The University of Nottingham

UNITED KINGDOM • CHINA • MALAYSIA

Evaluation of DNA Repair biomarkers in epithelial ovarian and breast cancers

AHMED HUSSIEN M. SHOQAFI

PhD thesis

Division of Cancer and Stem Cells

Faculty of Medicine

University of Nottingham

United Kingdom

June 2024

Acknowledgements

I would like to sincerely thank Prof. Srinivasan Madhusudan for his invaluable guidance and support during my research study. His advice and encouragement have been instrumental to my work, and I am truly grateful for his mentorship.

I want to thank my research group colleagues for their friendship and support during my research study. Additionally, I would like to thank all members of the Breast Pathology Group for their support and collaboration.

Finally, I would like to thank my family for their patience and support during this research process.

Abstract

DNA damage signalling and repair pathways play a crucial role in the regulation of genomic stability. Impaired DNA repair promotes genomic instability, a key route to the development of cancers. Cells have developed signalling pathways that are activated in response to DNA damage to detect and repair the damage that has occurred. Ataxia-Telangiectasia Mutated (ATM) and Ataxia-Telangiectasia and Rad3-related (ATR) kinases are activated in the presence of DNA damage and initiate a series of phosphorylation events that lead to the activation of downstream effectors. Some of these effectors include p53 and BRCA1, which regulate cell cycle, DNA repair, and apoptosis. The major DNA repair pathways are nucleotide excision repair (NER), which removes bulky DNA adducts; base excision repair (BER), which is involved in repairing small, non-helix-distorting base lesions; mismatch repair (MMR), which corrects replication errors and double-strand break repair which include homologous recombination (HR) and non-homologous end joining (NHEJ). All these pathways are regulated in a manner that is specific to the type of damage that needs to be repaired so that repair is as accurate as possible. Since conventional therapies for advanced epithelial ovarian cancer (EOC) and breast cancers have been found to be less effective, there has been a shift to search for new therapeutic approaches that aim at targeting the DNA repair pathways.

The host laboratory, using whole-exome sequencing in platinum-sensitive (PEO1, A2780) and platinum-resistant (PEO4, A2780cis) ovarian cancer cell lines, identified TP73 and POLE as potential predictors of platinum

resistance. In the current study, I have investigated the role of TP73 and POLE in EOC and breast cancers in detail.

TP73 is a member of the TP53 family of transcription factors that are involved in DNA repair, cell growth, migration, and death. In 331 EOC samples, I observed that high protein expression of TP73 was associated with higher tumour grade, late-stage disease and shorter progression free survival (PFS). In the large publicly available clinical cohort (n=522) and the cancer genome atlas (TCGA) ovarian cohort (n=182), TP73 transcript was upregulated in tumours compared to normal tissues and associated with shorter PFS. Preclinically, I have shown that overexpression of TP73 in A2780 platinum-sensitive ovarian cancer cells enhanced cell proliferation, invasion and increased DNA repair capacity. In clinical breast cancers, analysis of TP73 expression in 1,369 invasive breast cancers and 317 DCIS cases revealed that high cytoplasmic TP73 expression is significantly associated with aggressive disease features, including high tumour grade, ER negativity, triple-negative phenotype, and poor breast cancer-specific survival, particularly in the TP53 mutant subgroup. These findings highlight the prognostic and predictive significance of TP73 in EOC and breast cancers.

POLE has roles during DNA replication and repair pathways. I have investigated POLE expression in EOC and breast cancers. Immunohistochemical analysis of 331 EOC samples revealed that 75% exhibited low nuclear POLE expression, while 25% showed high expression. High POLE levels were significantly associated with higher tumour grade, poor progression free survival (PFS) and overall survival (OS).

The transcriptomic levels of POLE were analysed in patients with EOC, revealing that high POLE mRNA expression was significantly associated with poor progression free survival (PFS) and overall survival (OS) (All p=<0,05). Functional studies in platinum-resistant OVCAR 4 cells demonstrated that POLE knockdown increased cisplatin sensitivity, which was associated with double-strand break (DSB) accumulation, S-phase cell cycle arrest and increased apoptosis. The data supports the role of POLE in predicting response to platinum chemotherapy in EOC.

The study of 1,480 invasive breast cancer cases revealed that exhibited low nuclear POLE expression, which was associated with aggressive tumour features, poorer breast cancer specific survival (BCSS), and reduced response to endocrine therapy in ER+ and luminal subtypes. These findings suggest that POLE may be a predictive factor in ER+ breast cancers.

Taken together, the data provides evidence for the role of TP73 and POLE as potential biomarkers in EOC and breast cancers.

Publications

1. Alblihy A, Ali R, Algethami M, Ritchie AA, **Shoqafi A**, Alqahtani S, et al. Selective Killing of BRCA2-Deficient Ovarian Cancer Cells via MRE11 Blockade. International journal of molecular sciences. 2023;24(13):10966.
2. Alblihy A, Ali R, Algethami M, **Shoqafi A**, Toss MS, Brownlie J, et al. Targeting Mre11 overcomes platinum resistance and induces synthetic lethality in XRCC1 deficient epithelial ovarian cancers. NPJ precision oncology. 2022;6(1):51-.
3. Alblihy A, **Shoqafi A**, Toss MS, Algethami M, Harris AE, Jeyapalan JN, et al. Untangling the clinicopathological significance of MRE11-RAD50-NBS1 complex in sporadic breast cancers. NPJ breast cancer. 2021;7(1):143-.
4. Algethami M, Toss MS, Woodcock CL, Jaipal C, Brownlie J, **Shoqafi A**, et al. Unravelling the clinicopathological and functional significance of replication protein A (RPA) heterotrimeric complex in breast cancers. NPJ breast cancer. 2023;9(1):18-.
5. Ali R, Alabdullah M, Algethami M, Alblihy A, Miligy I, **Shoqafi A**, et al. Ligase 1 is a predictor of platinum resistance and its blockade is synthetically lethal in XRCC1 deficient epithelial ovarian cancers. Theranostics. 2021;11(17):8350-61.
6. Lashen A, Al-Kawaz A, Jeyapalan JN, Alqahtani S, **Shoqafi A**, Algethami M, et al. Immune infiltration, aggressive pathology, and poor survival outcomes in RECQL helicase deficient breast cancers. Neoplasia (New York, NY). 2024;47:100957-.
7. Lashen A, Algethami M, Alqahtani S, **Shoqafi A**, Sheha A, Jeyapalan JN, et al. The Clinicopathological Significance of the Cyclin D1/E1–Cyclin-Dependent Kinase (CDK2/4/6)–Retinoblastoma (RB1/pRB1) Pathway in Epithelial Ovarian Cancers. International journal of molecular sciences. 2024;25(7):4060.
8. Lashen A, Alqahtani S, **Shoqafi A**, Algethami M, Jeyapalan JN, Mongan NP, et al. Clinicopathological Significance of Cyclin-Dependent Kinase 2 (CDK2) in Ductal Carcinoma In Situ and Early-Stage Invasive Breast Cancers. International journal of molecular sciences. 2024;25(9):5053.
9. Mahmoodi A, **Shoqafi A**, Sun P, Giannakeas V, Cybulski C, Nofech-Mozes S, et al. High Expression of RECQL Protein in ER-Positive Breast Tumours Is Associated With a Better Survival. Frontiers in oncology. 2022;12:877617-.

Events, Poster, and Conferences

1. Pathology and precision medicine on Tuesday, January 30, 2024, at Royal Society of Medicine – London – UK

(***Clinicopathological and functional significance of TP73 transcription factor in epithelial ovarian cancers***)

2. Liverpool Pathology 2023 27-29 June 2023 – Liverpool – UK

(***Dissecting the clinicopathological significance of TP73 in sporadic breast cancers***)

3. NBCRC research day 15th May 2023 ah – Nottingham – UK
4. Sue Watson PGR Oral Presentation Event on 29th March 2022 – Nottingham – UK
5. Manchester Pathology 2021 6-8 July 2021 – Manchester – UK
6. Ovarian Cancer Masterclass 10 March 2020 – Nottingham – UK

Table of contents

List of Tables

List of Figures

List of abbreviations

Abbreviation	Definition
BC	Breast Cancer
BCA	Bicinchoninic Acid Assay
BER	Base Excision Repair
BRCA1	Breast Cancer Associated Gene1
BRCA2	Breast Cancer Associated Gene2
BSA	Bovine Serum Albumin
CIN	Chromosomal Instability
DAB	Diaminobenzidine Tetrahydrochloride
DCIS	Ductal Carcinoma in Situ
DDR	DNA Damage Response
dH2O	Distilled Water
DR	Direct Repair
DSBs	Double Strand Breaks
EMT	Epithelial-mesenchymal transition
EOC	Epithelial Ovarian Cancer
ER	Estrogen Receptor
FA	Fanconi Anaemia
FANCD2	Fanconi Anaemia Group D2 protein
FBS	Fetal Bovine Serum
GAPDH	Glyceraldehyde-3-Phosphate Dehydrogenase
HR	Homologous Recombination
H-Score	Histochemical-Score
ICL	Interstrand Cross-Link
IHC	Immunohistochemistry
IR	Ionising Radiation
MIN or MSI	Microsatellite Instability
MMR	Mismatch Repair
NAD+	Nicotinamide Adenine Dinucleotide
NER	Nucleotide Excision Repair

NGS	Next Generation Sequencing
NHEJ	Non-Homologous End Joining
NIN	Nucleotide Instability
NUH	Nottingham University Hospital
OSE	Ovarian surface epithelial
PARP1	Poly (ADP-ribose) Polymerase 1
PBS	Phosphate Buffered Saline
PBST	Phosphate Buffered Saline with Tween
ROS	Reactive Oxygen Species
RT-qPCR	Reverse transcriptase-quantitative polymerase chain reaction
SSBs	Single Strand Breaks
SSPS	Statistical Package for the Social Sciences
TBS	Tris Buffered Saline
TBS-T	Tris Buffered Saline with Tween
TCR	Transcription Coupled Repair
TMA	Tissue Microarray
W B	Western Blot

Chapter 1 Introduction

1.1 Hallmarks of Cancer and Therapeutic Targeting

All cancer cells exhibit common genetic, molecular, biochemical, and cellular characteristics known as the hallmarks of cancer. These hallmarks include angiogenesis, homologous recombination defects, immune system dysregulation and aberrant molecular signalling pathways (Hanahan, 2022; Werner & LeRoith, 2022).The essential role of these hallmarks contributes to the initiation, progression, and metastasis of tumours. Targeting these hallmarks are viable strategies in cancer treatment. Researchers have identified and developed therapeutic agents that can specifically target angiogenesis, homologous recombination defects or immune system dysregulation, and abnormal signal transduction. Moreover, evading growth suppressors, sustained proliferative signalling, resisting cell death, enabling replicative immortality, inducing angiogenesis, and activating invasion and metastasis are additional the hallmarks of cancer. Additionally, the ability to reprogram energy metabolism, evade immune destruction, promote tumour-promoting inflammation, genome instability and mutation, deregulate cellular energetics, and avoid immune destruction are also considered hallmarks of cancer, as outlined by (Hanahan & Weinberg, 2000; Hanahan & Weinberg, 2011) as shown in (**Figure 1-1**). In 2022, Douglas Hanahan expanded on the “Hallmarks of Cancer” by adding several new features that are important for understanding cancer biology. These new factors are phenotypic plasticity and disrupted differentiation, non-mutational epigenetic reprogramming, polymorphic microbiomes, and tumour-promoting inflammation, as shown in (**Figure 1-2**).

These hallmarks are suitable for therapeutic intervention as they provide potential targets for cancer treatment. For example, targeting oncogenes and their signalling networks can disrupt the enhanced activity of signal transduction pathways and inhibit the selective growth advantages of cancer cells (Carlberg et al., 2023). Furthermore, understanding the immunology of cancer hallmarks is crucial for optimizing therapeutic strategies, as immune dysfunction is central to cancer initiation and propagation (Milane, 2022; Senga & Grose, 2021). Additionally, targeting cell cycle kinases and checkpoint regulators can be explored as a potential strategy for developing new drugs against cancer (Selvaraj, 2023).

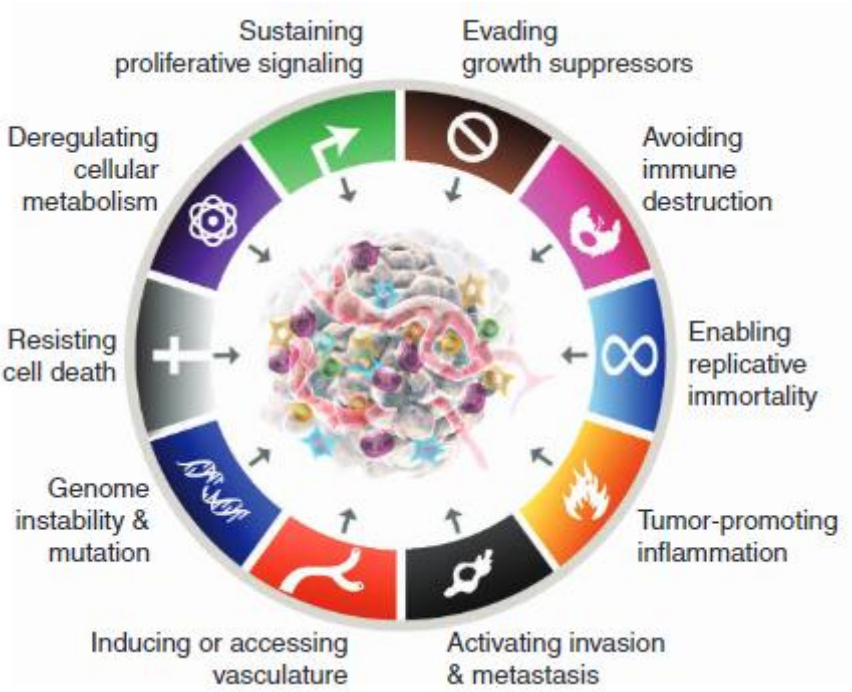

Figure 1-1. The hallmarks of cancer were originally introduced by Hanahan and Weinberg (2000, 2011). In 2022, Douglas Hanahan's updated model retains the original hallmarks, including sustaining proliferative signalling, evading growth suppression, resisting cell death, enabling replicative immortality, inducing angiogenesis, and activating invasion and metastasis. They later added emerging traits: genome instability, inflammation, reprogrammed energy metabolism, and immune evasion. Together, these hallmarks provide a framework for understanding cancer biology and its progression, highlighting critical pathways and processes that can be targeted for therapeutic interventions (Hanahan & Weinberg, 2000; Hanahan & Weinberg, 2011).

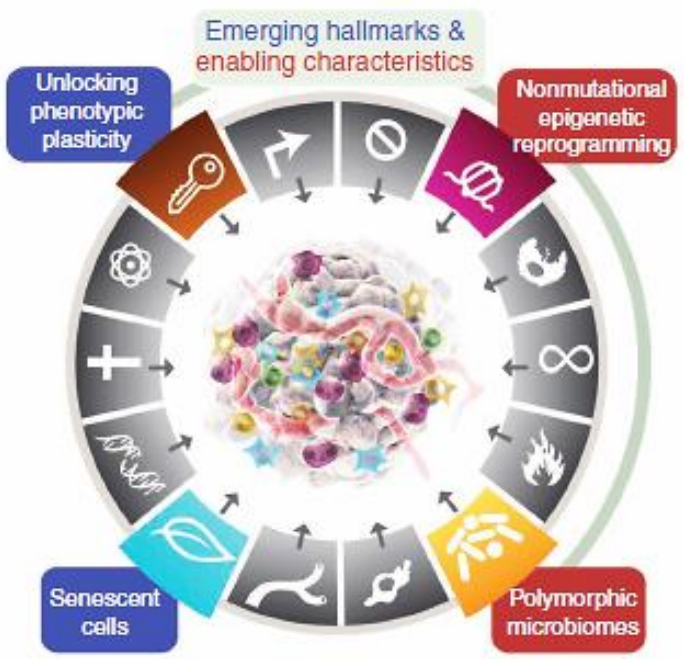

Figure 1-2. The updated hallmarks of the cancer model proposed by Douglas Hanahan in 2022 introduce new dimensions. These include phenotypic plasticity, which refers to cancer cells' ability to change their identity and resist differentiation, allowing ongoing proliferation. This update also identified non-mutational epigenetic reprogramming and the influence of the microbiome as enabling characteristics, suggesting they support the acquisition of hallmark traits by altering the tumour microenvironment and influencing cellular behaviour. The framework highlights the complex interplay between genetic, epigenetic, and environmental factors in cancer progression, providing a more comprehensive understanding of cancer biology (Hanahan, 2022).

1.1.1 Genome Instability and Mutations

Genomic instability refers to DNA damage or mutation in the genome, resulting in an increased risk of tumour formation (Mehrotra & Mittra, 2020). DNA damage can occur due to various reasons, including replication problems and radiation exposure, among other exogenous factors. But it can also result from normal cellular processes such as DNA replication and transcription which cause DNA damage and initiate DNA damage responses in the cell (Jilderda et al., 2021). Several strategies employed by cancer cells to hinder DNA repair fidelity culminate into genomic instability as a hallmark (Bhaswatee et al., 2021; Veschetti et al., 2023). Aneuploidy is an abnormal

number of chromosomes that is harmful and characteristic of cancer cells (Carlos, 2019). Understanding the mechanisms involved in genome instability and the associated pathways could facilitate the development of novel biomarkers and more effective cancer therapies.

Whole-genome duplication (WGD) is another common genomic abnormality in cancer that contributes to genome instability, leading to an elevated risk of DNA damage and chromosomal instability (Lau & Poon, 2023). In ovarian cancer, genomic instability is influenced by multiple factors, including cell cycle dysregulation and the suppression of DNA repair mechanisms such as BRCA2. Aurora Kinase A (AURKA) plays a critical role in this process by promoting centrosome amplification, aberrant mitotic progression, and chromosome segregation errors, all contributing to increased genomic instability (Yang et al., 2010). Loss of heterozygosity is commonly used to access whole-genome instability in ovarian cancer, with research showing the correlation between LOH and clinical outcomes observed in patients with this type of cancer (Korpanty et al., 2011). Additionally, a potential genomic instability score that can discriminate the outcome of BRCA1/2 mutations was suggested as well as predict the prognosis of women undergoing platinum-based chemotherapy for ovarian cancer (Zhang et al., 2014). Moreover, TP53 mutation-mediated genomic instability has also been implicated in chemoresistance and recurrence among epithelial ovarian cancers, where TP53 mutant groups had specific increases in multidrug resistance gene MDR1, among others (Zhang et al., 2017). Delaney and co-workers noted that autophagy gene haploinsufficiency drives chromosome instability while increasing migration, promoting early-stage ovarian tumours,

suggesting that autophagy contributes towards genomic instability in ovarian cancer (Delaney et al., 2020).

Cancer cells contain large numbers of mutations, from single nucleotide shifts to large-scale structural and numerical alterations of chromosomes. These mutations contribute to genome instability, which can be predisposed through inherited germline mutations or acquired somatic mutations. It has been found that numerous cancer-causing genes, approximately 82, are associated with germline mutations, 474 are linked to somatic mutations, and 513 are related to chromosomal alterations (Futreal et al., 2004).

Genomic instability can take many forms, such as point mutation, deletion, inversion, translocation, gene amplification, and aneuploidy. It can arise from acquired defects in any one of the DNA repair pathways (Tlsty et al., 1995). In cancer biology, DNA repair has significant implications for cancer diagnosis and treatment. Therefore, the loss of capacity to repair DNA is associated with the progression of the substantial majority of human tumours, which may lead to genomic instability (D’andrea, 2015).

Several studies have confirmed that hereditary germline mutation in either BRCA1 or BRCA2 is the most easily detectable risk factor for family histories of either ovarian or breast cancer. BRCA1 and BRCA2 proteins are involved in maintaining genomic instability by controlling homologous recombination (HR) and double-strand break repair in response to DNA damage (Berkenblit & Cannistra, 2005; Hahn & Weinberg, 2015; James et al., 2007; Moschetta et al., 2016; Welcsh & King, 2001).

Nucleotide instability (NIN), microsatellite instability (MIN), and chromosomal instability (CIN) are three classes of genomic instability. NIN refers to an increased rate of nucleotide substitutions; MIN involves changes in repetitive DNA sequences; and CIN involves the gain or loss of whole chromosomes or structural aberrations (Pikor et al., 2013). An understanding of these different classes of genomic instability is crucial for studying the mechanisms of cancer development and identifying potential therapeutic targets (Henninger & Pursell, 2014).

1.1.1.1 Microsatellite Instability (MIN or MSI)

Microsatellite instability is a genetic change characterised by the accumulation of mutations in microsatellite DNA repeat sequences. MSI is observed in various tumour types and plays a significant role in the development of cancer. It is associated with both sporadic and hereditary forms of cancer, such as Lynch syndrome (Amato et al., 2022; Kavun et al., 2023). The presence of microsatellite instability in tumours serves as a predictive biomarker for the sensitivity of tumours to immune checkpoint inhibitors (ICIs), particularly PD1/PD-L1 inhibitors (Geurts et al., 2023). MSI is detected using various assays, including immunohistochemistry, polymerase chain reaction, and next-generation sequencing (Kang et al., 2022). Studies have identified MSI-related genes and pathways involved in the DNA mismatch repair (MMR) system, including MLH1, MSH2, MSH6, and PMS2, which are associated with MSI in colorectal adenocarcinoma (COAD), providing insights into the causes and progression of MSI in colon cancer (Bhattarai et al., 2020). Glutathione peroxidase 2 (GPX2) has been identified as a key gene associated with microsatellite instability in colon

cancer (Cui et al., 2023). Additionally, MSI can occur in synchronous primary malignancies, such as gastric and colorectal cancer, and may contribute to their pathogenesis.

Microsatellite instabilities are short, two to six simple base pair, or tandem, sequence DNA repeats found in the genome. MIN arise when the DNA mismatch repair (MMR) mechanism is impaired, resulting in microsatellite extension, contraction, deletion, and spontaneous insertion (Li et al., 2020; Maxwell & Roskelley, 2015).

1.1.1.2 Chromosomal Instability (CIN)

Chromosomal instability (CIN) is a common feature of cancer development, contributing to tumour initiation and progression. CIN refers to variations in the number or structure of chromosomes within a tumour population. It can provide survival and adaptation advantages to cancer cells, but excessive CIN-induced chromosomal aberrations can be detrimental to cell survival and proliferation. Aggressive tumours adapt to cope with ongoing CIN and develop unique susceptibilities that can be targeted for therapy (Dhital & Rodriguez-Bravo, 2023). CIN is a mechanism that leads to the creation of genomic heterogeneity by altering the number and structure of chromosomes. It is observed not only in cancer but also in evolution and speciation. The patterns of chromosomal instability in cancer and speciation are strikingly similar, suggesting a common underlying mechanism (Comaills & Castellano-Pozo, 2023). CIN has implications for cancer diagnosis, prognosis, and response to therapy. However, the relationship between CIN and therapeutic response is complex, with conflicting findings reported

(Castellanos et al., 2023). Aneuploidy, a state of karyotype imbalance, can trigger CIN and contribute to the genetic diversity of cancer cells. Aneuploid cells undergo DNA replication stress, leading to continual CIN and the generation of genetically diverse cells with chromosomal abnormalities (Garribba et al., 2023). CIN is the most predominant type of genomic instability found in more than 90% of all malignancies. It is identified during the entire phase of neoplastic development, from premalignant to metastatic lesions (Maxwell & Roskelley, 2015; van Gent et al., 2001).

Chromosomal instability, characterised by an increased rate of gaining or losing whole chromosomes (W-CIN) or accumulating structural aberrations (S-CIN), is associated with tumorigenesis, cancer progression, treatment resistance, and clinical outcome. W-CIN is primarily caused by whole genome doubling, while S-CIN is strongly associated with homologous recombination deficiency (Zhang & Kschischo, 2022). Understanding the mechanisms and implications of CIN in cancer can provide insights into tumour progression and potentially lead to new therapeutic approaches.

1.1.1.3 Nucleotide Instability (NIN)

Nucleotide instability (NIN) arises from defects in DNA repair mechanisms, particularly the base excision repair (BER) and nucleotide excision repair (NER) pathways. These deficiencies lead to replication errors, manifesting as single nucleotide substitutions, deletions, or insertions. These alterations can disrupt gene structure and expression, ultimately threatening genomic integrity and contributing to tumorigenesis (Pikor et al., 2013).

NIN encompasses a range of base modifications and small sequence changes, including insertions and deletions. Such mutations often result from errors during DNA replication or faulty BER and NER pathways, which fail to correct these lesions (Maxwell and Roskelley, 2015; Tubbs and Nussenzweig, 2017). While less prevalent than chromosomal instability (CIN) or microsatellite instability, NIN has significant implications for cancer biology, particularly in its ability to alter key regulatory genes and promote tumour progression.

Despite its relative rarity, NIN's role in cancer development is profound. Subtle alterations at the nucleotide level can influence genomic stability, enhance mutational burdens, and drive the development of malignant phenotypes (Das et al., 2021). Understanding the mechanisms underlying NIN provides critical insights into its contribution to cancer pathogenesis and offers potential avenues for therapeutic intervention.

1.2 DNA Damage

DNA damage in the human body refers to changes in the structure of DNA that are not replicated during DNA replication. These damages can include chemical additions, disruptions to DNA bases, and the breaking of one or both DNA strands (Bernstein, 2013). DNA damage can lead to mutations if the damaged base is incorrectly replicated and can also cause rearrangements of chromosome structure (Lamghari et al., 2023). DNA damage can be induced by external physical and chemical agents as well as by normal metabolic processes within cells (Moreno-Villanueva, 2016). However, cells have evolved mechanisms of DNA repair to recognise and repair these damages before replication, avoiding mutations and maintaining genome integrity (Joaquin & Fernandez-Capetillo, 2012; Lewis & Dimri, 2023).

DNA can be damaged by various factors, both endogenous and exogenous. Endogenous sources of stress include methylation, alkylation, self-replication of DNA, cellular free radical formation, and exposure to DNA-damaging agents. Exogenous sources of stress include ultraviolet radiation, ionising radiation, and numerous chemical agents that can lead to various types of damage, such as base excision, double-strand breaks (DSBs), single-strand breaks (SSBs), and inter- or intra-strand cross-links as shown in (**Figure 1-3**) (Abbotts et al., 2014; Abbotts & Wilson, 2017; Hakem, 2008; Hoeijmakers, 2007; Madhusudan & Wilson, 2013). Evidence suggests that accumulating DNA damage could contribute to genomic instability, leading to more aggressive malignant tumours (Zheng et al., 2011). DNA repair pathways are

the key to maintaining genomic stability and integrity by repairing various types of damage to the DNA. There are several pathways involved in this process, such as base excision repair (BER), nucleotide excision repair (NER), mismatch repair (MMR), and double-strand break repair (DSBR), which can be further divided into non-homologous end joining (NHEJ) and homologous recombination (HR) (Jiang et al., 2020; Madhusudan & Wilson, 2013).

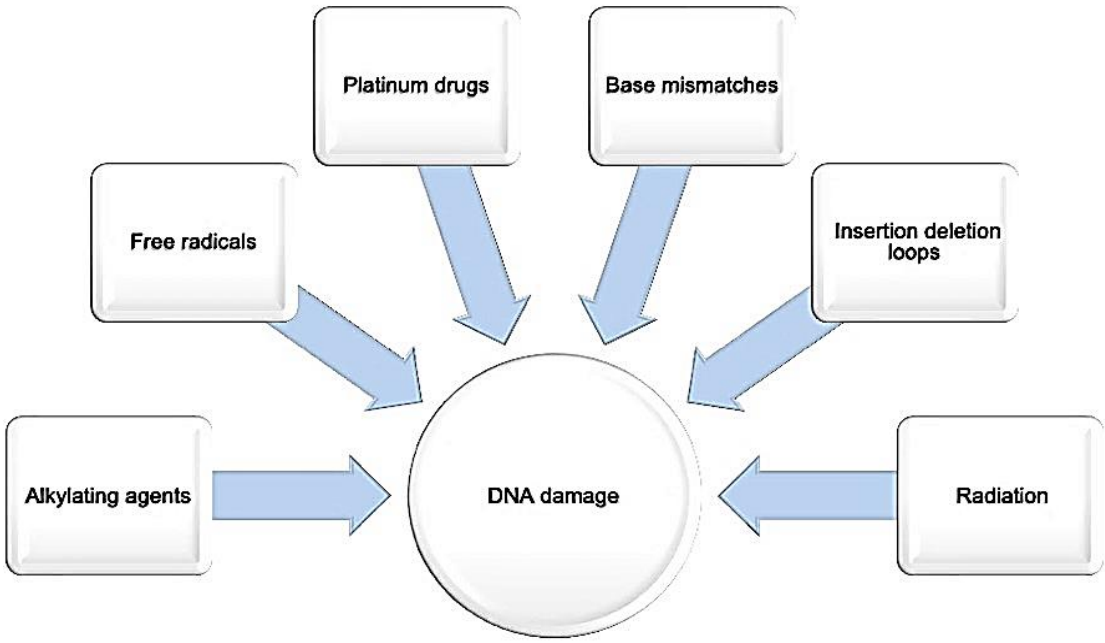

Figure 1-3. DNA damage arises from a combination of endogenous and exogenous factors. Endogenous sources include reactive oxygen species (ROS), and free radicals generated through cellular metabolism, which cause oxidative stress, leading to base modifications and strand breaks. Additionally, base mismatches and insertion-deletion loops can occur during DNA replication, particularly in microsatellite regions, resulting in replication errors and mutations if repair mechanisms fail. Exogenous sources, such as alkylating agents, add alkyl groups to DNA bases, disrupting their structure and function while ionizing radiation (e.g., X-rays) causes highly lethal double-strand breaks. Platinum-based chemotherapy drugs induce cross-links within and between DNA strands, effectively blocking replication in cancer cells but can pose a risk of damaging normal cells. These combined factors create complex DNA lesions that promote mutations, and cellular dysfunction, and contribute to the development of cancer (Abbotts et al., 2014; Abbotts & Wilson, 2017).

1.2.1 Endogenous

Endogenous DNA damage means the damage which takes place inside the cells by various endogenous DNA damaging agents. These agents can affect the DNA helix and thus cause wrong replication, transcription or protein synthesis (Yousefzadeh, 2022). Some endogenous DNA damaging agents include free radicals, reactive oxygen species (ROS), reactive nitrogen intermediates (RNI), reactive carbonyl species (RCS), lipid peroxidation products and alkylating agents. The formation of these reactive species can cause oxidative stress, and this can cause damage to the DNA bases, induce DNA strand breaks, and alter cell signalling mechanisms (Sharma et al., 2019). Endogenous DNA damage can have significant implications for human health, as it can lead to genetic abnormalities such as cancer, heart failure, Alzheimer's disease, and depression (Sharma et al., 2019). The human cell has antioxidant molecules and enzymes that help neutralize these free radicals and protect cells from the deleterious effects of oxidative stress (Bukunmi Ogunro et al., 2023). Endogenous DNA damage can ultimately lead to mutations and chromosome aberrations, which can have serious consequences for the cell's ability to proliferate and survive(Marnett & Plastaras, 2001; Tubbs & Nussenzweig, 2017).

1.2.1.1 Poly (ADP-ribose) polymerase 1 (PARP1)

Research into PARP1 has a long history. PARP1 was discovered as a DNA-dependent synthesis of a polyadenylic acid-like compound by Chambon et al., in 1963. Initially established as an ADP- ribose derived from the nicotinamide adenine dinucleotide (NAD+), labelled as poly (ADP-)

synthetase later became PARP1 (Chambon et al., 1963, Nishizuka et al., 1967, Cherney et al., 1987, Kurosaki et al., 1987). PARP1 is an extensively maintained, multi-functional enzyme in eukaryotes, composed of three major domains: an amino-terminal DNA-binding domain (DBD), a BRCT domain, and a carboxy-terminal catalytic domain. These domains work together to provide an early signal or warning for DNA damage. PARP1 catalyses the polymerisation of poly (ADP) ribose polymers on PARP1 itself and other proteins and histones that activate pathways for restoring DNA damage. PARP thus plays a significant role in the repair of base excision (BER) by detecting the degree of injury. In addition, due to its important function in restoring the DNA, inhibition of PARP induces genomic instability that can contribute to the conversion of single-strand breaks (SSBs) into double-strand breaks (DSBs) during DNA replication (Ame et al., 2004; Tubbs & Nussenzweig, 2017).

The BRCA gene plays a significant role in the repair of DSBs by homologous recombination (HR), as BRCA deficiency leads to poor capability of fixing damaged chromosomes via homologous recombination (HR). Hence the option of repairing is through the non-homologous joining pathway (NHEJ) which is error-prone (Madhusudan & Wilson, 2013).

1.2.1.1.1 Synthetic lethality

In 1922, Synthetic lethality was first identified by Calvin Bridges, who discovered the combinations of the gene mutations in Drosophila that confer lethality. Synthetic lethality involves two key concepts in developing novel cancer therapeutics. First, many genes that are considered synthetic lethal

with mutations in oncogenic drivers are not typically mutated in cancer itself as shown in (**Figure 1-4**) (Abbotts et al., 2014; Kaelin, 2005; Lord et al., 2015). This principle is especially appealing in the case of undruggable mutation, and the cells that have missed a tumour suppressor gene might have been more reliant on another gene, which may not be an oncogene, leading to a condition called non-oncogenic addiction. Second, the actions of medications that have little (or limited) therapeutic efficacy as single agents may be significantly potentiated when administered in conjunction with a second medication that is synthetically lethal to the first product (Beijersbergen et al., 2017; Huang et al., 2020; Lord & Ashworth, 2017; Lord et al., 2015).

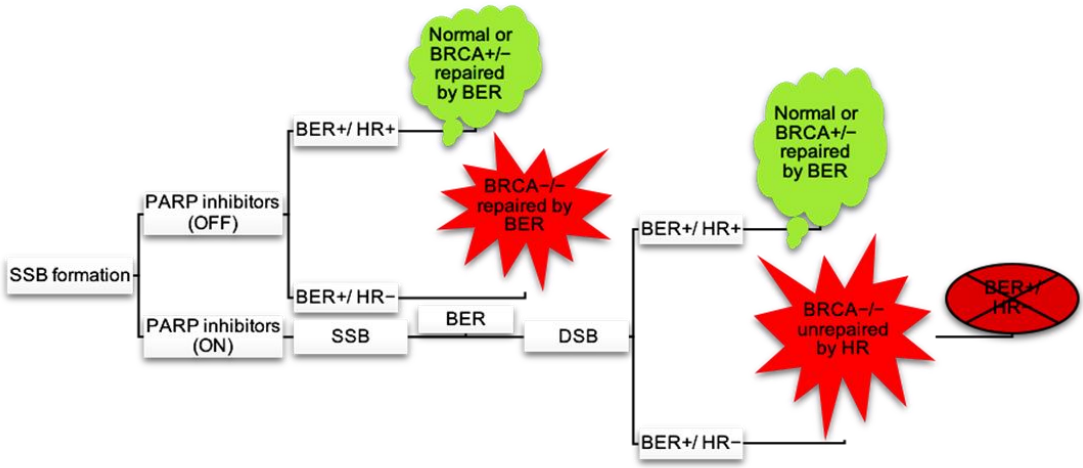

Figure 1-4. Synthetic lethality in BRCA−/− cells upon PARP inhibition. PARP inhibitors are designed to block the repair of single-strand DNA breaks through base excision repair (BER). In cells lacking functional BRCA1/2, which are already deficient in homologous recombination repair, PARPI treatment leads to accumulation of DNA damage that cannot be effectively repaired. This results in double-strand breaks, which, without repair, induce cell death. This mechanism specifically targets BRCA-deficient cancer cells while sparing healthy cells with intact DNA repair pathways (Abbotts et al., 2014; Lord et al., 2015).

1.2.2 Exogenous

Exogenous DNA damage defines the damage to DNA that occurs due to the exposure of DNA to various physical and chemical agents such as ionising radiation (IR), ultraviolet (UV) radiation, and chemical agents as mentioned in (Madhusudan & Wilson, 2013). In several studies, exogenous DNA damage has been assessed in cells. For instance, it was discovered that exogenous aldehydes like acetaldehyde, acrolein, etc., can react with DNA to form adducts which are potentially mutagenic and may explain the carcinogenic effects of exposure to air pollution or cigarette smoke (Medeiros, 2019). Another study also proposed a model to analyse exogenous DNA damage, and it was observed that it could affect the kinetics of damage accumulation in cells by increasing the level of reactive oxygen species (Guo et al., 2019). These agents can cause several damages to the DNA, such as single and double strand breaks, covalently bound chemical DNA adducts, oxidative induced lesions and DNA-DNA or DNA-protein cross-links as described by (Barnes et al., 2018). This information is valuable for the determination of risk associated with genotoxic agents as well as for the development of DNA repair treatments (Klapacz et al., 2016). Regularly conducting routine examinations to detect DNA damage is essential for early identification and intervention. This proactive approach not only facilitates timely therapeutic strategies but also helps mitigate the risk of subsequent complications. Other measures, such as adequate diets and refraining from smoking, can also help in the prevention of DNA damage, as indicated by (Hakem, 2008, Chatterjee and Walker, 2017).

1.2.2.1 Cisplatin

Cisplatin is a platinum-based compound also known as cis-(diammine) dichloridoplatinum (II), which was first discovered in 1845 by Dr. Michele Peyrone as shown in (**Figure 1-5**). At first, it was called "Peyrone's salt" and only after more than a century its cytotoxicity became known. Thereafter, cisplatin was shown to inhibit cell growth and received approval for animal experiments before getting FDA approval in 1978. It is the prototype of platinum-based chemotherapy agent that causes DNA adducts by binding to DNA thus preventing their replication. Although cisplatin is employed as the primary modality of treatment for different cancers, there are indications of efficacy against testicular tumours, ovarian tumours, head and neck tumours, bladder tumours, cervical tumours, oesophageal tumours and small cell lung carcinoma (Djordjević et al., 2023; Kopacz-Bednarska & Król, 2022; Prashanth et al., 2022). Cisplatin remains stable at room temperature but can slowly convert into its trans-isomer rendering it clinically ineffective in cross-linking over time.

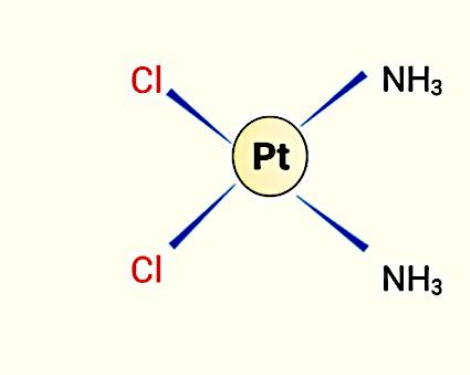

Figure 1-5. Cisplatin chemical structure (Messori & Merlino, 2016).

1.2.2.1.1 Mechanism of cisplatin

Cisplatin is a widely used chemotherapy drug that can be especially effective against different types of cancer, including testicular, ovarian, bladder and lung cancer (Zon and Bednarek, 2023). Its mechanism of action involves several steps mainly associated with interaction with DNA, leading to disruption of the normal cellular processes. Cisplatin enters cancer cells primarily through passive diffusion and copper transporters like Ctr1 (copper transporter 1), which can transport cisplatin into the cell. The aquation process occurs when cisplatin enters a cell, whereby its chloride ions are replaced by water molecules, forming highly reactive aquated cisplatin species. Aquated cisplatin forms covalent binding with purine bases in DNA adenine and guanine. This attachment takes place at the N7 positions for purine bases (Mei, 2021; Tchounwou et al., 2021). The distortion of the DNA helix due to cisplatin-DNA adducts formation impairs DNA function. Consequently, covalent bonding between DNA and cisplatin results in intra-strand and inter-strand cross-links in the deoxyribonucleic acid molecule, blocking DNA replication and transcription, thereby damaging DNA and activating apoptosis (programmed cell death) in cancerous cells.

1.3 DNA Repair

The DNA repair pathways play a significant role in maintaining genomic integrity. They are considered so crucial that germline mutations within DNA repair genes are linked with syndromes of predisposition to cancer, such as those in breast and ovarian cancer. Disruption of one or more DNA repair pathways via germline or sporadic mutation may speed up the rate of production of extra mutations by 100-1000 times. This increase in mutation rate is associated with the development of the "mutator phenotype," which can lead to carcinogenesis as shown in (**Figure 1-6**) (Abbotts et al., 2014; Madhusudan & Wilson, 2013).

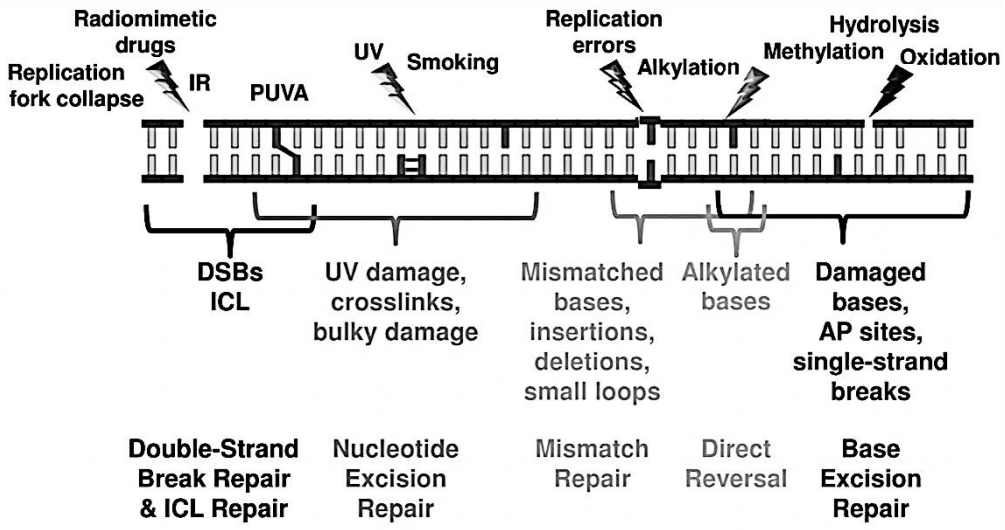

Figure 1-6. Overview of DNA damage and DNA repair pathways. Direct reversal repair is highlighted as a unique pathway that corrects specific DNA lesions without removing bases, commonly targeting damage like alkylation. Base excision repair (BER) corrects oxidative and small base lesions, while nucleotide excision repair (NER) addresses larger distortions like UV-induced damage for bulky DNA adducts. Mismatch repair (MMR) corrects replication errors. Double-strand break repair (DSBR) fix breaks through homologous recombination (HR) or non-homologous end joining (NHEJ). These pathways are essential for maintaining genomic stability and are central to cancer therapies. (Abbotts et al., 2014; Madhusudan & Wilson, 2013). *DNA Repair and Cancer: From Bench to Clinic* (1st ed.). CRC Press.

1.3.1 Direct Reversal Repair Pathway (DR)

Direct reversal repair is a form of DNA repair which does not require the prior excision, synthesis and ligation of the modified nucleic acid. It is also accurate and does not alter the genetic sequence (Madhusudan & Wilson, 2013). There are two classes of proteins that are directly involved in the direct reversal repair; these are O6-methylguanine-DNA methyltransferases (MGMT) and ALKBH α-ketoglutarate Fe (II) dioxygenases (FeKGDs) (Gutierrez & O'Connor, 2021; Gutierrez et al., 2018). Direct reversal repair is mainly involved in the repair of damage that has been caused by DNA alkylating agents such as MNNG, MNU and MMS. Alkylating agents can cause different kinds of damage to the DNA, and the direct reversal repair proteins are responsible for identifying and repairing these damaged areas to prevent any harm to the genome (Eker et al., 2009; Mishina et al., 2006; Yi & He, 2013).

O6-methylguanine-DNA methyltransferase (MGMT) is essential in the DNA repair process and the recovery of alkylated DNA, which affects the efficacy of chemotherapeutic agents. MGMT prevents mutations and tumorigenesis by removing methyl groups from the O6 position of guanine. This repair mechanism also contributes to chemoresistance against alkylating agents used in cancer treatment. Also, elevated level of MGMT expression is linked to resistance, as they repair the DNA damage these agents aim to induce. O6-benzyl guanine and lomeguatrib are inhibitors that affect DNA repair mechanisms, though they present challenges, including haematological toxicity, which poses risks to patient safety. Furthermore, modulating MGMT

expression via cell signalling pathways, including NF-κB and Wnt/β-catenin, may increase the therapeutic efficacy of alkylating drugs (Akcora-Yildiz et al., 2024; Bai et al., 2023; Chen & Wen, 2024; Yuexia Chen et al., 2023; Cropper et al., 2022). Understanding direct reversal repair mechanisms may help identify ways to overcome resistance to alkylating agents used in cancer therapy.

1.3.2 Single Strand Breaks and Repair Pathway (SSBs)

SSBs are one of the most frequent forms of DNA damage which occur during DNA replication, recombination and repair. SSB refers to the breakage of one of the two strands that form the DNA double helix while the other strand is left undamaged (Caldecott, 2008; Wilson III, 2007). Also, it can be caused by oxidative stress and as DNA repair intermediate during DNA repair. The repair of single-strand breaks can be done by three types of excision repair pathways, namely base excision repair (BER), nucleotide excision repair (NER) and mismatch repair (MMR) (Madhusudan & Wilson, 2013, Chatterjee & Walker, 2017).

1.3.2.1 Base Excision Repair (BER)

The Base Excision Repair (BER) pathway repairs various types of DNA damage, including oxidation, deamination, alkylation, and base loss. BER involves a series of enzymatic steps to remove the damaged base, incise the phosphodiester backbone, fill the resulting gap, and seal the nick as shown in (**Figure 1-7**) (Madhusudan & Wilson, 2013). BER is essential for maintaining genome stability and preventing cancer. BER carried out by a collection of enzymes, including DNA glycosylases, endonucleases,

polymerases, and ligases. Protein posttranslational modifications (PTMs) are crucial in regulating BER by controlling protein levels, enzymatic activities, interactions, and cellular localisation. Defects in BER components lead to reduced cell survival, increased mutation rates, and hypersensitivity to DNA-damaging agents (Maynard et al., 2009; Parsons & Grundy, 2023). Understanding the molecular details of BER and its regulation is essential for developing therapeutic strategies and improving cancer treatment.

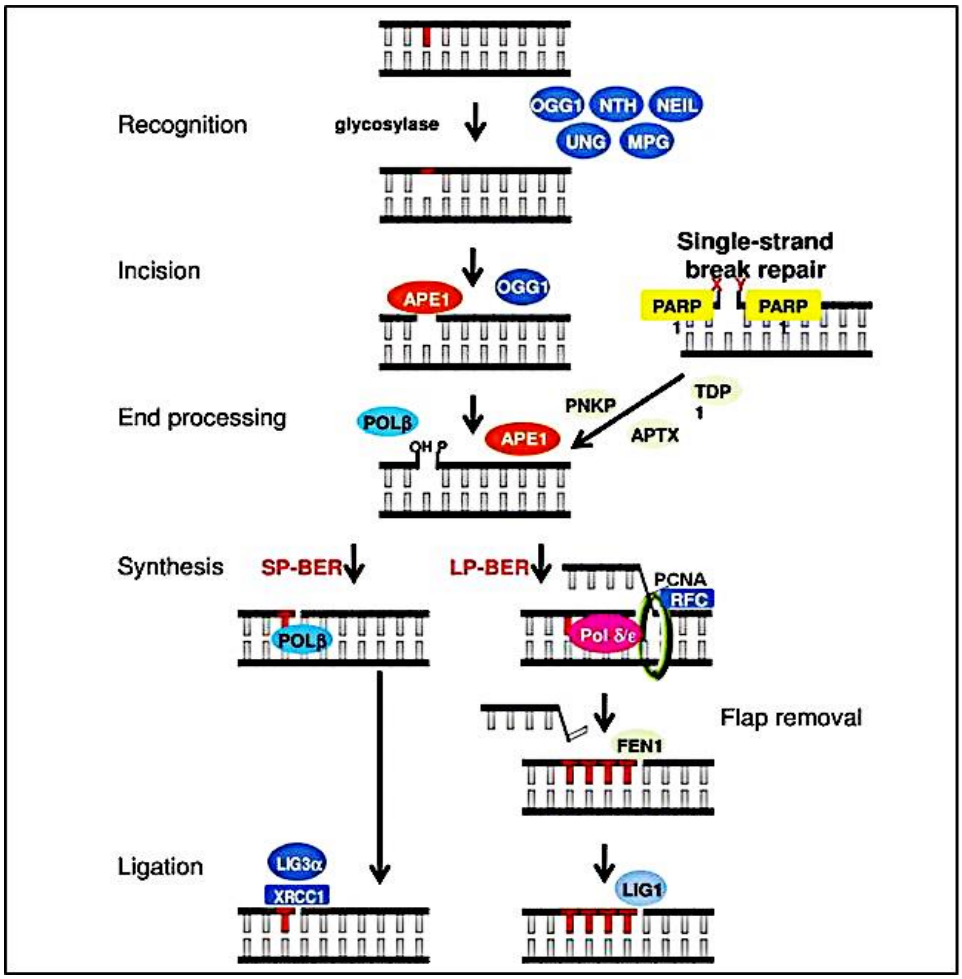

Figure 1-7. Schematic diagram of base excision repair mechanism. Madhusudan and Wilson describe base excision repair (BER) as a multistep process where a damaged base is first recognized and removed by a DNA glycosylase, creating a basic site. This site is then processed by an AP endonuclease, which cuts the DNA backbone. DNA polymerase adds a correct nucleotide, and the DNA ligase seals the strand, restoring DNA integrity. This pathway is crucial for repairing small, non-helix-distorting lesions caused by oxidation or alkylation (Madhusudan & Wilson, 2013). *DNA Repair and Cancer: From Bench to Clinic* (1st ed.). CRC Press.

1.3.2.2 Nucleotide Excision Repair (NER)

Nucleotide excision repair (NER) removes various types of DNA lesions, including those induced by UV irradiation and environmental toxins. NER comprises of two sub-pathways: global genome repair (GGR) and transcription-coupled repair (TCR). In GGR, lesions are identified throughout the genome, while in TCR, lesions are specifically recognized in transcribed DNA regions. The core factors involved in NER include XPC, CSB, XPB, and XPD. XPC is required to repair non-transcribed DNA lesions via GGR, while CSB is required to repair lesions in transcribed DNA via TCR. XPB and XPD are helicases that unwind the DNA duplex around the lesion during NER, as shown in (**Figure 1-8**) (Huang & Zhou, 2021; Lindsey-Boltz et al., 2023; Madhusudan & Wilson, 2013).

Nucleotide excision repair (NER) is a highly conserved DNA repair mechanism that removes DNA damage from the genome, including bulky adducts and base lesions(Krasikova et al., 2021). This fundamental process is present in all species, from bacteria to humans. NER is carried out by a complex multi-subunit enzyme system called excision nuclease or exonuclease. This enzyme system makes dual incisions around the damaged site, removing a 12-13 nucleotide-long oligomer in prokaryotes and a 27-29 nucleotide-long oligomer in humans (Friedberg, 2013; Reardon & Sancar, 2005). One of the unique features of NER is its ability to distinguish different types of damage from undamaged DNA and repair lesions in both the transcribed and non-transcribed strands. Defects in NER can lead to cancer. The process of NER involves several stages, including damage

recognition, verification, and removal of the damaged strand (Bessho et al., 1998).

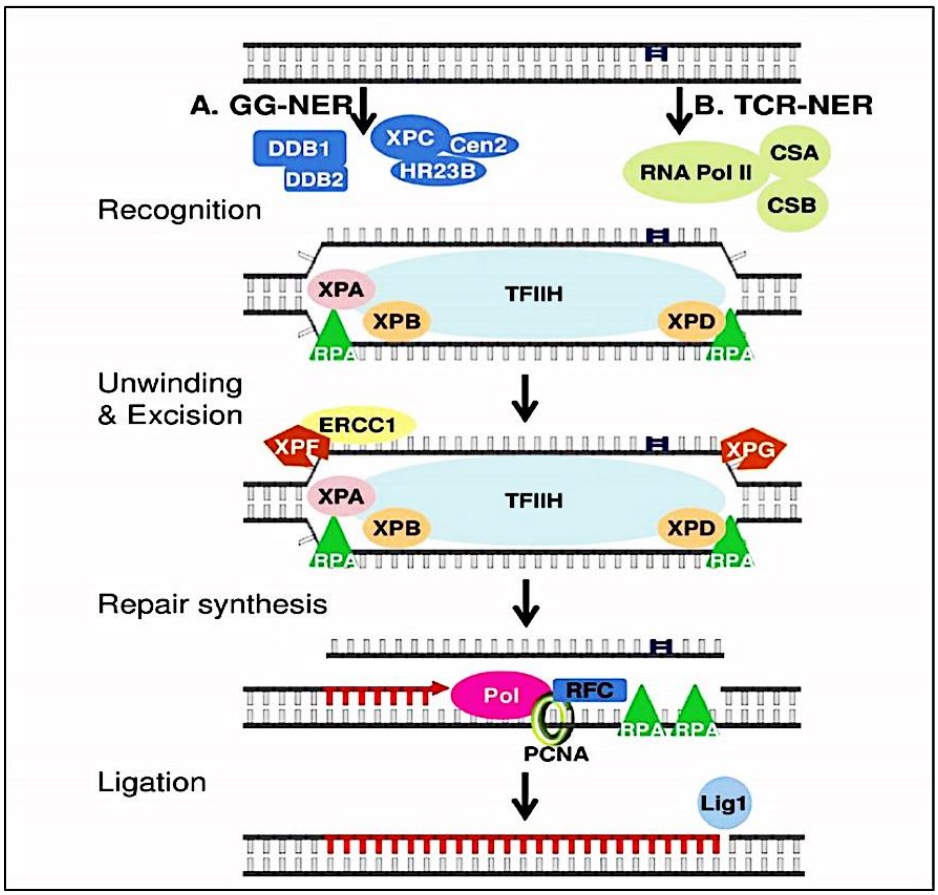

Figure 1-8. Nucleotide excision repair pathway mechanism. Madhusudan and Wilson outline nucleotide excision repair (NER) as a critical pathway for removing bulky DNA lesions, like those from UV radiation. NER involves damage recognition, unwinding by a helicase, and dual incisions around the lesion by endonucleases. The damaged section is excised, and DNA polymerase fills in the gap with the correct nucleotides. Finally, DNA ligase seals the repaired strand, restoring DNA integrity. This complex, multi-enzyme process is vital for preserving genomic stability. (Madhusudan & Wilson, 2013). *DNA Repair and Cancer: From Bench to Clinic* (1st ed.). CRC Press.

1.3.2.3 DNA Mismatch Repair (MMR)

DNA mismatch repair (MMR) is a process that corrects errors in DNA replication and other DNA transactions. Impaired MMR can have wide-ranging biological consequences. MMR proteins recognize and repair mismatches in the newly synthesized DNA strand, ensuring the fidelity of

replication. Mutations in MMR genes can lead to an increased risk of colorectal and other cancers. MMR also plays a role in the anti-recombination action on heteroduplexes. The mechanism of MMR involves various proteins such as MutS, MutL, and exonucleases, as shown in (**Figure 1-9**) (Madhusudan & Wilson, 2013). Dam methylation is a vital process for strand discrimination, which allows mismatched repair enzymes to distinguish between newly synthesized DNA strands and parental ones during replication. Dam methyltransferases can transfer a methyl group onto an adenine residue at specific DNA segments, such as GATC sites that affect protein–DNA binding and other cellular functions (Couturier & Lindas, 2018; Marinus & Casadesus, 2009). The repair mechanisms of MMR include short-patch repair and removal of oxidized bases (Geng & Hsieh, 2013; Kunkel & Erie, 2005; Marinus, 2012; Velmurugu & Velmurugu, 2017).

DNA mismatch repair (MMR) is a highly conserved genetic mechanism that is essential for the stability and functionality of DNA. It identifies and corrects errors that occur during DNA replication, such as base insertions, deletions, and misincorporations. When the MMR pathway malfunctions, it can result in various genomic alterations, including microsatellite instability, which is commonly observed in several types of malignancies. MMR exhibits a paradoxical effect on microsatellite expansion; while it suppresses certain types of expansion, it can also promote others in different contexts (Metaxas et al., 2023; Miller & Usdin, 2022). The biological significance of MMR is underscored by its association with Lynch syndrome, a genetic predisposition to various types of cancer. MMR is also involved in the maintenance of genetic information, replication and recombination editing, and the prevention

of genomic instability(Elez, 2021; Takedachi et al., 2022). Additionally, MMR has been linked to the accumulation of DNA damage and the ageing process, suggesting its role in promoting healthy ageing and reducing the incidence of age-related diseases (Wen et al., 2021).

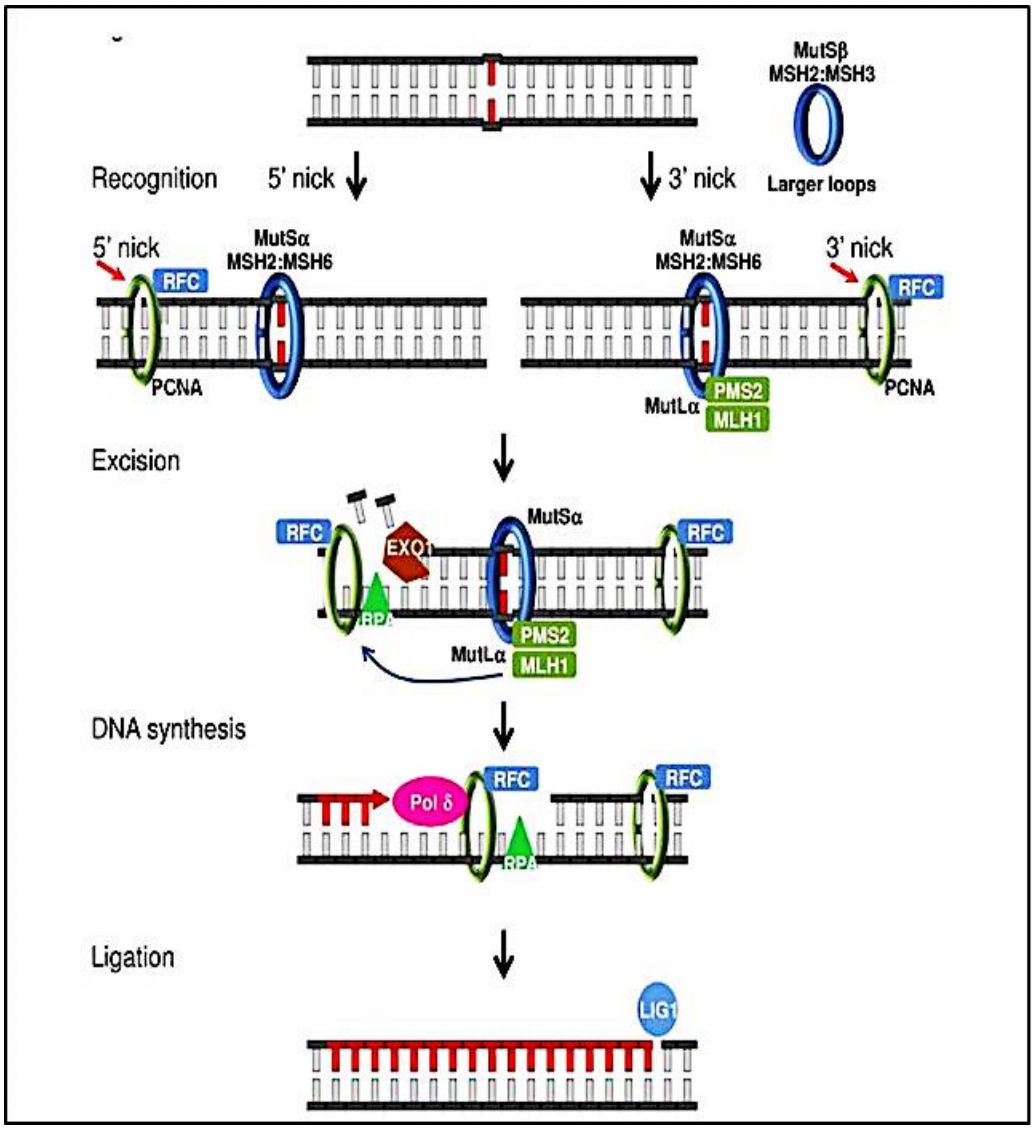

Figure 1-9. DNA mismatch repair mechanism. Madhusudan and Wilson describe the mismatch repair (MMR) mechanism as a crucial process for correcting DNA replication errors. The process begins with the recognition of mismatched bases by MMR proteins, which then bind to the error site. An endonuclease makes a cut in the DNA strand containing the mismatch, allowing for the excision of several nucleotides, including the erroneous base. DNA polymerase then synthesizes the correct sequence, followed by DNA ligase sealing the repaired strand, ensuring genomic stability (Madhusudan & Wilson, 2013). DNA Repair and Cancer: From Bench to Clinic (1st ed.). CRC Press.

1.3.3 Double Strand Breaks Repair Pathway (DSBs)

Double-strand breaks (DSBs) are cytotoxic lesions that occur when both strands of the DNA double helix are cleaved. DSBs can arise from various sources, including DNA replication, transcription, recombination, ionising radiation, and genome-editing nucleases (Chang et al., 2017; Khan & Ali, 2017; Surdutovich & Solov'yov, 2012). DSBs are considered the most toxic form of DNA damage and can lead to genetic instability, mutations, genome rearrangements, and loss of genetic material if not properly repaired (Barroso & Aguilera, 2021; Taverna Porro & Greenberg, 2015). Chromatin plays an active role in sensing, detecting, and repairing DSBs, with histone acetylation facilitating the recruitment of DSB repair proteins to sites of DNA damage (Aricthota et al., 2022). The selection of DSB repair pathways is crucial for genome editing, with non-homologous end joining (NHEJ) resulting in random mutations and homologous recombination (HR) inducing high-fidelity sequence-specific variations (Ali et al., 2022; Scully et al., 2019).

DSB repair is relevant because defects in this pathway may increase the risk of development of breast and ovarian cancer development. When two different chromosomes are incorrectly linked during DSB repair, chromosome translocations may occur; moreover, chromosome end-to-end fusions may occur by recombination at telomeres. Two primary mechanisms for repairing DNA double-strand breaks (DSBs) are non-homologous end joining (NHEJ) and homologous recombination (HR). NHEJ is a quick, error-prone process that directly ligates the broken DNA ends without the need for a homologous template, leading to small insertions or deletions. In contrast, HR is a high-

fidelity repair mechanism requiring a sister chromatid as a template to be active during the S and G2 phases of the cell cycle. These pathways are critical for maintaining cellular viability and genomic stability as shown in (**Figure 1-10**) (Madhusudan & Wilson, 2013).

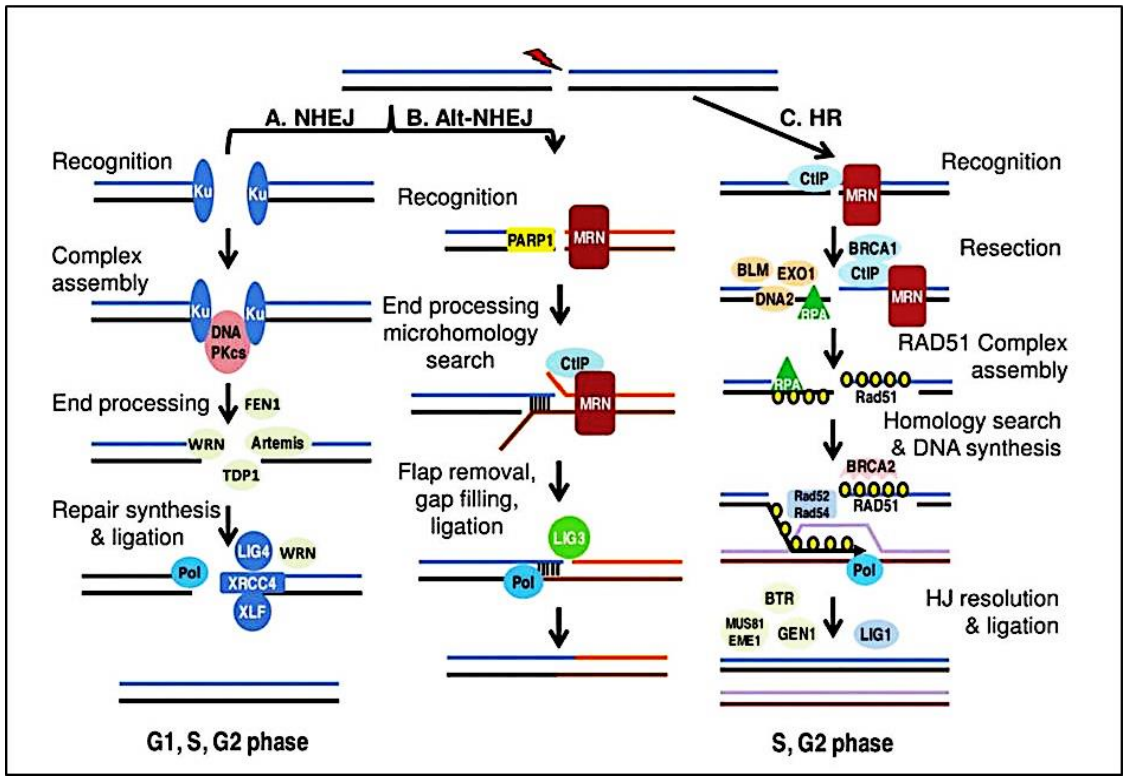

Figure 1-10. Double strand breaks repair pathway (DSBs) mechanisms. Madhusudan and Wilson describe the double-strand break repair (DSB) pathways, which are crucial for maintaining genomic integrity. There are two primary mechanisms: homologous recombination (HR) and non-homologous end joining (NHEJ). In HR, the broken ends are processed, and a homologous sequence serves as a template for accurate repair. In NHEJ, the ends are directly ligated together with Ku70, Ku80, and DNA ligase IV, factors enable efficient repair at the broken DNA ends, often with less fidelity. Both pathways are essential for resolving DSBs and preventing genomic instability (Madhusudan & Wilson, 2013). *DNA Repair and Cancer: From Bench to Clinic (1st ed.). CRC Press.*

1.3.3.1 Non-Homologous End Joining (NHEJ)

Non-homologous end joining (NHEJ) is an essential DNA repair pathway in human cells. It involves the direct joining of two ends of DNA, usually without requiring sequence homology. The main components of the NHEJ system in

eukaryotes are DNA-PKcs, Ku proteins, XRCC4, DNA ligase IV, and Artemis (Head et al., 2023; Mikhova et al., 2023; Poplawski & Blasiak, 2005). NHEJ (non-homologous end-joining) is the most common mechanism to repair DSBs but is associated with errors (Betermier et al., 2014). Non-homologous end joining (NHEJ) does not directly cause DNA double-strand breaks (DSBs); instead, it serves to repair them. DNA breakage occurs for various reasons, and NHEJ helps maintain chromosomal integrity by ligating broken DNA ends. However, this process often results in the loss of a few nucleotides from one or both ends, which can lead to minor genomic alterations (Chang et al., 2017). NHEJ is a DNA repair pathway that remains active across all cell cycle phases and can incorporate ribonucleotides into DNA during the ligation of double-strand breaks. This incorporation of RNA precursors into the DNA strand introduces an additional layer of flexibility to the repair process, allowing cells to modulate their response to DNA damage by different physiological conditions (Gago-Fuentes & Oksenych, 2020; Pryor et al., 2018; Ray & Raghavan, 2022; Zhao et al., 2020).

1.3.3.2 Homologous Recombination (HR)

Homologous Recombination (HR) is a pathway for DNA repair that is crucial for maintaining genomic stability. It facilitates the exchange of genetic material between two identical or nearly identical DNA sequences. HR deficiency is associated with an increased risk of several cancers, including breast and ovarian cancer (Yoon et al., 2023). HR deficiency can lead to chromosomal instability and copy number alterations (CNAs) in tumours. In the context of metastatic melanoma, HR deficiency has been observed in a

subset of patients, and PARP inhibitors have shown promise in treating tumours with HR mutations (Akinjiyan et al., 2023; Kim, 2023). HR deficiency is highly prevalent and is associated with CNAs and chromosome instability. CNAs have been identified as potential biomarkers for HR status and BRCA1/2 mutation status in HGSOC tumours. A whole genome sequencing classifier of HRD has been developed, which incorporates mutational features that can only be detected using WGS, achieving superior precision in identifying HRD tumours. In a study of platinum-responsive triple negative breast cancer (TNBC) patients, homologous recombination deficiency (HRD) testing using the OncoReveal™ HRD Panel identified HR alterations in 52.5% of patients, including BRCA1, BRCA2, PALB2, and BRIP1 alterations (Chai et al., 2022; Yimeng Chen et al., 2023; Hadi et al., 2023; Tan et al., 2023; Telli et al., 2016; Z. Zheng et al., 2023).

HRD has an important impact on the onset and progression of ovarian cancer (Mangogna et al., 2023). Studies show high frequencies of TP53 mutants, chromosomal instability, different molecular subtypes, and DNA copy number-dependent alterations in gene expression in high-grade serous ovarian cancer. These findings indicate that HRD is the beginning of a molecular cascade that impacts the evolution of this type of cancer (Abkevich et al., 2012; Frey & Pothuri, 2017). In this context, targeting defective homologous recombination represents an opportunity to exploit molecular differences between cells and normal cells, resulting in synthetic lethality specific to cancer among ovarian cancer patients (Konstantinopoulos et al., 2015).

1.3.4 Fanconi Anaemia pathway for, Interstrand Cross-Link Repair

Fanconi anaemia (FA) is a rare genetic disease that disrupts the interstrand crosslink repair pathway, leading to bone marrow failure and cancer predisposition. The Fanconi anaemia pathway is involved in the accurate repair and replication of DNA when Interstrand cross-links (ICLs) are present (Madhusudan & Wilson, 2013). ICLs are a form of DNA damage that disrupts crucial cellular processes like replication and transcription by creating covalent bonds between the complementary strands of the Watson-Crick double helix (Deans & West, 2011). While chemotherapy agents like cisplatin and mitomycin C are known to induce ICLs, the role of naturally occurring ICLs in diseases such as cancer is not fully understood. Lipid peroxidation products, especially malondialdehyde, are a significant endogenous source of ICLs, but the contribution of other DNA damages, like mono-adducts, to diseases and ageing symptoms related to ICL repair deficiencies remains unclear (Berrada et al., 2023; Hashimoto et al., 2016; Madhusudan & Wilson, 2013). Various cellular defence mechanisms, such as structure-specific nucleases and translesion synthesis polymerases, are involved in ICL bypass and replication fork rescue, as shown in (**Figure 1-11**). Aberrations in the repair mechanisms for ICLs can result in several hereditary disorders, including Fanconi anaemia (Garcia-de-Teresa et al., 2020). FA cells exhibit hallmarks of senescence, suggesting a relationship between FA and senescence, making FA a "senescence syndrome" (Helbling-Leclerc et al., 2021).

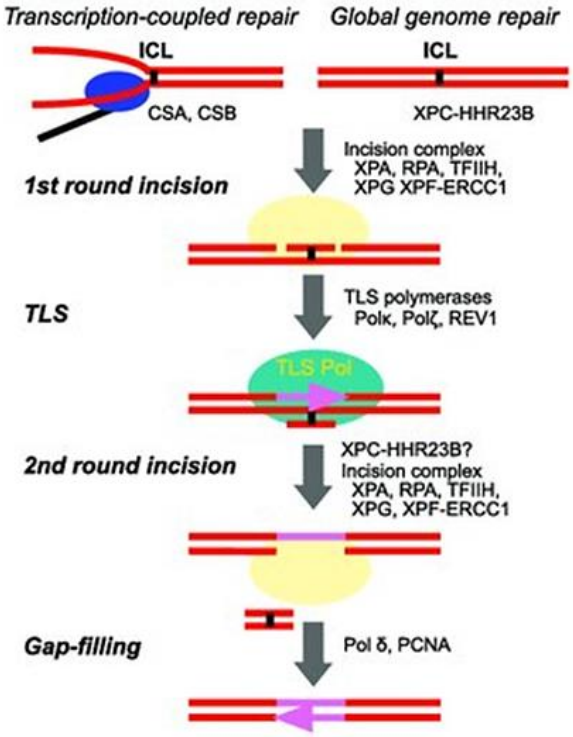

Figure 1-11. Schematic diagram of interstrand cross-links repair. Transcription-coupled nucleotide excision repair recruits the incision complex utilizing CSA and CSB. The XPC-HHR23B complex is crucial in initiating the process in non-transcribed regions. During the first incision round, XPA-RPA, TFIIH, XPF-ERCC1, and XPG collaborate to make an incision near the interstrand cross-link. Translesion synthesis polymerases, such as DNA polymerases, are responsible for replicating across the ICL by incorporating nucleotides at the damaged site. Finally, the second NER-associated incision complex completes the repair by excising the ICL lesion with an oligonucleotide strand (Hashimoto et al., 2016).

1.4 Breast Cancer

Breast cancer is the malignant abnormal proliferation of epithelial cells in the ducts or lobules of the breast. It is a leading cause of cancer in females, amounting to approximately one-third of all women's cancers (Rai et al., 2022). Histopathological and biological characteristics are different among these subtypes, which result in different responses to therapy and warrant diverse therapeutic approaches (Mir & Din, 2023; Mir & Qayoom, 2023). Breast cancer classification has undergone significant changes through the incorporation of molecular pathology as well as high-throughput molecular techniques. The traditional histological features of breast lesions continue to form the basis for classification, but molecular approaches have improved diagnostics, prognosis prediction, and treatment response assessments (Rakha et al., 2023). These molecular updates have led to changes in the World Health Organization (WHO) classification of breast tumours that include invasive carcinoma histology groupings; subtyping lobular carcinoma in situ (LCIS) and phyllodes tumour criteria have also been modified accordingly (Lebeau, 2021). Treatment for breast cancer may vary depending on its type and stage. Different treatment options include endocrine therapy, chemotherapy, radiation therapy, targeted therapy, and surgical interventions. Local therapy typically involves lumpectomy or mastectomy combined with radiation therapy. Systemic treatment, which may be administered before or after surgery, includes endocrine therapy, chemotherapy, and targeted therapy. (Leon & Richardson, 2021; Mumtaz et al., 2023; Trayes & Cokenakes, 2021).

1.4.1 Epidemiology

Breast cancer is the principal cause of death among women in some developed countries and the second most common reason for death from cancer among females (Bombonati & Sgroi, 2011; Wilkinson & Gathani, 2022). Annually in the world, more than two million women are diagnosed with breast cancer. In the UK, this disease has high incidence rates and is one of the leading causes of death in women (Ginsburg et. al., 2017; Landy et. al., 2016). It is also ranked fourth as a cause of cancer deaths, accounting for about 7% of all global cancer fatalities. Among older females globally, it comes in second as a cause of cancer deaths, with the total number being reported to be about 11,400 cases in 2017. During the period between years 2015-2017, there were approximately 55,200 new invasive breast cancers recorded and about 8,100 new carcinomas in situ cases that show how alarming this incidence rate has become (Cancer Research UK, 2017).

1.4.2 Pathogenesis and aetiology

Breast cancer is a complicated disease with numerous factors that contribute to its pathogenesis. These factors include age, genetic makeup, family history of the disease, diet, alcoholic intake, obesity, lifestyle choices, lack of exercise, hormonal aspects, and exposure to ionising radiation (Cohen et al., 2023; Pegington et al., 2023). Genetic mutations, for instance, in the BRCA1 and BRCA2 genes, are major genetic mutations that increase the risk of developing breast cancer (Chabuk et al., 2024). Hormonal factors such as early menarche, late menopause, and hormone replacement therapy have also been found to be related to increased risk (Admoun & Mayrovitz, 2022).

Environmental factors, for instance, certain chemicals, have been linked with the development of breast cancer (Hiatt et al., 2020). In addition, the breast and intestinal microbiota affect the development of breast cancer through the modulation of hormone metabolism and immune response (Tian et al., 2022). Although a lot of research has been conducted on the aetiology of breast cancer, there are still many aspects that are not well understood, hence the need to continue with research to establish other processes and factors involved.

1.4.3 Subtypes of Breast Cancer

Several types of breast cancer have different pathogenesis and morphological characteristics (Makki, 2015). Among these are infiltrating ductal carcinoma, infiltrating lobular carcinoma, tubular, mucinous, medullary, and adenoid cystic carcinoma as shown in (**Figure 1-12**) (Malhotra et al., 2010). Furthermore, histological grading of breast cancer plays a crucial role in sub-classifying the disease based on cellular differentiation, nuclear pleomorphism, and mitotic count, which helps determine the aggressiveness and prognosis (Rakha et al., 2022).

Many classifications exist for breast cancer. The most common classification is based on hormone receptor expression status, which includes oestrogen receptor (ER), Progesterone Receptor (PR) and Human Epidermal Growth Factor Receptor-2 (HER-2). These subtypes are luminal A, luminal B, HER2-positive, and triple-negative (Hashmi et al., 2023). There are other classifications based on molecular markers, such as miRNAs or mutations (Mir & Din, 2023; Orrantia-Borunda et al., 2022). For example, another

classification system has five intrinsic subgroups of breast cancer: Luminal A, Luminal B, HER2 enriched, normal and basal-like tumours as shown in (**Figure 1-13**) (Malhotra et al., 2010). Triple Negative Breast Cancer (TNBC) is a distinct subtype with a lack of three hormonal receptors and is further classified into six different groups: basal-like 1; basal-like 2; mesenchymal; mesenchymal stem-like; immunomodulatory; mesenchymal stem-like cell expressing CD44+CD24-/-and CD133+ cells lineage markers as well as luminal-androgen receptor (Yin et al., 2020).

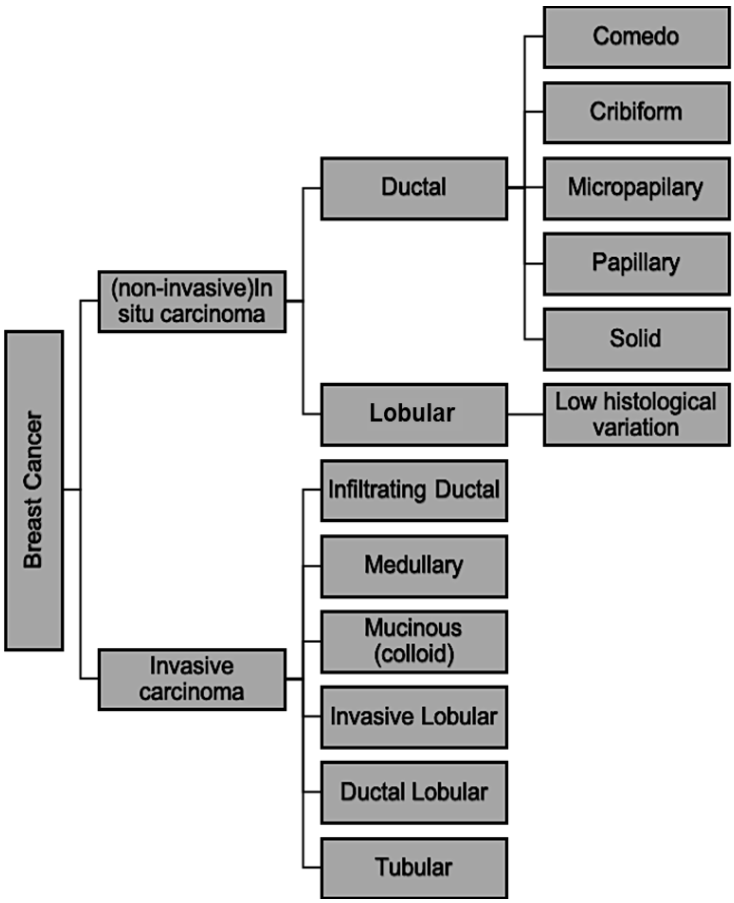

Figure 1-12. Histological classification of breast cancer subtypes, as discussed by Malhotra et al. (2010), focuses on identifying tumour types based on morphological and molecular characteristics. These include ductal carcinoma in situ (DCIS), invasive ductal carcinoma (IDC), lobular carcinoma, and other rare histological types like medullary, mucinous, and tubular carcinomas. IDC is the most common subtype, while others are distinguished by unique growth patterns and clinical behaviours. (Malhotra et al., 2010).

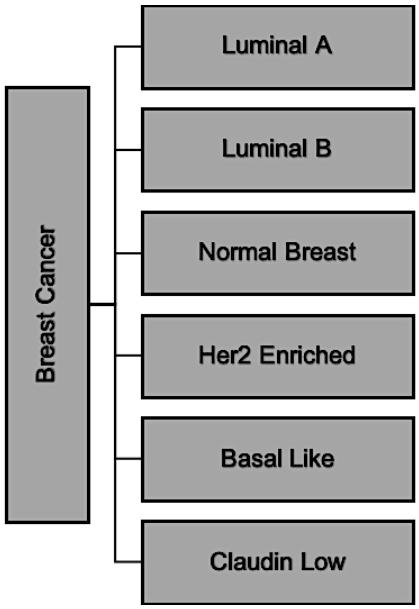

Figure 1-13. Molecular classification of breast cancer, as detailed by Malhotra et al. (2010), identifying subtypes based on gene expression profiles, enhancing our understanding of breast cancer heterogeneity. These subtypes include luminal A, luminal B, HER2-enriched, basal-like, and normal-like, each with distinct molecular markers, clinical outcomes, and responses to treatment. Luminal subtypes are hormone receptor-positive, HER2-enriched tumours overexpress HER2, and basal-like cancers are often triple-negative (Malhotra et al., 2010).

1.4.4 Breast cancer staging

Staging breast cancer is very important in the diagnosis and treatment planning of the patient. The staging system mainly used is the TNM staging system, which involves the assessment of the size of the primary tumour (T), the lymph node involvement (N), and the presence of distant metastases (M). The TNM staging system for breast cancer was created by the American Joint Committee on Cancer (AJCC) as a standardised way to evaluate the prognosis of patients with recently discovered breast cancer. In 2017, the AJCC published the 8th edition of the TNM system (Cabioglu et al., 2019; Giuliano et al., 2017). Furthermore, the Nottingham Prognostic Index (NPI) is a well-established tool for predicting the prognosis of breast cancer patients. It integrates tumour size, lymph node status, and histological grade. The NPI has been shown to be an independent risk factor for predicting locoregional

recurrence (LRR) in breast cancer patients. Based on NPI, a nomogram model was proposed in a study, and the discrimination and calibration of the nomogram were satisfactory, indicating the potential clinical utility of the nomogram for evaluating risk judgments (Zheng et al., 2024).Tumour size is one of the variables used in the NPI, and it is measured in centimetres, then divided by 10 and multiplied by 0. 2 in the formula as it is a significant factor in determining the prognosis. The stage of the lymph node ranges from 1 to 3, where a higher stage means a more involved lymph node and, therefore, a worse prognosis. Tumour grade, ranging from 1 to 3, is another component of the NPI, with higher grades indicating more aggressive cancer (Blamey et al., 2007; Green et al., 2016; Winzer et al., 2016).

1.5 Ductal carcinoma in situ (DCIS)

Ductal carcinoma in situ (DCIS) is a non-invasive breast cancer that arises from the cells lining the mammary ducts. It is characterised by the proliferation of malignant epithelial cells within the ducts, without invasion into the surrounding stroma (Alvarado-Cabrero, 2018). DCIS is associated with a high survival rate and accounts for 25% of all breast cancers diagnosed (Farante et al., 2022). The incidence of DCIS has increased with the expansion of screening mammography programs, and it is seen as a major driver of overdiagnosis and overtreatment. Diagnosis and classification of DCIS can be challenging due to under-sampling and interobserver variability. Imaging techniques such as mammography and MRI are used to detect and delineate the extent of DCIS, with MRI being more successful in some cases (Lagios, 2020).

DCIS can be defined as a group of diseases with varying characteristics where the proliferation of epithelial cells within the myoepithelial duct lobular lineage increases but without invading the adjacent stromal tissue. DCIS has a high degree of heterogeneity, which results in differential genomic profiles, morphology, and prognostic outcomes. It is also considered a significant risk factor for the subsequent recurrence of invasive breast carcinoma. (Bane, 2013). Intraductal carcinoma, or DCIS, is a non-invasive type of breast cancer caused by the proliferation of abnormal epithelial cells within the basement membrane. When the basement membrane layer is disrupted, the diagnosis changes from DCIS to invasive breast cancer. The presence of DCIS is a precursor to the development of invasive breast cancer. DCIS is defined by the World Health Organization as a proliferation of epithelial cells within the mammary ductal-lobular system characterised by variations in cytology that can range from subtle to severe, which may progress to invasive breast cancer.

Studies have shown that DCIS can recur locally even 15-25 years after initial diagnosis, highlighting the importance of long-term follow-up and monitoring (Page et al., 1995). The accuracy of diagnosing DCIS has improved with the use of directional, vacuum-assisted biopsy techniques, particularly in cases of atypical ductal hyperplasia (Burbank, 1997). The relevance of occult axillary micro metastasis in DCIS has been a topic of interest, as it may impact treatment decisions and patient outcomes (Lara et al., 2003). Additionally, patterns of chromosomal alterations in DCIS have been studied to understand the molecular mechanisms underlying the progression of DCIS to invasive breast cancer (Hwang et al., 2004). The prognostic significance of

morphologic features and biomarkers in DCIS has also been investigated to better predict patient outcomes (Cornfield et al., 2004). Some studies have explored the natural history of low-grade DCIS in women treated with biopsy only, revealing the need for long-term follow-up to monitor disease progression (Sanders et al., 2005). The molecular journey from DCIS to invasive breast cancer has been a focus of research to identify potential biomarkers for disease progression (Wiechmann et al., 2008). Furthermore, the malignant nature of human DCIS has been a subject of research to better understand the biology of this pre-invasive lesion (Espina et al., 2010).

1.5.1 Epidemiology

In the UK, approximately 7300 women are diagnosed yearly (Research, 2024; Tomlinson-Hansen et al., 2023). DCIS is often regarded as precursor towards invasive cancer (Peila et al., 2020). A study conducted in England found that ipsilateral DCIS was developed by 7% of women diagnosed with DCIS or invasive malignancy, while 5% developed contralateral DCIS (Shaaban et al., 2021). It accounts for about 15% of all breast cancer diagnoses in the United Kingdom, and as such, its incidence is significant (Timbres et al., 2023). A long-term study in England discovered that if these women underwent a mastectomy, their chances of getting invasive breast cancer would decrease significantly. Also, there was a population-based observational cohort study in England from 1988 to 2014 reviewing the epidemiology of DCIS and its impact on invasive breast cancer and breast cancer mortality outcomes (Chootipongchaivat et al., 2020; Mannu et al., 2020; Oxford, 2024). Understanding the epidemiology of this condition in the

UK is important for developing strategies for prevention and treatment approaches to this early-stage cancer.

1.5.2 Pathogenesis and aetiology

The pathogenesis of DCIS is a complex process involving various genetic abnormalities and biological consequences. Coene et al conducted a study (Coene et al.,1997) to characterize the early genetic abnormalities of chromosome 17q and their correlation with the overexpression of the c-ErbB-2 protein in DCIS. They found a significant association between chromosome 17q abnormalities and the extent of DCIS, highlighting the role of genetic amplification in the pathogenesis of breast cancer. In a study by Yonekura et al (Yonekura et al., 2018), the prognostic impact and pathogenesis of lymph node metastasis in DCIS were investigated. The authors suggested that DCIS with lymph node metastasis can be clinically treated in different stages, with implications for clinical management based on the pathogenesis of nodal metastasis. Furthermore, other studies (Osako et al., 2012 & Osako et al., 2013) explored the incidence of sentinel node micro-metastases and occult invasion in DCIS, respectively. Their findings shed light on the controversial pathogenesis of lymph node metastases in preinvasive breast cancer, emphasizing the importance of understanding the mechanisms underlying nodal metastasis in DCIS. Zhu et al (Zhu et al., 2020) identified key differentially expressed genes and gene mutations in breast DCIS using RNA-seq analysis, providing insights into the molecular mechanisms involved in the pathogenesis of DCIS. Additionally, another study (Wang et al., 2021) analysed hub genes associated with the pathogenesis of breast

cancer progression from DCIS to invasive ductal carcinoma, highlighting the dynamic changes in gene expression during disease progression.

The aetiology of DCIS is not fully understood, but several factors play a role in its development. Mutations in certain genes, such as BRCA1, BRCA2, and others related to cell growth and division, can increase the risk of developing DCIS (Lakhani et al., 2002). Estrogen and progesterone can influence the growth of breast cells. Hormone receptor-positive DCIS indicates that the cells are more likely to grow in response to hormonal stimulation(Allred et al., 2012; Colditz et al., 2004). Lifestyle factors like obesity, high-fat diets, lack of physical activity, and radiation exposure may contribute to the development of DCIS. DCIS begins with the proliferation of abnormal cells within abnormal cells within the breast milk ducts. These cells accumulate genetic changes that allow them to multiply rapidly, forming a mass of abnormal cells (Boyd et al., 2003; Ma et al., 2003; Suzuki et al., 2009).

1.6 Ovarian Cancer

1.6.1 Epidemiology

Ovarian cancer is the seventh most diagnosed cancer worldwide and the eighth most common cause of death in women due to cancer. Even though the incidence is rare, it remains the deadliest form of malignancy (Momenimovahed et al., 2019). Recent statistics from the World Health Organization (WHO) provided that around 140,200 women suffer from this illness every year, and about 225,500 cases will be diagnosed next year. A study shows that 3.6% of ovarian cancers in females have germline BRCA1 mutations, and 3.3% have germline BRCA2 mutations. The risk of ovarian cancer by age seventy is 44% for female carriers of the BRCA1 mutation. If one carries a BRCA2 mutation, then one has a 27% risk of developing ovarian cancer (Lisio et al., 2019).

1.6.2 Pathogenesis and aetiology

Ovarian cancer is a common gynaecologic malignancy and the prime cause of gynaecologic cancer-related death in women. The cause of ovarian cancer has not been fully understood, and early detection and prevention are difficult (Budiana et al., 2019). Recent studies show that high-grade serous ovarian carcinoma (HGSOC), which is the most prevalent type of ovarian cancer, originates from the fallopian tube. Mutations in genes involved in DNA damage repair, such as BRCA1 and BRCA2, are implicated in approximately 50% of HGSOC cases. Furthermore, CCNE1 amplification accounts for about 20% of all these cases, which influences HGSOC tumourigenesis

greatly (Kroeger & Drapkin, 2017). Several risk factors are responsible for ovarian cancer development. These include age-associated increased carcinogenesis, inflammation, lifestyle, reproduction, and sociodemographic factors (Reid et al., 2017; Sanchez-Prieto et al., 2022).

1.6.3 Subtypes of ovarian cancer

Ovarian cancer has four main types, which are epithelial ovarian cancer; germ cell ovarian cancer, sex cord-stromal ovarian cancer, and stromal cell ovarian cancer (**Figure 1-14**) (Chen et al., 2003; Ursu et al., 2022). EOC is the commonest, with approximately 90% of all cases (Hanafy et al., 2023). EOC comprises different subtypes that differ in their histological and molecular characteristics. The most common one is high-grade serous ovarian cancer (HGSOC), which has a poor prognosis. In addition, other frequently occurring ones, such as endometrioid and clear-cell carcinomas, often associated with endometriosis. In addition to these, there are also rarer subtypes like mucinous and low-grade serous ovarian carcinomas (**Figure 1-15**) (Bell, 2005; Karst & Drapkin, 2010).

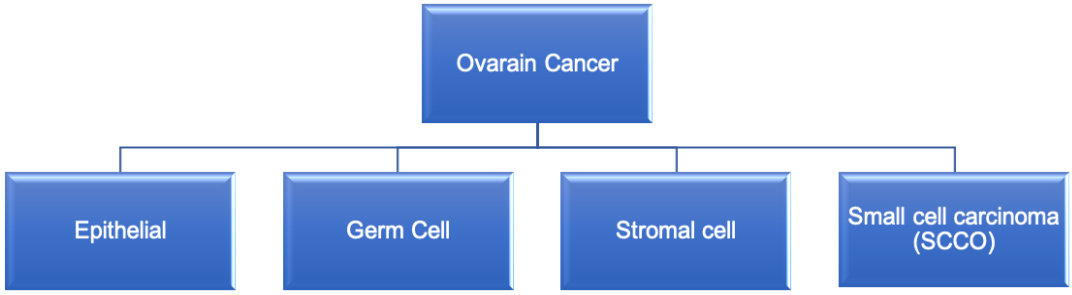

Figure 1-14. Four main cell types of ovarian cancer are classified by Chen et al. (2003). These main types include epithelial tumours, the most common, including high-grade serous, endometrioid, clear cell, and mucinous subtypes, each with distinct molecular features; germ cell tumours, arising from ovarian gametes, such as dysgerminomas and yolk sac tumours; sex cord-stromal tumours, originating from ovarian supporting tissue and including granulosa cell and Sertoli-Leydig tumours; and small cell carcinomas, a rare and highly aggressive type often affecting younger patients (Chen et al., 2003).

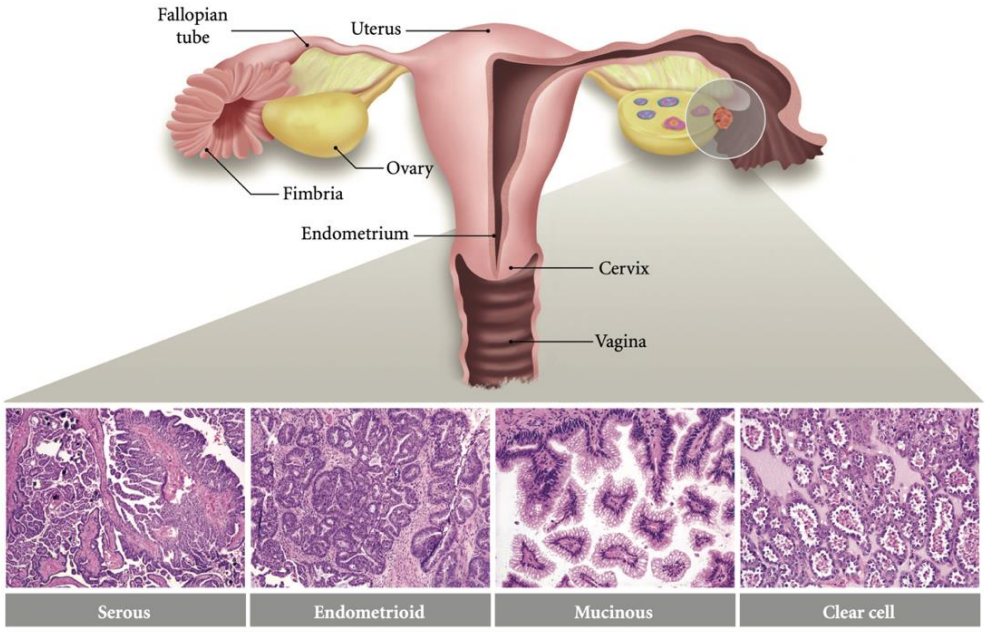

Figure 1-15. Subtypes of epithelial ovarian cancer described by (Karst & Drapkin, 2010). These histological subtypes of EOC include high-grade serous carcinoma (HGSC), the most common and aggressive subtype, frequently involving TP53 mutations; endometrioid carcinoma, associated with endometriosis and mutations in PTEN and ARID1A; clear cell carcinoma, also linked to endometriosis, with PIK3CA and ARID1A alterations; and mucinous carcinoma, characterised by KRAS mutations and rarer occurrence. These subtypes exhibit distinct genetic, molecular, and clinical features, influencing their prognosis and therapeutic response (Karst & Drapkin, 2010).

1.6.4 Ovarian cancer staging

The stage of ovarian cancer is crucial for determining the prognosis and guiding treatment decisions. Ovarian cancer is classified according to the FIGO staging system developed by the International Federation of Gynaecology and Obstetrics. Based on the FIGO 2014 staging system summarised in (**Table 1**), a study (Pereira et al., 2014) evaluated survival outcomes for patients with node-positive epithelial ovarian cancer. Using this system, survival was correlated with the location of peritoneal and extra-abdominal metastases. The revised FIGO staging system can provide patients with prognostic information and personalised management guidance (Javadi et al., 2016). A study (Kandukuri et al., 2014) compared the FIGO 2013 staging system with its predecessor from 1988, highlighting how the criteria have evolved. Another study (Duska et al., 2017) reviewed the clinical implications of updated classification systems for ovarian, fallopian tube, and primary peritoneal cancer. Several innovative approaches have also been investigated for staging ovarian cancer. Using near-infrared-guided surgery to map sentinel lymph nodes on the ovary, (Buddha et al., 2017) present a minimally invasive method for enhancing staging methods using technological advancements. The integration of machine learning techniques into prognostic systems for epithelial ovarian carcinomas has also been investigated by (Grimley et al., 2021). In this study, additional prognostic parameters were added to the conventional FIGO staging system to improve patient stratification and survival evaluation. The literature review of ovarian cancer staging systems emphasizes the importance of accurate classification for treatment decisions and prognostic assessment. A continuous evolution of

staging criteria, as well as the incorporation of new technologies and methodologies, continues to shape ovarian cancer management and research.

Table 1. FIGO staging system for ovarian cancers.

Stage I:	**T1-N0-M0**	**Tumour confined to the ovary.**
IA	T1a-N0-M0	Tumour limited to 1 ovary, no tumour on the surface.
IB	T1b-N0-M0	Tumour involves both ovaries, no tumour on the surface.
IC1	T1c1-N0-M0	Tumour limited to one or both ovaries with surgical spill.
IC2	T1c2-N0-M0	Tumour limited to one or both ovaries with capsule rupture before surgery.
IC3	T1c3-N0-M0	Tumour limited to one or both ovaries with malignant cells in the ascites.
Stage II:	**T2-N0-M0**	**Tumour involves one or two ovaries with pelvic extension.**
IIA	T2a-N0-M0	Extension and /or implant on uterus and fallopian tubes.
IIB	T2b-N0-M0	Extension to other pelvic intraperitoneal tissues.
Stage III:	**T1/T2-N1-M0**	**Tumour involves one or two ovaries.**
IIIA i	T3a2-N0/N1-M0	Positive retro-peritoneal lymph nodes≤10 mm.
IIIA ii	T3a2-N0/N1-M0	Positive retro-peritoneal lymph nodes>10 mm.
IIIA2	T3a2-N0/N1-M0	Microscopic extra peritoneal metastasis≤2cm + positive lymph nodes.
IIIB	T3b-N0/N1-M0	Macroscopic extra peritoneal metastasis>2cm + positive lymph nodes.
IIIC	T3c-N0/N1-M0	Macroscopic extra peritoneal metastasis>2cm + positive lymph nodes with extension to capsule of liver or spleen.
Stage IV:	**Any T, any N, M1**	**distant metastasis excluding peritoneal metastasis.**
IVA	Any T, any N, M1	Pleural effusion with positive cytology.
IVB	Any T, any N, M1	Hepatic or splenic metastasis, metastasis to extra abdominal organs.

1.7 Target Genes

1.7.1 Tumour Suppressor Proteins

The tumour suppressor genes are vital controllers of cellular functions that prevent cancers from occurring. Mutations in these genes are found in ovarian, lung, colorectal, head and neck, pancreatic, uterine, breast, and bladder cancers, among others, leading to the loss of their normal function (Joyce et al., 2024). Many tumour suppressor genes have roles during DNA repair. They rectify DNA damage before replication and transcription, reducing the chances of mutation (Alhmoud et al., 2020). Tumour suppressor genes can trigger programmed cell death or apoptosis in cells with severe DNA damage. Apoptotic process eliminates harmful cancer cells. Cancer is characterised by uncontrolled cell growth due to mutations or inactivation of tumour suppressor genes. Genetic alterations can result from inherited mutations, somatic mutations, or epigenetic modifications. Some prominent examples include TP53 (popularly known as ‘the guardian of the genome’), BRCA1 and BRCA2 genes linked with ovarian cancer and breast cancer, respectively, (Matsuda et al., 2020; Yoshida & Miki, 2004).

1.7.1.1 TP73

TP73, a TP53 protein family member, shares some similarities with the well-known tumour suppressor TP53 in controlling cell growth, apoptosis and tumour suppression (Kaghad et al., 1997; Li & Prives, 2007). Research indicates that TP73 is normally expressed at lower levels in non-cancerous cells but is highly expressed in cancerous ones. Some types of cancer have been associated with TP73 mutations that result in reduced function and

increased chances of getting the disease. TP73 is located on chromosome 1p36.32 (Ichimiya et al., 2000; Luo et al., 2022; Persson et al., 2023). TP73 has several domains including an N-terminal transactivation domain (NTD), a proline-rich region (PR), a DNA-binding domain (DBD), a sterile alpha motif (SAM), and a transactivation-inhibitory domain (TID) found at the C-terminus (Jancalek, 2014; Natan & Joerger, 2012).

TP73 not only interacts with Mdm2 and Mdm4 proteins to modulate TP53 activity and help inhibit tumours through TP53 activation, but it also interacts with other proteins such as p14/ARF, which is part of cell cycle regulators' network as well as the members of the Bcl-2 family, which are involved in regulating apoptosis. TP73 also regulates differentiation processes during cell division and senescence events thus able to control how cells pass these stages apart from regulating the cell cycle progression (Nishida et al., 2018; Stindt et al., 2015).

TP73 is a structural and functional homolog of TP53. However, unlike TP53, TP73 is rarely mutated in solid tumours(DeYoung & Ellisen, 2007; Osterburg & Dotsch, 2022). However, several isoforms can be transcribed from the TP73 locus. These include isoforms generated by alternative splicing in the 5´end including TA, ΔN, Δ Ex2TP73, ΔEx2/3TP73, Δ N´TP73 isoforms or C-terminal splice variants such as α, β, γ, δ, ε, ζ, η, η ∗, η1, and θ isoforms. The isoforms Δ Ex2TP73, ΔEx2/3TP73, and Δ NTP73 partially or entirely lack the transactivation domain and can have a dominant negative effect over the TA isoform. The ΔNTP73 isoforms along with ΔN, constitute the so called DN isoforms. Previous studies have shown that the TATP73 isoform is a tumour

suppressor but ΔNTP73 is oncogenic (Candi et al., 2014; Kong et al., 2023; Li & Prives, 2007; Maas et al., 2013; Vikhreva et al., 2018). Whereas total TP73 knockout mice show developmental abnormalities, TP73+/- heterozygous mice are prone to develop cancers. Moreover, TATP73−/− mice also show an increased susceptibility to cancer but ΔNTP73−/− mice do not (S. Logotheti et al., 2021; Oswald & Stiewe, 2008; Rozenberg et al., 2021; Rufini et al., 2011; Stiewe & Pützer, 2002). These data suggest complex biological functions for various isoforms of TP73. TP73 isoforms can form diverse protein–protein interactions with many nuclear (such as MDM2, YAP1, CDK complex, WT1, Sp1, MCL1, SUMO1, PTEN, MM1 and others) and cytoplasmic proteins (such as NGFR, PKP1, KCK, NEDL2, amphiphysinIIb-1 and others) to accomplish various biological functions. Although complex, the overall biological effect of TP73 isoforms is influenced by the TA/DN isoform ratio as opposed to the overexpression of a specific TP73 isoform or a specific class of TP73 isoforms in cells (Diaz et al., 2010; Irwin & Miller, 2004).

In cancers, TP73 is involved in genomic instability, pro-proliferative signalling, evasion of growth suppression, activation of invasion & metastasis, angiogenesis, immune evasion, altered cellular energetics, neo-neurogenesis and influence response to cytotoxic therapy. TP73 dysregulation has been reported in solid tumours. In breast cancer cell lines, TP73 transcripts are overexpressed. In human breast tumours, small reports suggest higher levels of TP73 in breast cancer tissue compared to normal breast tissue. However, the clinicopathological significance of TP73, in contrast to TP53, in breast cancer and ovarian cancer is largely unknown

(Dominguez et al., 2001; Duijf et al., 2019; Rodríguez et al., 2018; Schwartz et al., 1999).

1.7.2 DNA Polymerases

New DNA strands are synthesized during replication and DNA repair by DNA polymerases. DNA polymerases maintain the faithful copying of genetic information. Prokaryotes have well-known examples like DNA polymerase I, DNA polymerase III, and DNA polymerase II, while there are eukaryotic ones such as DNA polymerase α, δ, and ε. To accurately transmit hereditary information and repair damaged chromosomes, one must call upon specific enzymes. These enzymes play a crucial role in cellular growth and duplication. Genetic disorders, including cancer, can arise due to mutations in the genes that encode these enzymes. Therefore, therapeutic interventions should focus on this enzyme group. (Berdis, 2017; Garcia-Diaz & Bebenek, 2007; Strauss & Pursell, 2023).

1.7.2.1 DNA Polymerase Epsilon (POLE)

DNA Polymerase Epsilon (POLE) is a crucial enzyme for nuclear DNA replication in eukaryotic cells. This multi-subunit enzyme complex plays a central role in maintaining genomic stability and ensuring high fidelity during DNA replication. POLE is composed of four subunits, and it was identified in HeLa cell extracts with an approximate molecular weight of 260 kDa (Pospiech and Syvaoja, 2003). The POLE gene encodes the core catalytic subunit in humans and contains both the polymerase and exonuclease functions. The other subunits are POLE2 (the exonuclease subunit), POLE3, and POLE4. In yeast, these subunits are analogous to Pol2 (catalytic and

exonuclease), Pol12, and Dpb2. The catalytic subunit is involved in DNA polymerization, while the exonuclease subunit provides proofreading functions to correct errors during replication. POLE predominantly operates during the elongation phase of DNA replication, particularly contributing to synthesising the leading DNA strand. It is also involved in DNA repair mechanisms, particularly in the repair of double strand breaks and genetic recombination, thus safeguarding the integrity of the genetic code. Mutations within the exonuclease domain of POLE are significant because they can lead to high levels of single nucleotide substitutions and microsatellite stability, contributing to the development of cancers. For instance, such mutations account for 3% of colorectal cancers and 7% of endometrial cancers (Henninger & Pursell, 2014). These mutations fail to correct replication errors, leading to genomic instability and cancer progression. Several studies have demonstrated that alterations in the POLE gene can lead to an increase in neoantigen load, an increase in the number of lymphocytes circulating in tumours, and a potential response to immune therapy (Imboden et al., 2019). POLE's role in proofreading during DNA replication makes it a target for cancer therapies. Drugs designed to target POLE can be valuable in treating malignancies, including some solids such as melanoma, which may arise due to defective proofreading capabilities. Furthermore, gene therapy strategies could be developed to interfere with POLE's interactions with specific binding partners, disrupting its function and potentially inhibiting cancer growth. The multifunctional nature of POLE is highlighted by its distinct domains: the C-terminal zinc finger domain (ZF1) and the N-terminal region. The N-terminus recruits GHKL ATPase MORC1,

enhancing heterochromatin condensation, while ZF1 recognizes histone variants like H3K9me3-H4K20me2/3, promoting chromatin compaction through Polycomb-mediated trimethylation marks (Rousseau et al., 2022; Xing et al., 2022). Depletion of the non-catalytic domain of POLE1, located at its N-terminus, leads to a failure of DNA synthesis during replication initiation (Wang et al., 2022). Mutations in POLE can lead to significant genomic instability and cancer, making it a critical target for cancer research and therapeutic interventions. Understanding POLE's structure and functions enhances our ability to develop strategies to combat cancers associated with its mutations.

1.8 Hypothesis

Hypothesis (1)

Overexpression of TP73 (p73), has been strongly associated with tumour progression, chemoresistance, and poor prognosis in breast and ovarian cancers. Elevated TP73 levels may disrupt apoptotic pathways, promoting cell survival and increasing resistance to DNA-damaging agents such as platinum-based chemotherapy, especially in aggressive cancer subtypes. This makes TP73 a potential marker for predicting patient outcomes and therapeutic responses. The hypothesis that TP73 drives these oncogenic effects could be tested by evaluating the impact of TP73 overexpression on apoptosis, cell survival, and chemoresistance in breast and ovarian cancer models by correlating TP73 expression levels with clinical outcomes and treatment efficacy in patients. Understanding this relationship may provide insights into overcoming resistance and improving the effectiveness of cancer therapies.

Hypothesis (2)

High expression of DNA Polymerase Epsilon (POLE) in ovarian and breast cancers is associated with increased DNA replication fidelity and repair capacity, leading to enhanced tumour cell survival and resistance to chemotherapy. POLE overexpression may also contribute to genomic stability in cancer cells, facilitating tumour progression and poor clinical outcomes, particularly in subtypes with aggressive features.

This hypothesis can be tested by assessing the levels of POLE expression in tumour samples, evaluating its impact on DNA repair mechanisms and

chemotherapy resistance, and analysing patient outcomes about POLE expression across ovarian and breast cancer subtypes.

1.9 COVID-19 Impact statement

The COVID-19 pandemic significantly impacted this research. The nationwide lockdown, which began in March 2020, led to the closure of laboratories for five months, delaying research activities until August 2020. Even after reopening, progress remained slow due to reduced laboratory capacity, the enforcement of social distancing, and disruptions to supply chains. Although some challenges were mitigated, the circumstances limited the research to theoretical problem-solving, thereby restricting the practical, "hands-on" aspects of experimental studies. As a result, there were compromises in replicating experiments, particularly concerning the rigorous requirements for hypothesis testing. Given these constraints, we had to reduce the number of planned experiments, despite the original plan to conduct each experiment three times.

1.10 Aims of the Project

TP73:

1- To characterise the molecular mechanisms by which TP73 overexpression, contributes to tumour progression in ovarian and breast cancers.

- This aim focuses on understanding how TP73 regulate cell cycle, apoptosis, and DNA damage response pathways that drive cancer development.

2- To evaluate the impact of TP73 overexpression on chemoresistance, particularly to platinum-based therapies, in ovarian and breast cancer models.
   - This goal involves assessing whether elevated levels of TP73 are linked to resistance to DNA-damaging agents and exploring how targeting TP73 could improve therapeutic outcomes.
3- To determine the clinical significance of TP73 overexpression as a prognostic marker in ovarian and breast cancer subtypes.
   - This aim seeks to correlate TP73 expression with patient outcomes, tumour aggressiveness, and survival, potentially identifying TP73 as a biomarker for high-risk cancer patients.
4- To explore the therapeutic potential of targeting TP73 overexpression in combination with DNA repair markers to overcome drug resistance in ovarian and breast cancers.
   - This goal will investigate the efficacy of novel treatment strategies targeting TP73 in conjunction with other therapies, aiming to enhance sensitivity to chemotherapy and improve patient survival.

POLE:

1- To investigate the role of DNA Polymerase Epsilon (POLE) expression in regulating DNA replication and repair in ovarian and breast cancers.
   - This aim focuses on elucidating how POLE expression impacts genomic stability, replication fidelity, and the maintenance of cancer cell proliferation in these malignancies.

2- To assess the relationship between high POLE expression and chemo-resistance in ovarian and breast cancers, particularly to platinum-based therapies.

- This goal involves determining whether elevated POLE expression contributes to resistance to DNA-damaging agents and exploring POLE as a potential target for sensitizing cancer cells to chemotherapy.

3- To evaluate the prognostic significance of POLE expression in ovarian and breast cancer patients.

- This aim seeks to analyse whether POLE expression levels correlate with tumour aggressiveness, progression, and patient outcomes, identifying POLE as a potential biomarker for prognosis.

4- To explore the therapeutic potential of targeting POLE in combination with DNA repair inhibitors for the treatment of ovarian and breast cancers.

- This goal aims to assess whether inhibiting POLE function, in conjunction with DNA repair pathway inhibitors, can improve the efficacy of existing therapies and overcome drug resistance in these cancers.

Chapter 2 Materials and Methods

2.1 Materials

2.1.1 Cohort of study

2.1.1.1 Breast Cancer

TP73 and POLE expression was evaluated in a large cohort of 4221 cases of invasive BC collected from 1986 and 2006 at Nottingham University Hospitals (NUH), and their demographic data is summarised in (**Table 2**). All patients received standard surgery, including mastectomy or wide local excision, followed by radiotherapy. Anti-cancer treatment (Collaborative Group on Hormonal Factors in Breast) had not started yet before 1989. Previously, AT with respect to NPI score had been scheduled individually since this date using prognostic factors like oestrogen receptor-α status (ER-α), NPI and menopausal status. Patients with low-risk scores on the NPI scale (<3.4) did not receive AT.CMF regime was administered to high-risk premenopausal women with ER-α negative tumours; alternatively, they were treated with classical CMF chemotherapy plus HT if ER- α positive tumour. Postmenopausal patients who scored ≥3.4 on their NPI test results but whose tumours were ER- α positive received hormone therapy only, while others underwent a classical cyclophosphamide-methotrexate-fluorouracil chemotherapy regimen. The median follow-up time was about 111 months (range:1-233 months). Survival information, such as breast cancer-specific survival (BCSS), locoregional, and distant metastases (DM), was collected prospectively. BCSS was defined as the number of months from diagnosis to

death from breast cancer. DM-free survival is the time that elapses from the day of diagnosis to when DM recurs.

The Ethics approval for this cohort study was obtained from North-West–Greater Manchester Central Research Ethics Committee (NHSB-North Health Science Biobank), reference number 15/NW/0685. All patients' tissues used in research, including tumour material during surgery, were provided with informed consent forms. All samples used in this study were pseudo-anonymised, collected before 2006, and stored in compliance with the UK Human Tissue Act. Patients gave written informed consent in all cases. Throughout this study, we adhered strictly to Reporting Recommendations for Tumour Marker Prognostic Studies (REMARK) criteria, as advised by (McShane et al., 2006).

Table 2. ***Demographics of invasive breast cancer (IBC)***

Parameters	N %
Tumour size	
< 2cm	852 (58%)
≥ 2cm	628 (42%)
Grade	
1	253 (17%)
2	549 (37%)
3	678 (46%)
Tubular formation	
1	119 (8%)
2	456 (31%)
3	905 (61%)
Pleomorphism	
1	44 (3%)
2	500 (34%)
3	936 (63%)
Mitosis	
1	647 (44%)
2	294 (20%)
3	539 (36%)
HistologicalTumourType	
No Special Type (NST)	923 (62%)
Lobular	132 (9%)
Other special types	73 (5%)
NST mixed	352 (24%)
Lymphovascular Invasion	
Absent	1040 (70%)
Present	440 (30%)
Lymph Node status	
Negative	937 (63%)
Positive	543 (37%)
Nottingham Prognostic Index	
Good prognostic group	491 (33%)
Moderate prognostic group	769 (52%)
Poor prognostic group	220 (15%)
ER Status	
ER-	347 (24%)
ER+	1128 (76%)
PgR Status	
Negative	601 (41%)
Positive	857 (59%)
HER2 Status	
Negative	1264 (86%)
Positive	199 (14%)
Ki67 index	
Low	533 (48%)
High	580 (52%)
Molecular Classes	
Luminal A	478 (38%)
Luminal B	442 (36%)
HER2+	87 (7%)
Triple negative	235 (19%)
Menopausal Status	
Premenopausal	540 (36%)
Postmenopausal	940 (64%)
Age 50 Years	
< 50	481 (32%)
≥ 50	999 (68%)

2.1.1.2 Ductal carcinoma in situ (DCIS) cohort.

The study examined TP73 and POLE expression in a cohort of 776 patients with pure non-invasive ductal carcinoma in situ (DCIS) diagnosed between 1987 and 2012. The patients were identified from the Nottingham University Hospitals National Health System (NHS) database, and their demographic information is summarized in **(Table 3)**. Haematoxylin and eosin (H&E) staining was used to assess the samples, enabling the selection of representative tissue areas and avoiding haemorrhagic and necrotic tumour zones. High-resolution digital scanning of the slides was performed at 20x magnification using a PANORAMIC 250 FLASH III slide scanner from 3DHISTECH. Formalin-fixed paraffin-embedded (FFPE) tissue blocks for the pure DCIS cases were retrieved and evaluated to select representative blocks for constructing Tissue Microarrays (TMAs). Additionally, a cohort of 239 cases of invasive breast cancer (IBC) with a DCIS component diagnosed between 2000 and 2007 was identified and included in the study. The suitable blocks from these cases were assessed with H&E staining and retrieved for inclusion in the study. Furthermore, 50 normal breast tissues were identified from the NHS database and included in the study for comparative purposes with the DCIS cohort.

Table 3. ***Demographics of ductal carcinoma in situ (DCIS)***

Categories	N (%)
Age at time of diagnosis	
<50	87 (27%)
≥50	230 (73%)
Tumour size	
≤2cm	133 (42%)
>2cm	181 (58%)
Tumour grade	
Low grade	47 (15%)
Intermediate grade	85 (27%)
High grade	185 (58%)
Molecular subtype	
Luminal A	128 (54%)
Luminal B	44 (19%)
HER2 enriched	37 (16%)
Triple Negative	27 (11%)
Comedo type necrosis	
Absent	113 (36%)
Present	204 (64%)
ER Status	
Negative	68 (25%)
Positive	207 (75%)
PR Status	
Negative	115 (42%)
Positive	160 (58%)
HER2 Status	
Negative	226 (78%)
Positive	64 (22%)
Recurrence	
No recurrence	279 (88%)
Recurrence	38 (12%)
Ki67 expression	
Low (≤14)	192 (76%)
High (>14)	60 (24%)

2.1.1.3 Epithelial Ovarian Cancer

TP73 and POLE expression was assessed in 331 consecutive cases of epithelial ovarian cancer treated at Nottingham University Hospitals between 1997 and 2010. The International Federation of Obstetricians and Gynecologists Staging System for Ovarian Cancer determined the tumour stage. Tumour histology type, International Federation of Obstetricians and Gynecologists stage, grade, and chemotherapy regimen were included in the clinicopathological data. During first-line platinum chemotherapy, all patients developed progression or relapsed after 6 months, so data on platinum sensitivity/resistance were extracted from hospital computer systems and electronic patient records were analysed to retrieve tumour relapse information along with survival status (Alabdullah et al., 2021). Overall survival (OS) was calculated from the day of diagnosis or date of initiation of treatment to the date of death or last follow-up. Survival time between treatment initiation and progression was defined as progression free survival (PFS). (**Table 4**) shows the demographics and pathological characteristics of patients with EOC. The Nottingham Research Ethics Committee granted research ethics approval (REC Approval Number 06/Q240/153) to establish this ovarian cohort.

Table 4. ***Demographics of epithelial ovarian cancer***

Parameters	N (%)
Menopausal Status	
Pre-menopausal	17 (6%)
Peri-menopausal	16 (6%)
Post-menopausal	243 (88%)
Age at Surgery class	
<30	3 (1%)
31 to 60	120 (43%)
>61	155 (56%)
Surgical Pathology Type	
Serous	158 (57%)
Mucinous	41 (15%)
Endometriod	32 (12%)
Clear Cell	20 (7%)
Other	13 (4%)
Mixed	14 (5%)
Surgical Pathology Grade	
Low	39 (16%)
Intermediate	49 (20%)
High	155 (64%)
Surgical Pathology Stage	
1	107 (40%)
2	37 (14%)
3	116 (43%)
4	8 (3%)
Surgical Pathology Substage	
A	54 (26%)
B	28 (13%)
C	128 (61%)
Residual Tumour Following Surgery	
Non	176 (70%)
<1cm	28 (11%)
1-2cm	13 (5%)
>2cm	34 (14%)
Platinum Sensitivity	
Sensitive	215 (92%)
Resistant	20 (8%)

2.1.2 Primary Antibodies

Table 5. A list of primary antibodies used.

Name	Type	Incubation time	Concentration	Company	Clone
Anti-TP73	**Rabbit**	**4 C Over-night**	**1:5000**	**Abcam**	**Ab189896**
Anti-POLE	**Rabbit**	**1h RT**	**1:1000**	**Abcam**	**Ab226848**
Anti-TP53	**Mouse**	**4 C Over-night**	**1:1000**	**Cell signal**	**mAb48818**
Anti- Beta-actin	**Mouse**	**1h RT**	**1:5000**	**Abcam**	**Ab8226**
Anti- GAPDH	**Rabbit**	**1h RT**	**1:3000**	**Abcam**	**Ab9485**
Anti- YY1	**Rabbit**	**1h RT**	**1:2000**	**Abcam**	**Ab109228**
Anti-ERCC6	**Rabbit**	**4 C Over-night**	**1:500**	**Thermo**	**PA5-120625**
Anti-MLH1	**Mouse**	**4 C Over-night**	**1:500**	**Thermo**	**MA5-15431**
Anti-PMS1	**Mouse**	**4 C Over-night**	**1:1000**	**Thermo**	**PA5-86724**
Anti-XPA	**Rabbit**	**4 C Over-night**	**1:2000**	**Abcam**	**Ab85914**

RT = room temperature.

2.1.3 Compounds

The pharmacy at Nottingham University City Hospital (Nottingham, UK) supplied a 3.3 mM cisplatin solution, which was stored at room temperature.

2.1.4 Cell Line and Culture Media

ATCC (American Type Culture Collection) cell lines were obtained and cultured according to ATCC instructions. **Table 6** and **Table 7** shows the characteristics and culture media of each cell line. To ensure that the cell lines were not cross-contaminated or misidentified, ATCC used the Promega Power plex® 17 short tandem repeat (STR) system to authenticate them. A routine mycoplasma detection kit (R&D Systems; Abingdon, UK) was used to detect mycoplasmas monthly. Experimental cell lines were passaged up to 16 times before being terminated.

Table 6. A list of Ovarian cell lines has been used.

Cell line	Features	Culture media
A2780	Human ovarian carcinoma, endometrioid isolated from primary tumours of an untreated patient	RPMI (1640) +10% FBS + 1% penicillin/streptomycin
A2780cis	Cisplatin-resistant cell line developed by continuous exposure of A2780 cells to doses of cisplatin	RPMI (1640) +10% FBS + 1% penicillin/streptomycin
PEO1	Isolated from malignant effusion from peritoneal ascites of a patient with very poorly differentiated serous adenocarcinoma with a BRCA2 mutation 5193C>G (Y1655X)]	RPMI (1640) +10% FBS + 1% penicillin/streptomycin
PEO4	Derived from the same patient as PEO1 cells after the patient developed resistance to platinum chemotherapy due to restoration of the BRCA2 mutation	RPMI (1640) +10% FBS + 1% penicillin/streptomycin
OVCAR-4	a high-grade serous ovarian adenocarcinoma, a cell line established from a patient refractory to cisplatin, and is resistant to multiple chemotherapeutic agents	RPMI (1640) +10% FBS + 1% penicillin/streptomycin

Table 7. A list of Breast cell lines has been used.

Cell line	Features	Culture media
MCF7	Isolated from the breast tissue of a 69-year-old, white, female patient with metastatic adenocarcinoma.	RPMI (1640) +10% FBS + 1% penicillin/streptomycin
MDA-MB-231	Isolated from the breast tissue of a 51-year-old, white, female patient	RPMI (1640) +10% FBS + 1% penicillin/streptomycin
MCF10-A	Isolated in 1984 from the mammary gland of a white, 36-year-old female	DMEM-F12 +10% horse serum + insulin + cholera toxin+ epidermal growth factor (EGFR) + hydrocortisone + 1% penicillin-streptomycin
DCIS	Ductal carcinoma in situ	DMEM-F12 +10% horse serum + insulin + cholera toxin + EGFR + hydrocortisone +1% penicillin-streptomycin
T47D	The epithelial cells were obtained from a pleural effusion of a 54-year-old female with infiltrating ductal carcinoma of the breast.	RPMI (1640) +10% FBS + 1% penicillin/streptomycin

2.2 Methods

2.2.1 Tissue Microarray (TMA) and Immunohistochemistry (IHC)

Immunohistochemistry (IHC) is an antibody-based method used for research and diagnostic purposes to classify protein activity in tissue that conserves its structure and organization. Coons et al., who documented the discovery of a fluorescently associated antibody representing pneumococcal bacteria, first recorded IHC usage in 1942. IHC has since become an important tool in diagnosing and researching various medical conditions. It has also been used to identify cancerous cells, allowing doctors to diagnose and treat cancer. Furthermore, IHC can be used to study the effects of drugs on cells, tissues, and organs. (Oumarou Hama et al., 2022; Technology, 2020). Both in scientific testing laboratories and clinical settings, it is commonly used to detect antigens in biological samples. This type of technique is based on an antibody specifically designed to recognise epitopes in the target cell or tissue (Denmark, 2013). Optimisation of this specific binding arrangement is necessary to achieve the desired results.

Tissue Microarrays (TMAs) were placed in neutral-buffered formalin, which prevents diffusion issues and is embedded into the paraffin block. Staining was carried out on 4mm thick samples. Immunohistochemical staining was performed using Novolink Max Polymer Detection System (RE7280-K: 1250 tests) and Leica Bond Primary Antibody Diluent (AR9352), both prepared according to the manufacturer's instructions (Leica Microsystems).

Five decreasing alcohol concentrations (100%, 90%, 70%, 50% and 30%) were used to rehydrate the tissue slides after deparaffinization with xylene. Pre-treatment of TMA sections with sodium citrate buffer (pH 6.0) and microwave heating at 95°C for 20 minutes (Whirlpool JT359 Jet Chef 1000W). For 5 minutes, the slides were cooled down with tap water and dried. After that, an ImmeEdgeTM pen (H-4000) was used to make hydrophobic barriers on the TMA cores. The slides were then rinsed in TBS-Tween (500 mL of 1X TBS pH 7.6 with 500 µL of Tween 20), blocked for 5 min in Peroxidase Block (Novolink Max Polymer DS (1250) - RE7280-CE, Lecia, US), washed three times for five minutes each time with TBS-Tween before incubating them at room temperature for one hour with rabbit monoclonal TP73 (dilution 1:500), rabbit polyclonal POLE (dilution 1:100), and mouse monoclonal T53 [clone DO-7] (dilution 1:100) primary antibodies diluted in BONDTM antibody diluent (AR9352, Lecia, US) at optimised staining time (All antibodies details in **Table 5**). The next steps included washing the slides in TBS-Tween (3 × 5 min), adding post-primary (300 µL) for thirty minutes, after which washing was done using TBS-Tween (3 × 5 min); polymer (300 µL) was added for thirty minutes, and all slides were washed using TBS-Tween (3 × 5 min). DAB working solution was made up by mixing DAB chromogen with DAB substrate buffer at a ratio of 1:20. After adding it to the slides for five minutes; they were washed with TBS-Tween (3 × 5 min), counterstained using Hematoxylin for six minutes followed by dehydration as per Leica autostainer protocol. Mounting media-covered samples on the slide were placed under coverslips and allowed to dry overnight inside a fume hood.

2.2.2 Optimization of Primary Antibodies

The TMA slides were incubated with at least four different concentrations of each antibody to optimize them. The concentrations were selected based on the providers' recommendations.

The TP73 antibody's specificity was studied by applying positive and negative controls to test it. There is no staining in the negative control TMA sections stained without the TP73 antibody. For one hour, 1:500, 1:1000, 1:1500 and 1:2000 dilutions of TP73 antibody were tested. After one hour of incubation at a dilution of 1:500, there was optimal staining characterised by clear nuclear coloration with no background staining observed. Western blotting also confirmed that TP73 has high specificity in cell lysates from four ovarian and breast cell lines.

Positive and negative controls were used to assess the POLE antibody's specificity. No staining was observed in negative control TMA sections, without the POLE antibody applied. One-hour treatments for optimization included checking the activity of POLE antibodies at various dilutions such as 1:50, 1:100, 1:200 and 1:500 Dilutions. The optimal staining was seen at a 1:100 dilution following one-hour exposure. This showed a very clear nuclear staining without background stains. Also, western blotting has been done on lysates from breast and ovarian cell lines to test for their specificities concerning this antibody.

As a next step, full-face slides were stained with each antibody, and the staining was confirmed as homogeneous to ensure the TMA is valid for studying this antibody as shown in (**Figure 2-1**).

A.

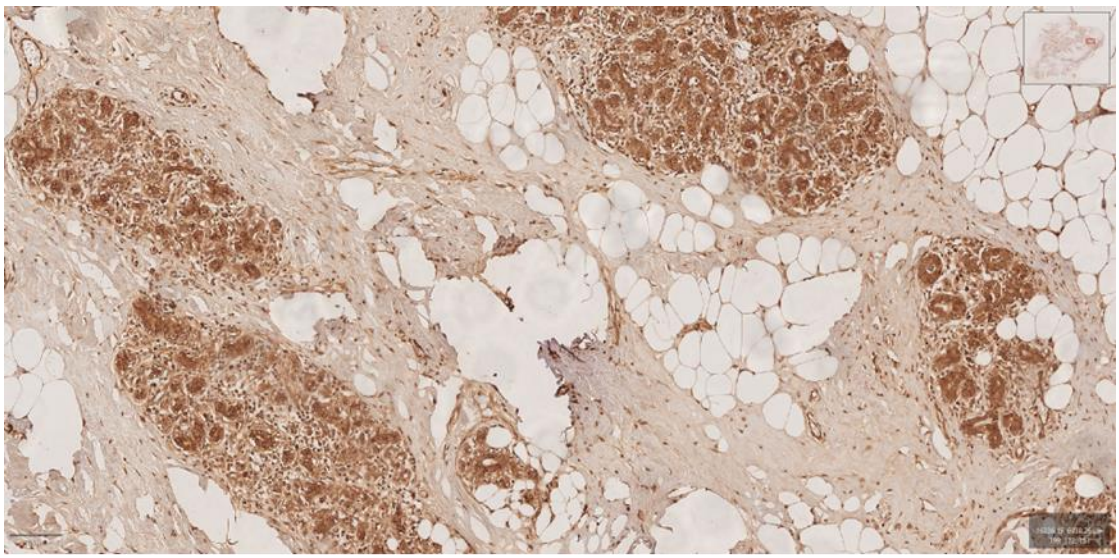

B.

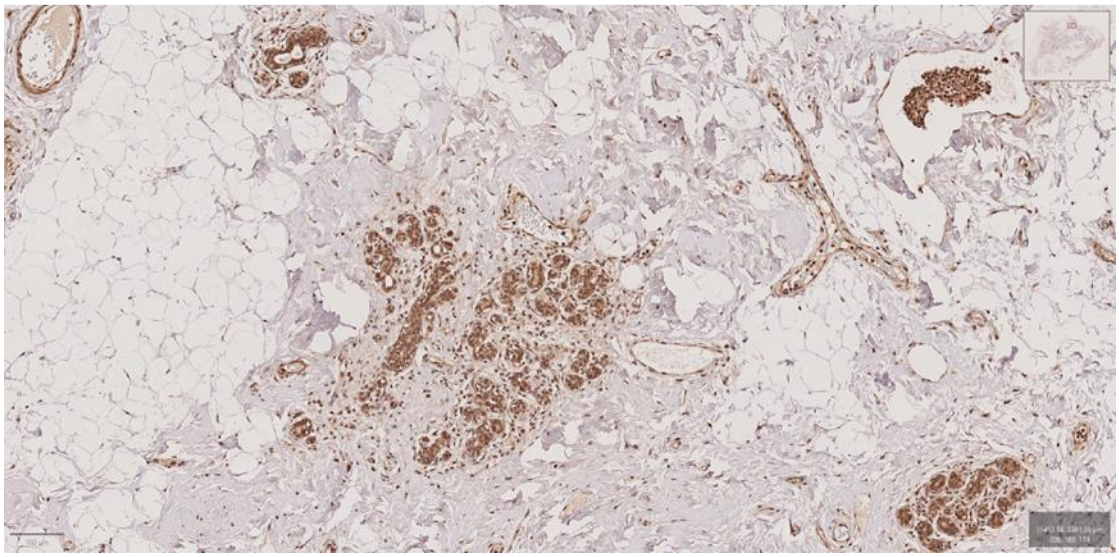

Figure 2-1. A. Full-face sections of breast cancer. Staining showed an even distribution of TP73 protein expression, which indicated the suitability of TMA to assess TP73 protein expression. B. Full-face sections of BC showed an even distribution of POLE protein expression, which indicated the suitability of TMA to assess POLE protein expression.

2.2.3 Evaluation of immunohistochemical staining

In a whole field inspection of the core, each marker was mapped to its sub-cellular location (nuclear, cytoplasm, cell membrane). The intensity of subcellular compartments was assessed and categorized as follows: 0 = no staining, 1 = weak staining, 2 = moderate staining, 3 = strong staining. In each category, tumour cell percentages were estimated (0–100%). The histochemical score (H-score) (range 0–300) is calculated based on the intensity and percentage of staining. Based on each marker's scoring system, a specific cut-off point can be determined.

2.2.4 Cell Line sub-culture

Cell lines were cultured at 37°C in 5% CO2/95% air. Each cell line was handled separately under sterile conditions using its respective reagents. To trypsinise the cells, the cell media was removed using pipetting, and the cells were washed with PBS (without Mg2+ and Ca2+). Then, 0.5 mg/mL trypsin-EDTA (Sigma Aldrich) was added to disrupt the cells' monolayers. The mixture was incubated at 37oC for 3-5 minutes, followed by adding fresh media (4:1 to trypsin) to deactivate the enzyme by dissolving the trypsin. The cell suspensions were centrifuged at 1000 rpm for 5 minutes, and the pellets were resuspended in fresh media and mixed well. An aliquot of the mixture was added to another flask, and the same procedure was followed for incubation.

2.2.5 Cryopreservation of Cell Lines

A cryopreservation method was used to preserve cells with passage numbers below 16. Cells were collected after trypsinisation. Cells were resuspended in 1 mL of cell line-specific media + 10% DMSO (9:1) and stored at -80°C in a freezing container (CLS432000-1EA, Sigma Aldrich). Cells were placed in liquid nitrogen the next day so they could be stored for a long time.

2.2.6 Preparation of Cell Lysates

By following the protocol previously described, samples were collected, counted, and lysed in RIPA buffer (R0278-500 mL, Sigma Aldrich), cocktail 2 (P5726-1 mL, Sigma Aldrich), and cocktail 3 (P0044-1 mL, Sigma Aldrich) with a protease inhibitor. Initially, the lysates were incubated on ice for 30 minutes, followed by vigorous agitation for 15 minutes. To remove cell debris, the lysates are centrifuged at full speed at 4°C for 12 minutes. Supernatants will be stored at -20°C for future use.

2.2.7 Cell Lysate Protein Quantification (BCA Assay)

Protein levels in cell lysates were quantified by the Pierce ™ BCA Protein Assay kit (Thermo Fisher 23225). Cu+ chelation is produced by decreasing proteins under alkaline conditions. This water-soluble, purple substance [Cu(I)BCA2]3- absorbs 562 nm of light intensely linearly. As a comparison, a serial dilution of BSA was developed using albumin ampules (2 mg/mL) and nuclease-free water (NFW), with 8µL of each dilution placed on a 96-well microplate. 8µL NFW of 4 wells have been used as blank sources. The lysates were packed with a dilution ratio of 1:5; each lysate well was packed with 8µL of diluted lysate.

BCA Working Reagent (WR) was developed by applying a 1:50 ratio of BCA Reagent A (BCA, Na2CO3, NaHCO3 and 0.1 M NaOH solution) to BCA Reagent B (4% CuSO4 solution). 200µL (WR) was inserted and incubated in each well at 37oC for 30 minutes. The microplate was cooled to room temperature (RT) and then placed into the plate reader to test 562 nm light absorbance. To remove residual absorbance, the null normalised estimate was subtracted from the survey averages and BSA levels. A typical curve, the concentration of proteins versus absorbance, was plotted using BSA absorbance to assess the concentration of sample proteins (µg/µL).

2.2.8 Bis-Tris (4-12%) Mini Gels Western blot

Bis-Tris (4-12%) and Tris-Acetate (3-8%) Mini Gels have been used to observe the band pattern at each antibody's molecular weight. Following the BCA protein assay protocol, a constant amount of protein (20 ug) must be prepared, labelled, and placed in microtubes for every sample. Using a ready-made SDS (4X) buffer, which was prepared by dividing the sample protein by 4 and adding a (10X Dithiothreitol DTT) reducing agent, which was prepared by dividing the sample protein by 9, the sample protein was then mixed together. The mixture was then scaled up with deionised water until the volume reached the target volume.

Samples should be heated for 5 minutes at 95°C, cooled for 5 minutes at 4°C, and then centrifuged for 3 minutes at 13,000 RPM. This is in order to minimise the amount of residual material. The 15-well mini-gel should be placed in the mini-gel tank and subsequently filled with 1x MES Running buffer containing antioxidants up to the line above the chamber of the gel. Once the protein ladder is loaded into the first well, add the right quantity to each well, then continue loading the rest of the samples. Put the lid on carefully and plug in the socket at 160V for 1 hour.

This will allow protein separation according to molecular weight. Once the gel has run for the required time, transfer the gel safely to the nitrocellulose membrane. Follow the steps of the western blot setup. During this stage, the arrangement and handling of the blot module should be considered; once done, set the blot module at 30 V for one hour and thirty minutes to allow the proteins to transfer into it. Immediately after the transfer time has ended,

immerse the membrane in a blocking solution (5% skimmed milk diluted with 0.1% PBST) for 1 hour at room temperature.

Following the application of the blocking solution, the primary antibody's dilution concentrations and incubation periods should be determined by the manufacturer. Housekeeping antibodies can be used as loading controls, along with specific dilution concentrations. These antibodies include GAPDH (Glyceraldehyde 3-phosphate dehydrogenase) with a molecular weight of 38 kDa and beta-Actin with a molecular weight of 42 kDa. Upon completion of the incubation period, wash three times with 1%PBST for five minutes each, and then incubate the secondary antibodies at room temperature for an hour with aluminium foil covering them because they are light sensitive. Use the manufacturer's dilution recommendations along with the identification of whether the antibody is anti-mouse or anti-rabbit to determine the dilution concentration. The nitrocellulose membrane needs to be washed three times with 1% PBST for five minutes each, and then it is ready for analysis by the LI-COR Odyssey.

2.2.9 NE-PER™ Nuclear and Cytoplasmic Extraction

Cell cultures can be separated and prepared gradually by NE-PER™ Nuclear and Cytoplasmic Extraction Reagents (Thermo Scientific 78833). 2 x 106 cells were seeded into T25 flasks, cultured overnight, and treated with 1-5 uM of cisplatin for 24 or 48 hours. After trypsinising the cells, we centrifuged them at 1000 rpm for 5 minutes at room temperature and transferred them to 1.5 mL Eppendorf tubes. Cold PBS was used to wash the cells, and the PBS was carefully discarded, leaving the pellets dry. Afterwards, the cells were vortexed vigorously in 200 µL of CER I for 15 seconds. Then, after incubation on ice for 10 minutes, 11 ul of cold CER II was added. The cells were vortexed vigorously for 5 seconds. Immediately after incubation on ice for 1 minute, vortexing for 5 seconds was followed by centrifugation at maximum speed for 5 minutes. Upon obtaining the cytoplasmic extract, the tubes are placed on ice until they are stored at -80°C for storage. Following the previous step, re-suspend the remaining cell pellets in 100 ul of cold-NER reagent and vortex for 15 seconds, then place them on ice for 40 minutes, vortexing continuously every 10 minutes. As a result, the samples were centrifuged at maximum speed for 10 minutes. After the nuclear extracts were collected, the samples were transferred into clean tubes and stored at -80°C until needed.

2.2.10 Next-Generation Sequencing (NGS)

Pre-clinically, next-generation sequencing was performed in two sets of ovarian cell lines. Platinum sensitive (PEO1, A2780) and resistant (PEO4, A2780cis) ovarian cancer cell lines (**Figure 2-2)**.

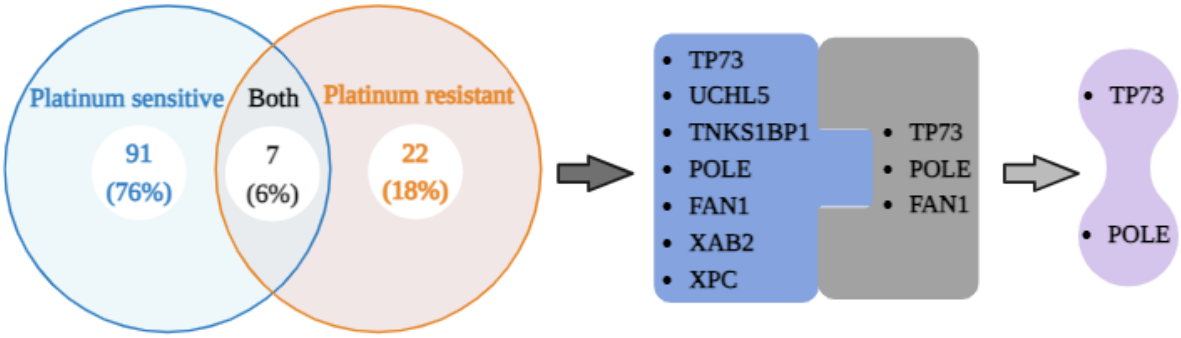

Figure 2-2. Whole-exome sequencing (WES) gene expression in a panel of platinum-sensitive and platinum-resistant ovarian cancer cell lines has identified TP73 and POLE as a potential key predictor of platinum resistance in ovarian cancer.

2.2.11 Clonogenic assay

A clonogenic assay is a type of assay used to assess the potential clonogenicity of cells. It involves exposing cells to a selective agent and counting the colonies that form. The clonogenicity of a cell is determined by the number of colonies that form. This assay is used to assess the ability of cells to form colonies and can be used to identify cells that have the potential for long-term survival. It can also be used to evaluate the effectiveness of treatments or drugs (Franken et al., 2006). Drug cytotoxicity and ionising radiation efficacy can be measured after the cells have been allowed to reproduce at least 5-6 times before the sample was collected. At the end of the experiment, colonies with at least 50 cells can be observed without a microscope. A crystal violet stain is applied to colonies to estimate survival relative to control colonies, and counts can be taken to evaluate survival.

Before performing a clonogenic survival assay with cytotoxic drugs, it is important to evaluate plating efficiency. The Plating Efficiency of a cell can be

defined as the ability of a single cell to form a colony on its own without any assistance. The cells were seeded in triplicate in 6-well plates at different densities and incubated under normal conditions for 14 days to test plating efficiency. The medium was removed immediately after incubation. A mixture of methanol and acetic acid was used to fix the cells for 10 minutes before processing. Following the staining of the colonies with crystal violet, the colonies were manually counted. By calculating the percentage of colonies formed and the number of cells seeded into each colony, the plating efficiency was calculated.

In the experiment, selected cell lines were seeded in 6-well plates under treated and untreated conditions. The suggested concentrations of cisplatin were used to assess cisplatin chemopotentiation. DMSO diluted in a culture medium was used as a control under each condition. The plates were incubated in 5% CO2/95% air at 37°C for 14 days. Upon completion of the incubation period, the media were removed, the cells were washed with PBS, and the cells were fixed in methanol and acetic acid for 10 minutes.

2.2.12 Cell cycle analysis using γ H2AX assay

The presence of phosphorylation of the histone H2AX is a reliable and rapid way to detect the formation of double-strand breaks (DSBs). Among the three types of histones H2A proteins, the γH2AX variant is the most sensitive to building DSBs. Several proteins play critical roles in DNA damage response, namely the phosphatidylinositol 3-kinase-like protein kinase (PIKKs) family, ATMs (Ataxia Telangiectasia Mutated), ATRs, DNA-PKs, and poly (ADP-ribose) polymerase (PARPs). During DSB (Double Strand Break), ATM

(Ataxia Telangiectasia Mutated), (DNA-PK), and ATR proteins are activated to repair the damage. There is evidence to suggest that PARP1 is responsible for the initial recruitment of the MRE11-NBS1-RAD50 complex to the sites of the DSB. As a result of the ATM and MRN complex phosphorylating γH2AX on ser139, the MRN complex further stabilises itself in positive feedback. A double-strand break occurs within each focus of γH2AX. To detect phosphorylated Histone γH2AX, cells are labelled with the anti-phospho-histone γH2AX, FITC conjugate antibody and can be visualised on flow cytometry (Sharma et al., 2012). A Propidium iodide (PI) stain was used to identify DNA in the cells by binding proportionally to the amount of DNA present. As a result of using the PI stain, it is possible to determine the amount of DNA in each phase of the cell cycle and the progression of cells throughout the cell cycle.

In 6-well plates, $1x10^5$ cells were seeded overnight. A day later, cells were treated with the indicated doses of drugs for 24 hours or 48 hours. Once the time point was complete, the medium was removed, and the cells were washed twice in cold PBS. Cells were trypsinised and collected by adding fresh media to stop trypsin action. Then, the cells were centrifuged at 1000 RPM for 5 minutes. The supernatant is discarded and washed twice with PBS, followed by centrifugation at 1000 RPM for 5 minutes. Cells were fixed in ice-cold 70% ethanol for 2 hours before running the experiment. Moreover, cells that have been fixed can be stored at -20°C for weeks. The fixation was removed by centrifuging and discarding the supernatant. Cell pellets were washed twice with cold PBS and then permeabilized with 50 ul of 1X permeabilization solution. 1 ul of Anti-phospho-Histone H2A.X (Ser139) FITC

conjugated (Merck) was added and incubated for 15 minutes with cells. In the next step, cells were incubated for 15 minutes with an RNAase solution (Invitrogen, UK) containing 5/mL. As a final step, 400 ul of propidium iodide solution (1 g/mL, Sigma, United Kingdom) were added to the cells. Cytoflex flow cytometry was used to analyse the cells. Kaluza software was used for data analysis.

2.2.13 Apoptosis Assay by Annexin V assay

As a process of maintaining tissue homeostasis, programmed cell death is also known as apoptosis. As apoptosis occurs, certain morphological features are observed, such as the loss of asymmetry and adhesion of the plasma membrane and chromatin condensation. As part of the apoptosis process, phosphatidylserine (PS) is translocated from the inner to the outer plasma membrane. An annexin V protein has a high affinity for PS and binds Ca2+-dependent phospholipids. Consequently, it can detect early apoptosis in cells that have translocated PS outside the plasma membrane. Detecting apoptosis will be easier with annexin V staining combined with propidium iodide (PI) or 7-Amino-Actinomycin (7-AAD). Annexin V or PI are not stained on viable cells with intact plasma membranes. Annexin V staining is positive for early apoptotic cells, but not for PI. Annexin V and PI are positive in late apoptotic cells, while Annexin V and PI are negative in necrotic cells as shown in (**Figure 2-3**) (Bratton et al., 1997; Vermes et al., 1995).

Cells were seeded into 6-well plates overnight at a density of $1x10^5$ per well. On the following day, cisplatin was administered for 24 and 48 hours to the cells. After the cells had been incubated for an appropriate amount of time,

the cells were harvested using trypsinization, washed twice with ice-cold PBS, and then re-suspended in 100 ul of 1X annexin V binding buffer (BD Pharmingen, USA). A 1µL fluorescein isothiocyanate (FITC) conjugated Annexin V antibody and 1µL propidium iodide were applied to cells on ice and incubated in a dark room for 15 minutes. CytoFlex system was used to analyse cells using a 488nm laser and a 575nm bandpass filter, and flow cytometry data were analysed using the Kaluza Analysis Software.

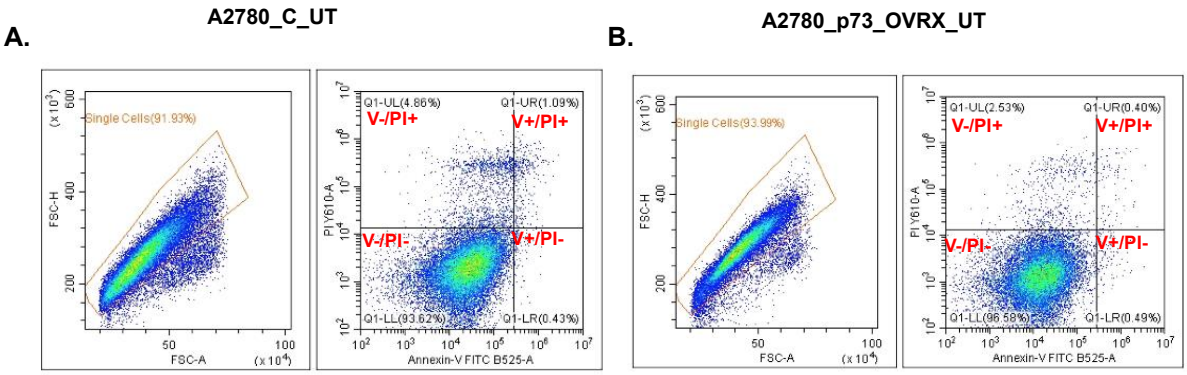

Figure 2-3. Annexin V and PI Staining were performed using follow cytometry. A. A2780_Wild type control cells. B. A2780_p73_Knock-in cells. Viable cells are both Annexin V and PI negative, early apoptosis cells are Annexin V positive and PI negative, late apoptosis cells are Annexin V and PI positive, and finally necrotic are Annexin V negative and PI positive.

2.2.14 Doubling time Assay

The doubling time of a cell population is an essential quantitative measure for characterizing cell growth kinetics. It represents the time taken for the number of cells to double and is typically determined from cell culture experiments. To perform this assay, cells are cultured in a specific growth medium under controlled temperature and CO_2 conditions. A known number of cells are seeded in a culture medium and allowed to grow over time. At regular intervals, the cells are counted by taking the initial cell count and subsequent counts at various time points. The formula for calculating the doubling time of cells is expressed as Doubling Time (hours) = T multiplied by ln (2) divided by ln (Nt/N0). In this formula, T refers to the incubation duration in hours, Nt represents the final cell count, and N0 is the initial cell count.

2.2.15 Migration Assay

Migration assays are used to study various physiological and pathological processes, including cell development, immune cell migration, angiogenesis, wound healing, and cancer metastasis. Cell migration is a crucial mechanism that contributes to the development and progression of cancer cells. In particular, the migration of tumour cells involves the movement of cells from the primary site to a different tissue, which is responsible for metastasis development. This process is a defining feature of aggressive tumour growth and is critical for understanding the underlying biology of cancer.

The wound-healing assay, also called a scratch assay, is a widely used technique in studying cell migration and the closure of a simulated "wound" in

a cell monolayer. This assay provides valuable insights into the cells' migratory and proliferative abilities. Its primary objective is to determine the physical gap within a cell monolayer and then monitor the cell migration process into that gap through photographs taken at different intervals (e.g., 0 hour, 24 hours, 48 hours, etc.) using Nikon Plate reading widefield. The gap culture rates can be measured automatically using software such as Image J (Fiji).

The wound-healing assay was performed using a 35-mm ibidi Culture-Inset 2 Well in a µ-Dish (Cat#: IB-81176; Thistle Scientific Ltd, Glasgow, UK), following the manufacturer's protocol. Cells with a density of 1.5×10^5 were suspended in 140 µL of cultured medium (10% FBS) and 70 µL of the suspension was added to each well. After incubating for 24 hours at 37°C and 5% CO2, the confluent layer of appropriate cell attachment was determined by gently removing the Culture-Insert 2 Well using sterile tweezers, followed by washing with DPBS. The cells were then washed with 1% FBS cultured media to focus on their migratory behavior and incubated for at least one hour. Finally, 2 mL of 1% FBS cultured medium was gently added to the dish and photographs were taken using an inverted microscope (Nikon Plate reading widefield) on the day the well was removed and the subsequent few days. The migration rate was calculated using an ImageJ analysis (Fiji).

2.2.16 Invasion Assay

The following protocol was performed to evaluate the invasive abilities of cells through a barrier mimicking the basement membrane by using a

Transwell invasion assay with Matrigel. On the first day, Transwell inserts (Cat#: 662638; Corning Transwell inserts, 24-well plate, 8.0 µm pore, Greiner Bio-One Ltd, UK) were placed in culture plates and coated with Matrigel. Matrigel was stored on ice or at 4 °C and then diluted with a cold serum-free medium as recommended by the manufacturer. The diluted Matrigel was stored on ice and piped an adequate amount into the upper chamber of each Transwell insert. Then, the inserts were incubated at 37 °C for 1-2 hours to allow the Matrigel to set and solidify.

Cells were trypsinised and resuspended in 1% RPMI + HU 1 mM medium. A total of 1.5×10^5 cells in 200 µL of the cell suspension was added to each insert, and 600 µL of 10% RPMI medium was added to the bottom chamber. Then, the cells were carefully incubated at 37°C in a 5% CO_2 atmosphere for 24 hours.

On the second day, the non-invaded cells on the upper surface of the membrane were gently wiped off using a cotton swab. The invaded cells on the underside of the membrane were then fixed with a suitable fixative like methanol or formaldehyde and stained with a staining solution like DAPI to facilitate visualization. The invaded cells were then observed under an inverted microscope, and the photographed total number of invaded cells was determined per high-power field. Quantitative data analysis was done using ImageJ (Fiji).

2.2.17 3D Spheroids

A 3D model was generated from adherent monolayer cells using Promocell 3D tumoursphere medium xenofree (catalog. no. C-28070) according to the

supplier's protocol. Before centrifugation, a small volume of 3D tumour sphere medium of 3-5 mL was added to trypsinised adherent cells. The cells were counted, and 4x104 cells/ml of the re-suspension were prepared, and each one ml was seeded into a Nunclon Sphera ultra-low attachment 6-well plate (Thermofisher, catalogue no.174932). In the next step, the cells were topped up with another one mL of tumour sphere medium. The cells were topped up with 0.5 mL of tumour sphere medium every three days. The formation of spheroids was regularly observed under the microscope. The passing of spheroid structures can be achieved by centrifuging the cell suspension containing the structures into a falcon. After washing with PBS, structures can be dissociated by resuspending in trypsin for three minutes. A single-cell suspension can be obtained by pipetting the spheres up and down. Spheroid structures can be formed by counting and dividing cells into new ultra-low attachment culture plates.

Using A2780 control and A2780_TP73_knock-in cell lines, 3D spheroid structures were tested, followed by untreated and cisplatin-treated cells for 24 hours or 48 hours. For staining, spheres were fixed in 37% formaldehyde at a 1:10 ratio for 30 minutes. The samples were stained with 2uM calcein AM and 1.5uM ethidium homodimer-1 (Live dead assay, Thermofisher), according to Debnath, (Debnath et al., 2003)Imaging was performed with a Leica SP2 confocal laser scanning microscope. At least 30 spheroids were analysed for each cell line. Cell viability was analysed and quantified using ImageJ (Fiji) image processing software.

2.2.18 Cell transfection

2.2.18.1 Transient transfection of cell lines by siRNA (Knock-down)

As part of the knockdown experiments, a total of two siRNA constructs for POLE were used (ID 117920, ID 119255; Thermo Fisher, UK). As a control construct, a negative scrambled siRNA construct (ID 4390843; Thermo Fisher, UK), as well as a siRNA construct selected for silencing, were also investigated. Constructs were resuspended in nuclease-free 50 ul water in stock solution (100 uM concentration). To prepare a working dilution of 10 uM as recommended by the manufacturer, we diluted the re-suspended constructs prepared with nuclease-free water before transfection. To deliver siRNA to cells, Lipofectamine RNAiMAX Transfection Reagent (Thermofisher, UK) was used in Opti-MEM low serum media (Thermofisher, UK). According to manufacturer's instructions, lipofectamine proportions were used. For transfection, 1-1.5 x10^6 cells were seeded overnight in T25 flasks to reach 60-70% confluency the next day. For each reaction, 20.8 ul Lipofectamine RNAiMAX were prepared in 0.75 mL Opti-MEM medium. Following this, 9.4 ul of 10 uM working siRNA solution was mixed with 0.75 mL Opti-MEM for 2-3 minutes and a negative control (scrambled). As a last step in the process, each diluted lipofectamine solution was then added to the diluted siRNA tube, the negative control tube, and incubated for 15 minutes before adding to the cells.

2.2.18.2 Transient transfection of cell line by pcDNA (Knock-in)

Plasmid HA-TP73α-pcDNA3 from Addgene (Cat. 22102) containing TP73 cDNA was used. The transfection cells were seeded in 6 well plates

overnight at 60-70% confluency. In the following day's experiment, 7.5 ul of lipofectamine 3000 were prepared in 500 ul of Opti-MEM medium along with 2 ug of plasmid dissolved in 500 ul of Opti-MEM medium and P3000 reagent. A diluted lipofectamine solution was added to a diluted DNA tube and incubated at room temperature for 15 minutes. The cells were then washed with Opti-MEM medium, and the transfection mixture was added to the plates and incubated overnight at 37°C in 5% CO2/95% air. The transfection medium was changed to a complete culture medium the next day. Following 48 hours, Neomycin (selected with G418) was used to isolate desired clones. A2780_TP73_Knock-in cells were selected at 400µg/mL of G418. Selection doses were determined pre-transfection using the G418 kill curve experiment in ovarian cells. In 10-14 days, A2780_TP73_Knock-in cells were maintained at 200 ug/mL of G418. Stable transfected colonies were amplified, and transfection efficiency was determined by western blot analysis.

2.2.19 Plasmid amplification

Amplification of plasmids is commonly achieved through bacterial transformation, propagation, and isolation of plasmid DNA. Techniques like bacterial culture, alkaline lysis, and column-based purification are routinely employed (Sambrook and Russell, 2001). Bacterial transformation with plasmids containing antibiotic resistance genes and subsequent selection on agar plates provides a means to enrich and amplify the plasmid of interest (Dower et al., 1988).

Verifying plasmids is paramount to ensure the correct insert, absence of mutations, and plasmid integrity. Several methods are employed for this

purpose, such as Polymerase Chain Reaction (PCR): PCR is a versatile tool for confirming the presence of the desired insert within the plasmid (Innis et al., 1990), restriction enzyme digestion with specific restriction enzymes that target unique sites within the plasmid and insert can verify the expected banding patterns (Roberts and Macelis, 2001), and DNA Sequencing the plasmid using Sanger or next-generation sequencing methods provides the most comprehensive verification, confirming the nucleotide sequence and identifying potential mutations (Sanger et al., 1977; Shendure et al., 2017). These methods collectively ensure the fidelity and authenticity of plasmids, a critical step in molecular biology research.

2.2.19.1 Bacterial strain

Escherichia coli (E. coli) DH5α. Genotype: lacZΔM15, recA1 mutation, endA mutation was used. Addgene ships plasmids as transformed bacteria in stab culture format (Cat. 22102).

2.2.19.2 Preparing LB broth and LB agar plates

To make 1 litre of Lysogeny Broth (LB) media, 25 g of LB powder (Sigma Aldrich, L3022) was dissolved in double-distilled water (ddH2O) and mixed well. The LB broth was autoclaved at 120°C for 15 minutes to sterilize it and was stored at 4°C.

LB agar was prepared by combining 2 g of LB powder and 2 g of bacterial agar (Sigma Aldrich, A5306) with 100 mL of double-distilled water (ddH2O). The mixture was thoroughly dissolved and then sterilised by autoclaving at 121°C for 15 minutes. The sterilised solution was stored at room temperature until needed. For agar plate preparation, 15-20 mL of the LB agar solution

was poured into 10 cm Petri dishes near a Bunsen burner. The plates were left to solidify at room temperature for 15-20 minutes.

According to the manufacturer's recommendation, 100 µg/mL of Bacterial Resistance antibiotic was incorporated into LB broth agar before use. A Bunsen burner was employed throughout the procedure to maintain aseptic conditions and minimize contamination risks.

2.2.19.3 Streaking Bacteria for Single Colonies

Bacteria were streaked for single colonies to isolate individual bacterial colonies on an agar plate. A vial of bacterial cells containing the desired plasmid was retrieved from Addgene and thawed on ice. An inoculation loop or toothpick was flame-sterilised until it glowed red and then cooled briefly. A small number of bacterial cells was aseptically picked from the vial using the sterilised loop or toothpick. The lid of the agar plate was lifted, and the bacterial cells were streaked across one section of the plate in a zigzag pattern. The loop or toothpick was flame-sterilised again before repeating the process as needed. The plate was then incubated overnight at 37°C.

2.2.19.4 Picking a colony and inoculating liquid bacterial culture.

A liquid culture was inoculated to propagate bacteria for plasmid amplification. A single colony was selected from the LB agar plate using a sterile pipette tip or toothpick and transferred into 5 mL of liquid LB medium containing the appropriate antibiotic. The tip or toothpick was swirled in the medium to ensure proper inoculation. The bacterial culture was covered with sterile aluminium foil or a loosely capped lid to allow aeration and incubated in a shaking incubator at 37°C with a shaking speed of 250-300 rpm for 12-

18 hours. Subsequently, the entire culture was transferred to 250 mL of LB broth supplemented with the same antibiotic. The subculture was incubated overnight to prepare the bacteria for further purification.

2.2.19.5 Plasmid purification

Following the supplier's protocol, the plasmid was purified using a Midi prep kit (Qiagen®, 12145). To begin with, the bacterial culture obtained from the previous transformation was spun down by centrifugation at 6000 RCF for 15 minutes at 4°C. The pellet was then resuspended in 4 mL of lysis buffer P1. An equal amount of buffer P2 was added, and the solution was mixed by inversion. The mixture was incubated at room temperature for 5 minutes. After incubation, 4 mL of buffer P3 was introduced to the mixture and left to incubate on ice for 20 minutes. This was followed by two consecutive 4°C centrifugations: first at 14,000–18,000 RCF for 10 minutes, then the supernatant from the first at ≥20,000 RCF for 15 minutes. Next, a Qiagen column was equilibrated with 4 mL of QBT buffer. The supernatant from the double-spinning process was transferred to the column to flow by gravity into the column’s resin. The column was washed twice with 10 mL of buffer QC. DNA was eluted using 5 mL of buffer QF and precipitated by adding 3.5 mL of isopropanol. The mix was then centrifuged at 4°C at ≥15,000 RCF for 30 minutes. The pellet was washed with 2 mL of 70% ethanol and centrifuged at ≥15,000 RCF for 10 min. Finally, the DNA pellet was dried for 10 minutes and dissolved in an appropriate volume of TE buffer, pH 8.0.

2.2.19.6 DNA quantification

A nanodrop UV spectrophotometer (NanoDrop™ 2000 UV - Thermo Scientific) was used to measure the absorbance at 260 nm to determine the quantity of isolated DNA. The concentration was calculated using the formula (A260 of 1.0 = 50 mg/mL pure DNA plasmid). Examining the A260 / A280 ratio is necessary to guarantee the purity of the plasmid DNA sample. A value between 1.9 and 2.1 can identify a highly purified plasmid DNA sample.

2.2.20 Plasmid verification

2.2.20.1 Diagnostic restriction digest

The two restriction enzymes were prepared according to the information provided in (**Table 8**) for the process of plasmid restriction digestion. The reaction was carried out in sterile PCR tubes, with all necessary components mixed and incubated at 37°C for 1 hour. The uncut plasmid was used as a control in this process. All reactions were stopped by inactivation at 65°C. BioLabs supplied all the restriction enzymes and buffers utilized in this experiment.

Table 8. Restriction digestion experiment

Component	**Uncut plasmid**	**Cut with both enzymes**
DNA (µg/µL)	1	1
10X Buffer (µL)	2	2
Restrction enzyme 1 (HindIII) (µL)	--	1
Restrction enzyme 2 (XbaI) (µL)	--	1
DW (µL)	17	15

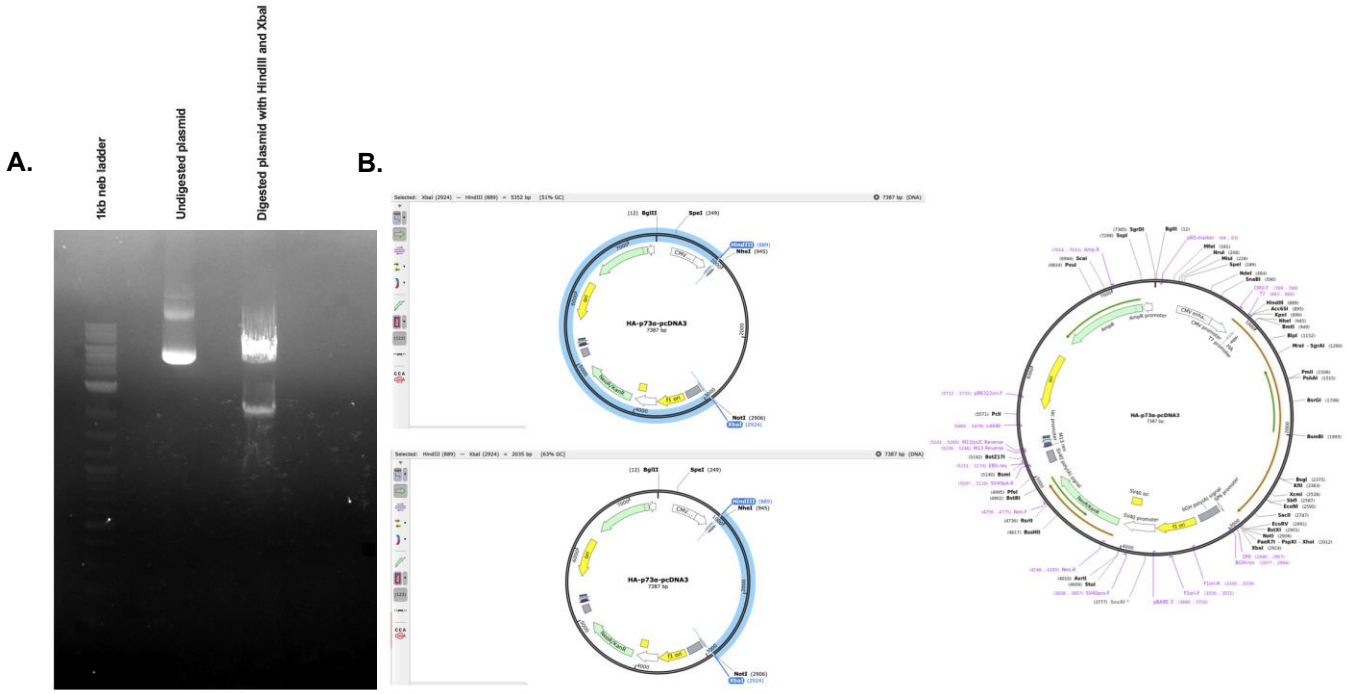

Figure 2-4. A. DNA electrophoresis agarose gel using restriction enzymes for pCDNA plasmid validation and confirmation. B. plasmid map shows the regions of restriction enzymes have been selected for confirmation by using SnapGene Viewer Version 7.0.3.

2.2.20.2 DNA electrophoresis using 2% Agarose gel

Agarose from Sigma Aldrich (A9539) was dissolved in a Tris-acetate EDTA (TAE) buffer consisting of 40 mM Tris-acetate from Sigma Aldrich (T1258) and 1mM EDTA from Sigma Aldrich (E1644) to make a 2% agarose gel. Using a microwave, a solution of agarose was heated to the point of becoming transparent and then cooled down on a bench for a few minutes. Next, 0.5 µg/mL Ethidium Bromide from Promega (H5041) was added to the mixture and swirled. Finally, the agarose solution was poured into a gel tray with a well-comb inserted and left to solidify at room temperature.

The gel's comb was taken out and the tray was put into an electrophoresis tank filled with TAE buffer. DNA gel loading dye was added to each restriction

reaction mix. A 5 µL of DNA ladder (Bioline, BIO-33056) was added to the first lane in the gel. The uncut plasmid was loaded into the second lane. A plasmid with both restriction enzymes was used in lane 3. The voltage was adjusted to 100 V and left to run until loaded samples were 80% away from the wells. The gel was imaged by a Gel DocTM EZ Gel Documentation System from Biorad as shown in Figure **2-4**). The bands were analysed using the software, Image LabTM. Bands were examined for backbone and insert sizes.

2.2.21 Primer validation

QuantiTect Primer Assays are genomewide, bioinformatically validated primer sets for use in LightCycler 480 SYBR Green-based real-time RT-PCR on any cycler. The products of (Hs_TP73_1_sg quantitect primer assay Gene Globe ID: QT00030240) was for target gene and Hs_GAPDH_1_SG QuantiTect Primer Assay Gene Globe ID: QT00079247) for housekeeping control.

2.2.22 RNA extraction

To study gene expression, RNA extraction is an important part of molecular biology, which isolates and analyses RNA molecules. This study provides valuable information that is crucial to the understanding of how cells function and how genes are regulated.

For extracting RNA from tissue culture cell lines, all necessary reagents and equipment were prepared, the working area was cleaned and free of RNases, and appropriate personal protective equipment (PPE) was worn, including gloves and lab coat. The extraction of total cellular RNA was carried

out using the RNeasy mini kit (Cat No; 74104, Qiagen) following the manufacturer's protocol. 2 x 10^6 pelleted cells were mixed with 350 µL of buffer RLT and then agitated. After that, 350 µL of 70% ethanol was added and mixed with the lysate. Next, 700 µL of the solution was transferred to a RNeasy spin column and centrifuged at 8000 xg for 15 seconds. The flow-through was discarded, and 350 µL of buffer RW1 was used to rinse the membrane. The flow-through was again discarded after a 15-second centrifugation at 8000 x g.

DNA digestion eliminated genomic DNA contamination using the DNase digestion kit (Cat No; 79254, Qiagen). The mixture was generated by mixing 70 uL of buffer RDD with 10 uL of DNase I stock solution in an Eppendorf tube, then centrifuging at 8000 xg for 15 seconds. Next, 80 µL of the DNase I mix was added directly to the RNeasy spin column membrane, which was then incubated at room temperature for 15 minutes. The RNeasy spin column was purified by adding 350 µL of buffer RW1. After another 15-second centrifugation at 8000 xg, the flow-through was discarded. RNeasy spin columns were washed with 500 µl of RPE buffer and centrifuged for 15 seconds at 8,000 x g. This step was repeated with another 500 µL of Buffer RPE, followed by centrifugation for 2 minutes at 8000 xg. After centrifugation, the RNeasy spin column was delicately transferred to a fresh 1.5 mL Eppendorf tube, and 40 µL of RNase-free water was applied directly to the spin column membrane. RNA elution was achieved by centrifugation for 1 minute at 8000 xg. The eluted RNA concentration (µg/µL) was determined by measuring the absorbance ratio at 260:280 nm using a spectrophotometer

system (Nanodrop 2000c, Thermo Scientific, USA), and the RNA was stored at -80°C for preservation.

2.2.23 cDNA reverse transcription

Following the QuantiTect Rev. Transcription Kit protocol (Qiagen, 205313), equal amounts of RNA were reverse transcribed into cDNA. A mix of RNA, nuclease free water and gDNA removal reagent was prepared and incubated at 42°C for 2-3 minutes. The reaction was stopped by cooling the mixture on ice or 4°C for 5 minutes. Then a mix of reverse transcriptase, reverse transcription buffer, and reverse transcription mix were added and incubated at 42 °C for 15 minutes. To stop the reaction, it was necessary to heat the mixture for 3 minutes at 95°C using a thermal cycler. cDNA was stored at -20°C until required.

2.2.24 Amplification factor and qPCR efficiency

In qPCR, the term "amplification factor" denotes the extent of DNA target amplification during the PCR process. This factor measures the degree to which the original DNA template is replicated after each PCR cycle. The amplification factor is determined by the formula 2^n, where "n" represents the number of PCR cycles.

One of the primary tasks when starting a qPCR assay is to determine amplification efficiency. It is crucial to understand efficiency and how to calculate it for precise data interpretation. The number of molecules in the target sequence should double during every replication cycle, indicating

100% amplification efficiency. To determine amplification efficiency, one approach is to create serial dilutions of the target and obtain their Ct values.

Plot the values on a logarithmic scale along with the corresponding concentrations, generate a linear regression curve through the data points, and determine the slope of the trend line. Finally, efficiency can be calculated using the equation: E = -1+10(-1/slope).

2.2.25 RT-qPCR

RNA was isolated from a panel of ovarian cell lines using the RNA Easy Mini kit from QIAGENUKUK). The concentration of the extracted RNA was determined through spectrophotometric analysis using a NanoDrop 2000c Spectrophotometer (Thermo Scientific). Subsequently, complementary DNA (cDNA) was synthesized from 0.5 µg of the total RNA using the RT2 first strand kit (Qiagen). The LightCycler ® 480 SYBR Green I Master Mix (Catalogue no. 04887352001, Roche) was used to conduct real-time quantitative polymerase chain reaction (qPCR) Using a primer set designed for the TP73 gene (TP73 Quanti Tect Primer Assay, catalogue no. QT00030240 from QIAGEN). To normalize gene expression, the glyceraldehyde-3-phosphate dehydrogenase housekeeping gene was utilized as an internal control (GAPDH Quanti Tect Primer Assay, catalogue no. QT00079247, QIAGEN). Each RNA sample underwent real-time PCR analysis in triplicate to ensure data reliability. No Template Control (NTC) samples were included to eliminate the possibility of reagent and surface contamination. The NTC samples contained all the reverse transcriptase-polymerase chain reaction (RT-PCR) reagents except for the RNA template.

Additionally, a minus reverse transcriptase (RT) control was employed to rule out the presence of genomic DNA contamination.

2.2.26 RT^2-Human DNA Repair Array

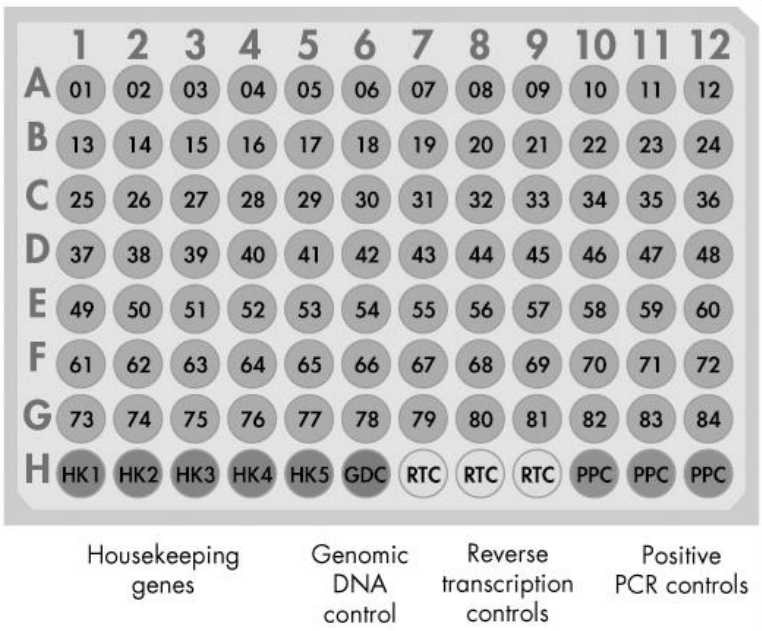

Figure 2-5. RT^2 Profiler PCR Array. RT^2 Profiler PCR Array Formats A, C, D, F, H: Wells A1 to G12 contain a real-time PCR assay for a pathway/disease/functionally related gene. Wells H1 to H5 contain a housekeeping gene panel to normalize array data (HK1–5). Well, H6 contains a genomic DNA control (GDC). Wells H7 to H9 contain replicate reverse-transcription controls (RTC). Wells H10 to H12 contain replicate positive PCR controls (PPC) (Hanahan, 2022; Qiagen, 2023)

The Qiagen RT2 Profiler PCR array is performed in a 96-well format, allowing the simultaneous analysis of 84 genes, as shown in (**Figure 2-5**). In addition to five housekeeping genes, the genomic DNA control (GDC) detects non-transcribed genomic DNA contamination with high sensitivity. The reverse-transcription control (RTC) tests the efficiency of the reverse-transcription reaction performed with the RT2 First Strand Kit by detecting a template synthesized from the built-in external RNA control included with the kit. The positive PCR control (PPC) consists of a pre-dispensed artificial DNA

sequence and the detection assay. This control tests the efficiency of the polymerase chain reaction itself.

Briefly, $2X10^6$ cells of A2780 control and A2780 (TP73_Overexpession) were collected by trypsinisation. Cells were washed with ice-cold PBS and lysed in 400µL of RLT buffer, and then the protocol for the Qiagen RNAeasy mini kit (catalogue no. 74104) was followed as per the supplier protocol for RNA purification. The purity and concentration of the extracted RNA were measured in the nanodrop 2000 (Thermofisher Scientific, UK). used 0.5µg of RNA to convert to cDNA using the RT2 first strand kit as per the supplier-provided protocol. The prepared cDNA was mixed with cyber green master mix and nuclease-free water and distributed on the EMT RT2 profiler array plates (catalogue no. PAHS-090Z). PCR was done in applied biosciences (qPCR ABI Viia 7) PCR thermal cycler.

2.2.27 Statistical Analyses

The correlation of clinical and pathological parameters was analysed using categorized data, and the Chi-squared test was used for all tests which had a 2-tailed distribution. The survival rates were calculated by using the Kaplan-Meier method, and the results were then compared with those calculated by the log-rank test. All analyses were conducted using Statistical Package for the Social Sciences (SPSS) software for Mac, version 29 from IBM, which was installed on the study computers. Statistical significance was determined by P values < 0.05.

GraphPad Prism7 software was used for the statistical analysis of the data. Student-T-tests were used to compare two groups in western blot

quantifications, clonogenic cell survival assays, and immunofluorescence quantifications. In contrast, a one-way ANOVA was used when comparing three or more groups, such as in the western blot and H2AX assay. Two-way ANOVA tests were used for several studies in cell cycle analysis and Annexin V assays that involved multiple comparisons. Using error bars, the standard error of the mean was represented between experiments. Furthermore, p-values were indicated as follows: P-values <0.05 =*, p-value <0.01 =**, p-value <0.001=***, p-value <0.0001=****.

A semi-quantitative H-score, considering the intensity of staining and the percentage of tumour cells stained, was utilised to estimate nuclear/cytoplasmic TP73 and POLE immunoreactivity. Cores containing <15% tumour cells were excluded from the assessment. Cases were scored blinded to clinicopathological and outcome data. X-tile plots are a sophisticated graphical tool for analysing biomarker data, segmenting it into three distinct populations based on expression levels: low, middle, and high to pinpoint optimal cut points. This approach facilitates the exploration of associations between biomarker levels and clinical outcomes, such as survival, employing robust statistical analyses like the log-rank test to evaluate significance (Camp et al., 2004). An H-score of ≤ 43 was used in the breast as the cut-off for TP73 cytoplasmic expression. The H-score of >110 was used as the positive POLE nuclear expression cut-off, and ≤20 was used as the cytoplasmic expression, respectively. A cut-off of 10% was determined to be optimal for dichotomizing TP53 expression between positive (mutant) and negative (wild type) tumours. The whole cohort was divided based on TP53 status into wild-type tumours (TP53 negative), and TP53 mutant

tumours (TP53 positive), and then clinicopathological variables were examined for interaction with TP53. In ovarian, an H-score of > 0 was used as the positive TP73 nuclear expression cut-off, and >140 was used as the positive TP73 cytoplasmic expression. H-score of >0 was used as the cut-off for positive POLE nuclear expression, and >100 was used as the cut-off for positive POLE cytoplasmic expression. Moreover, H-score of >3 was used as the cut-off for TP53. The univariate associations between the H-scores of the markers and pathological parameters were determined using the Chi-squared test. Survival rates were calculated using Kaplan–Meier survival curves and compared using the log-rank test. P-values < 0.05 were considered statistically significant. All statistical analyses were conducted by the Breast Pathology Group.

Chapter 3 TP73 in Ovarian Cancer

3.1 Introduction

Amongst different studies, the role of TP73 in ovarian cancer pathogenesis is unclear. In a study by Codegoni et al. (Codegoni et al., 1999), it was found that there are no significant distinctions in the allelic distribution and expression of TP73 between ovarian cancers and borderline tumours, suggesting that TP73 might not be important in the pathogenesis of ovarian cancer. Nevertheless, some ovarian cancer specimens and cell lines, as detected by Zwahlen et al. (Zwahlen et al., 2000), have shown the presence of the protein, indicating that TP73 could play a role in malignant ovarian tumour development. In their investigation of 100 ovarian carcinomas, (Concin et al., 2004) found that transdominant ΔTATP73 isoforms were upregulated in ovarian cancer, acting as epigenetic inhibitors of TP53. Another study (Concin et al., 2005) similarly explored whether these dominant-negative TP73 isoforms had clinical significance regarding susceptibility to chemotherapy or survival rates in ovarian cancer patients. Their findings illustrate how living organisms can endure stress conditions through gene or protein exchange. Moreover, polymorphisms in the MDM2 and TP73 genes could potentially affect their function or expression, leading to an increased risk of epithelial ovarian cancer (Couch et al.)among Chinese women. MDM2 interacts with TP73, a gene related to the well-known suppressor TP53, suggesting a genetic predisposition for developing EOC based on certain polymorphisms in these genes (Kang et al., 2008). They specifically proved that rather than being regulated by TP53 itself, apoptosis

responsiveness to cisplatin is governed by TP63, a member of its family (Muscolini et al., 2008). Furthermore, stage I and stage III Ovarian cancer patients were investigated for their expression levels of TP53 and TP73 isoforms. The study did not identify any association between TP53 and TP73 isoforms and the malignant progression of ovarian cancer (Marabese et al., 2008). Identically, when they investigated the expression of various genes in human ovarian carcinoma cell lines, which are known to express all three members of the TP53 gene family, namely TP53, TP63 and TP73, it was established that one could not be expressed without the other (Kim et al., 2011). Taken together, these data suggest that further investigation is required to understand the role of TP73 in ovarian cancer pathogenesis.

3.2 Aims of this study

1- Evaluate the role of TP73 expression in ovarian cancer

a- To investigate the expression patterns of TP73 in epithelial ovarian cancer (EOC) using immunohistochemistry (IHC) on tissue microarrays (TMAs) from 331 EOC patients treated at Nottingham University Hospitals.

b- To correlate TP73 expression (nuclear and cytoplasmic) with clinicopathological characteristics and patient outcomes, using the H-score for quantification of immunohistochemical staining.

2- Investigate the co-expression patterns of TP53 and TP73 in ovarian cancer

a- To determine the frequency and distribution of TP53/TP73 co-expression in ovarian tumours and its potential clinical relevance.

3- Assess the impact of TP73 on cisplatin sensitivity in ovarian cancer models

a- To evaluate TP73 expression in ovarian cancer cell lines with varying platinum sensitivities (PEO1, PEO4, A2780, A2780cis), both before and after cisplatin treatment, and correlate TP73 expression with drug response.

b- To assess the role of TP73 in regulating cisplatin sensitivity through functional assays, including clonogenic survival, cell cycle progression, γH2AX analysis, and apoptosis detection, post-cisplatin treatment.

4- Investigate the functional role of TP73 in ovarian cancer cell behaviour

a- To determine the effect of TP73 overexpression and knock-in on cell proliferation, migration, invasion, and EMT in ovarian cancer cell lines using 2D and 3D culture systems.

b- To explore the molecular mechanisms underlying TP73's role in regulating cisplatin sensitivity and tumour progression, through transcriptomic analysis (RT2 PCR profiler and RT-qPCR) and functional assays (invasion, migration, apoptosis, EMT markers).

3.3 Method

TP73 immunohistochemistry was performed on the TMAs of 331 epithelial ovarian cancer patients treated at Nottingham University Hospitals between 1997 and 2010. Immunohistochemistry protocol and antibody details are described in the Materials and Methods chapter. Immune staining was evaluated by the H-score (range 0–300). X-tile plots were strategically used to pinpoint the most effective cut-off points for precise stratification, enhancing our analysis. For positive TP73 nuclear expression, an H-score of >0 was used, and for positive TP73 cytoplasmic expression, an H-score of >140 was used. TP73 mRNA expression was analysed based on publicly available gene expression datasets for ovarian tumours (http://kmplot.com/analysis/index.php?p=service&cancer=ovar). A panel of ovarian cell lines, including PEO1 (BRCA2-deficient), PE04 (BRCA2-proficient), A2780 (Platinum sensitive), and A2780cis (Platinum resistant) were evaluated for TP73 expression before and after cisplatin treatment. Nuclear and cytoplasmic extracts were generated prior to cisplatin treatment and 24 to 48 hours after treatment, as described in the Materials and Methods chapter. Transient knock-in of TP73 by shRNA in A2780 was performed as per the protocol described in the Methods section. The clonogenic survival assay for cisplatin sensitivity in ovarian cell lines is detailed in Materials and Methods chapter. Functional studies, including cell cycle staining with propidium iodide, γH2AX double strand break analysis and apoptosis detection by annexin V, were analysed by flow cytometry. Detailed staining and analysis protocols are provided in the Materials and Methods chapter. In 2D and 3D models, platinum sensitivity was tested in

A2780 wild-type control and A2780 (TP73 knock-in) cell lines. Invasion and migration assays for studying EMT in the A2780 control and A2780 (TP73 knock-in) overexpression were performed using cell invasion assay and cell migration assay, respectively, as per the supplier protocol. Imaging was done using a Leica SP2 confocal laser scanning microscope. A doubling time assay was performed as described in the methods section. RT-qPCR for the A2780 control and A2780 (TP73-overexpression) were obtained in this study as described in the methods section. RT2 PCR profiler in A2780 and A2780_TP73_Knock_in were done as per Qiagen-guided protocol analysis and were performed using the provided software (https://www.qiagen.com/us/shop/genes-and-pathways/data-analysis-center-overview-page/). Data analysis was performed with GraphPad Prism-8 software. Error bars represent the standard error of the mean between experiments. P-values are indicated as P-values <0.05 =*, p-value <0.01 =**, p-value <0.001=*** and p-value <0.0001=****

3.4 Results

3.4.1 Clinical study

3.4.1.1 Overexpression of TP73 is Associated with Platinum Resistance in EOC

In a cohort of 331 patients with EOC, IHC staining was used to assess associations between TP73 expression and clinicopathological characteristics. A description of the demographics and pathological characteristics of the patients with EOC is presented in Chapter 2. Typical images of TP73 expression are shown in (**Figure 3-1**).

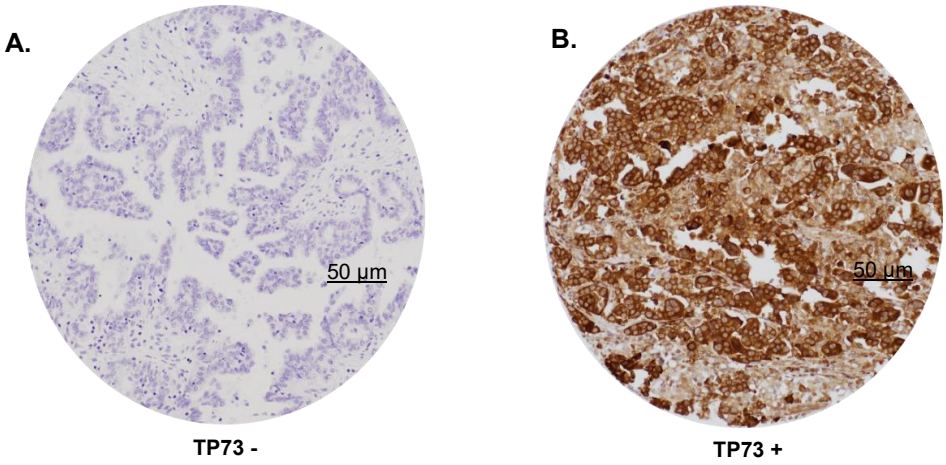

Figure 3-1. Immunohistochemical expression of TP73 in ovarian tumours. Representative images of negative and positive staining for TP73 in tumour microarrays at (x20 magnification; scale bar, 50 µm).

A study was then conducted to evaluate if TP73 expression was associated with the clinicopathological characteristics of EOC. TP73 protein expression was assessed in 278/332 tumours. Low nuclear TP73 expression was in 92% (256/278), and high was in 8% (22/278) of ovarian tumours. Low nuclear expression of TP73 was highly significantly associated with the Serous pathological type of ovarian cancer (*p=0.028*) (**Table 9**). On the other hand, a

high cytoplasmic TP73 expression was in 32% (89/278) and low cytoplasmic TP73 was seen in 68% (189/278) of ovarian tumours. A high cytoplasmic TP73 was significantly associated with aggressive clinicopathological features, including serous pathological type (*P=<0.0001*), high pathological grade (*p=0.006*), and advanced pathological stage (p=0.025). Whereas low cytoplasmic TP73 expression was significantly associated with non-residual tumours following surgery (*p=<0.0001*) (**Table 10**). High cytoplasmic TP73 was significantly linked with poor progression free survival (PFS) (*p<0.0001*) but not overall survival (OS) (*p=0.088*) (**Figure 3-2A, B**). The nuclear TP73 expression was not associated with progression free survival (PFS) (*p=0.731*) and overall survival (OS) (*p = 0.219*) (**Figure 3-2C, D**).

Nuclear and cytoplasmic co-expression of TP73 was seen in 84% (278/332) in EOC. A low nuclear/low cytoplasmic were seen in 64% (177/278), low nuclear/high cytoplasmic were seen in 28% (79/278), high nuclear/high cytoplasmic were seen in 4% (10/278), and high nuclear/low cytoplasmic were in 4% (12/278). Tumours with low nuclear/ high cytoplasmic TP73 levels were significantly associated with serous pathological type (*P=<0.0001*). Tumours with low nuclear/low cytoplasmic TP73 levels were significantly linked with non-residual tumours following surgery (*p=<0.003*) (**Table 11**). Additionally, high cytoplasmic/high nuclear TP73 expression was significantly associated with poor progression free survival (PFS) (*p<0.0001*) but not with overall survival (OS) (*p=0.166*) (**Figure 3-3A, B**).

Immunohistochemical staining for TP53 is a common practice for assessing mutational status in the diagnostic evaluation of various carcinomas, such as ovarian cancers. Strong and widespread expression of TP53 through

immunostaining is typically considered indicative of a TP53 gene mutation (Yemelyanova et al., 2011). TP53 immunohistochemical analysis was performed on 331 ovarian cancers to determine their characteristics. The analysis revealed that 224/331 (68%) of tumours had TP53 positivity. Tumours that had high levels of TP53 were found to have characteristics that were indicative of aggressive behaviour, such as serous pathological type (*p=0.001*) and high pathological grade (*p=0.001*) (**Table 12**). The analysis also showed that high TP53 expression was significantly associated with progression free survival (PFS) (*p=0.032*) but not with overall survival (OS) (*p=0.462*) in ovarian cancers (**Figure 3-4A, B**).

TP53 /TP73 co-expression analysis was performed on 331 cases of ovarian cancers. Among these, 49% (161/331) showed TP53/TP73 co-expression in ovarian tumours. The co-expression of high TP53 and high TP73 were significantly associated with serous pathological type (*p=0.011*). Low TP53 and high TP73 co-expression were significantly associated with high pathological grades (*p=0.046*). Additionally, the co-expression of low TP53 and low TP73 were significantly associated with non-residual tumours following surgery (*p=0.005*) (**Table 13**). The co-expression of low TP53 and high TP73 were significantly associated with poor progression free survival (PFS) (*p= 0.006*) but not with overall survival (OS) (*p=0.332*) (**Figure 3-5A, B**). This data indicates that overexpression of the TP73 protein is strongly associated with poor progression free survival (PFS) and may be a predictive marker for platinum resistance in EOC.

Table 9. TP73 nuclear expression in epithelial ovarian cancer

Parameters	*TP73 Nuclear expression*		*R^2*
	Low N (%)	*High N (%)*	*p value*
Menopausal_Status			
Pre-menopausal	16 (6%)	1 (4%)	0.188
Peri-menopausal	15 (6%)	1 (4%)	0.91
Post-menopausal	223 (88%)	20 (92%)	
Age at Surgery class			
<30	3 (1%)	0 (0%)	0.334
31 to 60	111 (43%)	9 (41%)	0.846
>61	142 (56%)	13 (59%)	
Surgical Pathology Type			
Serous	148 (58%)	10 (45%)	
Mucinous	38 (15%)	3 (14%)	12.586
Endometriod	30 (12%)	2 (9%)	**0.028**
Clear Cell	17 (7%)	3 (14%)	
Other	9 (3%)	4 (18%)	
Mixed	14 (5%)	0 (0%)	
Surgical Pathology Grade			
Low	36 (16%)	3 (15%)	0.435
Intermediate	46 (21%)	3 (15%)	0.804
High	141 (63%)	14 (70%)	
Surgical Pathology Stage			
1	100 (40%)	7 (35%)	2.325
2	36 (15%)	1 (5%)	0.508
3	105 (42%)	11 (55%)	
4	7 (3%)	1 (5%)	
Surgical Pathology Substage			
A	48 (24%)	6 (43%)	2.441
B	27 (14%)	1 (7%)	0.295
C	121 (62%)	7 (50%)	
Residual Tumour Following Surgery			
Non	165 (71%)	11 (59%)	2.435
<1cm	26 (11%)	2 (10%)	0.487
1-2cm	11 (5%)	2 (10%)	
>2cm	30 (13%)	4 (21%)	
Platinum Sensitivity			
Sensitive	200 (92%)	15 (88%)	0.249
Resistant	18 (8%)	2 (12%)	0.618

Table 10. TP73 cytoplasm expression in epithelial ovarian cancer

Parameters	*TP73 Cytoplasm expression*		R^2
	Low N (%)	*High N (%)*	*p value*
Menopausal_Status			
Pre-menopausal	12 (6%)	5 (6%)	3.051
Peri-menopausal	14 (8%)	2 (2%)	0.218
Post-menopausal	162 (86%)	81 (92%)	
Age at Surgery class			
<30	3 (2%)	0 (0%)	1.476
31 to 60	82 (43%)	38 (43%)	0.478
>61	104 (55%)	51 (57%)	
Surgical Pathology Type			
Serous	91 (48%)	67 (75%)	
Mucinous	38 (20%)	3 (3%)	25.679
Endometriod	21 (11%)	11 (13%)	**<0.0001**
Clear Cell	17 (9%)	3 (3%)	
Other	12 (7%)	1 (1%)	
Mixed	10 (5%)	4 (5%)	
Surgical Pathology Grade			
Low	33 (21%)	6 (7%)	10.322
Intermediate	36 (22%)	13 (16%)	**0.006**
High	92 (57%)	63 (77%)	
Surgical Pathology Stage			
1	83 (46%)	24 (28%)	9.362
2	25 (14%)	12 (14%)	**0.025**
3	68 (37%)	48 (56%)	
4	6 (3%)	2 (2%)	
Surgical Pathology Substage			
A	43 (29%)	11 (18%)	4.589
B	16 (11%)	12 (20%)	0.101
C	90 (60%)	38 (62%)	
Residual Tumour Following Surgery			
Non	129 (74%)	47 (61%)	20.008
<1cm	13 (8%)	15 (19%)	**<0.0001**
1-2cm	4 (2%)	9 (12%)	
>2cm	28 (16%)	6 (8%)	
Platinum Sensitivity			
Sensitive	149 (91%)	66 (93%)	0.282
Resistant	15 (9%)	5 (7%)	0.596

Table 11.TP73 cytoplasm/nuclear co- expression in epithelial ovarian cancer

Parameters	*TP73 Cyto / Nuc Co-expression*				R^2
	Cyto Low/ Nuc Low	*Cyto High/ Nuc Low*	*Nuc High/ Cyto High*	*Nuc High/ Cyto Low*	
	N (%)	*N (%)*	*N (%)*	*N (%)*	*p value*
Menopausal_Status					
Pre-menopausal	11 (6%)	5 (6%)	0 (0%)	1 (8%)	3.932
Peri-menopausal	13 (8%)	2 (3%)	0 (0%)	1 (8%)	0.686
Post-menopausal	152 (86%)	71 (91%)	10 (100%)	10 (84%)	
Age at Surgery class					
<30	3 (2%)	0 (0%)	0 (0%)	0 (0%)	1.842
31 to 60	77 (43%)	34 (43%)	4 (40%)	5 (42%)	0.934
>61	97 (55%)	45 (57%)	6 (60%)	7 (58%)	
Surgical Pathology Type					
Serous	86 (48%)	62 (79%)	5 (50%)	5 (42%)	
Mucinous	35 (20%)	3 (4%)	0 (0%)	3 (25%)	46.213
Endometriod	21 (12%)	9 (11%)	2 (20%)	0 (0%)	**<0.0001**
Clear Cell	16 (9%)	1 (1%)	2 (20%)	1 (8%)	
Other	9 (5%)	0 (0%)	1 (10%)	3 (25%)	
Mixed	10 (6%)	4 (5%)	0 (0%)	0 (0%)	
Surgical Pathology Grade					
Low	30 (20%)	6 (8%)	0 (0%)	3 (27%)	11.455
Intermediate	34 (23%)	12 (17%)	1 (11%)	2 (18%)	0.075
High	86 (57%)	55 (75%)	8 (89%)	6 (55%)	
Surgical Pathology Stage					
1	78 (46%)	22 (29%)	2 (22%)	5 (46%)	13.666
2	24 (14%)	12 (15%)	0 (0%)	1 (9%)	0.135
3	64 (37%)	41 (53%)	7 (78%)	4 (36%)	
4	5 (3%)	2 (3%)	0 (0%)	1 (9%)	
Surgical Pathology Substage					
A	39 (28%)	9 (16%)	2 (40%)	4 (45%)	8.503
B	15 (11%)	12 (21%)	0 (0%)	1 (10%)	0.204
C	86 (61%)	35 (63%)	3 (60%)	4 (45%)	
Residual Tumour Following Surgery					
Non	122 (75%)	43 (63%)	4 (51%)	7 (64%)	25.169
<1cm	12 (7%)	14 (20%)	1 (12%)	1 (9%)	**0.003**
1-2cm	4 (3%)	7 (10%)	2 (25%)	0 (0%)	
>2cm	25 (15%)	5 (7%)	1 (12%)	3 (27%)	
Platinum Sensitivity					
Sensitive	142 (92%)	58 (92%)	8 (100%)	7 (78%)	2.947
Resistant	13 (8%)	5 (8%)	0 (0%)	2 (22%)	0.4

Table 12. Associations between TP53 expression in epithelial ovarian cancer

Parameters	*TP53 expression*		R^2
	Low N (%)	*High N (%)*	*p value*
Age at Surgery class			
<30	1 (1%)	0 (0%)	1.57
31 to 60	48 (42%)	42 (38%)	0.456
>61	64 (57%)	69 (62%)	
Type_of_Surgery			
Biopsy	0 (0%)	3 (3%)	3.514
Early debulking	100 (90%)	96 (88%)	0.319
Interval debulking	9 (8%)	7 (6%)	
Delayed debulking	2 (2%)	3 (3%)	
Surgical Pathology Type			
Serous	47 (42%)	75 (67%)	20.298
Mucinous	21 (19%)	10 (9%)	**0.001**
Endometriod	18 (16%)	12 (11%)	
Clear Cell	14 (12%)	3 (3%)	
Other	8 (7%)	4 (4%)	
Mixed	5 (4%)	7 (6%)	
Surgical Pathology Grade			
Low	23 (26%)	8 (8%)	15.022
Intermediate	20 (22%)	16 (15%)	**0.001**
High	47 (52%)	79 (77%)	
Surgical Pathology Stage			
1	49 (47%)	38 (35%)	7.598
2	20 (19%)	14 (13%)	0.055
3	32 (31%)	52 (48%)	
4	3 (3%)	5 (4%)	
Surgical Pathology Substage			
A	24 (28%)	24 (28%)	0.00
B	11 (13%)	11 (13%)	1.00
C	51 (59%)	51 (59%)	
Residual Tumour Following Surgery			
Non	81 (78%)	64 (63%)	7.785
<1cm	10 (10%)	12 (12%)	0.051
1-2cm	5 (5%)	6 (6%)	
>2cm	7 (7%)	19 (19%)	
Platinum Sensitivity			
Sensitive	88 (91%)	88 (90%)	0.048
Resistant	9 (9%)	10 (10%)	0.827

Table 13.TP53/TP73 co-expression in epithelial ovarian cancer

Parameters	*TP53/TP73 co-expression*				R^2
	TP53 low/ TP73 low	*TP53 high/ TP73 low*	*TP53 high/ TP73 high*	*TP53 low/ TP73 high*	
	N (%)	*N (%)*	*N (%)*	*N (%)*	*p value*
Age at Surgery class					
<30	1 (2%)	0 (0%)	0 (0%)	0 (0%)	3.662
31 to 60	27 (45%)	18 (36%)	13 (38%)	5 (29%)	0.722
>61	32 (53%)	32 (64%)	21 (62%)	12 (71%)	
Surgical Pathology Type					
Serous	22 (37%)	32 (64%)	27 (79%)	13 (76%)	30.209
Mucinous	14 (23%)	7 (14%)	1 (3%)	1 (6%)	**0.011**
Endometriod	9 (15%)	2 (4%)	5 (15%)	1 (6%)	
Clear Cell	6 (10%)	2 (4%)	0 (0%)	1 (6%)	
Other	6 (10%)	3 (6%)	0 (0%)	0 (0%)	
Mixed	3 (5%)	4 (8%)	1 (3%)	1 (6%)	
Surgical Pathology Grade					
Low	14 (30%)	5 (11%)	2 (6%)	1 (7%)	12.795
Intermediate	8 (18%)	10 (21%)	5 (16%)	2 (13%)	**0.046**
High	24 (52%)	32 (68%)	25 (78%)	12 (80%)	
Surgical Pathology Stage					
1	25 (45%)	19 (39%)	10 (30%)	3 (19%)	8.235
2	11 (20%)	7 (14%)	5 (15%)	3 (19%)	0.511
3	18 (32%)	20 (41%)	17 (52%)	10 (62%)	
4	2 (3%)	3 (6%)	1 (3%)	0 (0%)	
Surgical Pathology Substage					
A	15 (33%)	12 (33%)	4 (17%)	2 (18%)	5.618
B	5 (11%)	2 (6%)	5 (22%)	2 (18%)	0.467
C	25 (56%)	22 (61%)	14 (61%)	7 (64%)	
Residual Tumour Following Surgery					
Non	44 (82%)	29 (62%)	17 (59%)	10 (67%)	23.375
<1cm	5 (9%)	3 (6%)	5 (17%)	3 (20%)	**0.005**
1-2cm	0 (0%)	1 (2%)	3 (10%)	2 (13%)	
>2cm	5 (9%)	14 (30%)	4 (14%)	0 (0%)	
Platinum Sensitivity					
Sensitive	51 (94%)	40 (87%)	27 (96%)	13 (93%)	2.859
Resistant	3 (6%)	6 (13%)	1 (4%)	1 (7%)	0.414

3.4.1.2 Associations Between TP73 Expression and Survival Outcomes in EOC

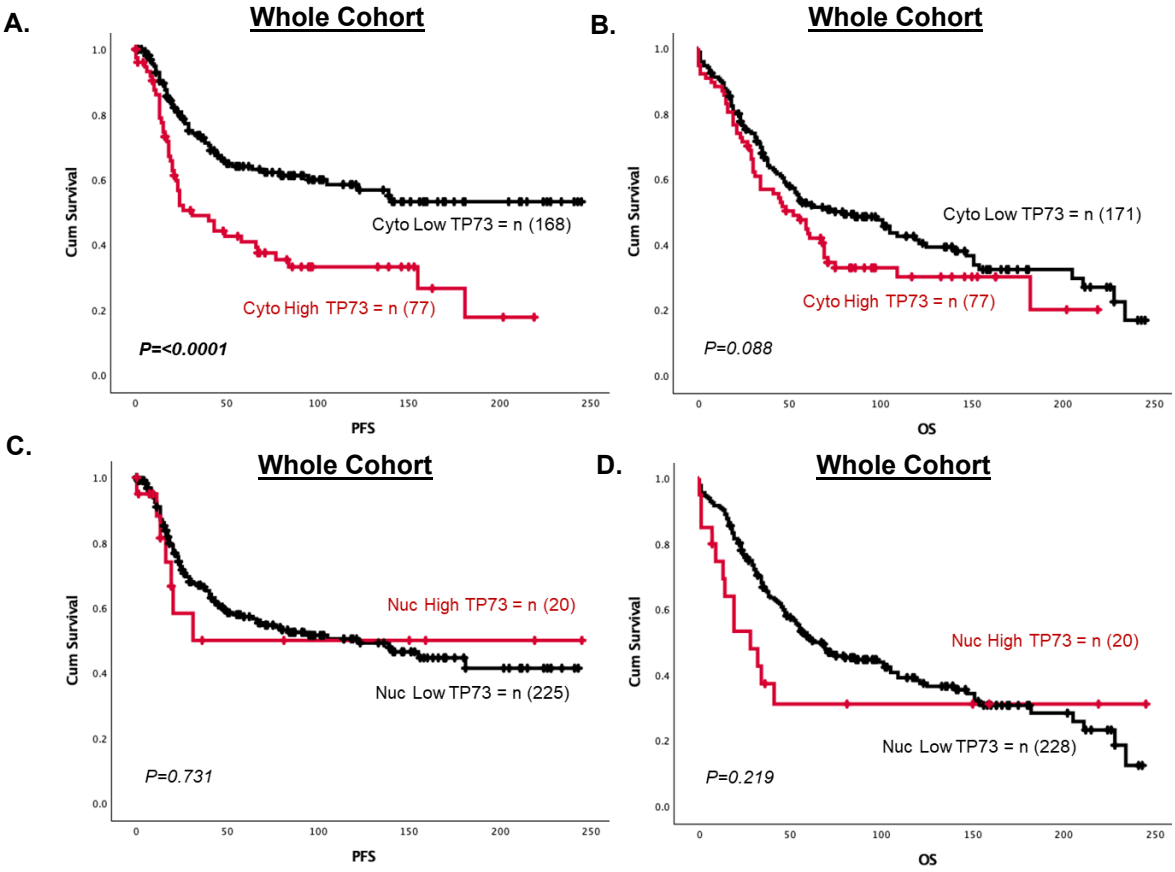

Figure 3-2. Kaplan-Meier survival curves for TP73 in ovarian tumours. A. Kaplan-Meier curve showing the correlation between cytoplasmic TP73 protein expression and progression-free survival (PFS) in the ovarian whole cohort. B. Kaplan-Meier curve showing the correlation between cytoplasmic TP73 protein expression and overall survival in the ovarian whole cohort. C. Kaplan-Meier curve showing the correlation between nuclear TP73 protein expression and progression-free survival (PFS) in the ovarian whole cohort. D. Kaplan-Meier curve showing the correlation between nuclear TP73 protein expression and overall survival in the ovarian whole cohort.

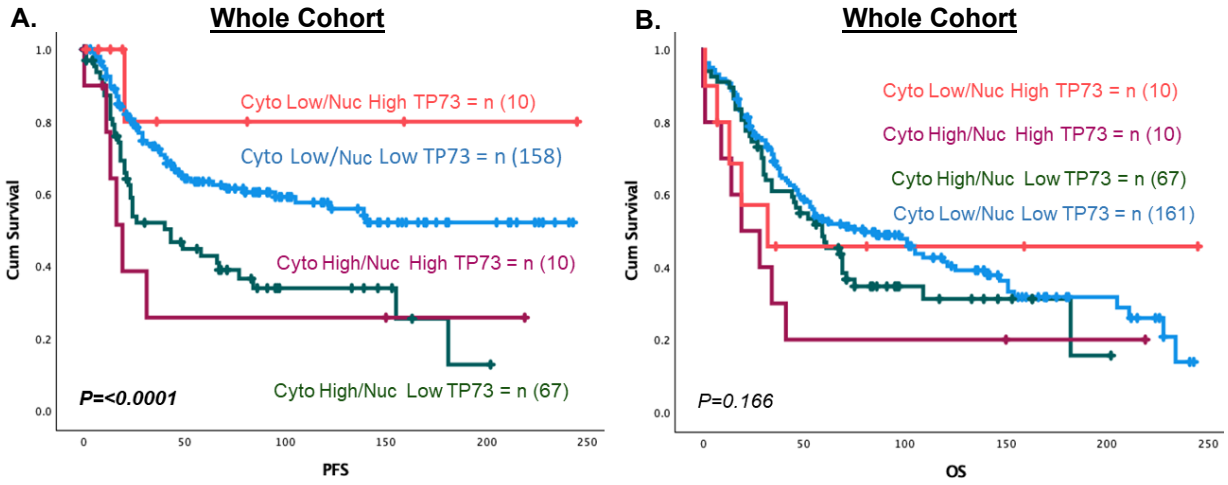

Figure 3-3. Kaplan Meier curve for nuclear/cytoplasmic TP73 co-expression in ovarian tumours. A. Kaplan-Meier curve showing the correlation between nuclear/cytoplasmic TP73 co-expression and progression-free survival (PFS) in the whole cohort. B. Kaplan-Meier curve showing the correlation between nuclear/cytoplasmic TP73 co-expression and overall survival in the whole cohort.

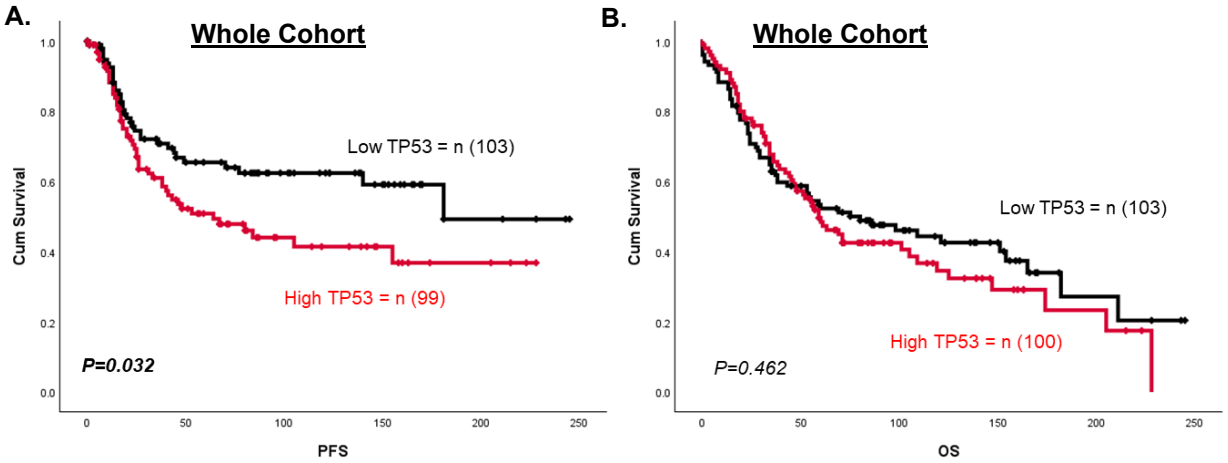

Figure 3-4. Kaplan Meier curve for TP53 expression in ovarian tumours. A. Kaplan-Meier curve showing the correlation between TP53 protein expression and progression-free survival (PFS) in the whole cohort. B. Kaplan-Meier curve showing the correlation between TP53 protein expression and overall survival in the whole cohort.

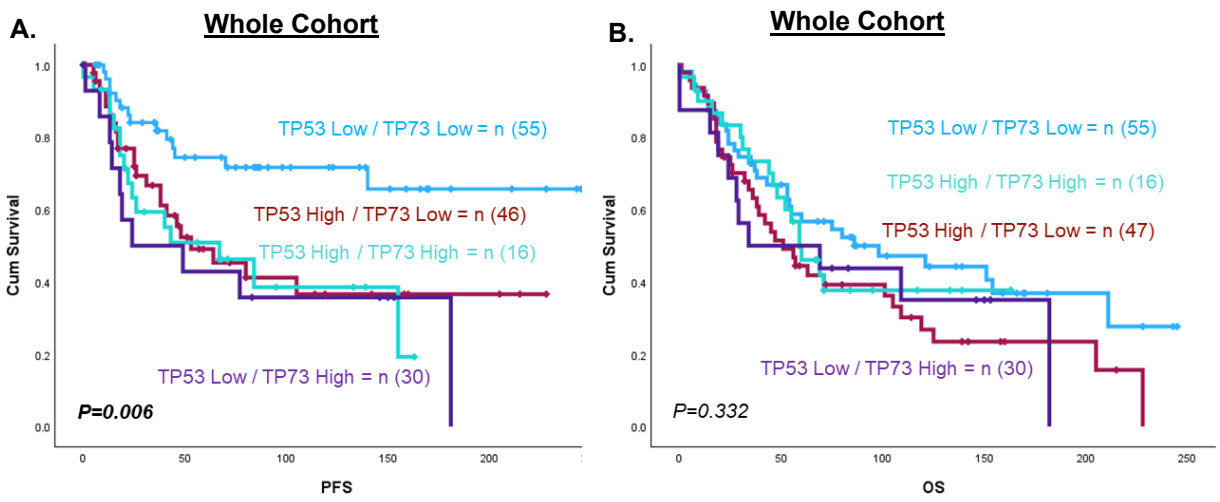

Figure 3-5. Kaplan Meier curve for TP53/TP73 co-expression in ovarian tumours. A. Kaplan-Meier curve showing the correlation between TP53/TP73 co-expression and progression-free survival (PFS) in the whole cohort. B. Kaplan-Meier curve showing the correlation between TP53/TP73 co-expression and overall survival in the whole cohort.

Our research group previously immune-profiled the expression of several DNA repair markers in the ovarian clinical cohort. Therefore, I investigated the correlations between TP73 expression and the levels of a various DNA repair markers. Firstly, moderate positive correlations were observed between the expression of TP73 and base excision repair (BER) related genes, including (LIG1, LIG3, LIG4, FEN1, NBS1, PTEN, MRE11, RAD50, PARP1, Polβ) (**Figure 3-6**). This result suggested a potential role of TP73 in BER.

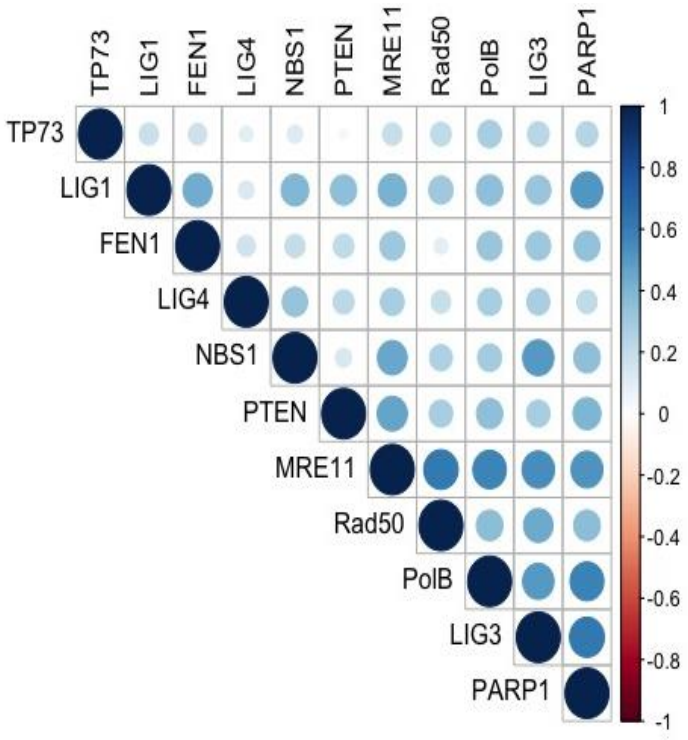

Figure 3-6. TP73 protein expression matrix in ovarian cancer. Correlation matrix showing the correlations between TP73 protein expression and the expression of other DNA repair biomarkers. 0 indicates no correlation. +1 means a positive correlation, while -1 indicates a negative correlation. The circle's intensity and size indicate the correlation, with red indicating a negative correlation and blue indicating a positive correlation.

Ovarian tumour tissue exhibited significantly higher TP73 mRNA expression compared to normal ovarian tissue (*P<0.0001*) (**Figure 3-7A**). The transcriptomic levels of TP73 were investigated in patients with EOC. High TP73 mRNA expression was significantly associated with poor PFS (*p=0.047*) (**Figure 3-7B**). In summary, these clinical analyses show that the protein and transcriptional expression levels of TP73 have predictive and prognostic significance in human EOC.

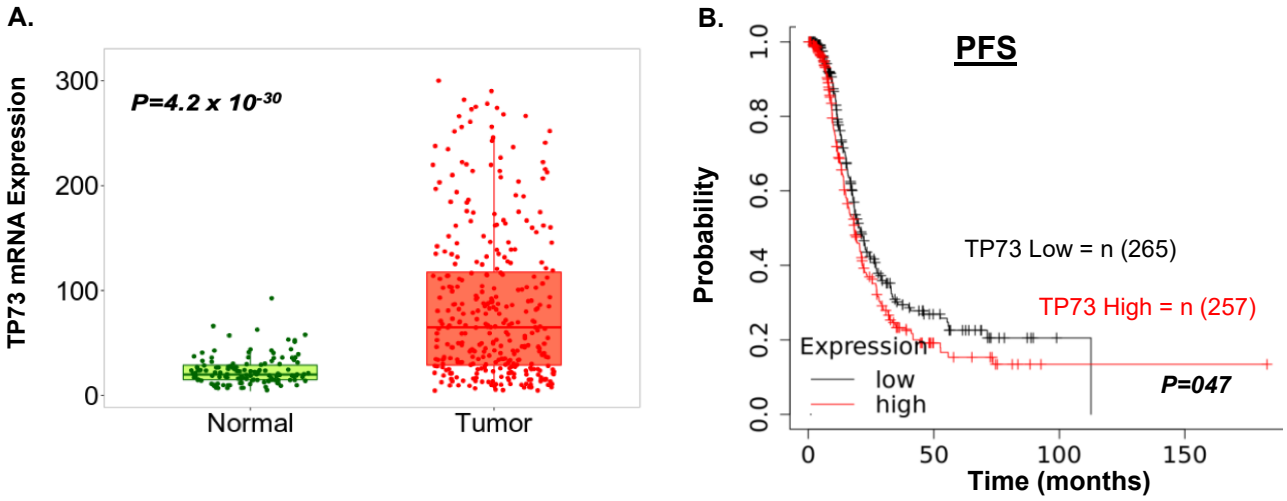

Figure 3-7. Transcriptional expression levels of TP73. A comparison of normal and tumorous ovarian tissue revealed differential TP73 mRNA expression. B. Clinicopathological studies of TP73 mRNA expression in OC. High TP73 mRNA expression was significantly associated with poor PFS.

TP73 overexpression is associated with aggressive clinicopathological characteristics. Additionally, high TP73 expression is correlated with poor prognosis for ovarian tumours. Similarly, elevated TP73 mRNA levels in EOC patients indicate unfavourable outcomes. This suggests the potential utility of this biomarker for therapeutic purposes and predicting responses to platinum compounds.

3.4.2 Pre-Clinical studies

IHC/transcript data findings showed that TP73 overexpression was significantly associated with the most aggressive clinicopathological features. TP73 overexpression was also an independent prognostic factor for survival. TP73 overexpression was associated with poor patient outcomes and may serve as a biomarker for prognosis and treatment. This data suggests that TP73 overexpression may be a key regulator of apoptosis, drug resistance, and cell proliferation, invasion and metastasis. Therefore, further preclinical studies are needed to investigate TP73's role in EOC.

In a panel of ovarian cancer cell lines, TP73 expression was evaluated by Western blotting. The intensities of TP73 (~70 kDa) and β-Actin (~42 kDa) bands were measured with LI-COR software. The TP73 readings were adjusted to β-Actin readings using Microsoft Excel 2011. GraphPad Prism, version 9 was used for data presentation and statistical analysis. The experiment was repeated three times (n=3) with independent samples, and the standard deviation (SD) is represented by the error bar (see Figure 3-8). The A2780 cell line is platinum-sensitive and established from a patient with untreated ovarian cancer. A2780cis cell line is platinum-resistant ovarian cancer developed by the continuous exposure of the A2780 cell line to increasing doses of cisplatin. PEO1 platinum-sensitive (BRCA2-deficient) cell line is derived from a patient with poorly differentiated serous adenocarcinoma treated with platinum-based drugs. PEO4 platinum-resistant (BRCA2-proficient) cell line was derived from a malignant effusion from the peritoneal ascites of the same patient after the development of clinical resistance to platinum treatment. OVCAR 4 is a cell line of high-grade serous

ovarian adenocarcinoma origin. It was derived from a patient who did not respond to cisplatin therapy and exhibited resistance to several other chemotherapeutic agents. The SK-OV-3 cell line is derived from human ovarian cancer and exhibits an epithelial-like morphology. These cells demonstrate resistance to cytotoxic drugs including cisplatin.

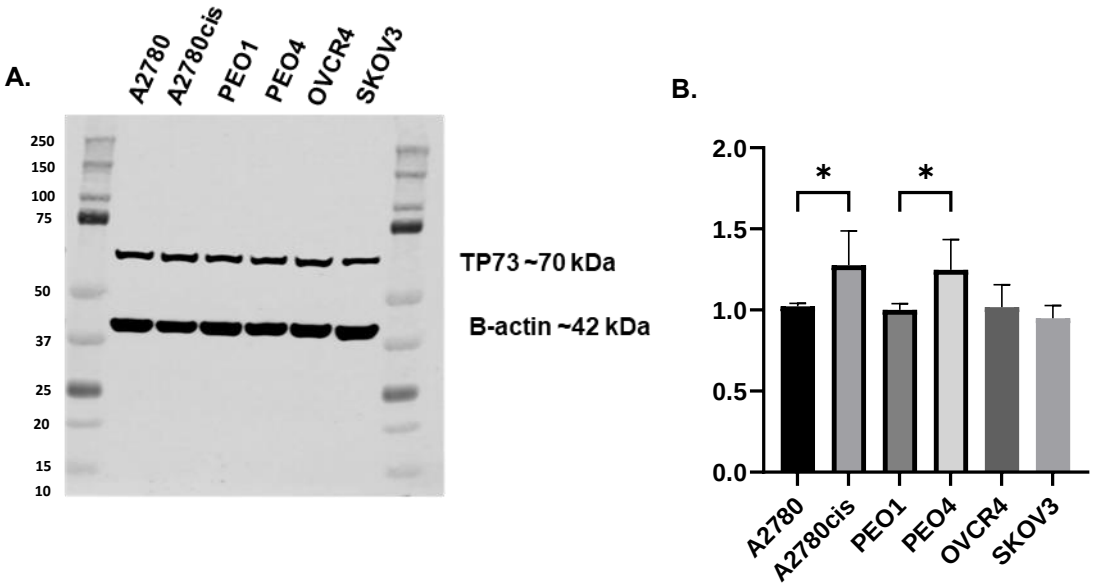

Figure 3-8. Western blot analysis for TP73. A.TP73 protein expression levels in a panel of ovarian cancer cell lines. B. Relative quantification of TP73 levels in ovarian cell lines. The readings for TP73 were normalized to those of β-actin using Microsoft Excel 2011. Data presentation and statistical analysis were performed using GraphPad Prism, version 9. The P value was calculated as follows, *p < 0.05. The experiment was performed for samples from three independent experiments n=3 and the error bar represent the standard deviation (SD).

In whole-cell lysates (**Figure 3-8**), the baseline TP73 protein level was high in A2780cis compared to A2780 cells. Similarly, the baseline TP73 protein level was high in PEO4 compared to PEO1 cells with (p=<*0.05*). To evaluate for induction of TP73 expression after cisplatin treatment, cells were treated with (1-5 uM) cisplatin for up to 48 h.

The level of TP73 significantly increased in all ovarian cell lines after 24 hours of cisplatin treatment. In A2780cis, the increase was higher than in A2780, and in PEO4, it was higher than in PEO1 (p=< 0.001) (**Figure 3-9**). TP73 level decreased after 48 hours of cisplatin treatment in A2780 compared to A2780cis and in PEO1 compared to PEO4.

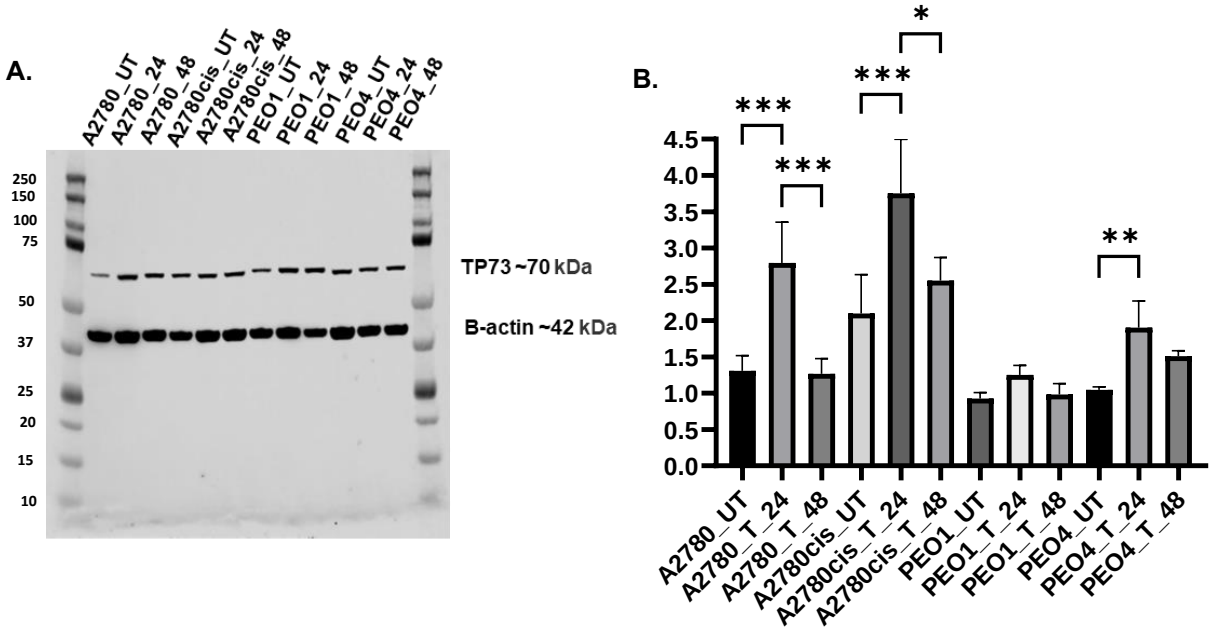

Figure 3-9. Western blot analysis for TP73 post cisplatin treated. TP73 protein expression levels in a panel of ovarian cancer cell lines before and after cisplatin-treated for 24h – 48h with relative quantification of TP73 levels in ovarian cell lines. Data presentation and statistical analysis were performed using GraphPad Prism, version 9. The P value was calculated as follows, *p <0.05, **p <0.01 and ***p <0.001. The experiment was performed for samples from three independent experiments n=3 and the error bar represent the standard deviation (SD).

After confirming the expression of TP73 protein in the ovarian cells, mRNA expression was determined by Quantitative real time PCR (RT-qPCR) using QuantiTect® Primers (Qiagen, UK) was as described in chapter 2. Relative expressions were calculated for each cell line and compared to their respective control cell lines. The mRNA expression of housekeeping GAPDH was used to standardize the samples. The relative expression of TP73

mRNA was calculated as the ratio between the expression of the TP73 gene and the expression of the housekeeping gene. Negative control was included in each experiment. GAPDH was used for all subsequent experiments. TP73 mRNA expression was detected in ovarian cancer cell lines at baseline, followed by cisplatin treatment for 24-48 hours (**Figure 3-10**).TP73 level was high after 24h cisplatin treatment in A2780cis compared to A2780 with no significant variance in PEO4 and PEO1. Moreover, TP73 level was decreased after 48h cisplatin treatment in all ovarian cell lines.

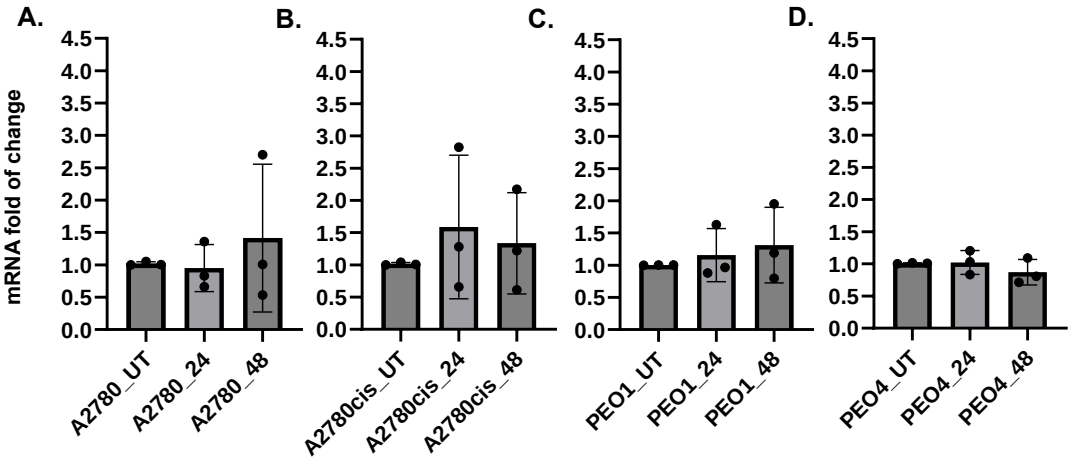

Figure 3-10. Real-time PCR analysis for TP73.TP73 mRNA level expression in a panel of ovarian cell lines following 24-48h cisplatin treatment. Values plotted are means ± SD of the fold-change (ratio of mRNA/GAPDH normalized to control). Graphs were produced, and statistical analysis was performed using GraphPad Prism 9.

To monitor TP73 sub-cellular localisation, the nuclear and cytoplasmic extracts were generated at baseline and following 2h, 4h, 8h, 24, and 48h of cisplatin therapy. In platinum-resistant A2780cis and PEO4 cells, platinum treatment increased TP73 nuclear and cytoplasmic sub-cellular localisation compared to platinum-sensitive A2780 and PEO1 cells. Furthermore, significant alterations were observed in the nuclear expression of TP73 in A2780 cells compared to the nuclear expression of TP73 in A2780cis after

4h, 8h, and 24h. While the TP73 cytoplasmic expression was significantly observed after the 24h. In addition, significant alterations were observed in the nuclear expression of TP73 in PEO1 cells compared to the nuclear expression of TP73 in PEO4 after 4h, 8h, 24h, and 48h. The TP73 cytoplasmic expression was significantly observed after the 2h, 4h, 8h, 24h and 48h. The data suggest that TP73 protein overexpression is subjected to sub-cellular localisation upon cisplatin treatment in the ovarian cell lines.

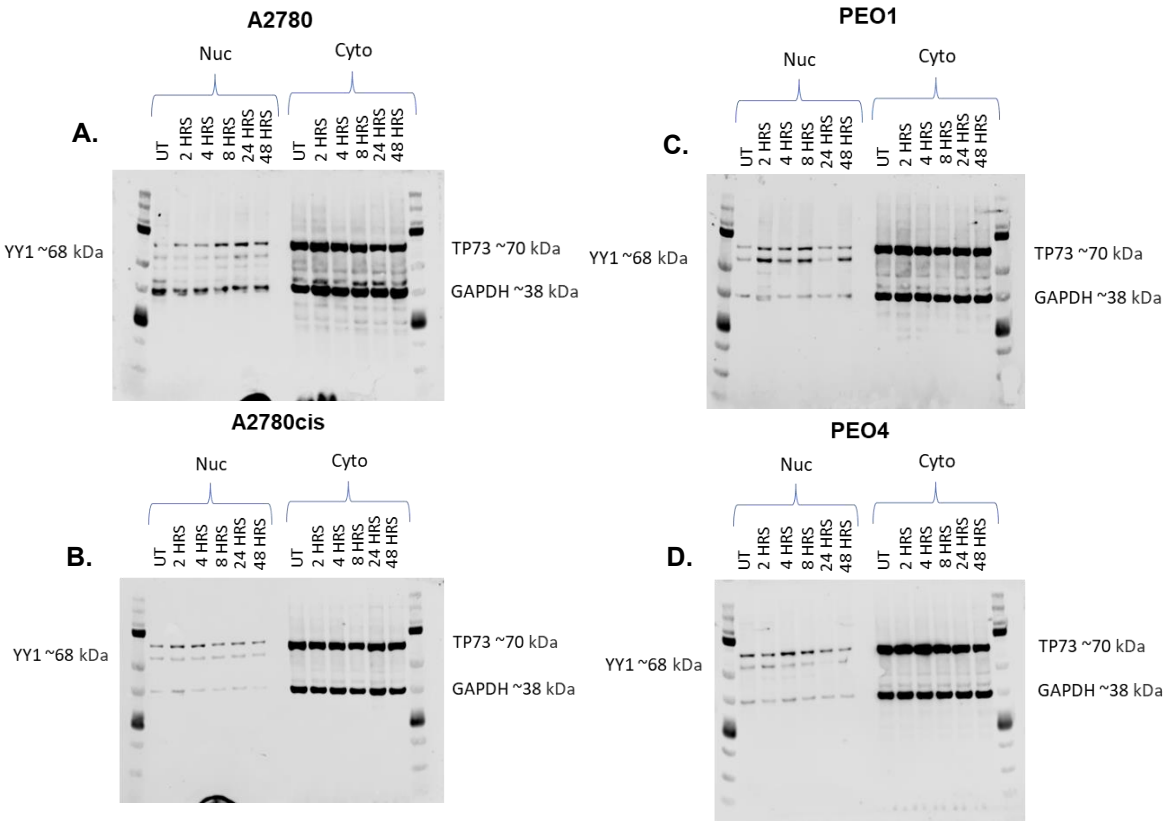

Figure 3-11. Representative western blots of TP73 nuclear and cytoplasmic expression in A2780, A2780cis, PEO1 and PEO4 following cisplatin-treated at different time points. The Materials and Methods chapter describes the nuclear and cytoplasmic extraction protocol. TP73 nuclear expression was normalised to YY1. TP73 cytoplasmic expression was normalised to GADPH. A. TP73 nuclear/cytoplasmic expression in A2780 cells in early points from 2 up to 48 hours of 2 μM cisplatin treatment. B. TP73 nuclear/cytoplasmic expression in A2780cis cells after 5 μM of cisplatin treatment from 2 up to 48 hours. C.TP73 nuclear /cytoplasmic expression in PEO1 cells after 2 up to 48 hours of 2 μM cisplatin treatment. D. TP73 nuclear expression in PEO4 cells after 2 up to 48 hours of 5 μM cisplatin treatment.

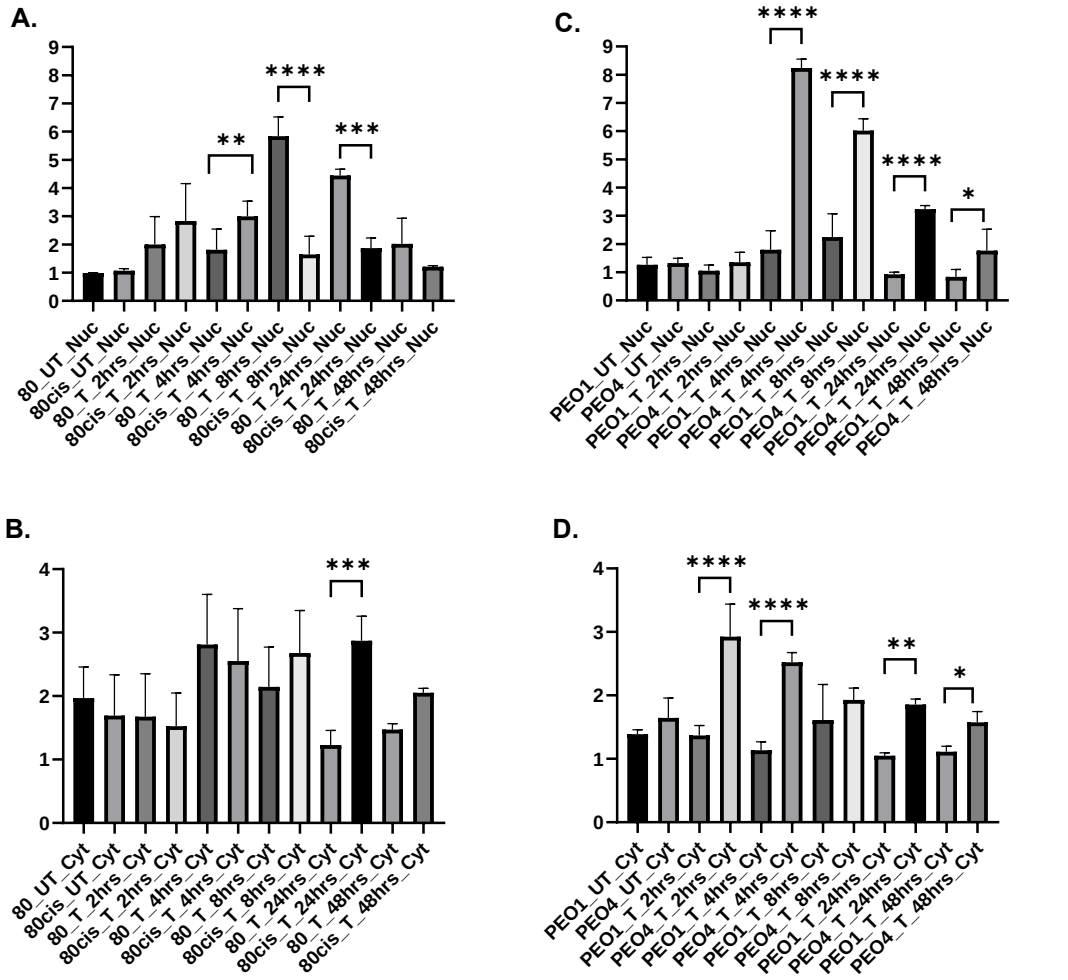

Figure 3-12. Nuclear and cytoplasmic analysis of TP73 in a panel of ovarian cells. A. Representative quantification of combined TP73 nuclear expression in A2780 and A2780cis following cisplatin-treated in various time points. B. Representative quantification of combined TP73 cytoplasmic expression in A2780 and A2780cis following cisplatin-treated in various time points. C. Representative quantification of combined TP73 nuclear expression in PEO1 and PEO4 following cisplatin-treated in various time points. Representative quantification of combined TP73 cytoplasmic expression in PEO1 and PEO4 following cisplatin-treated in various time points. Data presentation and statistical analysis were performed using GraphPad Prism, version 9. The P value was calculated as follows, *p <0.05, **p <0.01, ***p <0.001 and ****p <0.0001. The experiment was performed for samples from three independent experiments n=3 and the error bar

A2780 (platinum-sensitive) cell line was selected and transiently transfected with TP73 (pcDNA) to investigate the consequence of TP73 overexpression on proliferation, cell cycle, apoptosis, invasion, migration and platinum resistance. The successful knock-in of TP73 was validated using Western blot and qPCR (**Figure 3-13**).

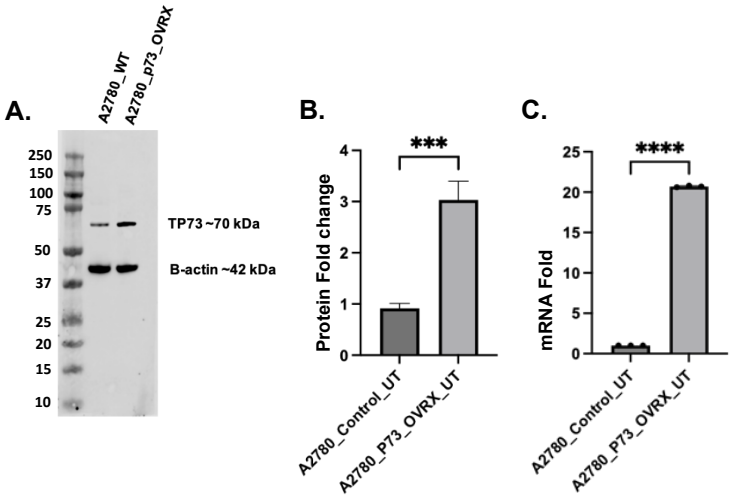

Figure 3-13. Western blot validation for TP73 overexpression. A. Western blot for TP73_Knock in (Overexpression) in A2780 cells. B. Quantification of P73 protein expression relative to β-Actin levels in A2780 and A2780_TP73_Knock-in cell line. C. TP73 mRNA level expression of TP73 in A2780 and A2780_TP73_knock-in cell line, values plotted are means ± SD of the fold-change (ratio of mRNA/GAPDH normalized to control).

The cell doubling time assay results showed a significantly slower growth rate in the A2780 wild-type control compared to A2780_TP73_Knock-in **(Figure 3-14)**. The data suggests that TP73 overexpression may play a role in cell growth and cell proliferation, but the molecular mechanism behind these effects remains to be elucidated. Clonogenic assays showed that A2780 TP73_Knock-in cells were significantly more resistant to cisplatin treatment than the wild type of control cells **(Figure 3-15 and Figure 3-16)**. Next, functional studies using FACS were conducted for TP73_Knock-in A2780 cells and A2780 wild types of control cells. After 24-48 hours of treatment with 1 μM cisplatin, A2780 wild types of cells exhibited significant accumulation of γH2AX compared to A2780 TP73_Knock-in cells. Accumulation of DSBs leads to activation of cell cycle checkpoints, resulting in cell cycle arrest, which allows the cells to repair DNA damage. Cells undergo apoptosis if the damage is irreparable. Thus, the effects of cisplatin

on the cell cycle and apoptosis were examined in the TP73 overexpression and control cells. After 24-48 hours of treatment with cisplatin, significantly higher proportions of cells arrested in the S phase and apoptotic cells were observed in the wild-type controls compared to TP73_Knock-in cells, as shown in **(Figure 3-17 and Figure 3-18)**.

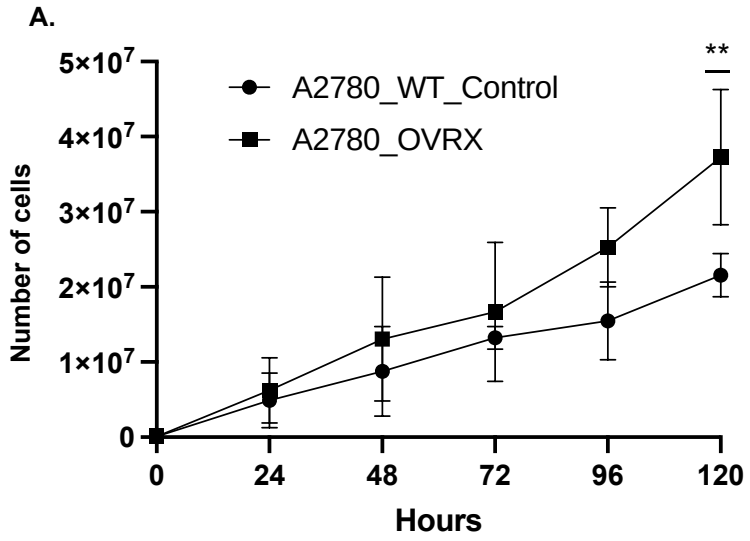

Figure 3-14. Representative the corresponding doubling times incubation for A2780 wild-type and A2780_TP73_Knock-in cells. The P-value was calculated as; **p<0.01. Data presentation and statistical analysis were performed using GraphPad Prism, version 9. The experiment was performed for samples from three independent experiments n=3 and the error bar represent the standard deviation (SD).

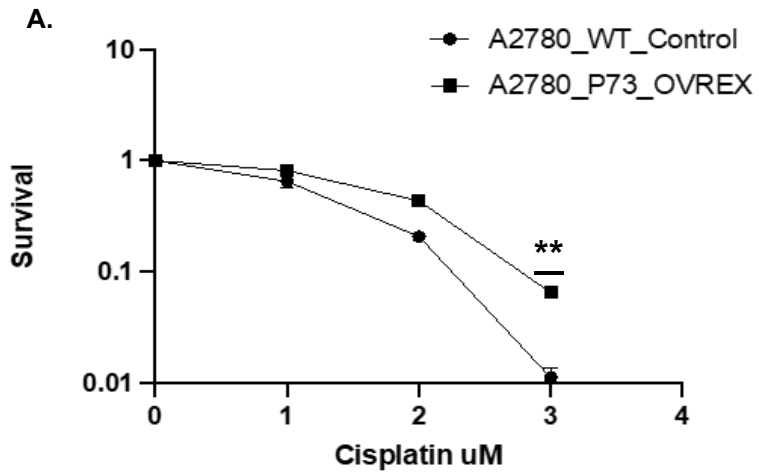

Figure 3-15. A plot of Clonogenic assay of cisplatin sensitivity in A2780 wild-type and A2780_TP73_Knock-in cells. A. Overexpression of TP73 increased cisplatin resistance in A2780 cells. The P-value was calculated as; **p<0.01. Data presentation and statistical analysis were performed using GraphPad Prism, version 9. The experiment was performed for samples from three independent experiments n=3 and the error bar represent the standard deviation (SD).

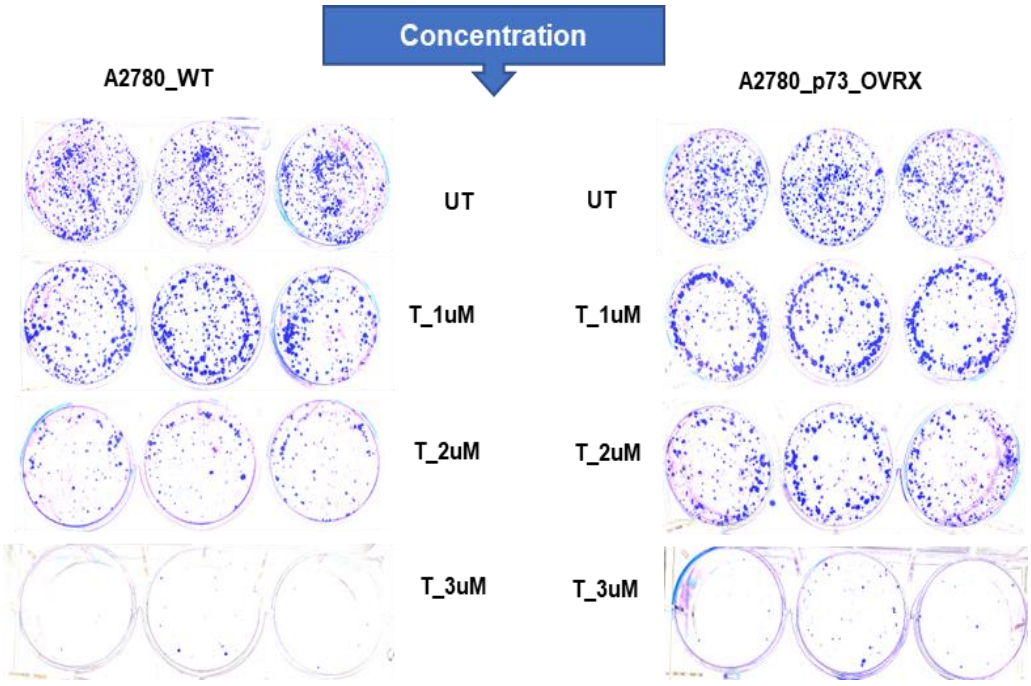

Figure 3-16. Clonogenic survival assay for A2780 (TP73_overexpression) in different doses of Cisplatin. A2780 control and TP73_Knock-in A2780 cells (350 cells/well) were plated into 6-well plates, incubated overnight, and then treated with the indicated doses of cisplatin for 14 days. Colonies were fixed and stained with crystal violet.

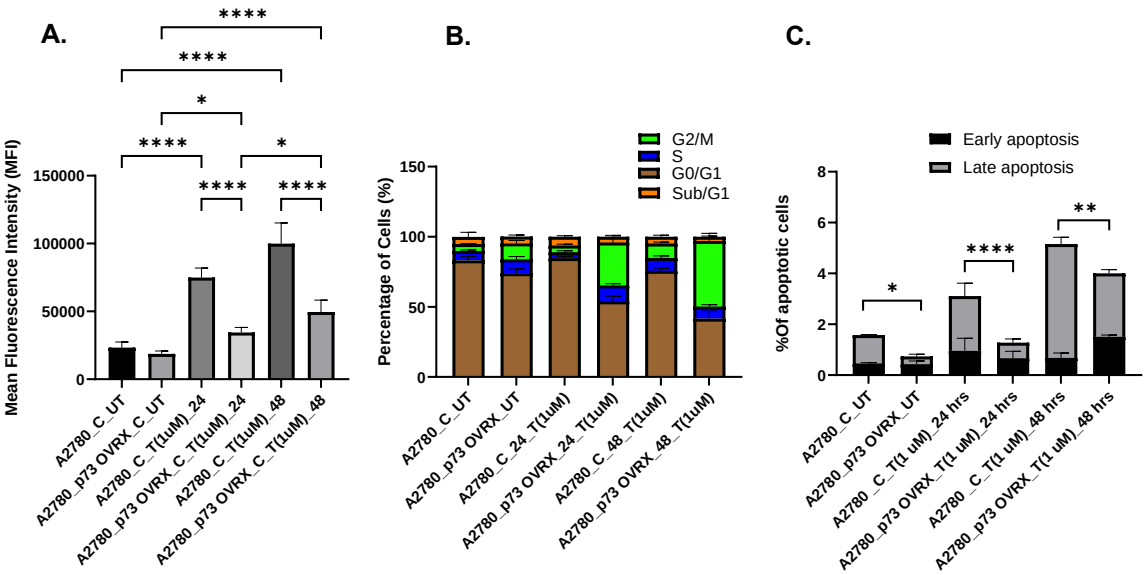

Figure 3-17.Cell cycle analysis of TP73. A. Functional studies of cisplatin sensitivity in A2780 control and A2780_TP73_Knock-in cells. Treated with 1μM cisplatin for 24-48h. B. γH2AX analysis by flow cytometry for A2780 control and A2780_TP73_Knock-in cells treated with 1μM cisplatin for UT-24-48h. UT = untreated cells; T = treated cells. Data presentation and statistical analysis were performed using GraphPad Prism, version 9. The P value was calculated as follows, *p <0.05, **p <0.01, ***p <0.001 and ****p <0.0001. The experiment was performed for samples from three independent experiments n=3 and the error bar represent the standard deviation (SD).

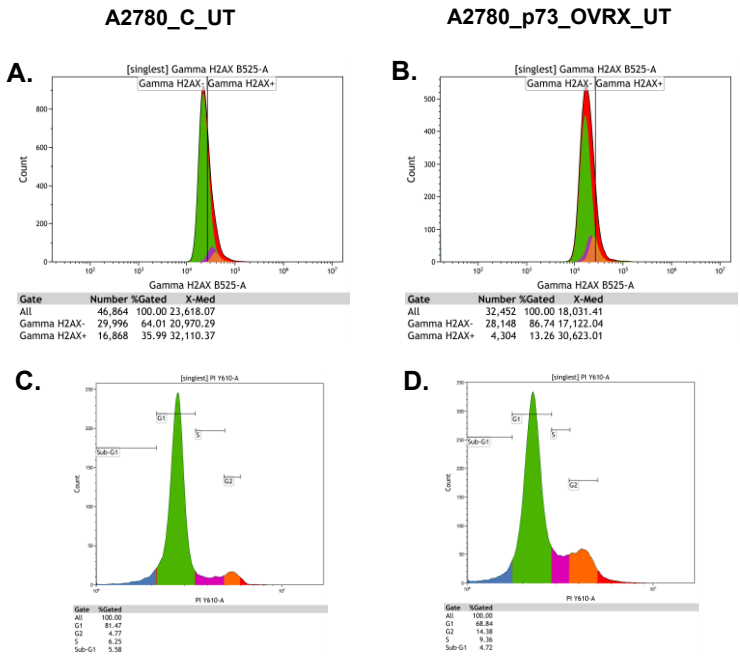

Figure 3-18. γH2AX and PI Staining were performed using follow cytometry. A. and B. A2780 wild-type control cells and A2780_p73_Knock-in cells analysis for γH2AX accumulations. C. and D. A2780 wild type control cells and A2780_p73_Knock-in cells analysis for cell cycle sub/G1, G1, S phase, G2/M arrest.

The findings presented so far indicated that the upregulation of the TP73 gene in ovarian cancer cells increases their resistance to cisplatin.TP73 overexpression may also promote invasion.To investigate this, A2780 wild-type control and A2780_TP73 knock-in ovarian cancer cells were seeded into an upper chamber coated with Matrigel, a matrix-like substance mimicking a barrier to simulate the metastatic process. ncubation, the cells may degrade the ECM and invade through the membrane pores to the lower chamber, which contains serum as a chemoattractant to drive invasion. Invaded cells are stained and quantified to assess invasiveness and evaluate the effects of drugs or genetic modifications on invasion behaviour. A2780_TP73 knock-in cells exhibited significantly higher invasive capacity and enhanced EMT than A2780 wild-type controls **(Figure 3-19)**.

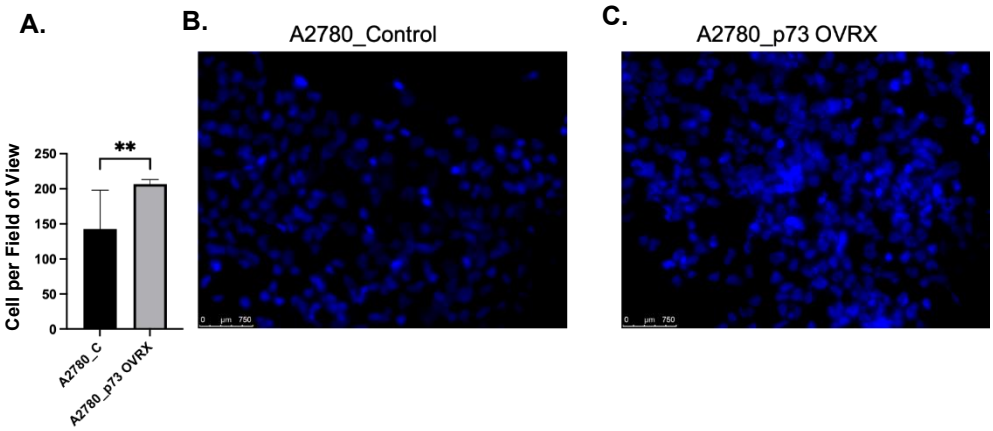

Figure 3-19. Invasion assay in A2780 and A2780_TP73_Knock-in cells. A. quantification of invasive cells for A2780 compared to A2780_TP73_Knock-in cells using Image J software (Fiji). The P value was calculated as **p <0.01. B. A2780 and A2780_TP73_Knock-in cells across a porous membrane coated with synthetic ECM inserts in 24 well plates stained with DAPI. Images were taken with a Nikon camera microscope at 20X magnification.

The study then assessed the impact of TP73 overexpression on migration ability. The study demonstrated a significant improvement in wound closure

in A2780_knock-in cells, which exhibited accelerated healing through enhanced migratory capacity. In contrast, A2780_wild type controls displayed reduced motility, resulting in slower wound closure rates (T24*: p = 0.001;* T48*: p=< 0.0001;* T72*: p=<0.0001;* T96*: p=<0.0001*) **(Figure 3-20).**

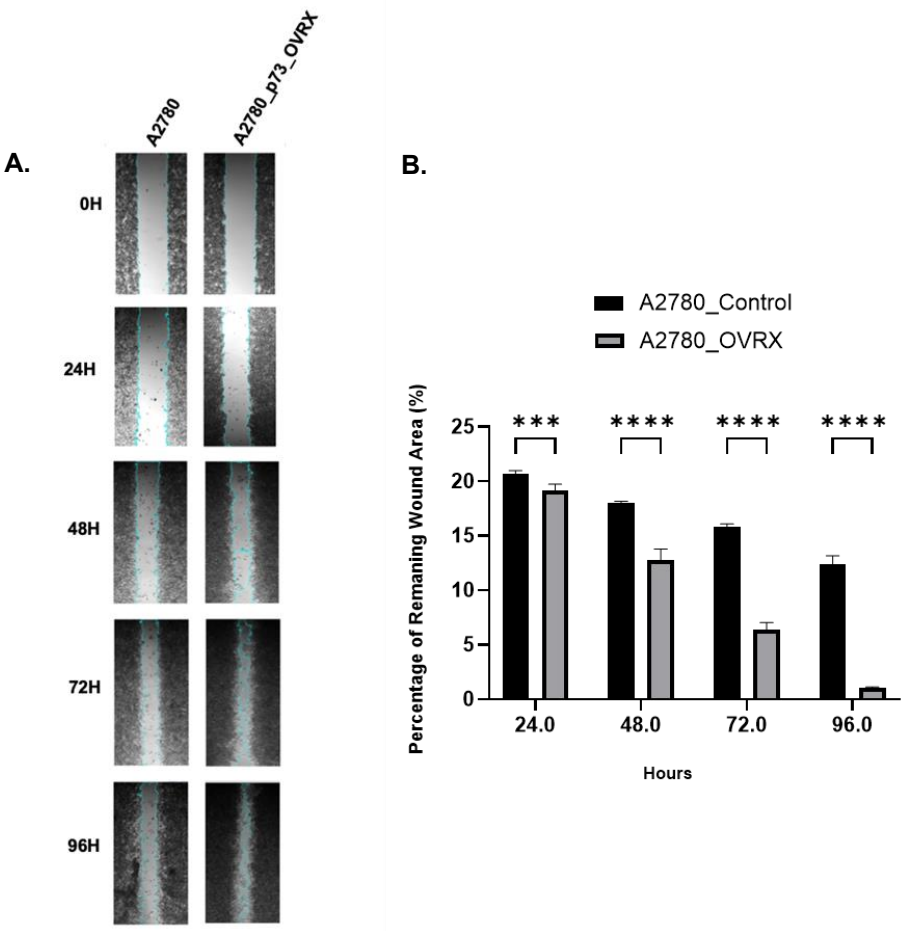

Figure 3-20. Wound-closure assays cell migration for ovarian cell lines. A. Representative images of the wound-closure assays in A2780 wild-type control and A2780_p73_Knock-in cells cell lines. B. Representative wound-closure measurement using ImageJ software (Fiji). Data presentation and statistical analysis were performed using GraphPad Prism, version 9. P values are indicated as follows: ***p < 0.001, ****p < 0.0001. The error bar indicates the standard error of the mean.

3D spheroids of A2780_TP73-knock-in and A2780_wild type control were tested for cisplatin sensitivity. A2780 wild-type control cells typically develop smaller, less compact spheroids. In contrast, TP73_knock-in cells exhibit the

formation of larger, denser spheroids. Quantification of viable/dead cells using calcein AM and ethidium homodimer showed a decrease in ethidium staining in A2780_TP73_knock-in compared to A2780_wild type control spheroids before and after cisplatin treatment for 24h and 48h **(Figure 3-21).** The data provides evidence that A2780_TP73_knock-in spheroids are resistant to cisplatin compared to A2780_wild type control spheroids.

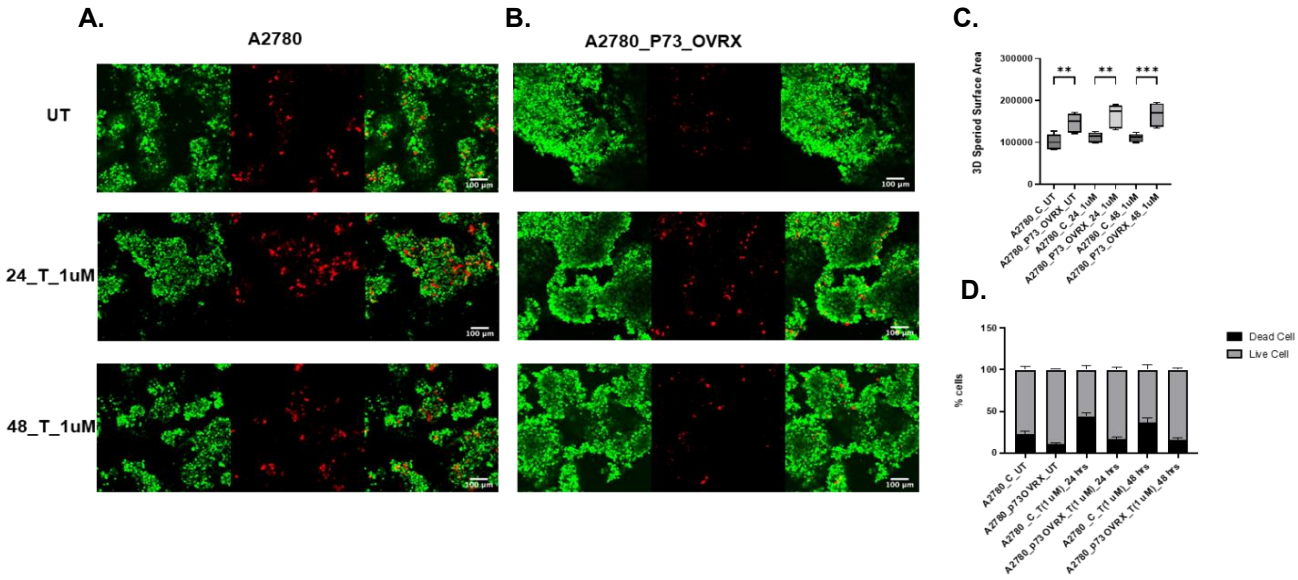

Figure 3-21. A. Representative photomicrographic images for 3D spheroids of A2780 control and A2780_TP73_Knock-in cells following with cisplatin-treated (1μM) for 24 - 48 h. B. Quantification of spheroids size by ImageJ software (Fiji). C. Quantification of spheroids cell viability by ImageJ software (Fiji). Figures are representative of three independent experiments. Data presentation and statistical analysis were performed using GraphPad Prism, version 9. The P value was calculated as follows, **p < 0.01 and ***p < 0.001. Error bars represent the standard error of the mean between experiments.

The data shown so far suggest that TP73 overexpression may influence the expression of certain DNA repair genes or pathways to promote cisplatin resistance. To explore this possibility, the DNA repair specific PCR expression array was performed.

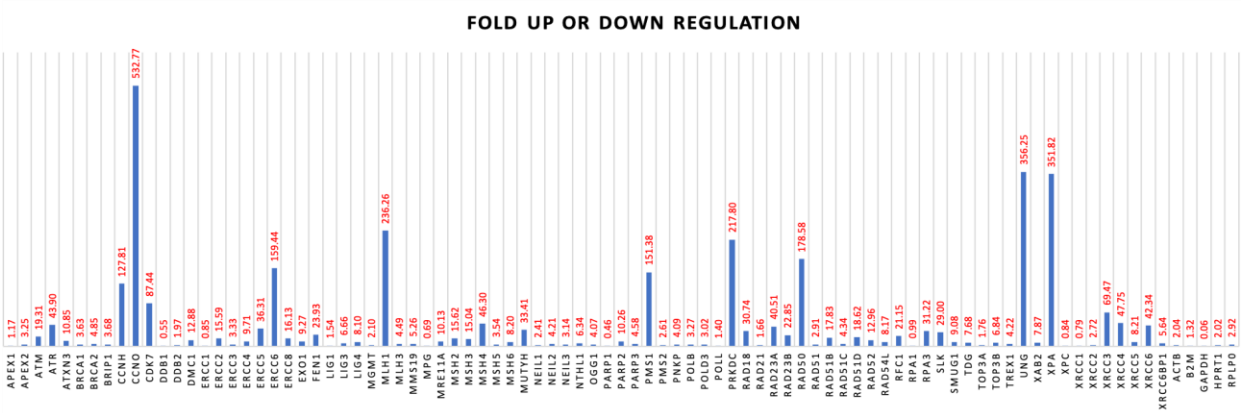

Figure 3-22. Real-time PCR analysis using RT^2 profiler human DNA repair array to assist expression of 84 genes involved in DNA damage signalling and repair in A2780 control and A2780_TP73_Knock-in ovarian cancer cells. The data demonstrated that the expression of several genes that are involved in DNA damage signalling and response such as (ATM, ATR, MRE11, PRKDC, RAD50), mismatch repair (MLH1, MSH2, MSH3, MSH4, PMS1), nucleotide excision repair (XPA, ERCC1, ERCC4, ERCC5, ERCC6), homologous recombination (XRCC3, RAD51), non-homologous end joining (XRCC4, XRCC6) and base excision repair (UNG) were upregulated in A2780_TP73_knock-in cells when compared with A2780 wildtype control cells. Analysis of the RT^2-PCR profiler was performed on the Qiagen website. Normalization against GADPH housekeeper expression was performed.

Using the Qiagen RT^2 Profiler PCR array assay to measure the expression levels of multiple genes involved in specific biological pathways between A2780 and A2780 (TP73_Overexpession) (**Figure 3-22)**. The Qiagen RT^2 Profiler PCR array assay can help identify which genes are upregulated or downregulated in response to TP73 overexpression. The RT^2 profiler is a high throughput assay that can concurrently detect the expression of 84 pathway-specific mediator genes. The assay comes in a 96-well plate format; each well is pre-coated with the specific primer. In addition to the 84 EMT-specific genes, there are 5 housekeeper genes for data normalisation and several quality control measures. The genomic DNA control (GDC) wells assist with detecting non-transcribed genomic DNA within the isolated mRNA. PCR positive control (PPC) specifically detects non-transcribed genomic DNA contamination with high sensitivity. The reverse-transcription

control (RTC) was performed earlier using the RT^2 first strand kit to determine the efficacy of the reverse transcription reaction.

Table 14. The top up-regulated genes involved in DNA repair.

Gene	Description
ERCC6	Excision Repair Cross-Complementation Group 6
PMS1	Postmeiotic Segregation Increased 1
MLH1	MutL Homolog 1
XPA	Xeroderma Pigmentosum, Complementation Group A

To further validate, Western blot analysis was performed in A2780_TP73_Knock-in and A2780 wild-type control cells for the top-upregulated genes involved in DNA repair (**Table 14**). Using the TP73 expression level as a positive control confirmed the TP73 overexpression within the A2780_TP73_knock-in cell line (**Figure 3-23A, B**). The expression level of ERCC6 was significantly higher in A2780_TP73_Knock-in compared to A2780 wild-type control cell lines (p=<*0.001*) **(Figure 3-23C, D).** A high expression level of PMS1 was significantly associated with A2780_TP73_Knock-in compared to A2780 wild-type control cell lines (p=<*0.001*) **(Figure 3-23E, F).** Similarly, a high MLH1 expression level was significantly linked with A2780_TP73_Knock-in compared to A2780 wild-type control cell lines (p=<*0.0001*) **(Figure 3-23G, H).** finally, the high expression level of XPA was significantly associated with A2780_TP73_Knock-in compared to A2780 wild-type control cell lines (p=<*0.001*) **(Figure 3-23I, J)**.

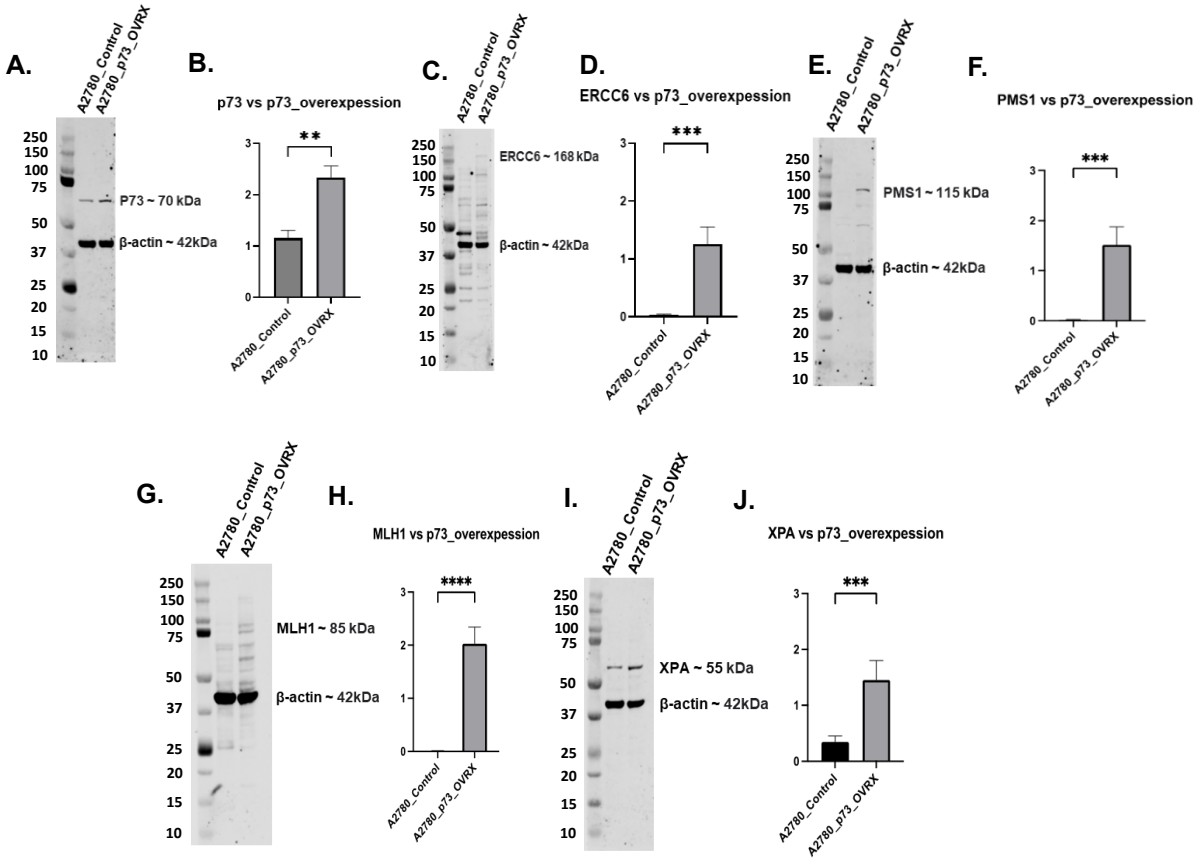

Figure 3-23. Western blots for A2780 and A2780_TP73_Knock-in cells for more validation regarding upregulating genes by TP73 overexpression. A. and B. TP73 protein expression levels normalized by B-actin with relative quantification. C. and D. ERCC6 protein expression levels normalized by B-actin with relative quantification. E. and F. PMS1 protein expression levels normalized by B-actin with relative quantification. G. and H. MLH1 protein expression levels normalized by B-actin with relative quantification. I. and J. XPA protein expression levels normalized by B-actin with relative quantification. The P value was calculated as follows, **p < 0.01 and ***p < 0.001. Data presentation and statistical analysis were performed using GraphPad Prism, version 9.

The upregulation of multiple DNA repair pathway genes, including ERCC6, PMS1, MLH1, and XPA, in p73-overexpressing cells likely enhances their ability to detect and repair platinum-induced DNA damage, thereby reducing the efficacy of platinum-based therapies. Platinum compounds exert cytotoxic effects by forming DNA adducts and crosslinks that disrupt DNA replication and transcription. However, increased expression of genes pivotal in DNA repair pathways may counteract these effects.

Specifically, XPA and ERCC6, key components of the nucleotide excision repair (NER) pathway, facilitate the recognition and removal of platinum-DNA adducts. Simultaneously, the upregulation of PMS1 and MLH1, crucial to the mismatch repair (MMR) pathway, helps correct replication errors arising from platinum-induced DNA damage. This coordinated activation of NER and MMR pathways reflects a robust and multifaceted DNA damage response that enables cells to tolerate and proliferate under chemotherapy-induced stress.

These observations highlight the complex interactions among DNA repair mechanisms, suggesting that targeting specific DNA repair pathways or their regulatory networks could provide novel therapeutic strategies to overcome platinum resistance in cancer.

3.5 Discussion

TP73 is a transcription factor that belongs to the TP53 tumour suppressor family. It has a high degree of structural and functional homology with TP53. Unlike TP53, TP73 is rarely mutated in cancer. TP73 isoforms have been shown to inhibit various hallmarks of cancer and can mimic the tumour-suppressive functions of TP53, even in TP53-mutated cells (Jost et al., 1997; Kaelin, 1999; Yang et al., 2000). TP73 plays a crucial role in tumour development, exhibiting both tumour-suppressive and oncogenic behaviours. It regulates apoptosis, the DNA damage response, angiogenesis, epithelial-mesenchymal transition, senescence, and maintaining genomic stability (Gonzalez-Cano et al., 2010; Tomasini et al., 2008). However, cancer cells have developed mechanisms to suppress TP73-mediated cell death, and inactive isoforms of TP73 are often overexpressed in cancers (Concin et al., 2004; Laubach et al., 2022; Müller et al., 2005). Understanding TP73 regulation and function may help TP73 developing targeted therapies for cancer and other pathological conditions (Zaika et al., 2001; Zawacka-Pankau et al., 2010). Previous research has highlighted the involvement of TP73 in the development of ovarian cancer. For example, a study by Ng et al (Ng et al., 2000) found increased TP73 expression in various ovarian cancer cell lines and human tumours. Similarly, (Zwahlen et al., 2000) reported higher TP73 mRNA splice variants and TP73 protein levels in invasive ovarian cancers compared to ovarian adenomas, though neither study explored clinicopathological correlations. A study in 100 ovarian tumours, (Concin et al., 2004) found frequent upregulation of the trans-dominant ΔTAp73 isoforms, which can inhibit TP53 epigenetically and are linked to

more aggressive disease characteristics. In a later study, Concin et al (Concin et al., 2005) showed that these ΔTAp73 isoforms contribute to cisplatin resistance, particularly in TP53-mutant ovarian cancers. Our current results suggest that tumours with low TP73 expression and wild-type TP53 are associated with better progression free survival (PFS), implying increased sensitivity to platinum-based therapies. TP73 overexpression has also been observed in other solid tumours, such as liver, bladder, prostate, and colorectal cancers (Stiewe and Putzer, 2002; Rufini et al., 2011; Logotheti et al., 2021), while TP73 loss has been documented in pancreatic cancers (Loukopoulos et al., 2007).

The TP73 locus can produce multiple isoforms, and evidence indicates that the balance between TA and ΔN splice variants may impact tumour biology and prognosis. Specifically, overexpression of ΔNp73 has been associated with aggressive features and poor outcomes in cancers such as neuroblastoma, prostate, head and neck, and cervical cancers (Stiewe and Putzer, 2002; Rufini et al., 2011; Logotheti et al., 2021). One limitation of our study is the inability to examine individual TP73 splice variants, as specific antibody clones for these isoforms were unavailable. For immunohistochemistry (IHC), we used a rabbit monoclonal anti-TP73 antibody (Abcam clone ab189896), which, according to the manufacturer, recognises a C-terminal fragment of TP73 (amino acids 380-636). This implies that the antibody detects all TP73 isoforms, and the expression levels observed reflect the total TP73 content in the cells.

Mutations in TP53 can result in its stabilisation and accumulation within cells, making TP53 overexpression a commonly used marker for TP53 mutation

status in tumours (Cole et al., 2016). Our finding that TP53 overexpression correlates with an aggressive tumour phenotype and shorter progression free survival (PFS) is consistent with previous clinical reports (Tuna et al., 2020). Additionally, our data show that tumours overexpressing both TP53 and TP73 have worse PFS than TP53 wild-type tumours with low TP73 levels. In TP53 wild-type tumours, TP73 overexpression is also linked to poorer clinical outcomes, suggesting that the interaction between TP53 and TP73 may significantly influence ovarian cancer progression. However, further mechanistic studies are needed to confirm this hypothesis. Our bioinformatics analyses also suggest that TP73 overexpression may alter DNA expression patterns, potentially driving a more aggressive tumour phenotype.

The clinicopathological and functional significance of TP73 in ovarian cancer remains largely unexplored. Our findings indicate that TP73 overexpression correlates with an aggressive phenotype characterised by high tumour grade, advanced-stage disease, and reduced progression free survival (PFS). Notably, significantly elevated levels of TP73 transcripts were observed in tumour tissues compared to normal tissues and were associated with shorter PFS. In preclinical models, TP73 overexpression in A2780 cells was associated with increased proliferation, invasion, spheroid formation, DNA repair capacity, upregulation of several DNA repair genes, and enhanced platinum resistance.

Chapter 4 TP73 in Breast Cancer

4.1 Introduction

TP73 shares structural and functional similarities with the widely known tumour suppressor TP53. The contribution of TP73 to breast cancer pathogenesis may differ depending on the isoform or circumstances in which the cancer develops (Oswald & Stiewe, 2008; Rufini et al., 2011). TP73, like TP53, has been implicated in regulating cell cycle progression and induction of apoptosis (Jost et al., 1997; Maas et al., 2013). TP73 acts as a tumour suppressor by promoting cell cycle arrest and cell death in response to various stress signals (Ozaki & Nakagawara, 2005; Zawacka-Pankau et al., 2010). TP73 splice variants are generated within cells through alternative splicing events and different promoters. Multiple TP73 isoforms generated by splicing at both the 5' and 3' ends and using alternative promoters have been described. These isoforms include TAp73 (C-terminally transactivation-proficient isoforms) and ΔNp73 (N-terminally truncated isoforms). The two isoforms can have opposing effects on cell fate, with TAp73 generally promoting apoptosis and ΔNp73 often exerting anti-apoptotic functions (Candi et al., 2014; Laubach et al., 2022; Vikhreva et al., 2018). Expression levels of TP73 in breast cancer tissues have been investigated as potential prognostic markers (C.-O. Leong et al., 2007). Some studies have suggested correlations between altered TP73 expression and clinical outcomes, including disease progression and patient survival (Chen, 2022; Gomez et al., 2018). The role of TP73 in breast cancer may vary among different molecular subtypes of the disease. Studies have explored whether TP73

expression levels or genetic variations are associated with specific breast cancer subtypes, providing insights into potential subtype-specific functions. TP73 has been implicated in the response to chemotherapy in breast cancer (Wang et al., 2023). Alterations in TP73 expression may influence the sensitivity of cancer cells to various chemotherapeutic agents (Gong et al., 1999). Post-translational modifications and interactions with other proteins can modulate TP73 activity (DeYoung & Ellisen, 2007; C. O. Leong et al., 2007; Omran et al., 2021).

4.2 Aims of this study

1- Examine TP73 expression in invasive breast cancer

a- To investigate the expression patterns of TP73 in invasive breast cancer using immunohistochemistry (IHC) on tissue microarrays (TMAs) from 4221 patients.

b- To correlate TP73 expression (specifically cytoplasmic) with clinicopathological features and patient outcomes, utilizing the H-score to quantify immune staining.

2- Evaluate the clinical and molecular significance of TP73/TP53 co-expression

a- To examine the link between TP73/TP53 co-expression and prognostic factors such as the Nottingham Prognostic Index (NPI), disease stage, and molecular subtypes (HER-2+, ER-/PR-, and TNBC).

3- Assess the expression of TP73 in breast cancer cell lines

a- To evaluate TP73 expression in a panel of breast cancer cell lines, including MCF10-A (normal epithelial), DCIS (ductal carcinoma in situ), MCF7 (ER+), T47D (ER+), and MDA-MB-231 (triple-negative).

b- To explore the potential differences in TP73 expression across various breast cancer subtypes and normal breast epithelial cells, providing insight into its role in breast cancer progression.

4.3 Method

Immunohistochemistry of TP73 was performed on TMAs of 4221 patients with invasive breast cancers. Patient demographics are summarized in chapter 2. The immunohistochemistry protocol and antibody details are described in Materials and Methods chapter. Evaluation of immune staining was performed by calculation of H-scores (range 0–300). For TP73 cytoplasmic expression, an H-score cut off of ≤ 43 was used. A panel of breast cell lines used in this study are MCF10-A, DCIS, MCF7, T47D, and MDA-MB-231. Media used to maintain all the cell lines as well as cell passaging, and storage are described in the Materials and Methods chapter. Assays used in this study include western blotting, as detailed in the Methods section. All experiments were repeated 3 times. Data analysis was performed on GraphPad Prism-7 software. Error bars represent the standard error of the mean between experiments. P-values are indicated as p-value <0.05 =*, p-value <0.01 =**, p-value <0.001=*** and p-value <0.0001=****.

4.4 Results

4.4.1 Clinical study

The expression of TP73 in ductal carcinoma in situ (DCIS) and invasive breast cancer (IBC) was examined by IHC staining to determine whether TP73 is associated with the clinicopathological features of BC. The expression of TP73 was examined in 776 cases of pure DCIS, 239 cases of invasive BC coexisting with DCIS, 4221 cases of invasive breast cancer, and 50 normal breast tissues. The demographics and pathological characteristics of these patients are described in Chapter 2.

The immunohistochemical staining revealed that TP73 protein was expressed within the nucleus and cytoplasmic of both normal and cancerous tissues as shown in (**Figure 4-1 and Figure 4-2**).

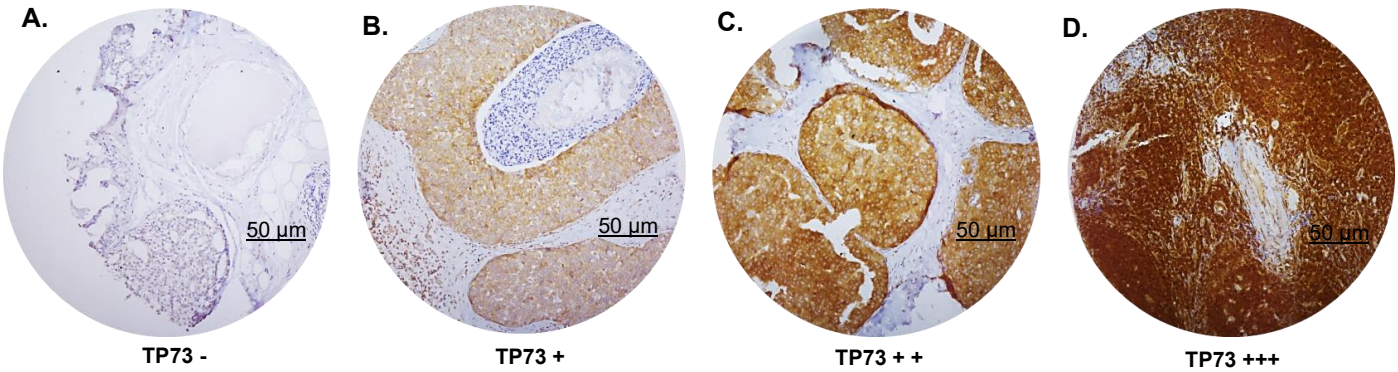

Figure 4-1. Immunohistochemistry staining of p73 in DCIS. Representative images of negative and positive staining in DCIS TMAs imaged at (x20 magnification; scale bar, 50 µm).

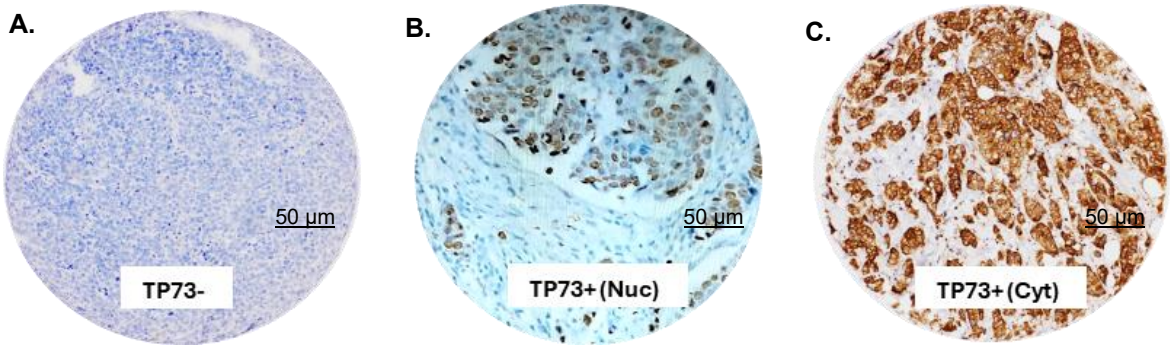

Figure 4-2. Immunohistochemistry staining of TP73 in invasive breast cancer. Representative images of negative and positive staining in invasive breast cancer TMAs imaged at (x20 magnification)

Table 15. TP73 cytoplasmic expression in ductal carcinoma in situ (DCIS)

Parameters	*TP73 Cytoplasmic Expression*		*R^2*
	Low (N%)	*High (N%)*	*p value*
Age 50 Years			
≤ 50	43 (23%)	44 (34%)	4.231
> 50	143 (77%)	87 (66%)	**0.04**
Tumour size			
≤ 2cm	80 (44%)	53 (41%)	0.229
> 2cm	104 (56%)	77 (59%)	0.632
Tumour grade			
Low	28 (15%)	19 (15%)	
Intermediate	48 (26%)	37 (28%)	0.233
High	110 (59%)	75 (57%)	0.89
Comedo necrosis			
No	66 (36%)	47 (36%)	0.005
Yes	120 (64%)	84 (64%)	0.943
Residual_tumour			
No	37 (47%)	17 (36%)	1.369
Yes	42 (53%)	30 (64%)	0.242
ER Status			
ER-	43 (26%)	25 (22%)	0.588
ER+	120 (74%)	87 (78%)	0.443
PR Status			
Negative	67 (41%)	48 (43%)	0.85
Positive	95 (59%)	65 (57%)	
HER2 Status			
Negative	135 (79%)	91 (76%)	0.25
Positive	36 (21%)	28 (23%)	0.617
Ki67			
Low	115 (78%)	77 (74%)	0.452
High	33 (22%)	27 (26%)	0.501
Molecular classes			
Luminal A	76 (55%)	52 (54%)	
Luminal B	23 (17%)	21 (22%)	3.737
HER2 Enriched	20 (14%)	17 (17%)	0.291
Triple negative	20 (14%)	7 (7%)	
Recurrence			
No	163 (88%)	116 (88%)	0.061
Yes	23 (12%)	15 (12%)	0.805

Table 16. TP73 nuclear expression in ductal carcinoma in situ (DCIS)

Parameters	*TP73 Nuclear Expression*		*R^2* *p value*
	Low (N%)	*High (N%)*	
Age 50 Years			
≤ 50	66 (26%)	21 (36%	2.417
> 50	192 (74%)	38 (64%)	0.12
Tumour size			
≤ 2cm	106 (41%)	27 (47%)	0.513
> 2cm	150 (59%)	31 (53%)	0.474
Tumour grade			
Low	39 (15%)	8 (13%)	
Intermediate	68 (26%)	17 (29%)	0.193
High	151 (59%)	34 (58%)	0.908
Comedo necrosis			
No	93 (36%)	20 (34%)	0.097
Yes	165 (64%)	39 (66%)	0.756
Residual tumour			
No	46 (44%)	8 (36%)	0.459
Yes	58 (56%)	14 (64%)	0.498
ER Status			
ER-	51 (23%)	17 (32%)	1.905
ER+	171 (77%)	36 (68%)	0.168
PR Status			
Negative	92 (41%)	23 (46%)	0.439
Positive	133 (59%)	27 (54%)	0.507
HER2 Status			
Negative	194 (82%)	32 (62%)	9.9
Positive	44 (18%)	20 (38%)	**0.002**
Ki67			
Low	157 (75%)	35 (80%)	0.331
High	51 (25%)	9 (20%)	0.565
Molecular classes			
Luminal A	108 (56%)	20 (46%)	
Luminal B	36 (19%)	8 (18%)	5.674
HER2 Enriched	25 (13%)	12 (27%)	0.129
Triple negative	23 (12%)	4 (9%)	
Recurrence			
No	226 (88%)	53 (90%)	0.227
Yes	32 (12%)	6 (10%)	0.634

Table 17. Cytoplasmic TP73/TP53 co-expression in ductal carcinoma in situ (DCIS)

Parameters	*Cytoplasmic_TP73 and TP53 co-expression*				R^2
	TP73 Low / TP53 Low	*TP73 High/ TP53 High*	*TP73 High/ TP53 Low*	*TP73 Low/ TP53 High*	*p value*
Age 50 Years					
≤ 50	23 (29%)	17 (33%)	17 (32%)	14 (26%)	0.613
> 50	57 (71%)	35 (67%)	37 (68%)	39 (74%)	0.893
Tumour size					
≤ 2cm	37 (46%)	18 (35%)	23 (43%)	21 (40%)	1.654
> 2cm	43 (54%)	33 (65%)	31 (57%)	32 (60%)	0.647
Tumour grade					
Low	14 (17%)	6 (12%)	9 (17%)	6 (11%)	
Intermediate	27 (34%)	13 (25%)	16 (29%)	11 (21%)	6.023
High	39 (49%)	33 (63%)	29 (54%)	36 (68%)	0.421
Comedo necrosis					
No	31 (39%)	20 (38%)	18 (33%)	18 (34%)	0.642
Yes	49 (61%)	32 (62%)	36 (67%)	35 (66%)	0.887
Residual tumour					
No	16 (50%)	6 (33%)	10 (42%)	9 (36%)	1.759
Yes	16 (50%)	12 (67%)	14 (58%)	16 (64%)	0.624
ER Status					
Negative	18 (23%)	17 (35%)	7 (14%)	15 (30%)	7.222
Positive	59 (77%)	31 (65%)	45 (86%)	35 (70%)	0.065
PgR Status					
Negative	27 (35%)	25 (51%)	15 (30%)	25 (49%)	7.017
Positive	50 (65%)	24 (49%)	35 (70%)	26 (51%)	0.071
HER2 Status					
Negative	64 (81%)	31 (63%)	45 (85%)	38 (73%)	8.065
Positive	15 (19%)	18 (37%)	8 (15%)	14 (27%)	0.045
Ki67					
Low	61 (84%)	33 (72%)	35 (78%	31 (65%)	6.13
High	12 (16%)	13 (28%)	10 (22%)	17 (35%)	0.105
Molecular classes					
Luminal A	46 (65%)	19 (42%)	27 (63%)	19 (42%)	
Luminal B	9 (12%)	9 (20%)	10 (23%)	12 (27%)	14.93
HER2 Enriched	9 (12%)	12 (27%)	5 (12%)	8 (18%)	0.093
Triple negative	8 (11%)	5 (11%)	1 (2%)	6 (13%)	
Recurrence					
No	69 (86%)	47 (90%)	46 (85%)	46 (87%)	0.727
Yes	11 (14%)	5 (10%)	8 (15%)	7 (13%)	0.867

Table 18. Nuclear TP73/TP53 co-expression and ductal carcinoma in situ (DCIS)

Parameters	*Nuclear_TP73 and TP53 co-expression*				R^2
	TP73 Low/ TP53 Low	*TP73 High/ TP53 High*	*TP73 High/ TP53 Low*	*TP73 Low/ TP53 High*	*p value*
Age 50 Years					
≤ 50	31 (28%)	8 (35%)	9 (41%)	23 (28%)	1.934
> 50	81 (72%)	15 (65%)	13 (59%)	59 (72%)	0.586
Tumour size					
≤ 2cm	50 (45%)	9 (41%)	10 (46%)	30 (37%)	1.415
> 2cm	62 (55%)	13 (59%)	12 (54%)	52 (63%)	0.702
Tumour grade					
Low	20 (18%)	2 (9%)	3 (14%)	10 (12%)	
Intermediate	36 (32%)	7 (30%)	7 (32%)	17 (21%)	6.578
High	56 (50%)	14 (61%)	12 (54%)	55 (67%)	0.362
Comedo necrosis					
No	41 (37%)	9 (39%)	8 (36%)	29 (35%)	0.114
Yes	71 (63%)	14 (61%)	14 (64%)	53 (65%)	0.99
Residual tumour					
No	24 (48%)	3 (30%)	2 (33%)	12 (36%)	1.939
Yes	26 (52%)	7 (70%)	4 (67%)	21 (64%)	0.585
ER Status					
Negative	18 (17%)	8 (36%)	7 (33%)	24 (32%)	8.022
Positive	90 (83%)	14 (64%)	14 (67%)	52 (68%)	**0.046**
PR Status					
Negative	34 (32%)	12 (52%)	8 (42%)	38 (49%)	7.468
Positive	74 (68%)	11 (48%)	11 (58%)	39 (51%)	0.058
HER2 Status					
Negative	96 (86%)	12 (55%)	13 (65%)	57 (72%)	13.447
Positive	16 (14%)	10 (45%)	7 (35%)	22 (28%)	**0.004**
Ki67					
Low	82 (82%)	14 (74%)	14 (78%)	50 (67%)	5.528
High	18 (18%)	5 (26%)	4 (22%)	25 (33%)	0.137
Molecular classes					
Luminal A	64 (66%)	7 (37%)	9 (50%)	31 (44%)	
Luminal B	16 (17%)	4 (21%)	3 (17%)	17 (24%)	14.984
HER2 Enriched	9 (9%)	6 (32%)	5 (28%)	14 (20%)	0.091
Triple negative	8 (8%)	2 (10%)	1 (5%)	9 (12%)	
Recurrence					
No	97 (87%)	21 (91%)	18 (82%)	72 (88%)	0.963
Yes	15 (13%)	2 (9%)	4 (18%)	10 (12%)	0.81

Table 19. Nuclear TP53 expression in ductal carcinoma in situ (DCIS)

Parameters	*TP53 Expression*		R^2
	Low (N%)	*High (N%)*	*p value*
Age 50 Years			
≤ 50	73 (27%)	56 (25%)	0.263
> 50	197 (73%)	168 (75%)	0.608
Tumour size			
≤ 2cm	131 (49%)	99 (45%)	0.754
> 2cm	139 (51%)	123 (55%)	0.385
Tumour grade			
Low	39 (15%)	24 (11%)	
Intermediate	79 (29%)	50 (22%)	5.872
High	152 (56%)	150 (67%)	0.053
Comed necrosis			
No	101 (37%)	74 (33%)	1.023
Yes	169 (63%)	150 (67%)	0.312
Residual tumour			
No	49 (45%)	38 (40%)	0.352
Yes	61 (55%)	56 (60%)	0.553
ER Status			
ER-	53 (21%)	65 (31%)	6.692
ER+	204 (79%)	144 (69%)	**0.01**
PR Status			
Negative	87 (34%)	103 (49%)	10.407
Positive	167 (66%)	107 (51%)	**0.001**
HER2 Status			
Negative	218 (83%)	151 (71%)	10.277
Positive	44 (17%)	62 (29%)	**0.001**
Ki67			
Low	187 (82%)	135 (70%)	8.465
High	41 (18%)	58 (30%)	**0.004**
Molecular classes			
Luminal A	133 (61%)	78 (43%)	
Luminal B	34 (16%)	43 (23%)	13.974
HER2 Enriched	26 (12%)	34 (19%)	**0.003**
Triple negative	24 (11%)	28 (15%)	
Recurrence			
No	237 (88%)	202 (90%)	0.713
Yes	33 (12%)	22 (10%)	0.398

Table 20. TP73 Cytoplasmic expression in breast cancer

Parameters	TP73 CYTOPLASMIC EXPRESSION		R^2
	Low (N%)	High (N%)	p value
Tumour size			
< 2cm	440 (52%)	400 (48%)	2.922
≥ 2cm	252 (48%)	277 (52%)	0.087
Grade			
1	114 (53%)	100 (47%)	15.241
2	302 (56%)	237 (44%)	**<0.0001**
3	276 (45%)	340 (55%)	
Tubular formation			
1	52 (53%)	46 (47%)	0.508
2	207 (51%)	196 (49%)	0.776
3	433 (50%)	435 (50%)	
Pleomorphism			
1	8 (44%)	10 (56%)	13.117
2	231 (58%)	166 (42%)	**0.001**
3	453 (47%)	501 (53%)	
Mitosis			
1	362 (55%)	298 (45%)	11.729
2	135 (50%)	134 (50%)	**0.003**
3	195 (44%)	245 (56%)	
HistologicalTumourType			
NST	424 (48%)	460 (52%)	16.248
ILC	69 (62%)	42 (38%)	**0.012**
Mixed NST and ILC	45 (54%)	38 (46%)	
Mixed NST and special type	14 (37%)	24 (63%)	
Pure special tumour type	14 (70%)	6 (30%)	
Metaplastic Carcinoma	2 (40%)	3 (60%)	
Tubular and Tubular Mixed	124 (54%)	104 (46%)	
LVI			
Absent	506 (52%)	474 (48%)	1.624
Present	186 (48%)	203 (52%)	0.203
Lymph Node status			
Negative	438 (52%)	408 (48%)	1.33
Positive	254 (49%)	269 (51%)	0.249
NPI			
GPG	261 (56%)	205 (44%)	
MPG	322 (47%)	357 (53%)	8.531
PPG	109 (49%)	115 (51%)	**0.014**
Stage			
1	438 (52%)	408 (48%)	
2	193 (51%)	184 (49%)	5.06
3	61 (42%)	85 (58%)	0.08
ER Status			
ER-	113 (41%)	161 (59%)	11.78
ER+	578 (53%)	516 (47%)	**0.001**
PgR Status			
Negative	269 (48%)	291 (52%)	2.34
Positive	418 (52%)	382 (48%)	0.126
HER2 Status			
Negative	592 (50%)	590 (50%)	0.634
Positive	99 (53%)	87 (47%)	0.426
TN			
Non- TN	614 (53%)	546 (47%)	17.738
TN	71 (37%)	123 (63%)	**<0.0001**
Molecular Classes			
Luminal	578 (53%)	516 (47%)	
HER2 Enriched	36 (55%)	30 (45%)	17.811
TNBC	71 (37%)	123 (63%)	**<0.0001**
Menopausal Status			
Pre	218 (47%)	247 (53%)	3.786
Post	474 (52%)	430 (48%)	0.052
Age 50 Years			
< 50	193 (45%)	233 (55%)	6.8
≥ 50	499 (53%)	444 (47%)	**0.009**

TP73 expression was evaluated in normal breast ducts of 57 samples, and only cytoplasmic staining was observed. In tumours, nuclear expression of TP73 was surprisingly rare, occurring in only 14 out of 1369 (1%) of tumours, and therefore unsuitable for clinicopathological association studies. Conversely, cytoplasmic staining of TP73 was observed in 677 out of 1369 (49.4%) tumours. A clinicopathological evaluation was conducted in breast cancer, and high cytoplasmic TP73 was significantly associated with features characteristic of aggressive behaviour, including high grade, pleomorphism, high mitotic index, high-risk Nottingham Prognostic Index (NPI), ER-negative, and triple-negative (TNBC) (*all p values ≤ 0.01*) (**Table 20**). In the entire cohort, high TP73 was associated with poor outcomes in terms of shorter breast cancer-specific survival (BCSS) (*p=0.017*) (**Figure 4-3A**). In ER+ breast cancers, high TP73 was borderline non-significant for shorter BCSS (*p= 0.056*) (**Figure 4-3B**) and non-significant in ER-breast cancers (*p =0.599*) (**Figure 4-3C**).

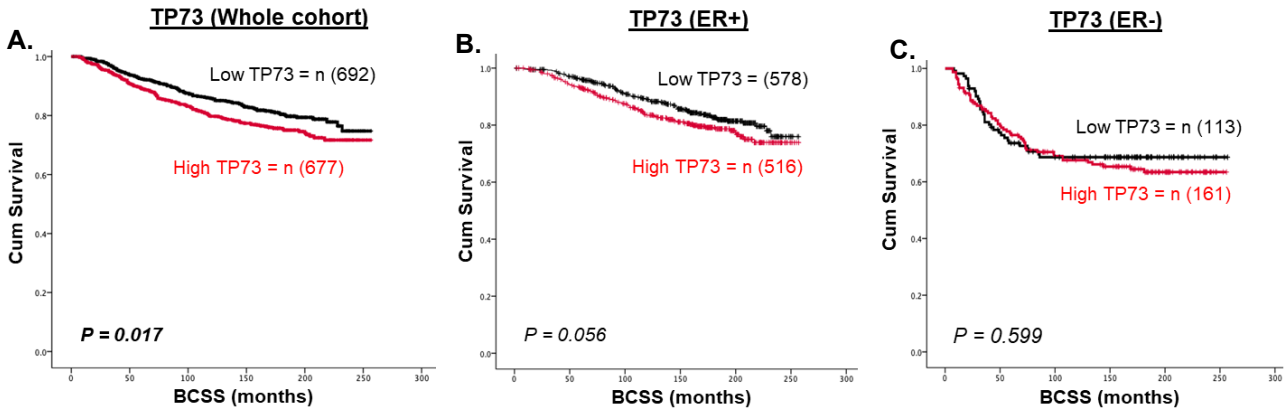

Figure 4-3. Clinicopathological studies of TP73 expression in breast cancer. A. TP73 expression and Kaplan-Meier curve for breast cancer-specific survival (BCSS) in the whole cohort. B. TP73 expression and Kaplan-Meier curve for BCSS in ER+ cohort. C.TP73 expression and Kaplan-Meier curve for BCSS in ER- cohort.

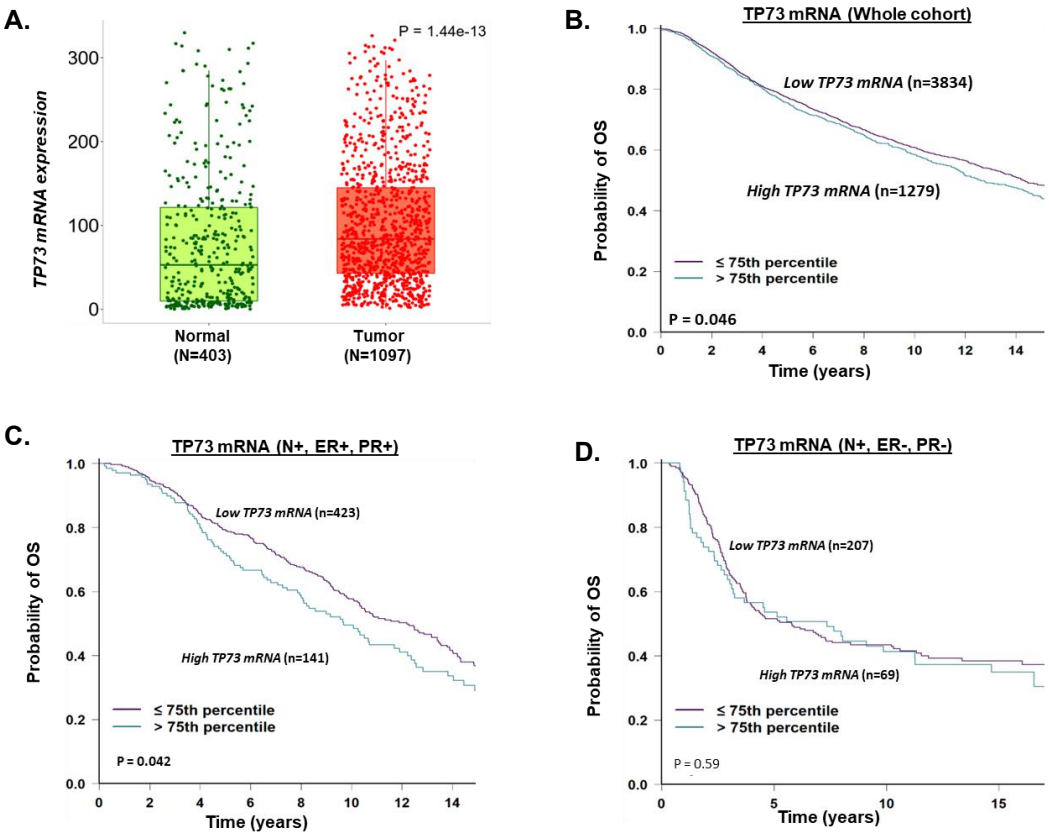

Figure 4-4. TP73 mRNA expression and breast cancer. A.TP73 transcripts in normal and breast cancer tissue. B.TP73 transcripts and Kaplan-Meier curve for breast cancer specific survival (BCSS) in the whole cohort. C. TP73 transcripts and Kaplan-Meier curve for BCSS in node positive (N+), ER+, PR- cohort. D. TP73 transcripts and Kaplan-Meier curve for BCSS in node positive (N+), ER-, PR-cohort.

Breast tumour tissue exhibited significantly higher TP73 mRNA expression compared to normal breast tissue (*P<0.0001*) (**Figure 4-4A**) . In the whole cohort, high TP73 mRNA expression was significantly associated with poor survival (**Figure 4-4B**). In lymph node+/ER+/PR+ breast cancers, high TP73 mRNA expression was strongly linked with poor survival (**Figure 4-4C**). However, no significant association was observed between high TP73 mRNA expression and poor survival in lymph node+/ER-/PR- breast cancers (**Figure 4-4D**).

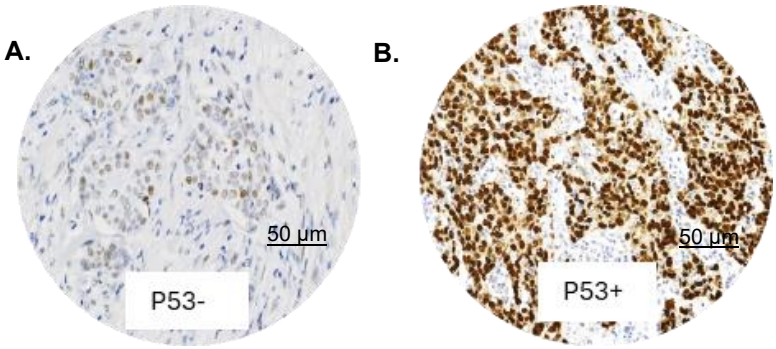

Figure 4-5. Immunohistochemistry staining of TP53 in breast cancer. A. Representative image of negative staining in invasive breast cancer TMAs. B. Representative image of positive staining in invasive breast cancer TMAs. Both were imaged at (x20 magnification; scale bar, 50 µm).

TP53 immunohistochemical analysis was performed on 1601 invasive breast cancers (IBC) to determine their characteristics **(Figure 4-5)**. The analysis revealed that 584/1601 (34.4%) of tumours had TP53 nuclear positivity. Tumours that were TP53 positive were found to have characteristics that were indicative of aggressive behaviour, such as high grade, de-differentiation, pleomorphism, high Mitotic index, lymphovascular invasion, high-risk Nottingham Prognostic Index (NPI), HER-2+, ER-negative and triple-negative breast cancers (TNBC) (*all p values ≤ 0.01*) (**Table 21**). The analysis also showed that high TP53 expression was associated with poor outcomes in terms of shorter breast cancer-specific survival (BCSS) (*p=0.006*) (**Figure 4-7A**), but this was not the case for ER+ (**Figure 4-7B**) or ER- tumours (**Figure 4-7C**) in the entire cohort.

TP73-TP53 co-expression analysis was performed on 1188 cases of invasive breast cancer (IBC). Among these, 19.1% (228/1188) showed highTP73 and highTP53 tumours, which were strongly associated with high grade, de-differentiation, pleomorphism, high mitotic index, lymphovascular invasion, high-risk Nottingham Prognostic Index (NPI), stage 3 disease, HER-2+, ER

negative, PR negative, and triple-negative breast cancers (TNBC) (*all p values ≤ 0.01*) (**Table 22**). The co-expression of high TP73 and high TP53 was linked with shorter breast cancer-specific survival (BCSS) (*p=0.001*) (**Figure 4-6A**) in the whole cohort, including ER+ (*p=0.040*) (**Figure 4-6B**) but not in ER- breast cancer (**Figure 4-6C**), indicating that TP73 dysregulation can potentially affect breast cancer pathogenesis and prognosis. Moreover, to examine whether TP73 dysregulation is an early event, we also examined a cohort of 317 non-invasive DCIS.

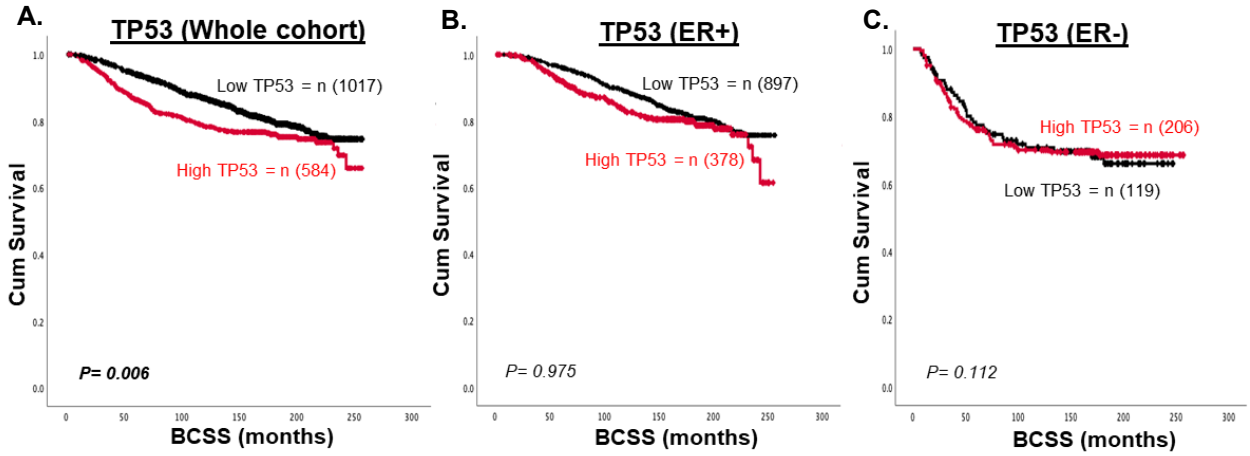

Figure 4-7. Clinicopathological studies of TP53 expression in breast cancer. TP53 expression and Kaplan-Meier curve for breast cancer-specific survival (BCSS) in the whole cohort. B. TP53 expression and Kaplan-Meier curve for BCSS in ER+ cohort. C. TP53 expression and Kaplan-Meier curve for BCSS in ER- cohort.

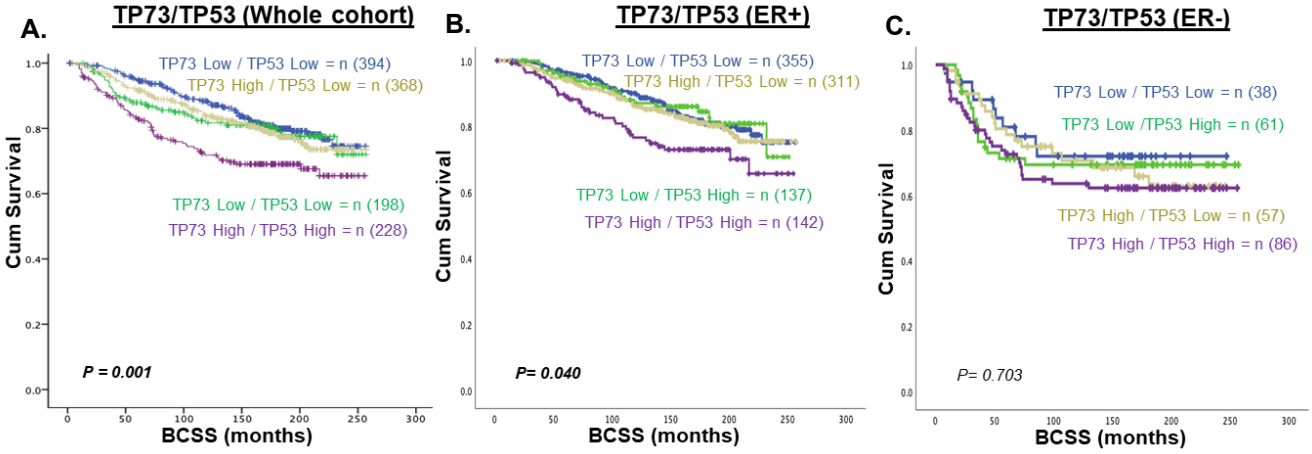

Figure 4-6. Clinicopathological studies of TP53/TP73 co-expression in breast cancer. A. TP73/TP53 co-expression and Kaplan-Meier curve for breast cancer-specific survival (BCSS) in the whole cohort. B. TP73-TP53 co-expression and Kaplan-Meier curve for BCSS in ER+ cohort. C. TP73-TP53 co-expression and Kaplan-Meier curve for BCSS in ER- cohort.

Table 21. TP53 expression in breast cancer

Parameters	TP53 EXPRESSION		R^2
	Low (N%)	High (N%)	P value
Tumour size			
< 2cm	634 (65%)	343 (35%)	2.03
≥ 2cm	383 (61%)	241 (39%)	0.154
Grade			
1	187 (78%)	52 (22%)	
2	474 (75%)	157 (25%)	128.278
3	356 (49%)	375 (51%)	**<0.0001**
Tubular formation			
1	84 (76%)	26 (24%)	
2	324 (68%)	153 (32%)	17.066
3	609 (60%)	405 (40%)	**<0.0001**
Pleomorphism			
1	17 (74%)	6 (26%)	
2	373 (81%)	85 (19%)	92.017
3	627 (56%)	493 (44%)	**<0.0001**
Mitosis			
1	581 (77%)	173 (23%)	
2	187 (60%)	125 (40%)	127.902
3	249 (46%)	286 (54%)	**<0.0001**
HistologicalTumourType			
NST	598 (57%)	459 (43%)	
ILC	108 (86%)	17 (14%)	
Mixed NST and ILC	68 (73%)	25 (27%)	
Mixed NST and special type	27 (66%)	14 (34%)	73.222
Pure special tumour type	13 (72%)	5 (28%)	**<0.0001**
Metaplastic Carcinoma	3 (60%)	2 (40%)	
Tubular and Tubular Mixed	200 (76%)	62 (24%)	
LVI			
Absent	744 (65%)	395 (35%)	5.505
Present	273 (59%)	189 (41%)	**0.019**
Lymph Node status			
Negative	637 (65%)	348 (35%)	1.357
Positive	380 (62%)	235 (38%)	0.244
NPI			
GPG	392 (73%)	141 (27%)	
MPG	494 (61%)	321 (39%)	40.584
PPG	131 (52%)	121 (48%)	**<0.0001**
Stage			
1	637 (65%)	348 (35%)	
2	291 (64%)	164 (36%)	4.905
3	89 (56%)	71 (44%)	0.086
ER Status			
ER-	119 (37%)	206 (63%)	127.185
ER+	897 (70%)	378 (30%)	**<0.0001**
PgR Status			
Negative	354 (54%)	300 (46%)	43.509
Positive	660 (70%)	279 (30%)	**<0.0001**
HER2 Status			
Negative	914 (66%)	469 (34%)	29.329
Positive	101 (47%)	114 (53%)	**<0.0001**
Ki67 index			
Low	458 (76%)	149 (24%)	60.599
High	319 (54%)	272 (46%)	**<0.0001**
Molecular Classes			
Luminal	897 (70%)	378 (30%)	
HER2 Enriched	25 (32%)	54 (68%)	127.187
TNBC	89 (38%)	146 (62%)	**<0.0001**
Menopausal Status			
Pre	337 (60%)	225 (40%)	4.732
Post	680 (65%)	359 (35%)	**0.03**
Age 50 Years			
< 50	296 (58%)	215 (42%)	10.148
≥ 50	721 (66%)	369 (34%)	**0.001**

Table 22. TP73/TP53 co-expression in breast cancer

Parameters	*TP73 Low/ TP53 Low* (N%)	*TP73 Low/ TP53 High* (N%)	*TP73 High/ TP53 Low* (N%)	*TP73 High/ TP53 High* (N%)	R^2 p value
Tumour size					
< 2cm	251 (35%)	120 (17%)	221 (31%)	127 (17%)	3.923
≥ 2cm	143 (30%)	78 (17%)	147 (31%)	101 (22%)	0.27
Grade					
1	75 (43%)	17 (10%)	59 (34%)	22 (13%)	
2	192 (42%)	58 (13%)	157 (34%)	50 (11%)	100.357
3	127 (23%)	123 (22%)	152 (27%)	156 (28%)	**<0.0001**
Tubular formation					
1	34 (43%)	8 (10%)	24 (30%)	13 (17%)	
2	128 (37%)	49 (14%)	119 (34%)	52 (15%)	17.558
3	232 (31%)	141 (18%)	225 (30%)	163 (21%)	**0.007**
Pleomorphism					
1	2 (13%)	4 (27%)	7 (47%)	2 (13%)	
2	158 (48%)	29 (9%)	106 (33%)	33 (10%)	70.951
3	234 (28%)	165 (19%)	255 (30%)	193 (23%)	**<0.0001**
Mitosis					
1	230 (42%)	64 (12%)	191 (35%)	62 (11%)	
2	80 (34%)	37 (16%)	70 (30%)	48 (20%)	97.101
3	84 (21%)	97 (24%)	107 (26%)	118 (29%)	**<0.0001**
HistologicalTumourType					
NST	221 (28%)	156 (20%)	237 (30%)	178 (22%)	
ILC	49 (55%)	6 (7%)	28 (31%)	6 (7%)	
Mixed NST and ILC	23 (35%)	8 (12%)	25 (38%)	10 (15%)	
Mixed NST and special type	9 (28%)	3 (9%)	13 (41%)	7 (22%)	67.693
Pure special tumour type	9 (65%)	2 (14%)	1 (7%)	2 (14%)	**<0.0001**
Metaplastic Carcinoma	2 (40%)	0 (0%)	1 (20%)	2 (40%)	
Tubular and Tubular Mixed	81 (43%)	23 (12%)	63 (33%)	23 (12%)	
LVI					
Absent	295 (35%)	132 (16%)	261 (31%)	146 (18%)	9.529
Present	99 (28%)	66 (19%)	107 (30%)	82 (23%)	**0.023**
Lymph Node status					
Negative	255 (35%)	117 (16%)	218 (30%)	131 (18%)	4.22
Positive	139 (30%)	81 (17%)	150 (32%)	97 (21%)	0.239
NPI					
GPG	158 (42%)	53 (14%)	117 (31%)	51 (13%)	
MPG	185 (31%)	99 (16%)	200 (33%)	122 (20%)	36.012
PPG	51 (25%)	46 (23%)	51 (25%)	55 (27%)	**<0.0001**
Stage					
1	255 (36%)	117 (16%)	218 (30%)	131 (18%)	
2	107 (32%)	61 (18%)	113 (34%)	55 (16%)	19.231
3	32 (25%)	20 (15%)	37 (28%)	42 (32%)	**0.004**
ER Status					
ER-	38 (16%)	61 (25%)	57 (24%)	86 (35%)	88.699
ER+	355 (38%)	137 (14%)	311 (33%)	142 (15%)	**<0.0001**
PgR Status					
Negative	138 (28%)	90 (19%)	134 (27%)	125 (26%)	28.459
Positive	255 (36%)	107 (16%)	233 (33%)	103 (15%)	**<0.0001**
HER2 Status					
Negative	353 (35%)	147 (14%)	328 (32%)	189 (19%)	31.615
Positive	40 (24%)	51 (30%)	40 (24%)	39 (22%)	**<0.0001**
Ki67 index					
Low	177 (40%)	63 (14%)	155 (35%)	50 (11%)	37.687
High	119 (27%)	89 (20%)	126 (29%)	104 (24%)	**<0.0001**
Molecular Classes					
Luminal	355 (38%)	137 (14%)	311 (33%)	142 (15%)	
HER2 Enriched	10 (17%)	22 (37%)	8 (13%)	20 (33%)	99.265
TNBC	27 (16%)	37 (21%)	45 (26%)	65 (37%)	**<0.0001**
Menopausal Status					
Pre	119 (28%)	78 (18%)	138 (33%)	88 (21%)	7.721
Post	275 (36%)	120 (16%)	230 (30%)	140 (18%)	0.052
Age 50 Years					
< 50	109 (28%)	70 (18%)	126 (32%)	89 (22%)	9.541
≥ 50	285 (36%)	128 (16%)	242 (31%)	139 (17%)	**0.023**

4.4.2 Pre-Clinical studies

Subsequent analysis was conducted on TP73 protein levels in a panel of cell lines including normal (MCF10A), DCIS (MCF10A_DCIS), ER+ invasive breast cancer (MCF-7, T47D), and triple-negative (MDA-MB-231) (**Figure 4-8**) breast cancer cells display high TP73 expression compared with normal epithelial cells (MCF10A).

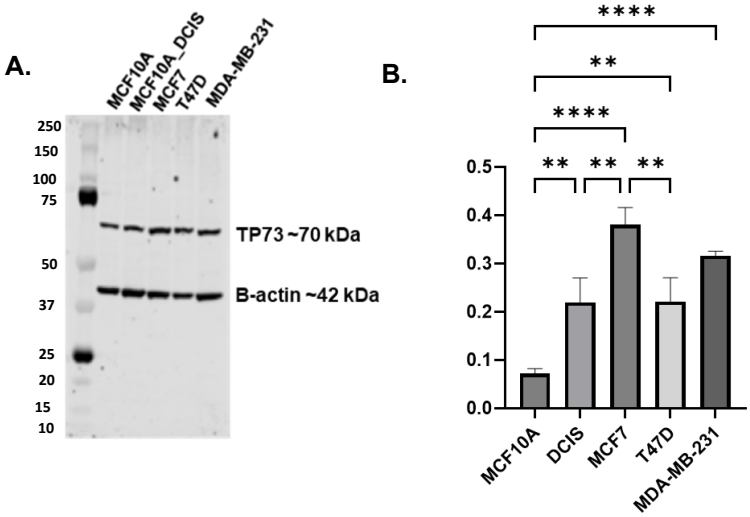

Figure 4-8. Expression of TP73 in breast cancer. A. panel of normal (MCF10A), DCIS (MCF10A_DCIS), ER+ (MCF7, T47D) and triple negative (MDA-MB-231) breast cancer cell lines was analysed by Western blotting. B. Relative quantification of TP73 protein expression. The band intensities of TP73 and β-actin were quantified using LI-COR software. The readings for TP73 were normalized to those of β-actin using Microsoft Excel 2011. Data presentation and statistical analysis were performed using GraphPad Prism, version 9. The P value was calculated as follow, **p < 0.01, ***p < 0.001 and ****p < 0.0001. The experiment was performed for samples from three independent experiments n=3 and the error bar represent the standard deviation (SD).

4.5 Discussion

TP73 plays a crucial role in various biological processes such as neurodevelopment, tissue homeostasis, and cancer pathogenesis, as indicated by multiple studies. Due to the presence of different splice variants of TP73 with distinct biological functions, the exact contribution of TP73 in breast cancer development is yet to be determined (Kong et al., 2023; Melino, 2020; Rufini et al., 2011; Stiewe & Pützer, 2002). In this study, we conducted the most extensive research to date on TP73 expression in clinical breast cancers. At the transcriptomic level, TP73 mRNA expression was higher in tumour tissue than in normal tissue, and this was associated with shorter survival outcomes. We then conducted an immunohistochemical evaluation of TP73 in a large cohort of breast cancer patients. Interestingly, only cytoplasmic TP73 staining was observed in invasive breast cancer, while nuclear TP73 staining was rare. A high cytoplasmic TP73 protein level was associated with aggressive phenotypes and poor survival. Previous research has shown that Wwox, a tumour suppressor protein, is involved in TP73 cytoplasmic sequestration(Pospiech et al., 2018). However, it is unclear whether the functional association between Wwox and TP73 could account for the cytoplasmic staining of TP73 observed in our study (Aqeilan et al., 2004; Stella Logotheti et al., 2021).

To validate our hypothesis, further mechanistic investigations are necessary. Previously conducted research indicated that inhibition of TP73's apoptotic activity can be achieved through WWOX. Furthermore, TP73's apoptotic activity may also be impeded by its cytoplasmic localisation and interaction

with other proteins, such as HCK and amphiphysin IIb-1 (Hussain et al., 2018; Li et al., 2021; Wang et al., 2019; Zhao et al., 2021). These factors may contribute to the aggressive phenotypes observed in our study. We did not investigate individual TP73 splice variants due to the unavailability of specific antibody clones. Instead, we employed a rabbit monoclonal anti-TP73 antibody (Abcam clone - ab189896) that recognizes the C-terminal fragment of TP73 containing amino acids 380-636. The antibody recognizes all splice variants, and the levels indicate total TP73 expression in cells for our IHC studies.

Our research suggests that TP73 has no bearing on clinical outcomes in DCIS, indicating its role only in the pathogenesis of invasive cancers. However, in tumours with mutant TP53, high TP73 levels were linked to aggressive pathology and shorter patient survival.

Recent studies suggest that TP53 mutants can bind to and sequester TP73, inhibiting its pro-apoptotic function. In previous research, both suppressor and oncogenic isoforms of TP73 were found to be significantly co-upregulated in tumours of 60 breast cancer samples(Steffens Reinhardt et al., 2023; Taverniti et al., 2023). TP73 overexpression was also observed in breast cancer cell lines and human breast cancer tissue in a small study. However, the clinical significance of TP73 and its impact on survival in the context of TP53 variants was not investigated in these studies. TP73 overexpression has also been reported in other solid tumours, including ovarian cancer, bladder, prostate, oesophageal and colorectal cancers (Inoue & Fry, 2014; Orzol et al., 2015; Rodríguez et al., 2018). In a large study of 193 patients with hepatocellular carcinomas (Moll & Slade, 2004; Müller et

al., 2005), TP73 overexpression was considered an independent prognostic factor. Overexpression of TP73 is linked with aggressive tumours in neuroblastomas and meningiomas (Tábuas-Pereira et al., 2022). In contrast, TP73 loss has been observed in pancreatic cancers (Thakur et al., 2016). Previous studies have shown that the TA and δN splice variant expression ratio could influence biology and prognosis. In some cancers, δNTP73 overexpression has been associated with aggressive features and poor prognosis. However, in the current study on breast cancer, we did not observe any significant differences in splice variant expression in the large TCGA-BC dataset (Hagiwara et al., 2020; Mucaki & Rogan, 2019; Smith & Kitzman, 2023).

Chapter 5 POLE in Ovarian Cancer

5.1 Introduction

Polymerase Epsilon (POLE) is a critical DNA polymerase enzyme in eukaryotic cells responsible for DNA replication and repair processes. As one of the four major DNA polymerases in eukaryotes, POLE plays a central role in ensuring genomic stability and the fidelity of DNA replication. This overview highlights POLE's structure, functions, and significance in DNA metabolism (Van Gool et al., 2015; Mehnert et al., 2016). POLE is a multi-subunit enzyme complex composed of several subunits. In yeast, the core catalytic subunit is Pol2, accompanied by the exonuclease subunit (also Pol2) and two smaller non-catalytic subunits (Pol12 and Dpb2). In humans, the core catalytic subunit is referred to as POLE, the exonuclease subunit as POLE2, and the smaller subunits as POLE3 and POLE4. This complex exhibits a specific structural organization, with the catalytic subunit involved in DNA polymerization and the exonuclease subunit facilitating proofreading activities to correct errors during replication. POLE predominantly operates during the elongation phase of DNA replication, significantly contributing to the synthesis of the leading DNA strand. The enzyme is recognized for its high fidelity in DNA synthesis, a crucial aspect of maintaining genomic stability. Besides its role in DNA replication, POLE is also involved in DNA repair mechanisms, particularly in the repair of double strand breaks and genetic recombination. Its accuracy in DNA synthesis is vital in these repair processes to safeguard the integrity of the genetic code. POLE's importance in genome stability is underscored by its essential role in DNA replication,

which is central to preserving genetic information. Mutations in POLE or its subunits can lead to genomic instability and are associated with various genetic disorders and cancers, emphasizing the enzyme's critical role in genome maintenance. In patients with colorectal cancer and POLE mutations, the median age at diagnosis is 54.5 years compared to 67.2 years in patients with wild-type POLE. They are often diagnosed at an earlier stage of the disease (Dong et al., 2022; Xing et al., 2022).

In 2013, Alexandrov et al. found over 20 mutational signatures among 4,938,362 mutations in 7042 tumours. There was a tenth signature linked to POLE mutations in colorectal cancer and endometrial cancer. Similarly, another study (Zou et al., 2014) observed that among Chinese patients suffering from ovarian endometrioid carcinoma, there were frequently observed mutations of POLE1 P.S297F mutation. A similar trend was seen in another study done by (Hoang et al., 2015), which focused on the prevalence of POLE exonuclease domain mutations among patients with ovarian endometrioid carcinomas and implicated POLE mutation in this subtype of cancer again.

The available data indicates that POLE mutations have role in ovarian cancer pathogenesis, particularly in endometrioid carcinoma (Davila et al., 2021; León-Castillo et al., 2020). Research has demonstrated that POLE exhibit high rates of mutation, with specific mutations such as P286R, S297F, V411L, and A456P identified as potential hotspots. These mutations are more commonly found in endometrioid ovarian cancer compared to other subtypes, suggesting a potential role in the development of this specific type of cancer (Hoang et al., 2015).

In 2014, Billingsley et al. analysed TCGA data to understand the incidence and prognostic significance of newly identified hotspot mutations in DNA polymerase epsilon (POLE) in endometrial cancer. They observed that these mutations are usually repaired by MMR mechanisms or DNA Polymerase Epsilon, which repairs most replication errors before they result in permanent damage. DNA Polymerase Epsilon is crucial as a proofreading exonuclease during DNA synthesis within mitochondria and nuclear genomes. Additionally, another study (Andrianova et al., 2017) focused on human cancers with somatic mutations in DNA polymerases delta and epsilon. They found that polymerase delta generated more mismatches than polymerase epsilon, which were subsequently repaired by the mismatch repair system. In particular, Hamanishi et al (Hamanishi et al., 2017) proposed that immune checkpoint inhibitors would target ultra-mutated genes such as the POLE gene. Potentially, these genetic changes can predict therapeutic responses in endometrial and ovarian cancer.

POLE mutations are promising for immunotherapy due to their association with high mutation burden (TMB) and response to immune checkpoint inhibitors (ICIs) in various cancers, including non-small cell lung cancer (NSCLC) and colon cancer (Liu et al., 2023; S. Zheng et al., 2023). Research indicates that POLE mutations lead to an ultra-mutated phenotype, making tumours more susceptible to immunotherapy (Hu et al., 2021). Additionally, POLE mutations result in a loss of proofreading function, leading to the accumulation of mutant genes in cells, which can serve as a potential molecular marker for predicting the efficacy of immunotherapy in different types of cancers (Ma et al., 2022). Whilst the role of POLE in endometrial

cancer has been well defined, the role of POLE in ovarian remains less well established.

5.2 Aims of this study

1- Evaluate POLE expression in ovarian cancer tissues

a- To investigate the expression of POLE in ovarian cancer tissues using immunohistochemistry (IHC) on tumour microarrays (TMAs) from 331 patients treated at Nottingham University Hospitals.

b- To quantify POLE nuclear and cytoplasmic expression using H-scores.

c- To correlate POLE expression with clinicopathological features and patient outcomes, assessing its potential as a prognostic marker for ovarian cancer.

2- Investigate the clinicopathological significance of POLE/TP53 co-expression

a- To explore the relationship between POLE/TP53 co-expression and key tumour characteristics, including histological subtype, tumour grade, stage, and patient outcomes.

3- Assess the role of POLE in chemoresistance

a- To evaluate POLE expression in ovarian cancer cell lines, including platinum-sensitive (A2780) and platinum-resistant (A2780cis), as well as in BRCA2-deficient (PEO1) and BRCA2-proficient (PEO4) models.

b- To assess the potential association of POLE expression with chemoresistance, particularly in platinum-resistant cell lines, and to determine whether POLE is involved in the regulation of drug sensitivity.

4- Investigate the functional role of POLE in ovarian cancer cells

a- To explore the functional consequences of POLE knockdown in ovarian cancer cells using siRNA transfection in OVCAR 4 and other ovarian cell lines.

b- To evaluate the impact of POLE depletion on key cellular processes, including proliferation, cell cycle progression, and apoptosis, using clonogenic assays, flow cytometry, and other functional assays.

5- Examine POLE expression at the mRNA level

a- To analyse publicly available gene expression datasets (e.g. KM-Plot) for POLE mRNA expression in ovarian tumours and correlate POLE mRNA levels with clinical outcomes such as overall survival (OS) and progression free survival (PFS).

5.3 Method

Immunohistochemical staining was performed to detect POLE expression in tumour microarrays (TMA) from 331 ovarian cancer patients treated at Nottingham University Hospitals between 1997 and 2010. The staining was performed utilizing an anti-POLE rabbit polyclonal antibody (ab226848, Abcam) at a dilution of 1:100 for 1 hour at room temperature. X-tile plots were utilized to determine the optimal cut-off values for stratification purposes. For positive POLE nuclear expression, an H-score >0 was used, while an H-score >100 was used for positive POLE cytoplasmic expression. POLE mRNA expression was analysed based on publicly available gene expression datasets for ovarian tumours (http://kmplot.com/analysis/index.php?p=service&cancer=ovar). The study

used the following cell lines: A2780 (platinum-sensitive), A2780cis (platinum-resistant), PEO1 (BRCA2 deficient), PEO4 (BRCA2 proficient), and OVCAR 4. The siRNA transfection protocol described in the Materials and Methods chapter was used to carry out the siRNA knock-down of POLE in ovarian cells. The clonogenic, cell cycle and apoptosis protocols for OVCAR 4_POLE_Knockdown were described in the Materials and Methods chapter.

5.4 Results

5.4.1 Clinical study

5.4.1.1 Overexpression of POLE is associated with Platinum Resistance in EOC

IHC staining was conducted to assess the associations between POLE expression and the clinicopathological features of a cohort of 331 patients with EOC. The demographics and pathological characteristics of the patients with EOC are presented in Chapter two. Typical images of POLE expression are shown in (**Figure 5-1**).

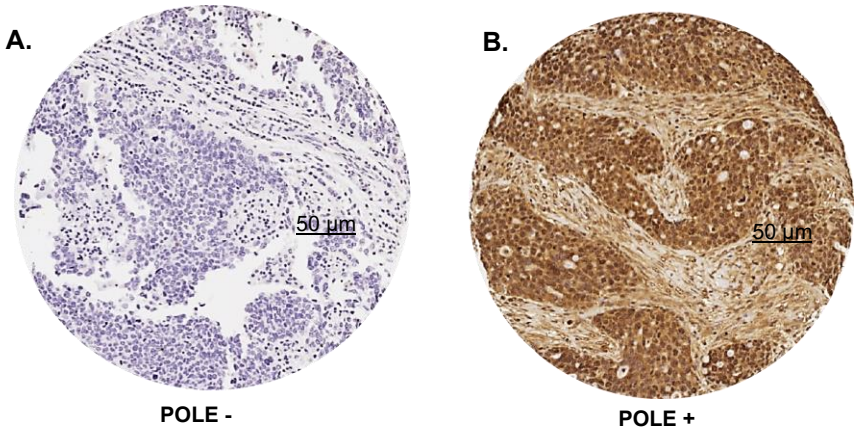

Figure 5-1. Immunohistochemical expression of POLE in epithelial ovarian tumours. Representative images of negative and positive staining for POLE in tumour microarrays at (x20 magnification; scale bar, 50 µm).

A study was then conducted to investigate the association between POLE expression and the clinicopathological features of EOC. A low nuclear POLE expression was in 75% (215/288), and high nuclear POLE expression was in 25% (73/288) of ovarian tumours. A high nuclear expression of POLE was highly significantly associated with the high tumour grade of ovarian cancer (*p=0.017*) (**Table 23**). High cytoplasmic POLE expression was observed in

49% (143/288) of ovarian tumours and low cytoplasmic was in 51% (145/288) of ovarian tumours. High nuclear POLE expression was significantly associated with poor progression free survival (PFS), (*p=0.021;* **Figure 5-2A**) and overall survival (OS), (*p=0.014;* **Figure 5-2B**) in EOC.

Low nuclear/low cytoplasmic expression of POLE was in 37% (107/288), low nuclear/high cytoplasmic was seen in 38% (109/288), high nuclear/high cytoplasmic expression of POLE was seen in 13% (37/288), and high nuclear/low cytoplasmic expression of POLE was seen in 12% (35/288). Tumours with high nuclear/ high cytoplasmic POLE levels were significantly associated with serous pathological type (P=0.032) (**Table 25**). The analysis showed that high nuclear/cytoplasmic expression was strongly associated with progression free survival (PFS) (p=0.001) and overall survival (OS) (p=0.001) in EOC (**Figure 5-3A, B**).

TP53 immunohistochemical analysis was performed on 331 ovarian cancers to determine their characteristics, as shown previously in chapter 3.

POLE – TP53 co-expression analysis was performed on 331 cases of ovarian cancers. Among these, 60% (197/331) showed POLE/TP53 co-expression in ovarian tumours. The co-expression of high POLE and high TP53 were significantly associated with serous pathological type (p=0.036) and high pathological grade (p=0.009). The co-expression of high POLE and high TP53 were significantly associated with non-residual tumours following surgery (p=0.034) (**Table 26**). The analysis also showed that low TP53/ low POLE co-expression was significantly associated with better progression free survival (PFS) (p=0.039), but not with overall survival (OS) (p=0.072) in

ovarian cancers as shown in (**Figure 5-4A, B**). The data taken together indicated that POLE may influence ovarian cancer pathogenesis, response to platinum therapy and prognosis.

Table 23. POLE nuclear expression in epithelial ovarian cancer

Parameters	*POLE Nuclear expression*		*R2*
	Low N (%)	*High N (%)*	*p value*
Menopausal Status			
Pre-menopausal	14 (7%)	2 (3%)	2.022
Peri menopausal	13 (6%)	3 (4%)	0.364
Post menopausal	186 (87%)	68 (93%)	
Age at Surgery class			
<30	3 (1%)	0 (0%)	1.974
31 to 60	85 (40%)	34 (47%)	0.373
>61	127 (59%)	39 (53%)	
Type of Surgery			
Biopsy	3 (1%)	1 (1%)	0.298
Early debulking	191 (90%)	66 (91%)	0.96
Interval debulking	13 (6%)	5 (7%)	
Delayed debulking	5 (3%)	1 (1%)	
Surgical Pathology Type			
Serous	120 (56%)	41 (56%)	8.044
Mucinous	34 (16%)	4 (6%)	0.154
Endometroid	26 (12%)	12 (16%)	
Clear Cell	13 (6%)	9 (12%)	
Other	10 (5%)	3 (4%)	
Mixed	12 (5%)	4 (6%)	
Surgical Pathology Grade			
Low	33 (18%)	4 (6%)	8.134
Intermediate	41 (23%)	10 (16%)	**0.017**
High	108 (59%)	50 (78%)	
Surgical Pathology Stage			
1	83 (40%)	25 (35%)	3.273
2	28 (14%)	15 (21%)	0.351
3	86 (42%)	31 (43%)	
4	8 (4%)	1 (1%)	
Surgical Pathology Substage			
A	42 (26%)	12 (21%)	0.473
B	23 (14%)	8 (14%)	0.79
C	97 (60%)	36 (65%)	
Residual Tumour Following Surgery			
Non	140 (71%)	43 (66%)	1.529
<1cm	23 (12%)	8 (12%)	0.675
1-2cm	8 (4%)	5 (8%)	
>2cm	25 (13%)	9 (14%)	
Platinum Sensitivity			
Sensitive	174 (92%)	50 (86%)	1.803
Resistant	15 (8%)	8 (14%)	0.179

Table 24. POLE cytoplasmic expression in epithelial ovarian cancer

Parameters	*POLE Cytoplasm expression*		*R2*
	Low N (%)	*High N (%)*	*p value*
Menopausal Status			
Pre-menopausal	8 (6%)	8 (6%)	1.128
Peri menopausal	10 (7%)	6 (4%)	0.569
Post menopausal	124 (87%)	130 (90%)	
Age at Surgery class			
<30	1 (1%)	2 (1%)	1.117
31 to 60	63 (44%)	56 (39%)	0.572
>61	79 (55%)	87 (60%)	
Type of Surgery			
Biopsy	2 (1%)	2 (2%)	9.622
Early debulking	126 (90%)	131 (91%)	**0.022**
Interval debulking	13 (9%)	5 (3%)	
Delayed debulking	0 (0%)	6 (4%)	
Surgical Pathology Type			
Serous	72 (50%)	89 (61%)	4.227
Mucinous	21 (15%)	17 (12%)	0.517
Endometroid	22 (15%)	16 (11%)	
Clear Cell	11 (8%)	11 (8%)	
Other	7 (5%)	6 (4%)	
Mixed	10 (7%)	6 (4%)	
Surgical Pathology Grade			
Low	19 (16%)	18 (14%)	1.134
Intermediate	21 (18%)	30 (23%)	0.567
High	77 (66%)	81 (63%)	
Surgical Pathology Stage			
1	59 (43%)	49 (35%)	6.728
2	16 (12%)	27 (20%)	0.081
3	61 (44%)	56 (40%)	
4	2 (1%)	7 (5%)	
Surgical Pathology Substage			
A	31 (27%)	23 (22%)	1.946
B	13 (11%)	18 (18%)	0.378
C	71 (62%)	62 (60%)	
Residual Tumour Following Surgery			
Non	99 (74%)	84 (66%)	5.223
<1cm	14 (10%)	17 (13%)	0.156
1-2cm	3 (2%)	10 (8%)	
>2cm	18 (14%)	16 (13%)	
Platinum Sensitivity			
Sensitive	108 (89%)	116 (92%)	0.576
Resistant	13 (11%)	10 (8%)	0.448

Table 25. POLE cytoplasmic/nuclear co-expression in epithelial ovarian cancer

Parameters	*POLE _Cyt/Nuc co-expression*				R^2
	Cyto Low/ Nuc Low	*Cyto High/ Nuc Low*	*Nuc High/ Cyto High*	*Nuc High/ Cyto Low*	
	N (%)	*N (%)*	*N (%)*	*N (%)*	*p value*
Menopausal Status					
Pre-menopausal	7 (7%)	7 (6%)	1 (3%)	1 (3%)	3.094
Peri menopausal	8 (8%)	5 (5%)	1 (3%)	2 (6%)	0.797
Post menopausal	91 (85%)	96 (89%)	35 (94%)	32 (91%)	
Age at Surgery class					
<30	1 (1%)	2 (2%)	0 (0%)	0 (0%)	4.26
31 to 60	44 (41%)	41 (38%)	15 (40%)	19 (54%)	0.642
>61	62 (58%)	66 (60%)	22 (60%)	16 (46%)	
Type of Surgery					
Biopsy	2 (2%)	1 (1%)	1 (3%)	0 (0%)	11.836
Early debulking	94 (89%)	98 (90%)	34 (91%)	31 (89%)	0.223
Interval debulking	9 (9%)	4 (4%)	1 (3%)	4 (11%)	
Delayed debulking	0 (0%)	5 (5%)	1 (3%)	0 (0%)	
Surgical Pathology Type					
Serous	55 (51%)	65 (59%)	24 (65%)	17 (49%)	17.288
Mucinous	20 (19%)	14 (13%)	3 (8%)	1 (3%)	0.302
Endometroid	14 (13%)	12 (11%)	4 (11%)	8 (23%)	
Clear Cell	7 (7%)	7 (6%)	5 (13%)	3 (8%)	
Other	5 (5%)	5 (4%)	1 (3%)	2 (6%)	
Mixed	6 (6%)	6 (5%)	0 (0%)	4 (11%)	
Surgical Pathology Grade					
Low	16 (19%)	17 (17%)	1 (3%)	3 (10%)	8.922
Intermediate	17 (20%)	24 (25%)	6 (19%)	4 (13%)	0.178
High	52 (61%)	57 (58%)	25 (78%)	24 (77%)	
Surgical Pathology Stage					
1	42 (41%)	42 (40%)	8 (22%)	16 (46%)	18.282
2	8 (8%)	20 (19%)	7 (19%)	8 (23%)	**0.032**
3	50 (49%)	36 (35%)	20 (56%)	11 (31%)	
4	2 (2%)	6 (6%)	1 (3%)	0 (0%)	
Surgical Pathology Substage					
A	23 (28%)	19 (24%)	4 (17%)	8 (26%)	4.651
B	11 (13%)	12 (15%)	6 (25%)	2 (6%)	0.589
C	49 (59%)	49 (61%)	14 (58%)	21 (68%)	
Residual Tumour Following Surgery					
Non	73 (72%)	68 (71%)	17 (53%)	25 (79%)	10.228
<1cm	11 (11%)	12 (13%)	5 (16%)	3 (9%)	0.332
1-2cm	2 (2%)	6 (6%)	4 (12%)	1 (3%)	
>2cm	15 (15%)	10 (10%)	6 (19%)	3 (9%)	
Platinum Sensitivity					
Sensitive	85 (89%)	90 (96%)	27 (82%)	22 (92%)	6.472
Resistant	11 (11%)	4 (4%)	6 (18%)	2 (8%)	0.091

Table 26. POLE/TP53 co-expression in epithelial ovarian cancer

Parameters	*POLE/TP53 co-expression*				R^2
	POLE Low/ TP53 Low	*POLE High/ TP53 Low*	*POLE High/ TP53 High*	*POLE Low/ TP53 High*	
	N (%)	*N (%)*	*N (%)*	*N (%)*	*p value*
Menopausal_Status					
Pre-menopausal	4 (8%)	4 (9%)	0 (0%)	3 (5%)	7.16
Peri menopausal	4 (8%)	2 (5%)	3 (7%)	1 (2%)	0.306
Post menopausal	40 (84%)	37 (86%)	40 (93%)	56 (93%)	
Age at Surgery class					
<30	0 (0%)	1 (2%)	0 (0%)	0 (0%)	4.558
31 to 60	19 (39%)	20 (46%)	18 (41%)	22 (37%)	0.602
>61	30 (61%)	23 (52%)	26 (59%)	38 (63%)	
Surgical Pathology Type					
Serous	21 (43%)	18 (41%)	30 (68%)	43 (72%)	26.184
Mucinous	6 (12%)	9 (20%)	4 (9%)	4 (7%)	**0.036**
Endometriod	10 (21%)	6 (14%)	3 (7%)	7 (12%)	
Clear Cell	5 (10%)	7 (16%)	2 (5%)	1 (1%)	
Other	3 (6%)	3 (7%)	1 (2%)	2 (3%)	
Mixed	4 (8%)	1 (2%)	4 (9%)	3 (5%)	
Surgical Pathology Grade					
Low	10 (27%)	9 (24%)	4 (10%)	4 (7%)	17.03
Intermediate	5 (13%)	10 (27%)	3 (7%)	11 (19%)	**0.009**
High	22 (60%)	18 (49%)	33 (83%)	42 (74%)	
Surgical Pathology Stage					
1	19 (43%)	20 (49%)	15 (35%)	19 (32%)	11.743
2	7 (16%)	10 (24%)	6 (14%)	7 (12%)	0.228
3	16 (36%)	11 (27%)	21 (49%)	29 (49%)	
4	2 (5%)	0 (0%)	1 (2%)	4 (7%)	
Surgical Pathology Substage					
A	10 (28%)	10 (32%)	12 (31%)	8 (19%)	2.627
B	4 (11%)	5 (16%)	4 (10%)	6 (15%)	0.854
C	22 (61%)	16 (52%)	23 (59%)	27 (66%)	
Residual Tumour Following Surgery					
Non	36 (82%)	34 (85%)	26 (63%)	33 (61%)	18.072
<1cm	4 (10%)	5 (12%)	7 (17%)	5 (9%)	**0.034**
1-2cm	2 (4%)	1 (3%)	2 (5%)	4 (8%)	
>2cm	2 (4%)	0 (0%)	6 (15%)	12 (22%)	
Platinum Sensitivity					
Sensitive	40 (95%)	35 (92%)	36 (92%)	47 (87%)	2.143
Resistant	2 (5%)	3 (8%)	3 (8%)	7 (13%)	0.543

5.4.1.2 Associations Between POLE Expression and Survival Outcomes in EOC

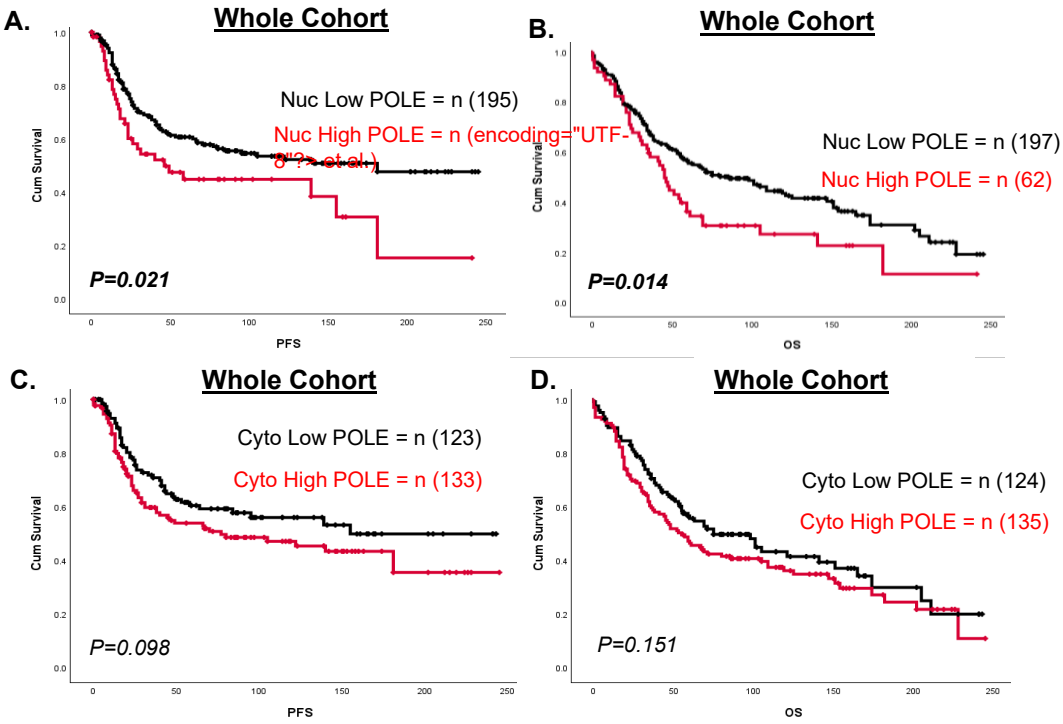

Figure 5-2. Kaplan Meier curve for POLE expression in ovarian tumours. A. Kaplan-Meier curve showing the correlation between nuclear POLE protein expression and progression-free survival (PFS) in the whole cohort. B. Kaplan-Meier curve showing the correlation nuclear POLE protein expression and overall survival in the whole cohort. C. Kaplan-Meier curve showing the correlation between cytoplasmic POLE protein expression and progression-free survival (PFS) in the whole cohort. D. Kaplan-Meier curve showing the correlation cytoplasmic POLE protein expression and overall survival in the whole cohort.

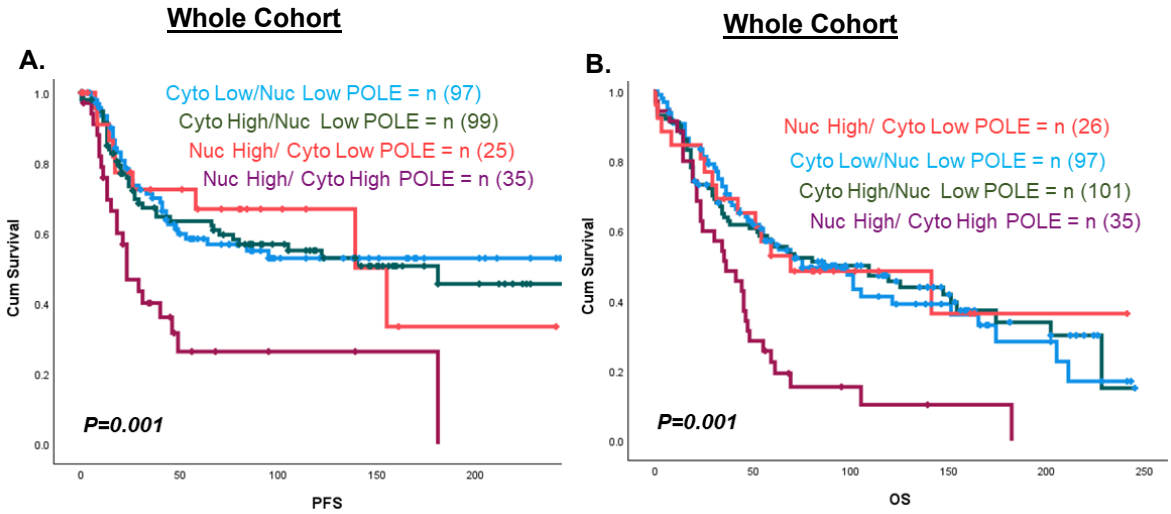

Figure 5-3. Kaplan Meier curve for nuclear/cytoplasmic POLE co-expression in ovarian tumours. A. Kaplan-Meier curve showing the correlation between nuclear/cytoplasmic POLE co-expression and progression-free survival (PFS) in the whole cohort. B. Kaplan-Meier curve showing the correlation between nuclear/cytoplasmic POLE co-expression and overall survival in the whole cohort.

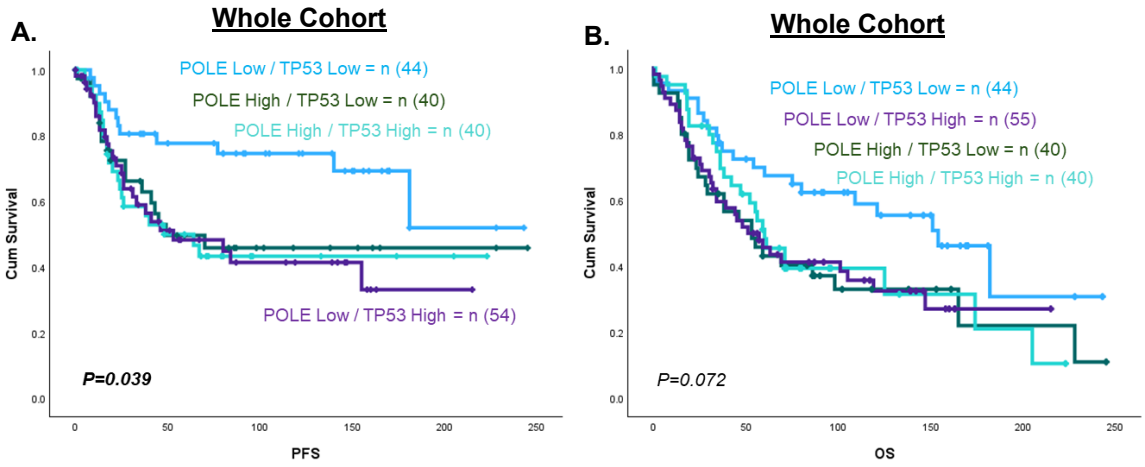

Figure 5-4. Kaplan Meier curve for POLE/TP53 co-expression in ovarian tumours. A. Kaplan-Meier curve showing the correlation between POLE/TP53 co-expression and progression-free survival (PFS) in the whole cohort. B. Kaplan-Meier curve showing the correlation between POLE/TP53 co-expression and overall survival in the whole cohort.

The transcriptomic levels of POLE were investigated in patients with EOC. High POLE mRNA expression was significantly associated with poor progression free survival (PFS) (*p=0.0028*) and overall survival (OS) (*p=0.038*) **(Figure 5-5)**. In summary, these clinical analyses show that the protein and transcriptional expression levels of POLE have predictive and prognostic significance in human EOC.

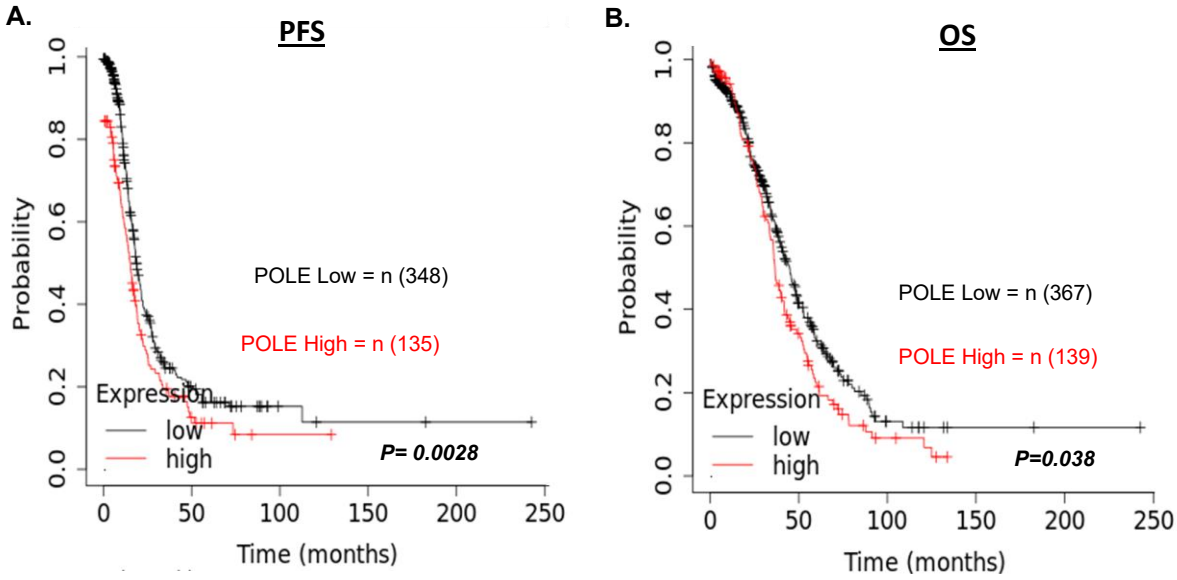

Figure 5-5. Clinicopathological studies of POLE mRNA expression in ovarian tumours. A. Kaplan-Meier curve showing the correlation between POLE mRNA expression and progression-free survival (PFS). B. Kaplan-Meier curve showing the correlation between POLE mRNA expression and overall survival (OS).

5.4.2 Pre-clinical studies

5.4.2.1 Depletion of POLE Enhances the Cisplatin-Sensitivity of EOC Cell Lines

Pre-clinical evaluation of POLE was conducted in platinum-sensitive and resistant EOC cell lines. First, the baseline levels of POLE were examined in A2780, A2780cis, PEO1, and PEO4 cells using western blotting of whole cell lysates (**Figure 5-6**). It was found that the level of POLE protein in A2780cis was slightly higher, but not significantly compared to A2780 cells. In addition, the protein level of POLE was significantly higher in PEO4 cells than in PEO1 cells. The higher expression of POLE in the cisplatin-resistant cell lines A2780cis and PEO4 cells than the corresponding cisplatin-sensitive A2780 and PEO1 cell lines suggests POLE may play a role in platinum resistance in the EOC cell line.

To evaluate the predictive significance of POLE for platinum sensitisation, cells were treated with (1-5) μM cisplatin for 24 to 48 hours. POLE levels significantly increased in all ovarian cell lines after 24 hours of cisplatin treatment. In A2780cis, POLE was higher than in A2780 cells. Similarly, in PEO4, POLE was higher than in PEO1 cells (**Figure 5-7**). However, POLE levels decreased after 48 hours of cisplatin treatment in all cell lines.

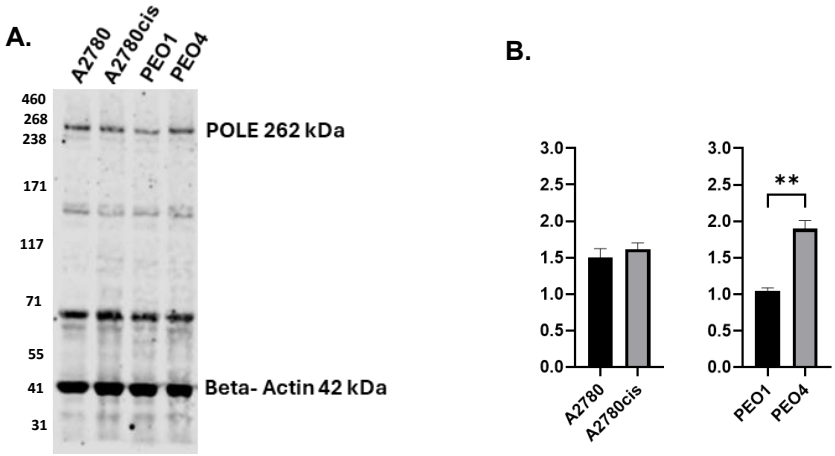

Figure 5-6. POLE protein levels in A2780, A2780cis, PEO1, and PEO4 cells. A. Western blot analysis and B. relative quantification of POLE levels in OC cell lines. High POLE protein levels were observed in A2780cis and PEO4 cells. The band intensities of POLE and β-actin were quantified using LI-COR software. The readings for POLE were normalized to those of β-actin using Microsoft Excel 2011. Data presentation and statistical analysis were performed using GraphPad Prism, version 9. The P value was calculated as follows, *p < 0.05, **p < 0.01 and ***p < 0.001. The experiment was performed for samples from three independent experiments n=3 and the error bar represent the standard deviation (SD).

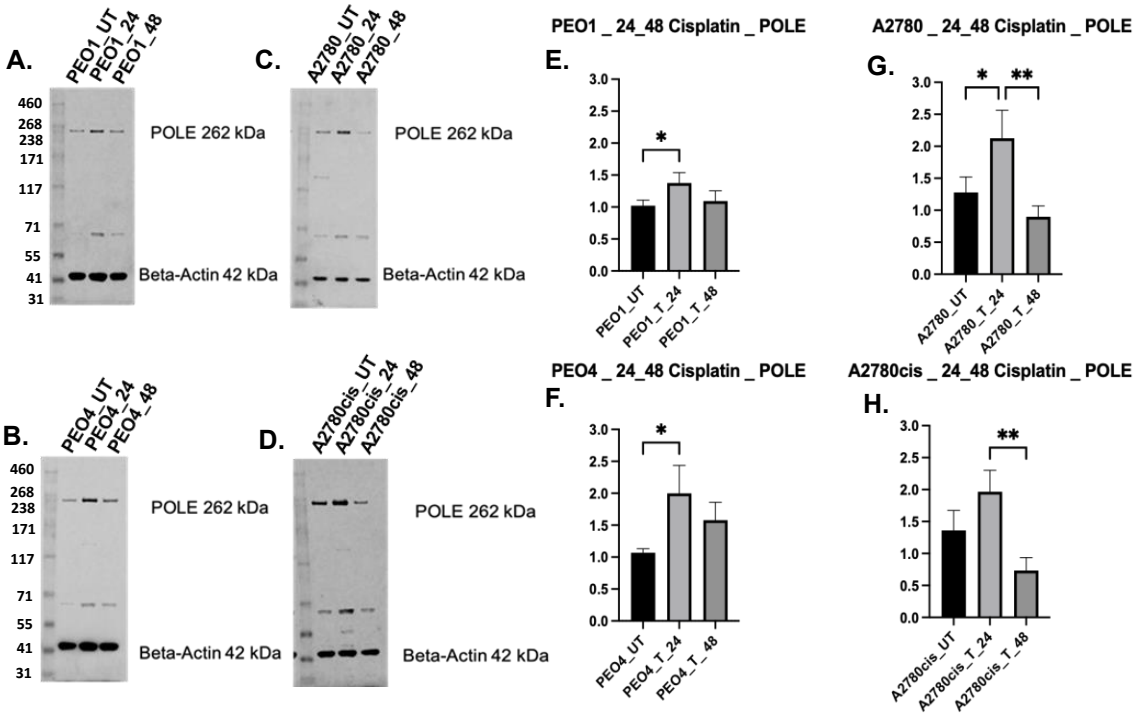

Figure 5-7. Western blot analysis for POLE protein expression levels in a panel of ovarian cancer cell lines before and after cisplatin-treated for 24h – 48h with Relative quantification of POLE levels in ovarian cell lines. Data presentation and statistical analysis were performed using GraphPad Prism, version 9. The P value was calculated as follows, *p < 0.05, **p < 0.01 and ***p < 0.001. The experiment was performed for samples from three independent experiments n=3 and the error bar represent the standard deviation (SD).

Following confirmation of the POLE protein expression in epithelial ovarian cells, mRNA expression was determined by Quantitative real-time PCR (RT-qPCR) using QuantiTect® Primers (Qiagen, UK), as described in the materials and methods chapter. Relative expressions were calculated for each cell line and compared to their respective control cell lines, using GAPDH as the housekeeping gene for standardization. The relative expression of POLE mRNA was calculated as the ratio between the expression of the POLE gene and the expression of the housekeeping gene. A negative control was included in each experiment. Baseline POLE mRNA expression was detected in ovarian cancer cell lines. Following cisplatin treatment for 24-48 hours, we investigated POLE transcript expression. POLE levels were high after 24 hours of cisplatin treatment in A2780cis compared to A2780. Similarly, POLE levels were high after 24 hours of cisplatin treatment in PEO4 compared to PEO1. However, POLE mRNA levels decreased after 48 hours of cisplatin treatment in all ovarian cell lines except A2780 cells (**Figure 5-8**).

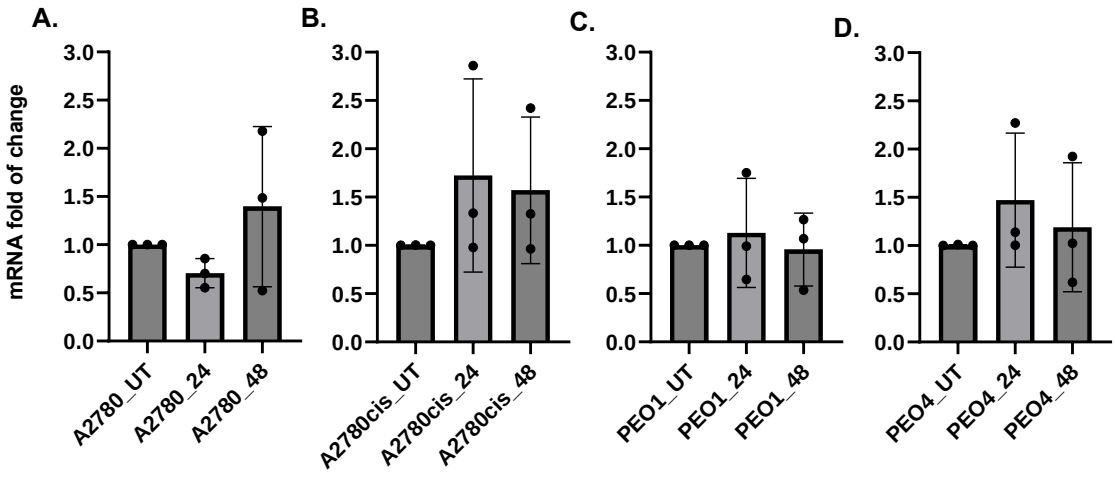

Figure 5-8. Real-time PCR analysis for POLE mRNA level expression in a panel of ovarian cell lines following 24-48h cisplatin treatment. Values plotted are means ± SD of the fold-change (ratio of mRNA/GAPDH normalized to control). Graphs were produced, and statistical analysis was performed using GraphPad Prism 9.

I then proceeded to generate transient knockdown (KD) of POLE using siRNAs in OVCAR 4 ovarian cancer cell line. OVCAR 4 is derived from a patient who did not respond to cisplatin therapy and showed resistance to other chemotherapeutic agents. It is of high-grade serous ovarian adenocarcinoma origin. The POLE knockdown was successful in OVCAR 4 cell lines on day 3 and day 5 compared to OVCAR 4 scrambled control (**Figure 5-9**).

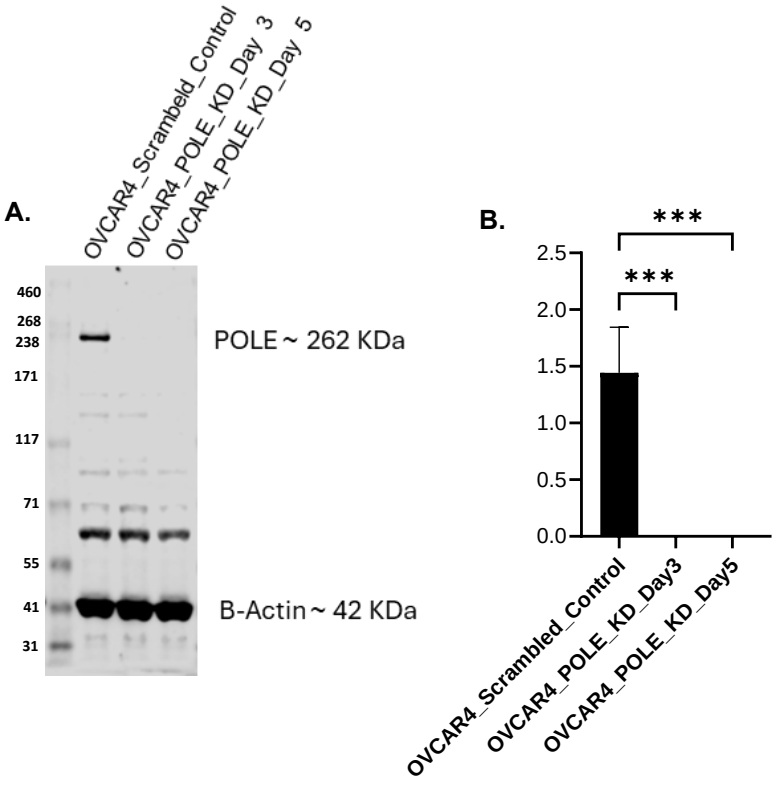

Figure 5-9. Knockdown of POLE in OVCAR4 cells using a siRNA. A. Representative western blot and B. quantification of POLE protein levels in OVCAR4 control and silenced cells. POLE was successfully knocked down on day 3 and day 5 in OVCAR4 cells. The P-value was calculated as *** $p<0.001$. D3 = day 3, D5 = day 5. Data presentation and statistical analysis were performed using GraphPad Prism, version 9. The experiment was performed for samples from three independent experiments n=3 and the error bar represent the standard deviation (SD).

Clonogenic assays showed that POLE_KD_OVCAR 4 cells were significantly more sensitive to cisplatin treatment than the scrambled control cells (**Figure *5-10* and Figure *5-11***). The results of the cell doubling time assay revealed a noticeably slower growth rate in OVCAR 4_POLE_KD cells compared to the OVCAR 4_scrambled control (**Figure *5-12***). This suggests that POLE depletion may influence DNA replication in epithelial ovarian cancer cells. However, the specific molecular mechanisms underlying these effects have yet to be fully understood and further investigation is needed. Next, functional studies using FACS were conducted for POLE_KD and scrambled control cells. After 24 hours of treatment with 1 μM cisplatin, POLE-depleted cells exhibited significant accumulation of γH2AX in the nucleus, a surrogate marker of DSBs. Accumulation of DSBs leads to activation of cell cycle checkpoints, resulting in cell cycle arrest, which allows the cells to repair DNA damage. Cells undergo apoptosis if the damage is irreparable. Thus, the effects of cisplatin on the cell cycle and apoptosis were examined in the POLE-deficient and control cells. After 24 hours of treatment with cisplatin, significantly higher proportions of cells arrested in the S phase and apoptotic cells were observed in POLE_KD cells compared with the scrambled controls (**Figure *5-13***).

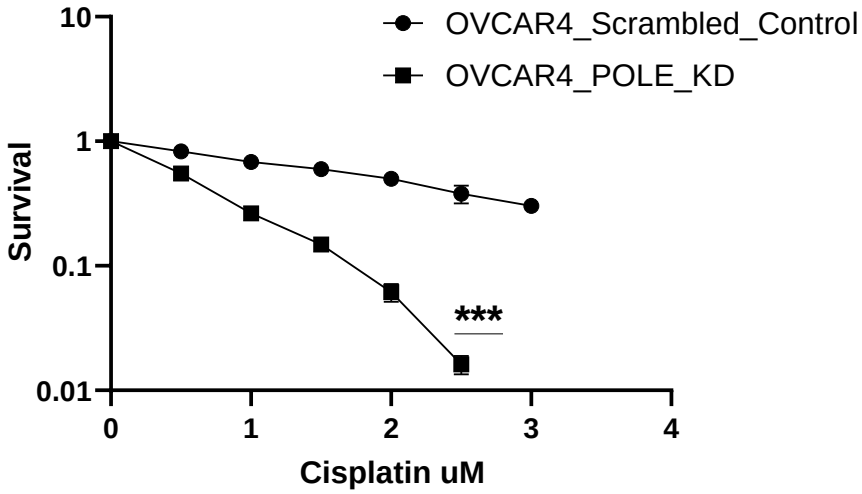

Figure 5-10. A Plot of Clonogenic assay of cisplatin sensitivity in OVCAR4 and POLE_KD_OVCAR4 cells. Depletion of POLE increased cisplatin sensitivity in OVCAR4 cells. The P-value was calculated as; ***p<0.001. Data presentation and statistical analysis were performed using GraphPad Prism, version 9. The experiment was performed for samples from three independent experiments n=3 and the error bar represent the standard deviation (SD).

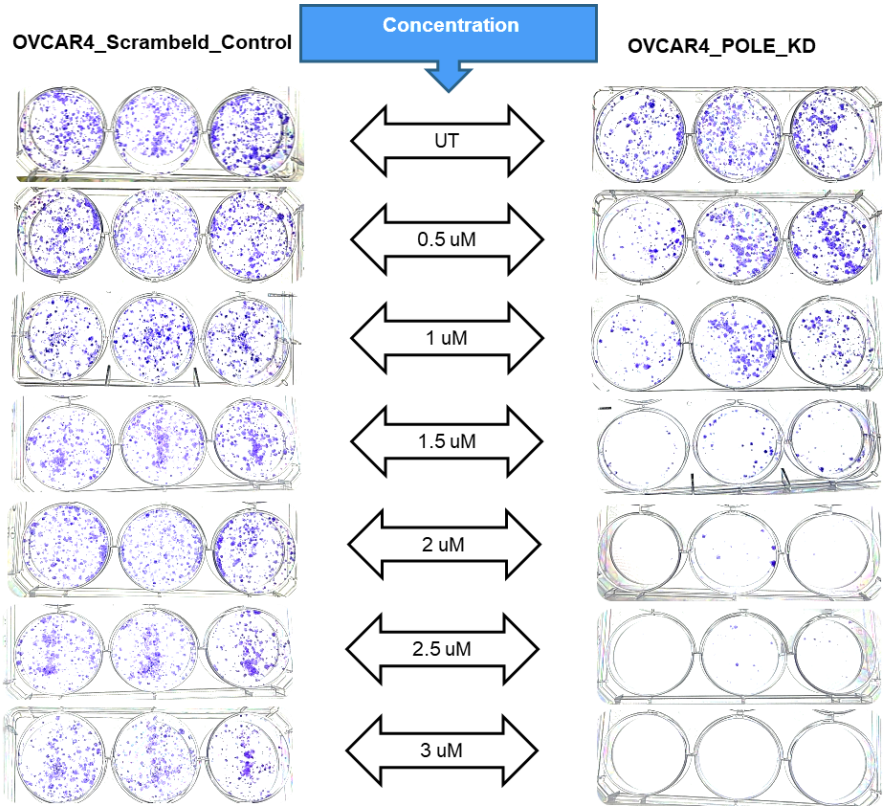

Figure 5-11. Clonogenic survival assay of cisplatin sensitivity in OVCAR4 and POLE_KD_OVCAR4 cells. OVCAR4 scrambled control and POLE_KD_OVCAR4 cells (300 cells/well) were plated into 6-well plates, incubated overnight, and then treated with the indicated doses of cisplatin for 14 days. Colonies were fixed and stained with crystal violet.

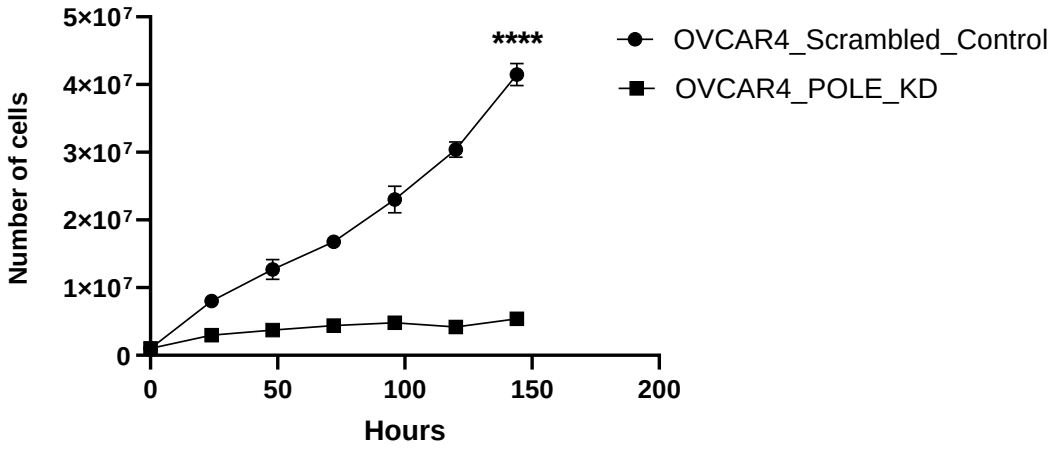

Figure 5-12. Representative the corresponding doubling times incubation for OVCAR4 scrambled control and POLE_KD_OVCAR4 cells. The P-value was calculated as; ****p<0.0001. Data presentation and statistical analysis were performed using GraphPad Prism, version 9. The experiment was performed for samples from three independent experiments n=3 and the error bar represent the standard deviation (SD).

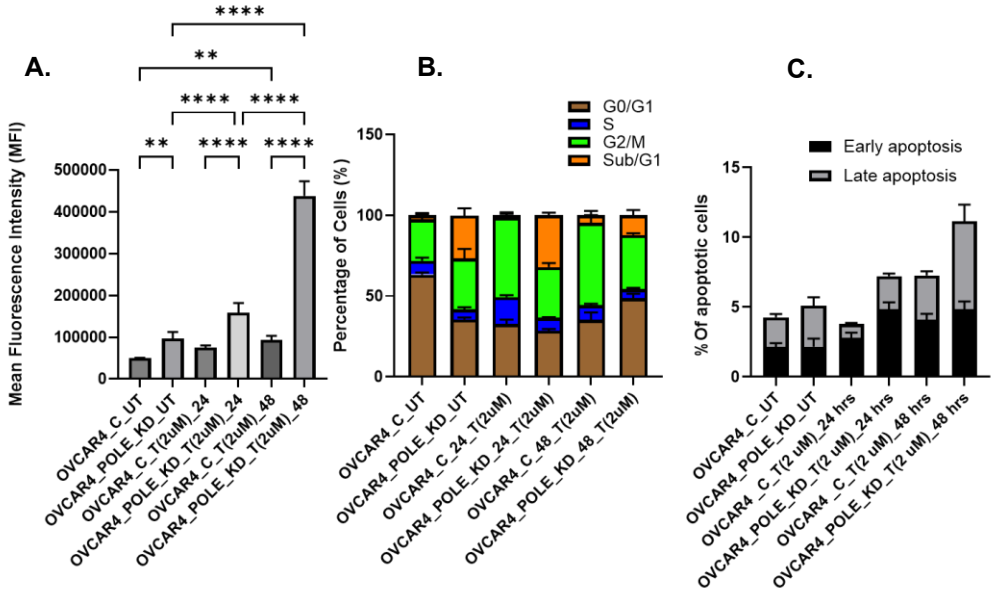

Figure 5-13. Functional studies of OVCAR4 cells using flow cytometry. A. Percentages of γH2Ax-positive cells; one-way ANOVA. OVCAR4_POLE_KD treated cells revealed a significant accumulation of γH2AX-positive cells. B. Cell cycle analysis of UT and treated cells, two-way ANOVA. OVCAR4_POLE_KD treated cells showed S-phase cell cycle arrest. C. Annexin V analysis of UT and treated cells: two-way ANOVA. OVCAR4_POLE_KD treated cells demonstrated significant increases in apoptotic cells. Kaluza Analysis Software. UT = untreated cells; T = treated cells. Data presentation and statistical analysis were performed using GraphPad Prism, version 9. The P value was calculated as follows, *p <0.05, **p <0.01, ***p <0.001 and ****p <0.0001. The experiment was performed for samples from three independent experiments n=3 and the error bar represent the standard deviation (SD).

5.5 Discussion

DNA polymerase epsilon (POLE) plays a critical role in DNA proofreading and replication (Rayner et al., 2016). Mutations in POLE have been associated with ultramutated tumours and have shown a positive response to immune checkpoint inhibitor (ICI) therapy (Johanns et al., 2016; Le et al., 2017). Studies have shown that POLE mutations are prevalent in various cancer types, including liver hepatocellular carcinoma (HCC), colorectal cancer, and endometrial cancer. These mutations result in a high tumour mutation burden and increased neoantigen load, leading to enhanced immunogenicity and a favourable response to immunotherapy(Church et al., 2013; Deng et al., 2004). Patients with pathogenic POLE mutations have shown improved clinical benefit rates, progression-free survival, overall survival, and longer treatment duration compared to those with benign variants. The number of co-occurring mutations does not seem to affect the response to ICI therapy. Further studies are needed to validate POLE mutations as predictive biomarkers for ICI therapy (Bellido et al., 2016; Mehnert et al., 2016).

Previous studies have investigated the role of DNA polymerase epsilon (POLE) in ovarian cancer. One study found that POLE mutations were present in 4.5% of ovarian endometrioid carcinomas, with a higher prevalence in low-grade tumours (Levine et al., 2013). Additionally, a study used whole genome sequencing data to identify the genomic positions of replication origins in POLE-mutated tumours, providing insights into the association between replication origins and DNA features (Bicknell et al.,

2011). Finally, a study in yeast cells showed that cancer-associated POLE exonuclease domain alleles drive ultra-mutagenesis, leading to a mutation pattern like cancer (Williams et al., 2013).

In the current study, overexpression of POLE was associated with aggressive clinicopathologic features and poor prognosis in ovarian cancers. The data provides evidence that POLE overexpression may represent a novel prognostic marker and predictive biomarker for platinum sensitivity in EOC.

Based on preclinical data, PEO4 and A2780cis cells showed higher POLE basal levels than A2780 and PEO1 cells, which exhibited lower basal levels. The upregulation of POLE gene expression in platinum-resistant cell lines could increase DNA repair capacity and replication stress processing thereby contributing to platinum resistance. Targeting POLE in these cells may offer potential benefits as a therapeutic strategy to improve outcomes in platinum-resistant ovarian cancers. Furthermore, DSB accumulations and S-phase arrest were increased along with higher apoptosis rates after depleting POLE in A2780cis cells; this finding shows that depletion of POLE might result in greater sensitivity towards cisplatin treatment cells. Taken together, the data provides evidence that POLE could be a promising predictive and prognostic factor in EOC.

Chapter 6 POLE in Breast Cancer

6.1 Introduction

Breast cancer is a multifaceted disease with various subtypes and characteristics that impact patient prognosis and treatment options. Recent research has emphasised the significance of DNA polymerase, specifically polymerase epsilon (POLE), in the development and progression of breast cancer (Alanazi et al., 2020; Schuh et al., 2018). POLE is a crucial enzyme involved in DNA replication and repair, and its dysfunctional activity has been associated with breast cancer (Couch et al., 2013; Malhotra et al., 2010). Recent studies on genomics have discovered that POLE mutations are present in breast cancer patients (Bellido et al., 2016). These mutations are more common in specific subtypes of breast cancer, such as luminal and HER2-enriched breast cancers. It is important to note that POLE mutations are linked to a hypermutator phenotype, which leads to a higher mutation rate. This hypermutation may result in the accumulation of genetic changes that stimulate tumour progression and cause resistance to therapy (Garmezy et al., 2022; Mardis, 2019).

POLE is a gene that helps to maintain the stability of DNA. The dysfunction of this gene is linked to an increased risk of cancer (Fouad & Aanei, 2017). Previous studies have shown that mutations in the POLE gene may cause sporadic breast cancer. POLE is expressed in many tissues and is crucial in cell division (Temko et al., 2018). During cell division, POLE is responsible for replicating DNA in Genomic Instability. Dysregulation or mutations in POLE can cause errors in DNA replication, which increases mutation rate and

causes genomic instability (Temko et al., 2018) (Henninger & Pursell, 2014). In cases of breast cancer, high levels of genomic instability can lead to tumour heterogeneity and may impact treatment responses. POLE plays an essential role in DNA repair, and its mutations can result in hypermutator phenotype in cells (Eggink et al., 2017). The clinicopathological significance of POLE in breast cancers is largely unknown.

6.2 Aims of this study

1- Assess POLE expression in invasive breast cancer tissues

a- To investigate the expression of POLE in invasive breast cancer tissues using immunohistochemistry (IHC) on tumour microarrays (TMAs) from 4221 breast cancer patients.

b- To evaluate POLE cytoplasmic and nuclear expression using H-scores.

c- To correlate POLE expression with clinicopathological features and clinical outcomes, assessing its potential as a prognostic marker in breast cancer.

2- Investigate the prognostic significance of nuclear and cytoplasmic POLE expression in breast cancer subtypes

a- To evaluate the relationship between POLE expression levels and breast cancer-specific survival (BCSS) in ER+, HER2-enriched, and triple-negative breast cancer (TNBC) cohorts.

3- Assess the predictive utility of POLE expression in endocrine therapy outcomes

a- To determine the association between nuclear and cytoplasmic POLE expression and survival outcomes in ER+ patients receiving endocrine therapy.

4- Examine POLE expression in a panel of breast cancer cell lines

a- To evaluate POLE expression in various breast cancer cell lines, including normal mammary epithelial cells (MCF10-A), ductal carcinoma in situ (DCIS), estrogenic receptor-positive (ER+) invasive breast cancer (MCF7, T47D), and triple-negative breast cancer (TNBC) cells (MDA-MB-231).

b- To investigate differences in POLE expression between different breast cancer subtypes and assess the relationship between POLE expression and tumour characteristics.

6.3 Method

Immunohistochemistry of POLE was performed on TMAs of 4221 patients with invasive breast cancers. Patient demographics are summarized, and the immunohistochemistry protocol and antibody details are described in the Materials and Methods chapter. Evaluation of immune staining was performed by calculation of H-scores (range 0–300). For cytoplasmic expression of POLE, a H-score of ≤ 20 was used, and for nuclear expression, a H-score of >110. A Western blot was performed on a panel of breast cell lines, including MCF10-A, DCIS, MCF7, T47D, and MDA-MB-231, after confirming the specificity of the antibody. Media used to maintain all the cell lines, as well as cell passaging and storage, are described in the Materials and Methods chapter. Assays used in this study include western

blotting, as detailed in the Materials and Methods chapter as well. All experiments were repeated 3 times. Data analysis was performed on GraphPad Prism-9 software. Error bars represent the standard error of the mean between experiments. P-values are indicated as P-values <0.05 =*, p-value <0.01 =** & p-value <0.001=***.

6.4 Results

6.4.1 Clinical study

6.4.1.1 Deficiency of POLE is Associated with Aggressive Breast Cancer

The expression of POLE in ductal carcinoma in situ (DCIS) and invasive breast cancer (IBC) was examined by IHC staining to determine whether POLE is associated with the clinicopathological features of BC. The expression of POLE was examined in 776 cases of pure DCIS, 239 cases of invasive BC coexisting with DCIS, 4221 cases of invasive breast cancer, and 50 normal breast tissues. The demographics and pathological characteristics of these patients are described in Materials and Methods chapter.

The immunohistochemical staining revealed that POLE protein was expressed within the nucleus and cytoplasmic of breast tissues **(Figure 6-1).**

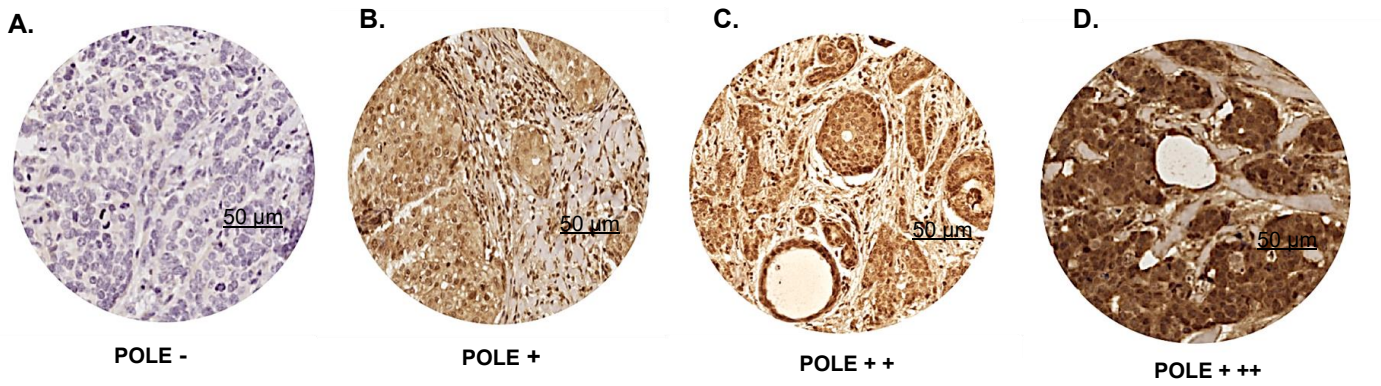

Figure 6-1. Immunohistochemistry staining of POLE in breast cancer. Representative images of negative and positive staining in TMAs imaged at (x20 magnification; scale bar, 50 µm).

Full-face tissue sections revealed a homogenous staining pattern, indicating the suitability of TMA for POLE expression evaluation as described in the Materials and Methods chapter. The next step was to determine the relationship between POLE expression and BC clinicopathological characteristics. The Pearson's chi-square test was used to evaluate the significance of the associations between the clinicopathological characteristics of BC and POLE expression.

POLE nuclear expression was low in 85% (297/349) of the cases of DCIS and high in 15% (52/349). It was found that patients with POLE- nuclear expression in DCIS had no significant association with clinicopathological features (**Table 27**). POLE cytoplasmic expression was low in 83% (290/349) and high in 17% (59/349) of the DCIS cases. It was observed that no significant association between POLE cytoplasmic expression of DCIS and clinicopathological features (**Table 28**). This data suggests that POLE does not influence DCIS pathogenesis.

Table 27. POLE nuclear expression in ductal carcinoma in situ (DCIS)

Parameters	*POLE Nuclear Expression*		R^2
	Low (N%)	*High (N%)*	*p value*
Age 50 Years			
≤ 50	77 (26%)	12 (23%)	0.189
> 50	220 (74%)	40 (77%)	0.664
Tumour size			
≤ 2cm	129 (44%)	21 (41%)	0.115
> 2cm	166 (56%)	30 (59%)	0.734
3 Tier Grade			
Low	36 (12%)	7 (13%)	0.309
Intermediate	79 (27%)	12 (23%)	0.857
High	182 (61%)	33 (64%)	
Comedo Type Necrosis			
No	110 (37%)	15 (29%)	1.291
Yes	187 (63%)	37 (71%)	0.256
Residual_Tumour			
No	59 (51%)	6 (33%)	1.917
Yes	57 (49%)	12 (67%)	0.166
ER Status			
ER-	61 (25%)	13 (30%)	0.463
ER+	186 (75%)	31 (70%)	0.496
PgR Status			
Negative	103 (41%)	20 (48%)	0.707
Positive	150 (59%)	22 (52%)	0.4
HER2 Status			
Negative	213 (79%)	31 (72%)	0.997
Positive	57 (21%)	12 (28%)	0.318
Ki67			
Low	181 (78%)	25 (68%)	1.806
High	52 (22%)	12 (32%)	0.179
Molecular Classes with Ki-67			
Luminal A	116 (54%)	16 (46%)	2.675
Luminal B	43 (20%)	6 (17%)	0.445
HER2 Enriched	32 (15%)	9 (26%)	
TNBC	25 (11%)	4 (11%)	
Recurrence			
No	261 (88%)	47 (90%)	0.268
Yes	36 (12%)	5 (10%)	0.605

Table 28. POLE cytoplasmic expression in ductal carcinoma in situ (DCIS)

Parameters	*POLE Cytoplasmic Expression*		R^2
	Low (N%)	*High (N%)*	*p value*
Age 50 Years			
≤ 50	70 (24%)	19 (32%)	1.679
> 50	220 (76%)	40 (68%)	0.195
Tumour size			
≤ 2cm	130 (45%)	20 (34%)	2.589
> 2cm	157 (55%)	39 (66%)	0.108
3 Tier Grade			
Low	35 (12%)	8 (14%)	0.178
Intermediate	75 (26%)	16 (27%)	0.915
High	180 (62%)	35 (59%)	
Comedo Type Necrosis			
No	101 (35%)	24 (41%)	0.73
Yes	189 (65%)	35 (59%)	0.393
Residual_Tumour			
No	50 (47%)	15 (56%)	0.672
Yes	57 (53%)	12 (44%)	0.412
ER Status			
ER-	64 (27%)	10 (20%)	0.939
ER+	177 (73%)	40 (80%)	0.333
PgR Status			
Negative	105 (43%)	18 (35%)	1.039
Positive	139 (57%)	33 (65%)	0.308
HER2 Status			
Negative	197 (77%)	47 (84%)	1.416
Positive	60 (23%)	9 (16%)	0.234
Ki67			
Low	168 (76%)	38 (78%)	0.052
High	53 (24%)	11 (22%)	0.819
Molecular Classes with Ki-67			
Luminal A	107 (52%)	25 (57%)	2.119
Luminal B	40 (19%)	9 (20%)	0.548
HER2 Enriched	37 (18%)	4 (9%)	
TNBC	23 (11%)	6 (14%)	
Recurrence			
No	255 (88%)	53 (90%)	0.171
Yes	35 (12%)	6 (10%)	0.68

A total of 1480 invasive breast cancer cases were suitable for scoring and evaluation. Low nuclear POLE levels were seen in 79% of tumours (n= 1162/1480), and high nuclear POLE levels were observed in 21% of tumours (n= 318/1480) (**Table 29**). A low nuclear POLE level was significantly associated with aggressive features including tumour size, high tumour grade, high mitotic index, Nottingham Prognostic Index (NPI), Ki67 index and triple negative ($p<0.05$). In contrast, high nuclear POLE level was significantly associated with less aggressive features including ER+, PR+, and luminal A molecular classes ($p<0.01$). This data suggests that nuclear POLE level may be influence aggressiveness of breast cancer.

High cytoplasmic POLE level was seen in 73% of tumours (n= 1077/1480), and low cytoplasmic POLE level was seen in 27% of tumours (n= 403/1480) (**Table 30**). A high cytoplasmic POLE level was significantly associated with high pleomorphism and no special histological tumour type ($p\leq0.01$). In contrast, a low cytoplasmic POLE level was not significantly associated with any clinicopathological features based on ($p>0.05$).

Nuclear and cytoplasmic co-expression of POLE in invasive breast cancer: 58% (858/1480) of tumours were low nuclear/high cytoplasmic, 21% (315/1480) were low nuclear/low cytoplasmic, 16% (230/1480) were high nuclear/high cytoplasmic and 5 % (77/1480) were high nuclear/low cytoplasmic (**Table 31**). Tumours with low nuclear/ high cytoplasmic POLE levels were significantly associated with no special histological type ($p<0.01$). Tumours with high nuclear/ high cytoplasmic POLE levels were significantly linked with tumour size and high pleomorphism ($p\leq0.01$). Furthermore,

tumours with high nuclear/ low cytoplasmic POLE levels were strongly associated with tumour grade, Mitosis, and luminal A molecular classes (*p=<0.05*) (**Table 31**).

Normal breast tissues exhibited high levels of POLE protein expression. The levels of POLE expression of both nuclear and cytoplasmic were significantly lower in DCIS and IBC than in the normal breast tissues (*p<0.0001*) (**Figure 6-2A, B**). The local recurrence-free interval was not significantly shorter for patients with low POLE nuclear DCIS compared to those with high POLE DCIS (*p=0.5470*) (**Figure 6-2C**). Moreover, the local recurrence-free interval was not significantly shorter for patients with low POLE cytoplasmic DCIS compared to those with high POLE DCIS (*p=0.48*) (**Figure 6-2 D**).

Table 29. POLE Nuclear expression in breast cancer

Parameters	POLE Nuclear Expression		R^2
	Low (N%)	High (N%)	p value
Tumour size			
< 2cm	645 (56%)	207 (65%)	9.393
≥ 2cm	517 (44%)	111 (35%)	**0.002**
Grade			
1	186 (16%)	67 (21%)	12.883
2	416 (36%)	133 (42%)	**0.002**
3	560 (48%)	118 (37%)	
Tubular formation			
1	84 (7%)	35 (11%)	5.016
2	358 (31%)	98 (31%)	0.081
3	720 (62%)	185 (58%)	
Pleomorphism			
1	33 (3%)	11 (3%)	1.84
2	384 (33%)	116 (37%)	0.399
3	745 (64%)	191 (60%)	
Mitosis			
1	476 (41%)	171 (54%)	19.241
2	233 (20%)	61 (19%)	**<0.0001**
3	453 (39%)	86 (27%)	
Histological Tumour Type			
NST	740 (64%)	183 (57%)	6.8
Lobular	97 (8%)	35 (11%)	0.08
Other special types	51 (4%)	22 (7%)	
NST mixed	274 (24%)	78 (25%)	
LVI			
Absent	810 (70%)	230 (72%)	0.82
Present	352 (30%)	88 (28%)	0.365
Lymph Node status			
Negative	732 (63%)	205 (65%)	0.232
Positive	430 (37%)	113 (35%)	0.63
NPI			
GPG	367 (32%)	124 (39%)	6.529
MPG	615 (53%)	154 (48%)	**0.038**
PPG	180 (15%)	40 (13%)	
ER Status			
ER-	297 (26%)	50 (16%)	13.489
ER+	861 (74%)	267 (84%)	**<0.0001**
PgR Status			
Negative	491 (43%)	110 (35%)	6.583
Positive	652 (57%)	205 (65%)	**0.01**
HER2 Status			
Negative	991 (86%)	273 (87%)	0.025
Positive	157 (14%)	42 (13%)	0.875
Ki67 index			
Low	401 (46%)	132 (54%)	4.515
High	467 (54%)	113 (46%)	**0.034**
Molecular Classes			
Luminal A	353 (36%)	125 (47%)	15.889
Luminal B	347 (36%)	95 (35%)	**0.001**
HER2+	70 (7%)	17 (6%)	
Triple negative	204 (21%)	31 (12%)	
Menopausal Status			
Pre	420 (36%)	120 (38%)	0.273
Post	742 (64%)	198 (62%)	0.601
Age 50 Years			
< 50	381 (33%)	100 (31%)	0.205
≥ 50	781 (67%)	218 (69%)	0.651

Table 30. POLE Cytoplasmic expression in breast cancer

Parameters	POLE Cytoplasmic Expression		R^2
	Low (N%)	High (N%)	p value
Tumour size			
< 2cm	225 (56%)	627 (58%)	0.683
≥ 2cm	178 (44%)	450 (42%)	0.408
Grade			
1	71 (17%)	182 (17%)	0.305
2	152 (38%)	397 (37%)	0.858
3	180 (45%)	498 (46%)	
Tubular formation			
1	28 (7%)	91 (8%)	0.901
2	125 (31%)	331 (31%)	0.637
3	250 (62%)	655 (61%)	
Pleomorphism			
1	20 (5%)	24 (2%)	9.701
2	145 (36%)	355 (33%)	**0.008**
3	238 (59%)	698 (65%)	
Mitosis			
1	169 (42%)	478 (44%)	3.59
2	93 (23%)	201 (19%)	0.166
3	141 (35%)	398 (37%)	
Histological Tumour Type			
NST	238 (59%)	685 (63%)	10.65
Lobular	51 (13%)	81 (7%)	**0.01**
Other special types	23 (6%)	50 (5%)	
NST mixed	91 (22%)	261 (25%)	
LVI			
Absent	291 (72%)	749 (70%)	0.996
Present	112 (28%)	328 (30%)	0.318
Lymph Node status			
Negative	260 (65%)	677 (63%)	0.346
Positive	143 (35%)	400 (37%)	0.556
NPI			
GPG	134 (33%)	357 (33%)	1.007
MPG	215 (53%)	554 (52%)	0.604
PPG	54 (14%)	166 (15%)	
ER Status			
ER-	97 (24%)	250 (23%)	0.16
ER+	303 (76%)	825 (77%)	0.689
PgR Status			
Negative	157 (40%)	444 (42%)	0.486
Positive	238 (60%)	619 (58%)	0.486
HER2 Status			
Negative	341 (86%)	923 (87%)	0.118
Positive	56 (14%)	143 (13%)	0.732
Ki67 index			
Low	148 (51%)	385 (47%)	1.727
High	141 (49%)	439 (53%)	0.189
Molecular Classes			
Luminal A	128 (40%)	350 (38%)	5.399
Luminal B	103 (32%)	339 (37%)	0.145
HER2+	30 (10%)	57 (6%)	
Triple negative	57 (18%)	178 (19%)	
Menopausal Status			
Pre	154 (38%)	386 (36%)	0.713
Post	249 (62%)	691 (64%)	0.399
Age 50 Years			
< 50	144 (36%)	337 (31%)	2.637
≥ 50	259 (64%)	740 (69%)	0.104

Table 31. POLE CO-expression (Nuclear/Cytoplasmic) in breast cancer

Parameters	*Cyto Low/ Nuc Low* (N%)	*Cyto High/ Nuc Low* (N%)	*Nuc High/ Cyto Low* (N%)	*Nuc High/ Cyto Low* (N%)	R^2 p value
Tumour size					
< 2cm	172 (55%)	478 (56%)	154 (67%)	48 (62%)	11.361
≥ 2cm	143 (45%)	380 (44%)	76 (33%)	29 (38%)	**0.01**
Grade					
1	54 (17%)	134 (15%)	50 (22%)	15 (19%)	16.28
2	107 (34%)	315 (37%)	88 (38%)	39 (51%)	**0.012**
3	154 (49%)	409 (48%)	92 (40%)	23 (30%)	
Tubular formation					
1	22 (7%)	62 (7%)	29 (12%)	6 (8%)	8.861
2	100 (32%)	261 (30%)	73 (32%)	22 (28%)	0.182
3	193 (61%)	535 (63%)	128 (56%)	49 (64%	
Pleomorphism					
1	14 (4%)	20 (2%)	5 (2%)	5 (7%)	18.669
2	100 (32%)	291 (34%)	71 (31%)	38 (49%)	**0.005**
3	201 (64%)	547 (64%)	154 (67%)	34 (44%)	
Mitosis					
1	119 (38%)	364 (42%)	121 (52%)	43 (56%)	23.685
2	77 (24%)	157 (18%)	45 (20%)	15 (19%)	**0.001**
3	119 (38%)	337 (40%)	64 (28%)	19 (25%)	
Histological Tumour Type					
NST	196 (62%)	547 (64%)	141 (61%)	39 (51%)	23.2
Lobular	29 (9%)	74 (9%)	13 (6%)	16 (21%)	**0.006**
Other special types	18 (6%)	33 (4%)	17 (7%)	5 (6%)	
NST mixed	72 (23%)	204 (23%)	59 (26%)	17 (22%)	
LVI					
Absent	230 (73%)	588 (68%)	169 (73%)	53 (69%)	3.588
Present	85 (27%)	270 (32%)	61 (27%)	24 (31%)	0.31
Lymph Node status					
Negative	208 (66%)	531 (62%)	153 (66%)	45 (58%)	3.558
Positive	107 (34%)	327 (38%)	77 (34%)	32 (42%)	0.313
NPI					
GPG	102 (32%)	269 (31%)	92 (40%)	28 (36%)	7.779
MPG	170 (54%)	451 (53%)	109 (47%)	39 (51%)	0.255
PPG	43 (14%)	138 (16%)	29 (13%)	10 (13%)	
ER Status					
ER-	87 (28%)	211 (25%)	40 (17%)	9 (12%)	14.35
ER+	226 (72%)	645 (75%)	190 (83%)	67 (88%)	**0.002**
PgR Status					
Negative	134 (43%)	359 (42%)	87 (38%)	21 (28%)	7.541
Positive	175 (57%)	486 (58%)	142 (62%)	54 (72%)	0.057
HER2 Status					
Negative	262 (84%)	740 (87%)	194 (84%)	68 (92%)	4.96
Positive	50 (16%)	107 (13%)	36 (16%)	6 (8%)	0.175
Ki67 index					
Low	110 (49%)	296 (46%)	94 (52%)	33 (59%)	5.173
High	116 (51%)	353 (54%)	88 (48%)	23 (41%)	0.16
Molecular Classes					
Luminal A	92 (37%)	266 (36%)	89 (44%)	31 (54%)	25.623
Luminal B	82 (32%)	267 (37%)	74 (37%)	19 (33%)	**0.002**
HER2+	28 (11%)	42 (6%)	15 (7%)	2 (3%)	
Triple negative	50 (20%)	155 (21%)	24 (12%)	6 (10%)	
Menopausal Status					
Pre	118 (38%)	307 (36%)	84 (36%)	31 (40%)	0.786
Post	197 (62%)	551 (64%)	146 (64%)	46 (60%)	0.853
Age 50 Years					
< 50	116 (37%)	268 (31%)	72 (31%)	25 (33%)	
≥ 50	199 (63%)	590 (69%)	158 (69%)	52 (67%)	

In the whole cohort, low POLE nuclear expression was associated with poor outcomes in terms of shorter breast cancer specific survival (BCSS) (*p=0.008*) (**Figure 6-3A**) and high POLE cytoplasmic expression was associated with poor outcomes in terms of shorter breast cancer specific survival (BCSS) (*p=0.235*) (**Figure 6-3B**). Moreover, high cytoplasmic/low nuclear co-expression POLE was significantly associated with poor outcomes in terms of shorter breast cancer specific survival (BCSS) (*p=0.015*) (**Figure 6-3C**).

Among the patients with ER+ breast cancer who received endocrine therapy, low nuclear POLE expression was associated with poorer BCSS (*p=0.015)* (**Figure 6-4A**). There was no significant association between cytoplasmic expression and BCSS (*p=0.36*) (**Figure 6-4B**). The data suggests that low POLE expression may predict a limited response to endocrine therapy. In luminal classes, low nuclear POLE was also associated with shorter BCSS (*p=0.009*) (**Figure 6-5A**). There was no significant association between cytoplasmic POLE and BCSS (*p=0.586*) (**Figure 6-5B**). In both nuclear and cytoplasmic POLE expression was not significantly associated with any survival outcome in endocrine naive, HER2, TNBC, chemo-treated, and chemo-naive breast cancers (*p=>0.05*) (**Figure 6-4C, D and Figure 6-5C, D, E, F and Figure 6-6A, B, C, D**).

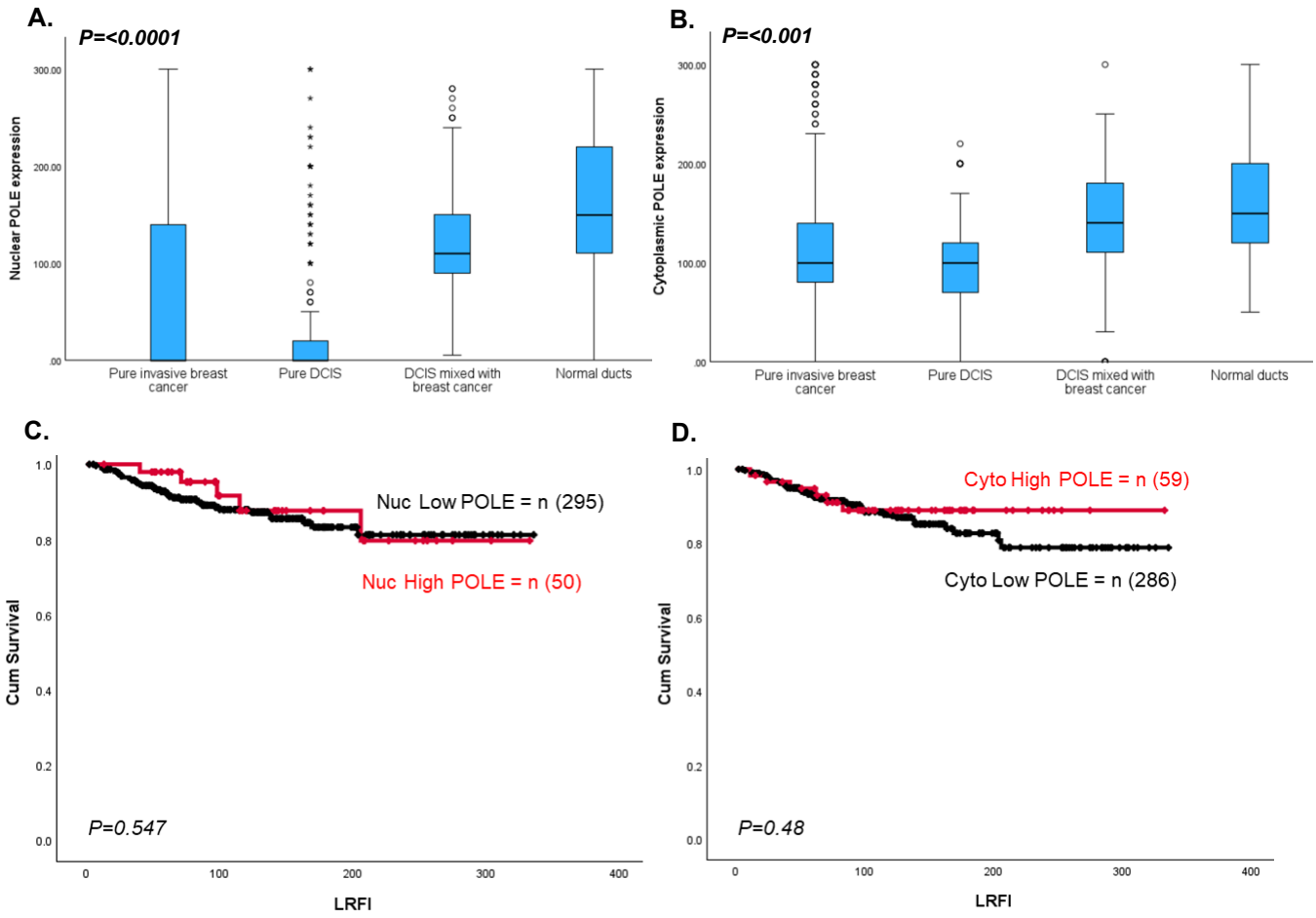

Figure 6-2. Clinicopathological studies of POLE expression in DCIS. A. Box plot showing mean nuclear POLE expression (H-score) in normal breast tissues, pure DCIS, and DCIS mixed tumours. B. Box plot showing mean cytoplasmic POLE expression (H-score) in normal breast tissues, pure DCIS, and DCIS mixed tumours. C. Kaplan-Meier analysis of nuclear POLE expression and the recurrence-free interval (LRFI) for patients with DCIS. D. Kaplan-Meier analysis of cytoplasmic POLE expression and the recurrence-free interval (LRFI) for patients with DCIS.

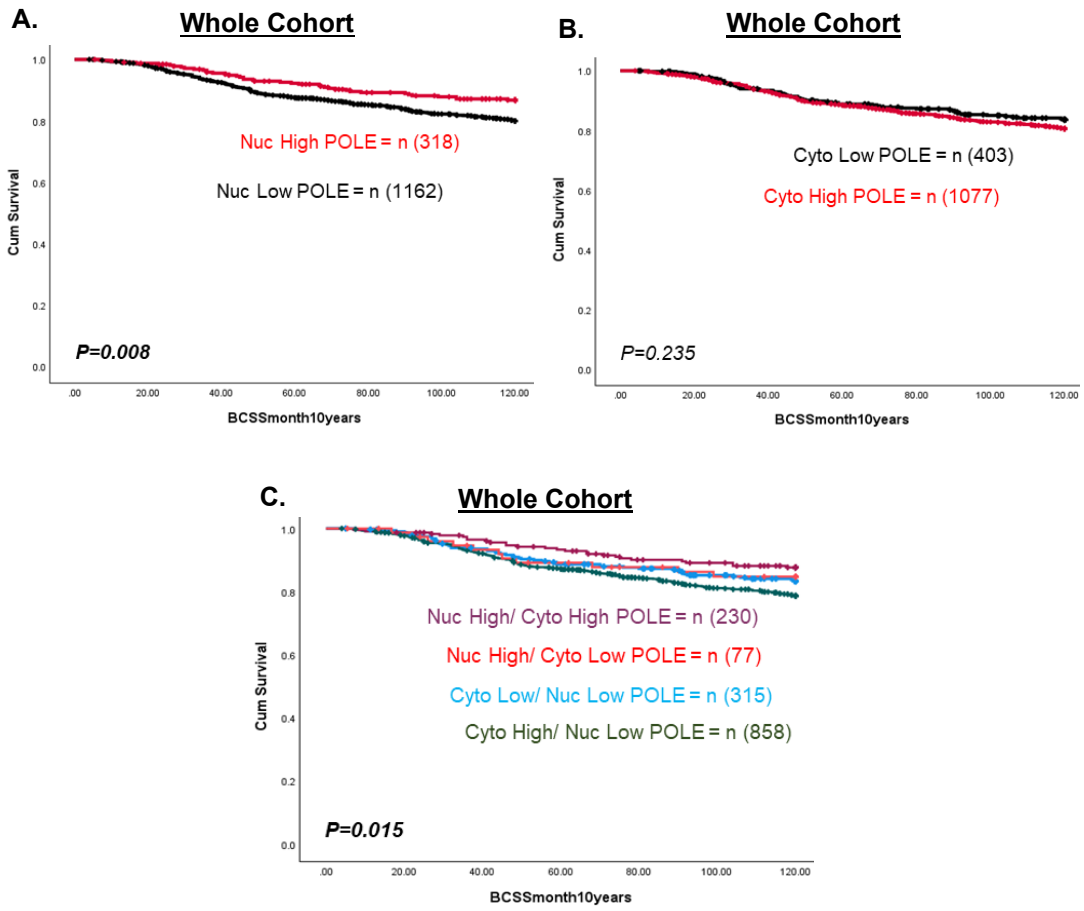

Figure 6-3. Clinicopathological studies of POLE expression in the whole breast cancer cohort. A. Kaplan–Meier curves of nuclear POLE expression and BCSS for the whole cohort. B. Kaplan–Meier curves of cytoplasmic POLE expression and BCSS for the whole cohort. C. Kaplan-Meier curve for POLE nuclear & cytoplasmic co-expression and BCSS for the whole cohort.

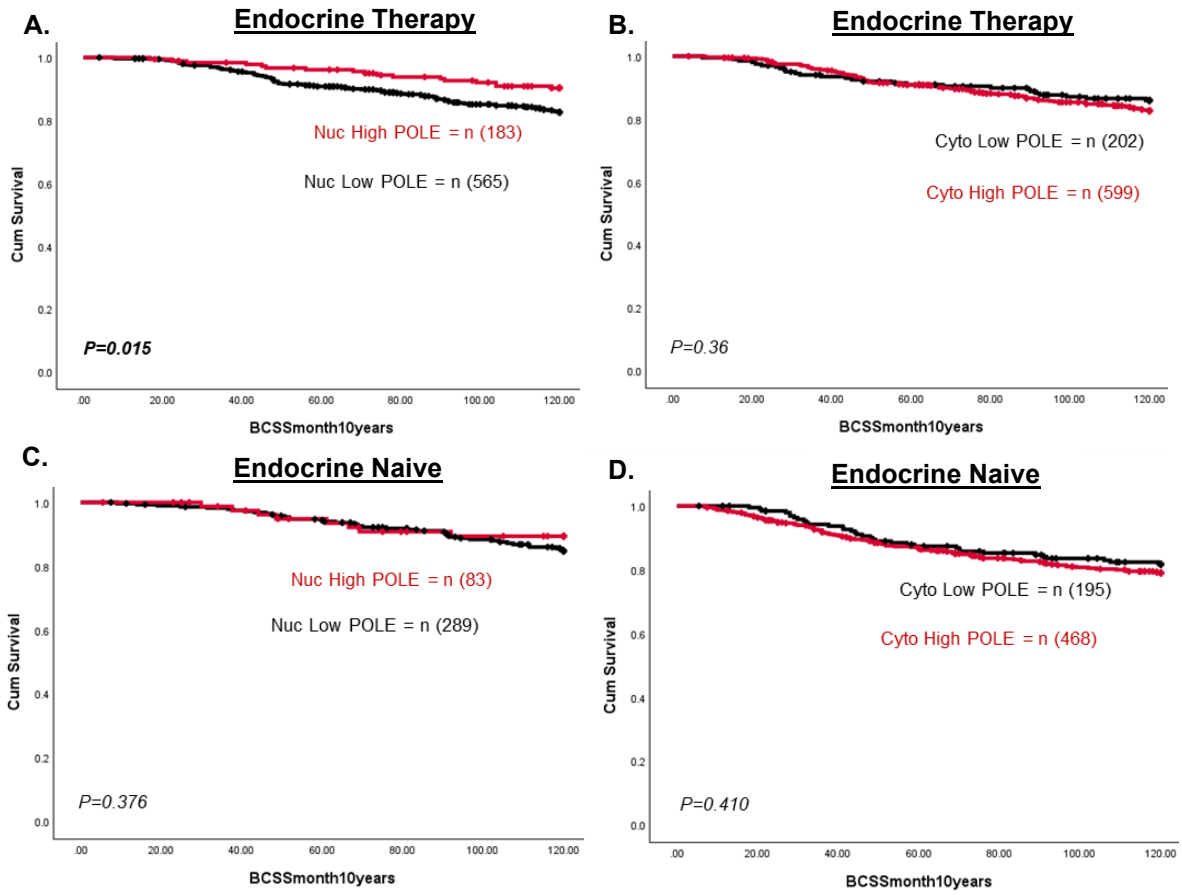

Figure 6-4. Clinicopathological studies of POLE expression and survival curves in breast cancer. A. Kaplan-Meier curve of nuclear POLE expression and BCSS for endocrine therapy. B. Kaplan-Meier curve of cytoplasmic POLE expression and BCSS for endocrine therapy. C. Kaplan-Meier curve of nuclear POLE expression and BCSS for endocrine naive. D. Kaplan-Meier curve of cytoplasmic POLE expression and BCSS for endocrine naive.

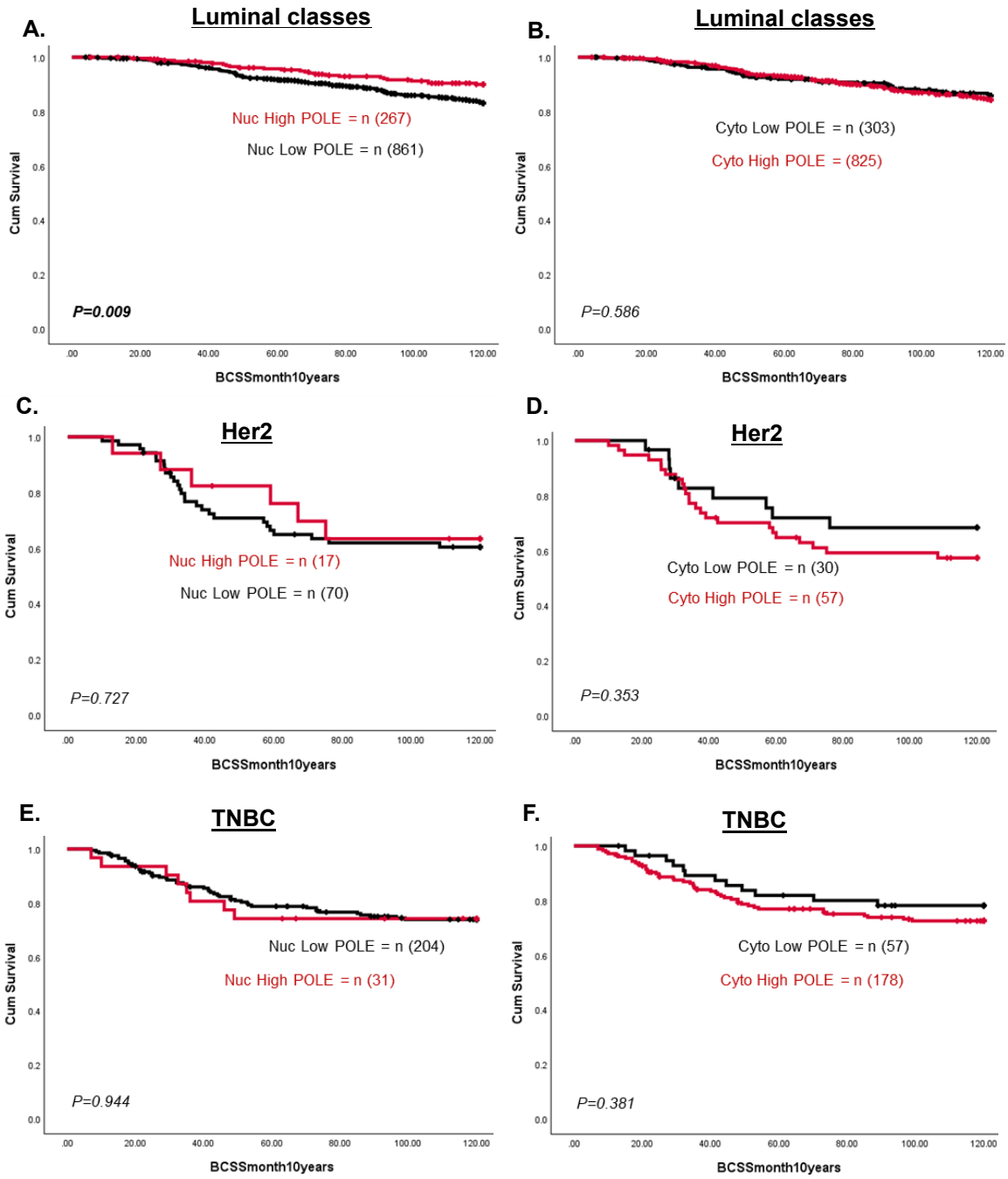

Figure 6-5. Clinicopathological studies of POLE expression and survival curves in breast cancer. A. Kaplan-Meier curve of nuclear POLE expression and BCSS for luminal classes. B. Kaplan-Meier curve of cytoplasmic POLE expression and BCSS for luminal classes. C. Kaplan-Meier curve of nuclear POLE expression and BCSS for HER2-enriched. D. Kaplan-Meier curve of cytoplasmic POLE expression and BCSS for HER2-enriched. E. Kaplan-Meier curve of nuclear POLE expression and BCSS for TNBC. F. Kaplan-Meier curve of cytoplasmic POLE expression and BCSS for TNBC.

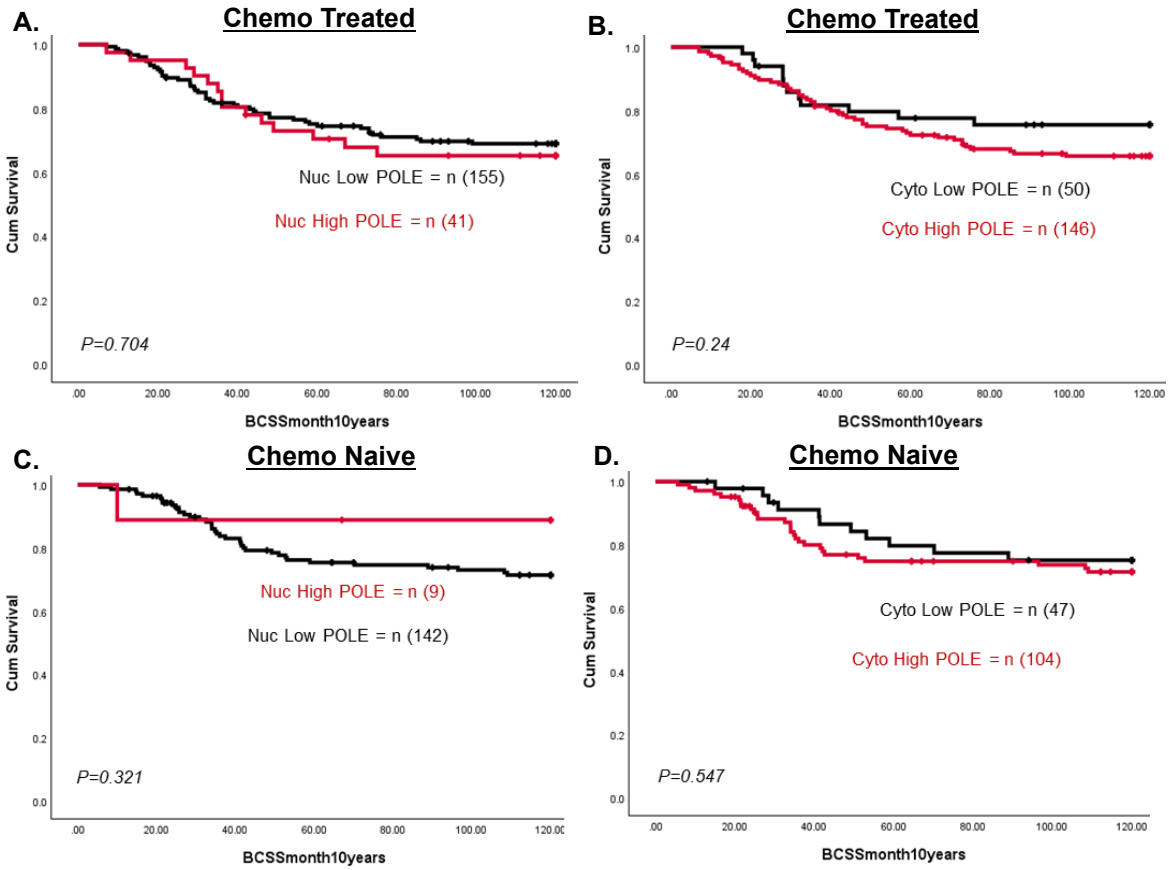

Figure 6-6. Clinicopathological studies of POLE expression and survival curves in breast cancer. A. Kaplan-Meier curve of nuclear POLE expression and BCSS for chemo-treated. B. Kaplan-Meier curve of cytoplasmic POLE expression and BCSS for chemo-treated. C. Kaplan-Meier curve of nuclear POLE expression and BCSS for chemo-naive. D. Kaplan-Meier curve of cytoplasmic POLE expression and BCSS for chemo-naive.

6.4.2 Pre-Clinical studies

The expression of the POLE protein was assessed in a panel of breast cell lines, including normal (MCF10A_DCIS), ER+ invasive breast cancer (MCF-7, T47D), and triple-negative breast cancer (MDA-MB-231) cell lines. In Western Blot (WB) analysis, both normal breast cells and ductal carcinoma in situ (DCIS) cells showed no detectable expression of the POLE protein. This finding contrasts with the immunohistochemistry (IHC) data, which indicated the presence of POLE protein. Furthermore, the expression of the POLE protein was significantly lower in the MDA-MB-231 breast cancer cell line compared to the higher levels observed in the MCF7 and T47D breast cancer cell lines as shown in (**Figure 6-7)**.

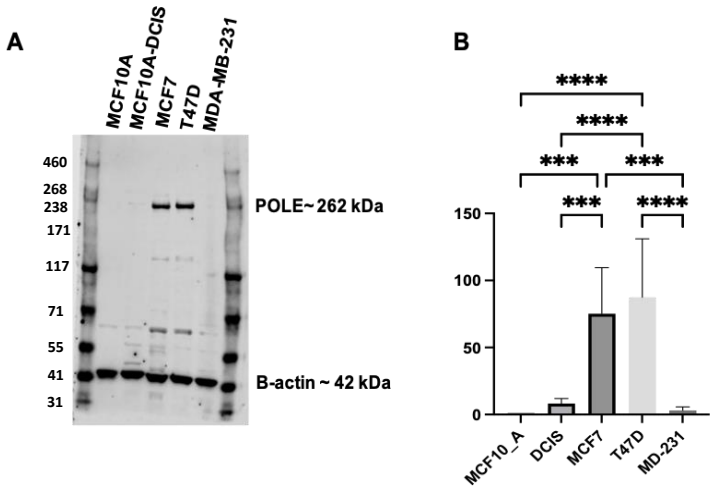

Figure 6-7. Expression of POLE in breast cancer. A panel of normal (MCF10A), DCIS (MCF10A_DCIS), ER+ (MCF7, T47D) and triple negative (MDA-MB-231) breast cancer cell lines was analysed by Western blotting. The readings for POLE were normalized to those of β-actin using Microsoft Excel 2011. Data presentation and statistical analysis were performed using GraphPad Prism, version 9. The P value was calculated as follows, *p > 0.05, **p > 0.01 and ***p > 0.001. The experiment was performed for samples from three independent experiments n=3 and the error bar represent the standard deviation (SD).

6.5 Discussion

Recent research has shed light on the role of DNA polymerases, including polymerase epsilon (POLE), in breast cancer clinicopathology(Stojic et al., 2004). POLE is a key enzyme involved in DNA replication and repair, and its dysregulation may have a role in breast cancer development and progression. The catalytic subunit of DNA polymerase epsilon (POLE) is a large, multi-domain protein called P261, which is encoded by the POLE gene. P261 is responsible for the polymerase activity of POLE and plays a crucial role in DNA replication and repair. It ensures the high fidelity of DNA synthesis during these processes. Aberrations in these pathways can lead to genomic instability, a hallmark of cancer (Henninger & Pursell, 2014). In breast cancer, the dysregulation of POLE has been associated with genomic mutations and chromosomal aberrations. These alterations contribute to the acquisition of oncogenic mutations, tumour heterogeneity, and the development of aggressive cancer subtypes (Hammarlund et al., 2023; Ma et al., 2022) . The genomic instability associated with POLE mutations can confer resistance to standard therapeutic approaches, such as chemotherapy and targeted therapies. The high mutation rate may allow the tumour to rapidly adapt and evolve, making treatment more challenging (Haradhvala et al., 2016).

The present study shows that deficiency in the expression of the protein POLE is a common feature of breast cancer and its precursor lesion, ductal carcinoma in situ (DCIS). Furthermore, low POLE protein expression was significantly associated with aggressive phenotypes and poor clinical

outcomes. The relationship between poor prognosis and reduced levels of POLE expression was demonstrated at both mRNA and protein levels. Taken together, these results indicate the importance of the POLE complex in BC tumorigenesis, progression, and treatment response.

This study also found that POLE is associated with response to endocrine therapy, especially anti-hormonal agents. BC management uses endocrine therapy for hormone receptor-positive patients. However, this study showed that lower POLE levels were linked to decreased responsiveness to these drugs, suggesting that POLE may be a predictive factor in ER+ breast cancers.

High POLE expression in ER+ invasive breast cancer and certain ovarian cancer cell lines suggests its role in promoting tumour progression through enhanced DNA replication and repair capacity. This may contribute to the survival of cancer cells under genotoxic stress (e.g., chemotherapy). Elevated POLE levels could serve as a biomarker for aggressive tumour behaviour, highlighting the need for targeted interventions. Lower POLE expression in triple-negative breast cancer (TNBC) compared to ER+ subtypes, suggests subtype-specific regulatory mechanisms. These findings could guide subtype-specific therapeutic strategies. For example, targeting POLE in ER+ cancers may reduce resistance, while addressing other vulnerabilities in TNBC is essential.

Chapter 7 General Discussion

Breast cancer and ovarian cancer are major women's health challenges worldwide, characterised by intricate nature and heterogeneity (Kossai et al., 2018; Zardavas et al., 2015). Breast cancer early diagnosis has significantly improved due to screening programs (Su et al., 2023; Yu, 2023). In contrast, ovarian cancer is often diagnosed at later stages, which substantially impacts overall survival rates (Savinova & Gataullin, 2022). Breast cancer benefits from standardised screening methods that lead to personalised treatment approaches. Conversely, there is a lack of standardised screening for ovarian cancer, with the current emphasis on biomarkers and multimodal algorithms for early detection (BAROS et al., 2022; Funston et al., 2022; Hossain et al., 2022). BRCA1/2 mutations are among the common risk factors for both diseases, necessitating specific biomarkers for early identification (Antoniou et al., 2003, Zhang et al., 2011). The survival outcomes of synchronous and metachronous BC and OC cases vary, with the former being more favourable than the latter (Buys et al., 2011, Kuchenbecker et al., 2017). In contrast to ovarian or endometrial cancer, where long-term oral contraceptive use is associated with reduced risk, it has a minor impact on breast cancer development (Gierisch et al., 2013). Prior research has focused on alterations in genes like AKT2, BRCA1, BRCA2, RASSF1A and CHD5 in breast and ovarian cancer pathogenesis. According to Bellacosa et al (Bellacosa et al.,1995), AKT2 changes were higher in ovarian than breast cancer, implying that this gene could be specifically involved in the oncogenesis of ovarian tumours. BRCA1 and BRCA2 mutations have different penetrance rates in ovarian or breast carcinoma (Risch et al., 2001).

Similarly, CHD5 somatic mutations were detected in ovarian but not breast cancers (Gorringe et al., 2008). Furthermore, B-cell signatures in breast and ovarian cancers were examined by Iglesia et al (Iglesia et al., 2014), indicating an anti-tumour B-cell response in certain subtypes. Gao et al (Gao et al., 2016) conducted a Mendelian randomisation study to explore whether adiposity traits are causally linked to breast and ovarian cancer risks. Pulliam et al (Pulliam et al., 2018) suggested combining DNA methyltransferase inhibitor (DNMTi) with PARP inhibitor (PARPi) therapy to counter PARPi resistance in treating breast and ovarian cancers, regardless of BRCA mutations. These studies have provided important insights into genetic, genomic, and epigenetic factors, as well as other features of ovarian and/or breast carcinomas. They also suggest new therapeutic approaches for improving treatment outcomes.

The TP53 family members, including TP73, have been found to have a tumour suppressor function. While TP53 is frequently mutated in cancers, TP73 are rarely mutated. Studies have shown that TP73 activators may be able to replace mutant TP53 and act as anti-cancer drugs (Cai et al., 2022). Aberrant splicing that results in overexpression of ΔNTP73, which are dominant-negative isoforms, is frequently found in human cancers and is associated with poor clinical outcomes (Inoue & Fry, 2014).

POLE, or DNA polymerase epsilon, plays a key role in the replication of nuclear DNA in eukaryotes. This enzyme is made up of four subunits, with the largest one being encoded by a gene called POLE that possesses both catalytic polymerase activity as well as exonuclease function. About 3% of

colorectal cancers and 7% of endometrial cancers arise from mutations within this region of the protein, which leads to the unusually frequent occurrence of single base substitutions and increased microsatellite instability compared with what is normally observed (Henninger et al., 2014).

There is a tight link between p73 and DNA polymerase epsilon (POLE) regarding carcinogenesis. Both proteins are involved in DNA repair and replication processes, which are vital to maintaining genomic stability. In response to damage caused by internal and external sources such as X-rays or toxic chemicals, the proteins act as a sensor of DNA errors activating self-destructive programs in cells. There is a possibility that they play a similar role in DNA damage response pathways.

This study considered TP73 expression in epithelial ovarian cancer and its relationship with the clinicopathologic characteristics and prognosis. In these EOC cases, immunohistochemical (IHC) analysis was performed on 331 tumours patients; we found that TP73 overexpression is linked with aggressive clinicopathological features and poor prognosis in ovarian s. It is also worth noting that high levels of TP73 mRNA were associated with adverse events among individuals suffering from EOC, which means this could serve as a prognostic marker while predicting response towards platinum-based chemotherapy.

The research findings from the preclinical study indicate that cisplatin-sensitive cell populations exhibit a significantly reduced expression of TP73 compared to their cisplatin-resistant. In platinum-resistant cell lines, raised amounts of TP73 led to an increase in resistance against platinum drugs by

enhancing DNA repair capability while decreasing the accumulation of DNA double-strand breaks. Additionally, when overexpressed in cisplatin-sensitive cells, elevated levels of TP73 conferred substantial resistance to platinum exposure, thereby causing S-phase arrest within cell cycles coupled with reduced apoptotic cellular death. In summary, according to these findings, TP73 overexpression plays a crucial role in determining sensitivity or resistance to platinum-based drugs used in treating epithelial ovarian cancer (EOC). Therefore, targeting TP73 may offer potential benefits as a therapeutic strategy to improve outcomes for these patients.

This study investigated the expression and potential roles of TP73 in breast cancer. I found that TP73 mRNA expression was higher in tissue compared to normal tissue, and this was associated with shorter survival outcomes. I also observed that a high cytoplasmic TP73 protein level was associated with aggressive phenotypes and poor survival, with cytoplasmic staining being more common than nuclear staining in invasive breast cancer.

The study suggests that TP73 may not impact clinical outcomes in ductal carcinoma in situ (DCIS) but could play a role in the pathogenesis of invasive breast cancers, especially in s with mutant TP53, where high TP73 levels were linked to aggressive pathology and shorter patient survival. Mechanistically, TP73's apoptotic activity may be inhibited by its cytoplasmic localisation and interaction with other proteins, such as Wwox, HCK, and amphiphysin IIb-1.

Previous studies have shown that TP73 overexpression is associated with aggressive features and poor prognosis in various cancers, including ovarian,

bladder, prostate, oesophageal, and colorectal cancers, as well as neuroblastomas and meningiomas. However, the specific impact of TP73 on survival in the context of TP53 variants in breast cancer has not been extensively investigated. Overall, the study highlights the complex expression pattern of TP73 in breast cancer and suggests that further mechanistic investigations are necessary to fully understand the role of TP73 in breast cancer pathogenesis and its potential as a therapeutic target.

The study also highlights the role of POLE expression in ovarian cancer, particularly its association with clinicopathologic features and prognosis. Among 331 ovarian cancer cases, overexpression of POLE was linked to aggressive clinicopathologic characteristics and poor prognosis. High levels of POLE mRNA were also associated with worse outcomes in epithelial ovarian cancer patients, suggesting that POLE could serve as a prognostic and predictive biomarker for platinum sensitivity in EOC.

In preclinical experiments, it was found that cisplatin-resistant PEO4 and A2780cis cells had higher basal levels of POLE compared to cisplatin-sensitive A2780 and PEO1 cells. Upregulation of POLE in platinum-resistant cell lines enhanced DNA repair mechanisms and replication stress processing, contributing to platinum resistance. Depleting POLE in OVCAR 4 cells led to increased DNA double-strand break accumulation, S-phase arrest, and higher apoptosis rates, indicating that reducing POLE expression could increase sensitivity to cisplatin treatment in these cells. Overall, the study suggests that POLE expression is a key determinant of platinum

sensitivity in EOC, and that targeting POLE could be an effective therapeutic approach for treating ovarian cancer.

This study highlights the significance of POLE expression in breast cancer and ductal carcinoma in situ (DCIS). I found that low POLE protein expression is a common feature in BC and DCIS, and it is associated with aggressive phenotypes and poor clinical outcomes. This association between reduced POLE expression and poor prognosis was observed at both the mRNA and protein levels, suggesting that POLE plays an important role in BC tumourigenesis, tumour progression, and treatment response.

Additionally, the study demonstrated that POLE expression is associated with the response to endocrine therapy. Endocrine therapy is a common approach for managing hormone receptor-positive BC. However, the study showed that tumours with lower POLE levels were less responsive to these drugs, implying that they may be less effective in tumours with low POLE expression. Overall, these findings suggest that POLE expression could serve as a biomarker for predicting treatment response and prognosis in BC, particularly in the context of endocrine therapy for hormone receptor-positive tumours.

Limitations of the study

This study had some limitations. First, nuclear expression of TP73I breast cancer was detected in only 14 out of 1369 (1%) tumours, which clearly showed that it is of limited value for analysing clinicopathological associations. Second, the breast cancer cell line experiments should be extended to include knock-in and knock-out models for TP73 and POLE to gain better insight into their functions. Additionally, while POLE expression was analysed, its mutation status was not assessed, potentially overlooking significant functional implications.

The immunohistochemistry (IHC) study was retrospective, and the cell line experiments involved only a single representative cell line for gene knock-in and knock-out studies, limiting the findings' robustness. Additionally, the study used a narrow selection of platinum-sensitive and platinum-resistant cell lines, which may not encompass the complete range of resistance mechanisms found in ovarian and breast cancers. This limitation reduces the generalizability of the results.

The functional roles of TP73 are not yet fully understood. Depending on the cellular context, TP73 can function as either a tumour suppressor or an oncogene. However, the study's limited exploration of the tumour microenvironment and epigenetic modifications prevents a comprehensive understanding of these dual roles. Furthermore, the inability to differentiate between TP73 isoforms (TAp73 and ΔNp73) and their interactions with TP53 complicates understanding their unique contributions to tumour suppression, oncogenesis, and therapy resistance. The study also did not examine how

TP73 and TP53 (whether wild-type or mutant) co-regulate downstream targets, which could provide valuable insights into their combined or opposing roles in cancer progression and treatment response.

Although the study analysed elevated POLE expression, this measure may not always reflect functional activity, especially when mutations exist. Additionally, the research did not investigate POLE's interactions with non-platinum-based therapies, such as PARP inhibitors or immune checkpoint inhibitors, which are important in the context of DNA repair defects.

Future directions

One of the major characteristics of many human cancers is genomic instability, which is a consequence of the dysregulation of DNA repair mechanisms. These DNA repair defects may also alter drug responses in different cancers. Accordingly, DNA repair factors are considered promising biomarkers for prognosis and prediction of response to cancer therapy (D'andrea, 2015).The current study provides evidence supporting the potential of TP73 and POLE as DNA repair biomarkers for breast and ovarian cancers.

It is be important to further validate TP73 and POLE biomarkers for diagnosis, staging and management of the disease. Further preclinical studies will be required to understand the functional significance of TP53 and POLE alterations in breast and ovarian cancer cells. Synthetic lethality approach for treating cancers with POLE mutations should be an area of future investigation.

The differential expression of TP73 isoforms TAp73 and ΔNp73 offers the potential to employ these markers for prognosis and treatment outcome prediction. High levels of ΔNp73 may be useful in predicting chemoresistance, and clinicians may use it to select patients who will not benefit from platinum-based therapies and work towards developing new strategies for treatment. ΔNp73, which promotes tumour cell survival, could also be a potential therapeutic target. Blockade of ΔNp73 or the restoration of TAp73 could be potential therapeutic approaches. Small molecule inhibitors,

RNA-based therapies, or CRISPR technology-based therapeutic approaches could be investigated to target TP73 in cancer therapy.

TP73's involvement in DNA repair pathways also opens possibilities for synthetic lethality strategies. Combining drugs like PARP inhibitors with agents that modulate TP73 activity could selectively kill tumour cells while sparing normal cells, particularly those that rely on TP73-mediated DNA repair. TP73's role in apoptosis and DNA repair may also influence the tumour microenvironment and immune responses. Tumours with altered TP73 activity could exhibit changes in immune activity, making TP73-targeted therapies promising when used with immune checkpoint inhibitors. Understanding how promoter methylation and histone modifications regulate TP73 expression is important, and exploring demethylating agents or histone deacetylase inhibitors to restore TAp73 activity in resistant tumours should be evaluated. Similarly, preclinical studies should also explore whether combinations of ΔNp73 inhibitors with DNA-damaging agents or PARP inhibitors can effectively treat platinum-resistant ovarian cancers.

Regarding POLE, which is involved in repairing cisplatin-induced DNA damage, the inhibition of POLE may enhance the effectiveness of chemotherapy in platinum resistant ovarian cancer. Future studies should focus on using RNA interference or small-molecule inhibitors to suppress POLE activity in resistant cell lines. POLE's interaction with base excision repair (BER) proteins suggests that targeting both POLE and BER pathways, especially in tumours that depend on these repair mechanisms, could induce synthetic lethality. Furthermore, the POLE mutations that cause hypermutated immunogenic tumours may also open new possibilities for

immunotherapy. Prospective studies should analyse the frequency of POLE mutations in ovarian cancer and their effect on tumour mutation load, inflammatory cell recruitment, and the potential use of immune checkpoint blockade.

The transient upregulation of POLE during cisplatin treatment indicates that it is regulated by stress pathways such as ATR/CHK1 signalling. Targeting these pathways could block the adaptive response and enhance cisplatin efficacy. POLE's activity may also influence the tumour microenvironment by altering cytokine production or immune cell infiltration. Future research should also determine if blocking POLE can modify the immune environment in ovarian tumours and thus enhance the efficacy of immunotherapies.

In conclusion, the research work described here provides evidence that TP73 and POLE are promising biomarkers and therapeutic targets in breast and ovarian cancers.

Conclusions

In conclusion, this research shows that BC and OC development and progression are influenced by TP73 and POLE proteins. These findings also suggest that the response to therapy and survival outcomes may be determined by TP73 and POLE expression in patients with BC or OC, which makes them a possible biomarker for predicting therapeutic responses among these patients. Besides, it could help design personalised treatment plans so as not only to improve the efficiency of care but also to provide more opportunities for effective treatment in individuals diagnosed with breast cancer or ovarian cancer.

References

Abbotts, R., Thompson, N., & Madhusudan, S. (2014). DNA repair in cancer: emerging targets for personalized therapy. *Cancer Manag Res*, *6*, 77-92. https://doi.org/10.2147/CMAR.S50497

Abbotts, R., & Wilson, D. M., 3rd. (2017). Coordination of DNA single strand break repair. *Free Radic Biol Med*, *107*, 228-244. https://doi.org/10.1016/j.freeradbiomed.2016.11.039

Abkevich, V., Timms, K. M., Hennessy, B. T., Potter, J., Carey, M. S., Meyer, L. A., Smith-McCune, K., Broaddus, R., Lu, K. H., Chen, J., Tran, T. V., Williams, D., Iliev, D., Jammulapati, S., FitzGerald, L. M., Krivak, T., DeLoia, J. A., Gutin, A., Mills, G. B., & Lanchbury, J. S. (2012). Patterns of genomic loss of heterozygosity predict homologous recombination repair defects in epithelial ovarian cancer. *Br J Cancer*, *107*(10), 1776-1782. https://doi.org/10.1038/bjc.2012.451

Admoun, C., & Mayrovitz, H. N. (2022). The Etiology of Breast Cancer. *Exon Publications*, 21-30.

Akcora-Yildiz, D., Ozkan, T., Cetintav, B., Yukselten, Y., Calis, S., Sevim-Nalkiran, H., Turkel, N., Gunduz, M., Ozen, M., & Beksac, M. (2024). Inhibition of O6-methylguanine-DNA-methyltransferase (MGMT) by lomeguatrib reduces multiple myeloma cell viability and impairs DNA repair in MGMT-proficient cells. *Chemical Biology & Drug Design*, *103*(2), e14465.

Akinjiyan, F. A., Morecroft, R., Phillipps, J., Adeyelu, T., Elliott, A., Park, S. J., Butt, O. H., Zhou, A. Y., & Ansstas, G. (2023). Homologous Recombination Deficiency (HRD) in Cutaneous Oncology. *Int J Mol Sci*, *24*(13), 10771. https://doi.org/10.3390/ijms241310771

Alanazi, M., Parine, N. R., Shaik, J. P., Al Naeem, A., & Aldhaian, S. (2020). Targeted sequencing of crucial cancer causing genes of breast cancer in Saudi patients. *Saudi J Biol Sci*, *27*(10), 2651-2659. https://doi.org/10.1016/j.sjbs.2020.05.047

Alhmoud, J. F., Woolley, J. F., Al Moustafa, A. E., & Malki, M. I. (2020). DNA Damage/Repair Management in Cancers. *Cancers (Basel)*, *12*(4). https://doi.org/10.3390/cancers12041050

Ali, A., Xiao, W., Babar, M. E., & Bi, Y. (2022). Double-stranded break repair in mammalian cells and precise genome editing. *Genes*, *13*(5), 737.

Allred, D. C., Anderson, S. J., Paik, S., Wickerham, D. L., Nagtegaal, I. D., Swain, S. M., Mamounas, E. P., Julian, T. B., Geyer, C. E., Jr., Costantino, J. P., Land, S. R., & Wolmark, N. (2012). Adjuvant tamoxifen reduces subsequent breast cancer in women with estrogen receptor-positive ductal carcinoma in situ: a study based on NSABP protocol B-24. *J Clin Oncol*, *30*(12), 1268-1273. https://doi.org/10.1200/JCO.2010.34.0141

Alvarado-Cabrero, I. (2018). Ductal Carcinoma In Situ. *Practical Atlas of Breast Pathology*, 227-237.

Amato, M., Franco, R., Facchini, G., Addeo, R., Ciardiello, F., Berretta, M., Vita, G., Sgambato, A., Pignata, S., Caraglia, M., Accardo, M., & Zito Marino, F. (2022). Microsatellite Instability: From the Implementation of the Detection to a Prognostic and Predictive Role in Cancers. *International journal of molecular sciences*, *23*(15), 8726. https://doi.org/10.3390/ijms23158726

Ame, J. C., Spenlehauer, C., & de Murcia, G. (2004). The PARP superfamily. *Bioessays*, *26*(8), 882-893. https://doi.org/10.1002/bies.20085

Aqeilan, R. I., Palamarchuk, A., Weigel, R. J., Herrero, J. J., Pekarsky, Y., & Croce, C. M. (2004). Physical and functional interactions between the Wwox tumor suppressor protein and the AP-2γ transcription factor. *Cancer Research*, *64*(22), 8256-8261.

Aricthota, S., Rana, P. P., & Haldar, D. (2022). Histone acetylation dynamics in repair of DNA double-strand breaks. *Front Genet*, *13*, 926577. https://doi.org/10.3389/fgene.2022.926577

Bai, P., Fan, T., Wang, X., Zhao, L., Zhong, R., & Sun, G. (2023). Modulating MGMT expression through interfering with cell signaling pathways. *Biochemical Pharmacology*, 115726.

Barnes, J. L., Zubair, M., John, K., Poirier, M. C., & Martin, F. L. (2018). Carcinogens and DNA damage. *Biochem Soc Trans*, *46*(5), 1213-1224. https://doi.org/10.1042/BST20180519

BAROS, A., POTORAC, A., TURCAN, N., SECARA, D., MUNTEANU, O., PARIZA, G., & CIRSTOIU, M. M. (2022). Correlation Between Early Diagnosis of Ovarian Neoplasm and Long-Term Prognosis. *Medicina Moderna*, *29*(2).

Barroso, S. I., & Aguilera, A. (2021). Detection of DNA Double-Strand Breaks by gamma-H2AX Immunodetection. *Methods Mol Biol*, *2153*, 1-8. https://doi.org/10.1007/978-1-0716-0644-5_1

Beijersbergen, R. L., Wessels, L. F. A., & Bernards, R. (2017). Synthetic Lethality in Cancer Therapeutics [review-article]. *Annual Review of Cancer Biology*, *1*(1), 141-161. https://doi.org/10.1146/annurev-cancerbio-042016-073434

Bell, D. A. (2005). Origins and molecular pathology of ovarian cancer [OriginalPaper]. *Mod Pathol*, *18 Suppl 2*(2), S19-32. https://doi.org/10.1038/modpathol.3800306

Bellido, F., Pineda, M., Aiza, G., Valdes-Mas, R., Navarro, M., Puente, D. A., Pons, T., Gonzalez, S., Iglesias, S., Darder, E., Pinol, V., Soto, J. L., Valencia, A., Blanco, I., Urioste, M., Brunet, J., Lazaro, C., Capella, G., Puente, X. S., & Valle, L. (2016). POLE and POLD1 mutations in 529 kindred with familial colorectal cancer and/or polyposis: review of reported cases and recommendations for genetic testing and surveillance. *Genet Med*, *18*(4), 325-332. https://doi.org/10.1038/gim.2015.75

Berdis, A. J. (2017). Inhibiting DNA Polymerases as a Therapeutic Intervention against Cancer. *Frontiers in molecular biosciences*, *4*, 78-78. https://doi.org/10.3389/fmolb.2017.00078

Berkenblit, A., & Cannistra, S. A. (2005). Advances in the management of epithelial ovarian cancer. *J Reprod Med*, *50*(6), 426-438.

Bernstein, C. (2013). DNA Damage, DNA Repair and Cancer. https://doi.org/10.5772/53919

Berrada, S., Martinez-Balsalobre, E., Larcher, L., Azzoni, V., Vasquez, N., Da Costa, M., Abel, S., Audoly, G., Lee, L., Montersino, C., Castellano, R., Combes, S., Gelot, C., Ceccaldi, R., Guervilly, J. H., Soulier, J., & Lachaud, C. (2023). A clickable melphalan for monitoring DNA interstrand crosslink accumulation and detecting ICL repair defects in Fanconi anemia patient cells. *Nucleic Acids Res*, *51*(15), 7988-8004. https://doi.org/10.1093/nar/gkad559

Bessho, T., Sancar, A., Eckstein, F., & Lilley, D. M. J. (1998). Nucleotide Excision Repair in Man. *DNA Repair*, *12*, 141-155. https://doi.org/info:doi/10.1007/978-3-642-48770-5_7

Betermier, M., Bertrand, P., & Lopez, B. S. (2014). Is non-homologous end-joining really an inherently error-prone process? *PLoS Genet*, *10*(1), e1004086. https://doi.org/10.1371/journal.pgen.1004086

Bhaswatee, D., Bipasha, C., Aditya, K., & Vishwa Jyoti, B. (2021). Genome Instability and DNA Repair in Cancer. https://doi.org/10.5772/intechopen.95736

Bhattarai, M., Juhari, W. K. W., Lama, R., Pun, C. B., Yusof, W., Rahman, W. F. W. A., Zakaria, A. D., Noordin, K. B. A. A., Shrestha, T. R., & Zilfalil, B. A. (2020). MLH1 and MSH2 mismatch repair protein profile using immunohistochemistry in Nepalese colorectal cancer patients. *Medical Journal of Indonesia*, *29*(2), 183-189.

Bicknell, L. S., Bongers, E. M., Leitch, A., Brown, S., Schoots, J., Harley, M. E., Aftimos, S., Al-Aama, J. Y., Bober, M., Brown, P. A., van Bokhoven, H., Dean, J., Edrees, A. Y., Feingold, M., Fryer, A., Hoefsloot, L. H., Kau, N., Knoers, N. V., Mackenzie, J., . . . Jackson, A. P. (2011). Mutations in the pre-replication complex cause Meier-Gorlin syndrome. *Nat Genet*, *43*(4), 356-359. https://doi.org/10.1038/ng.775

Blamey, R., Ellis, I., Pinder, S., Lee, A., Macmillan, R., Morgan, D., Robertson, J., Mitchell, M., Ball, G., & Haybittle, J. (2007). Survival of invasive breast cancer according to the Nottingham Prognostic Index in cases diagnosed in 1990–1999. *European Journal of Cancer*, *43*(10), 1548-1555.

Bombonati, A., & Sgroi, D. C. (2011). The molecular pathology of breast cancer progression. *J Pathol*, *223*(2), 307-317. https://doi.org/10.1002/path.2808

Boyd, N. F., Stone, J., Vogt, K. N., Connelly, B. S., Martin, L. J., & Minkin, S. (2003). Dietary fat and breast cancer risk revisited: a meta-analysis of the published literature. *Br J Cancer*, *89*(9), 1672-1685. https://doi.org/10.1038/sj.bjc.6601314

Bratton, D. L., Fadok, V. A., Richter, D. A., Kailey, J. M., Guthrie, L. A., & Henson, P. M. (1997). Appearance of Phosphatidylserine on Apoptotic Cells Requires Calcium-mediated Nonspecific Flip-Flop and Is Enhanced by Loss of the Aminophospholipid Translocase. *The Journal of biological chemistry*, *272*(42), 26159-26165. https://doi.org/10.1074/jbc.272.42.26159

Budiana, I. N. G., Angelina, M., & Pemayun, T. G. A. (2019). Ovarian cancer: Pathogenesis and current recommendations for prophylactic surgery. *J Turk Ger Gynecol Assoc*, *20*(1), 47-54. https://doi.org/10.4274/jtgga.galenos.2018.2018.0119

Bukunmi Ogunro, O., Elizabeth Fakayode, A., & El-Saber Batiha, G. (2023). Involvement of Antioxidant in the Prevention of Cellular Damage. In *Importance of Oxidative Stress and Antioxidant System in Health and Disease*. IntechOpen. https://doi.org/10.5772/intechopen.108732

Cabioglu, N., Yavuz, E., & Aydiner, A. (2019). Breast Cancer Staging. *Breast Cancer: A Guide to Clinical Practice*, 99-122.

Cai, B. H., Hsu, Y. C., Yeh, F. Y., Lin, Y. R., Lu, R. Y., Yu, S. J., Shaw, J. F., Wu, M. H., Tsai, Y. Z., Lin, Y. C., Bai, Z. Y., Shih, Y. C., Hsu, Y. C., Liao, R. Y., Kuo, W. H., Hsu, C. T., Lien, C. F., & Chen, C. C. (2022). P63 and P73 Activation in Cancers with p53 Mutation. *Biomedicines*, *10*(7), 1490. https://doi.org/10.3390/biomedicines10071490

Caldecott, K. W. (2008). Single-strand break repair and genetic disease. *Nat Rev Genet*, *9*(8), 619-631. https://doi.org/10.1038/nrg2380

Camp, R. L., Dolled-Filhart, M., & Rimm, D. L. (2004). X-tile: a new bio-informatics tool for biomarker assessment and outcome-based cut-point optimization. *Clin Cancer Res*, *10*(21), 7252-7259. https://doi.org/10.1158/1078-0432.CCR-04-0713

Candi, E., Agostini, M., Melino, G., & Bernassola, F. (2014). How the TP53 Family Proteins TP63 and TP73 Contribute to Tumorigenesis: Regulators and Effectors. *Human mutation*, *35*(6), 702-714. https://doi.org/10.1002/humu.22523

Carlberg, C., Velleuer, E., & Molnár, F. (2023). Oncogenes, Signal Transduction and the Hallmarks of Cancer. In C. Carlberg, E. Velleuer, & F. Molnár (Eds.), *Molecular Medicine* (pp. 423-433). Springer International Publishing. https://doi.org/10.1007/978-3-031-27133-5_25

Carlos, A. R. (2019). Genomic Instability: DNA Repair and Cancer. *Molecular and Cell Biology of Cancer*.

Castellanos, G., Valbuena, D. S., Pérez, E., Villegas, V. E., & Rondón-Lagos, M. (2023). Chromosomal Instability as Enabling Feature and Central Hallmark of Breast Cancer. *Breast cancer targets and therapy*, *15*, 189-211. https://doi.org/10.2147/BCTT.S383759

Chabuk, S. K., Hameed, A. K., Naser, S. A. A., & Al-Fahham, A. A. (2024). The Epidemiology and Pathophysiology of Breast Cancer. *International Journal of Health & Medical Research*, *03*(09). https://doi.org/10.58806/ijhmr.2024.v3i09n02

Chai, Y., Chen, Y., Zhang, D., Wei, Y., Li, Z., Li, Q., & Xu, B. (2022). Homologous Recombination Deficiency (HRD) and BRCA 1/2 Gene Mutation for Predicting the Effect of Platinum-Based Neoadjuvant Chemotherapy of Early-Stage Triple-Negative Breast Cancer (TNBC): A Systematic Review and Meta-Analysis. *J Pers Med*, *12*(2), 323. https://doi.org/10.3390/jpm12020323

Chang, H. H. Y., Pannunzio, N. R., Adachi, N., & Lieber, M. R. (2017). Non-homologous DNA end joining and alternative pathways to double-strand break repair. *Nat Rev Mol Cell Biol*, *18*(8), 495-506. https://doi.org/10.1038/nrm.2017.48

Chen, L., & Wen, A. (2024). Unveiling the role of O(6)-methylguanine-DNA methyltransferase in cancer therapy: insights into alkylators, pharmacogenomics, and others. *Frontiers in oncology*, *14*. https://doi.org/10.3389/fonc.2024.1424797

Chen, V. W., Ruiz, B., Killeen, J. L., Cote, T. R., Wu, X. C., & Correa, C. N. (2003). Pathology and classification of ovarian tumors. *Cancer*, *97*(10 Suppl), 2631-2642. https://doi.org/10.1002/cncr.11345

Chen, Y. (2022). Identification of the Potential Correlation between Tumor Protein 73 and Head and Neck Squamous Cell Carcinoma. *Dis Markers*, *2022*, 6410113. https://doi.org/10.1155/2022/6410113

Chen, Y., Qu, W., Tu, J., & Qi, H. (2023). Implications of Advances in Studies of O6-Methylguanine-DNA- Methyltransferase for Tumor Prognosis and Treatment. *Frontiers in Bioscience-Landmark*, *28*(9), 197. https://doi.org/10.31083/j.fbl2809197

Chen, Y., Wang, X., Du, F., Yue, J., Si, Y., Zhao, X., Cui, L., Zhang, B., Bei, T., & Xu, B. (2023). Association between homologous recombination deficiency and outcomes with platinum and platinum-free chemotherapy in patients with triple-negative breast cancer. *Cancer Biology & Medicine*, *20*(2), 155.

Chootipongchaivat, S., van Ravesteyn, N. T., Li, X., Huang, H., Weedon-Fekjaer, H., Ryser, M. D., Weaver, D. L., Burnside, E. S., Heckman-Stoddard, B. M., de Koning, H. J., & Lee, S. J. (2020). Modeling the natural history of ductal carcinoma in situ based on population data. *Breast Cancer Res*, *22*(1), 53. https://doi.org/10.1186/s13058-020-01287-6

Church, D. N., Briggs, S. E. W., Palles, C., Domingo, E., Kearsey, S. J., Grimes, J. M., Gorman, M., Martin, L., Howarth, K. M., Hodgson, S. V., Kaur, K., Taylor, J., & Tomlinson, I. P. M. (2013). DNA polymerase epsilon and [delta] exonuclease domain mutations in endometrial cancer. *Human molecular genetics*, *22*(14), 2820-2828. https://doi.org/10.1093/hmg/ddt131

Cohen, S. Y., Stoll, C. R., Anandarajah, A., Doering, M., & Colditz, G. A. (2023). Modifiable risk factors in women at high risk of breast cancer: a systematic review. *Breast Cancer Res*, *25*(1), 45. https://doi.org/10.1186/s13058-023-01636-1

Colditz, G. A., Rosner, B. A., Chen, W. Y., Holmes, M. D., & Hankinson, S. E. (2004). Risk factors for breast cancer according to estrogen and progesterone receptor status. *J Natl Cancer Inst*, *96*(3), 218-228. https://doi.org/10.1093/jnci/djh025

Collaborative Group on Hormonal Factors in Breast, C. (2012). Menarche, menopause, and breast cancer risk: individual participant meta-analysis, including 118 964 women with breast cancer from 117 epidemiological studies. *Lancet Oncol*, *13*(11), 1141-1151. https://doi.org/10.1016/S1470-2045(12)70425-4

Comaills, V., & Castellano-Pozo, M. (2023). Chromosomal Instability in Genome Evolution: From Cancer to Macroevolution. *Biology (Basel, Switzerland)*, *12*(5), 671. https://doi.org/10.3390/biology12050671

Couch, F. J., Wang, X., McGuffog, L., Lee, A., Olswold, C., Kuchenbaecker, K. B., Soucy, P., Fredericksen, Z., Barrowdale, D., Dennis, J., Gaudet, M. M., Dicks, E., Kosel, M., Healey, S., Sinilnikova, O. M., Bacot, F., Vincent, D., Hogervorst, F. B. L., Peock, S., . . . Antoniou, A. C. (2013). Genome-Wide Association Study in BRCA1 Mutation Carriers Identifies Novel Loci Associated with Breast and Ovarian Cancer Risk. In *PLoS Genet* (Vol. 9). https://doi.org/10.1371/journal.pgen.1003212

Couturier, M., & Lindas, A. C. (2018). The DNA Methylome of the Hyperthermoacidophilic Crenarchaeon Sulfolobus acidocaldarius. *Front Microbiol*, *9*, 137. https://doi.org/10.3389/fmicb.2018.00137

Cropper, J. D., Alimbetov, D. S., Brown, K. T. G., Likhotvorik, R. I., Robles, A. J., Guerra, J. T., He, B., Chen, Y., Kwon, Y., & Kurmasheva, R. T. (2022). PARP1-MGMT complex underpins pathway crosstalk in O6-methylguanine repair. *Journal of Hematology & Oncology*, *15*(1). https://doi.org/10.1186/s13045-022-01367-4

Cui, Z., Xu, L., Wu, H., Wang, M., Lu, L., & Wu, S. (2023). Glutathione peroxidase 2: A key factor in the development of microsatellite instability in colon cancer. *Pathology, research and practice*, *243*, 154372-154372. https://doi.org/10.1016/j.prp.2023.154372

D'andrea, A. D. (2015). *4 - DNA Repair Pathways and Human Cancer*. Elsevier Inc. https://doi.org/10.1016/B978-1-4557-4066-6.00004-4

Davila, J. I., Chanana, P., Sarangi, V., Fogarty, Z. C., Weroha, S. J., Guo, R., Goode, E. L., Huang, Y., & Wang, C. (2021). Frequent POLE-driven hypermutation in ovarian endometrioid cancer revealed by mutational signatures in RNA sequencing. *BMC Med Genomics*, *14*(1), 165. https://doi.org/10.1186/s12920-021-01017-7

Deans, A. J., & West, S. C. (2011). DNA interstrand crosslink repair and cancer. *Nat Rev Cancer*, *11*(7), 467-480. https://doi.org/10.1038/nrc3088

Debnath, J., Muthuswamy, S. K., & Brugge, J. S. (2003). Morphogenesis and oncogenesis of MCF-10A mammary epithelial acini grown in three-dimensional basement membrane cultures. *Methods*, *30*(3), 256-268. https://doi.org/10.1016/s1046-2023(03)00032-x

Deng, G., Bell, I., Crawley, S., Gum, J., Terdiman, J. P., Allen, B. A., Truta, B., Sleisenger, M. H., & Kim, Y. S. (2004). BRAF mutation is frequently present in sporadic colorectal cancer with methylated hMLH1, but not in hereditary nonpolyposis colorectal cancer. *Clinical Cancer Research*, *10*(1), 191-195.

Denmark, D. (2013). Dako Publishes Sixth Edition of Immunohistochemistry Guidebook NYSE:A.

DeYoung, M. P., & Ellisen, L. W. (2007). p63 and p73 in human cancer: defining the network. *Oncogene*, *26*(36), 5169-5183. https://doi.org/10.1038/sj.onc.1210337

Dhital, B., & Rodriguez-Bravo, V. (2023). Mechanisms of chromosomal instability (CIN) tolerance in aggressive tumors: surviving the genomic chaos. *Chromosome research*, *31*(2), 15-15. https://doi.org/10.1007/s10577-023-09724-w

Diaz, R., Gonzalez-Sancho, J. M., Soldevilla, B., Silva, J., Garcia, J. M., Garcia, V., Pena, C., Herrera, M., Gomez, I., Bonilla, F., & Dominguez, G. (2010). Differential regulation of TP73 isoforms by 1alpha,25-dihydroxyvitamin D3 and survivin in human colon and breast carcinomas. *Genes Chromosomes Cancer*, *49*(12), 1135-1142. https://doi.org/10.1002/gcc.20821

Djordjević, M., Ilić, J., & Stojanovic, N. M. (2023). CISPLATIN-AN OVERVIEW OF ITS EFFICIENCY AND TOXICITY. *Facta Universitatis, Series: Medicine and Biology*, 025-035.

Dominguez, G., Silva, J. M., Silva, J., Garcia, J. M., Sanchez, A., Navarro, A., Gallego, I., Provencio, M., Espana, P., & Bonilla, F. (2001). Wild type p73 overexpression and high-grade malignancy in breast cancer. *Breast Cancer Res Treat*, *66*(3), 183-190. https://doi.org/10.1023/a:1010624717311

Dong, S., Zakaria, H., & Hsiehchen, D. (2022). Non-Exonuclease Domain POLE Mutations Associated with Immunotherapy Benefit. *Oncologist*, *27*(3), 159-162. https://doi.org/10.1093/oncolo/oyac017

Duijf, P. H. G., Nanayakkara, D., Nones, K., Srihari, S., Kalimutho, M., & Khanna, K. K. (2019). Mechanisms of Genomic Instability in Breast Cancer. *Trends in molecular medicine*, *25*(7), 595-611. https://doi.org/10.1016/j.molmed.2019.04.004

Eggink, F. A., Van Gool, I. C., Leary, A., Pollock, P. M., Crosbie, E. J., Mileshkin, L., Jordanova, E. S., Adam, J., Freeman-Mills, L., Church, D. N., Creutzberg, C. L., De Bruyn, M., Nijman, H. W., & Bosse, T. (2017). Immunological profiling of molecularly classified high-risk endometrial cancers identifies POLE-mutant and microsatellite unstable carcinomas as candidates for checkpoint inhibition. *Oncoimmunology*, *6*(2), e1264565-e1264565. https://doi.org/10.1080/2162402X.2016.1264565

Eker, A. P., Quayle, C., Chaves, I., & van der Horst, G. T. (2009). DNA repair in mammalian cells: Direct DNA damage reversal: elegant solutions for nasty problems. *Cell Mol Life Sci*, *66*(6), 968-980. https://doi.org/10.1007/s00018-009-8735-0

Elez, M. (2021). Mismatch Repair: From Preserving Genome Stability to Enabling Mutation Studies in Real-Time Single Cells. *Cells*, *10*(6), 1535. https://doi.org/10.3390/cells10061535

Farante, G., Toesca, A., Magnoni, F., Lissidini, G., Vila, J., Mastropasqua, M., Viale, G., Penco, S., Cassano, E., Lazzeroni, M., Bonanni, B., Leonardi, M. C., Ripoll-Orts, F., Curigliano, G., Orecchia, R., Galimberti, V., & Veronesi, P. (2022). Advances and controversies in management of breast ductal carcinoma in situ (DCIS). *Eur J Surg Oncol*, *48*(4), 736-741. https://doi.org/10.1016/j.ejso.2021.10.030

Fouad, Y. A., & Aanei, C. (2017). Revisiting the hallmarks of cancer. *Am J Cancer Res*, *7*(5), 1016-1036.

Franken, N. A., Rodermond, H. M., Stap, J., Haveman, J., & van Bree, C. (2006). Clonogenic assay of cells in vitro. *Nat Protoc*, *1*(5), 2315-2319. https://doi.org/10.1038/nprot.2006.339

Frey, M. K., & Pothuri, B. (2017). Homologous recombination deficiency (HRD) testing in ovarian cancer clinical practice: a review of the literature. *Gynecol Oncol Res Pract*, *4*(1), 4. https://doi.org/10.1186/s40661-017-0039-8

Friedberg, E. C. (2013). Nucleotide Excision Repair: Biology. *Encyclopedia of Biological Chemistry*, 337-340. https://doi.org/info:doi/10.1016/B978-0-12-378630-2.00254-1

Funston, G., Crosbie, E. J., Hamilton, W., & Walter, F. M. (2022). Detecting ovarian cancer in primary care: can we do better? In (Vol. 72, pp. 312-313): British Journal of General Practice.

Gago-Fuentes, R., & Oksenych, V. (2020). Non-homologous end joining factors XLF, PAXX and DNA-PKcs support neural stem and progenitor cells development. *bioRxiv*, 2020.2012. 2001.406629.

Garcia-de-Teresa, B., Rodriguez, A., & Frias, S. (2020). Chromosome Instability in Fanconi Anemia: From Breaks to Phenotypic Consequences. *Genes (Basel)*, *11*(12), 1528. https://doi.org/10.3390/genes11121528

Garcia-Diaz, M., & Bebenek, K. (2007). Multiple functions of DNA polymerases. *CRC Crit Rev Plant Sci*, *26*(2), 105-122. https://doi.org/10.1080/07352680701252817

Garmezy, B., Gheeya, J., Lin, H. Y., Huang, Y., Kim, T., Jiang, X., Thein, K. Z., Pilie, P. G., Zeineddine, F., Wang, W., Shaw, K. R., Rodon, J., Shen, J. P., Yuan, Y., Meric-Bernstam, F., Chen, K., & Yap, T. A. (2022). Clinical and Molecular Characterization of POLE Mutations as Predictive Biomarkers of Response to Immune Checkpoint Inhibitors in Advanced Cancers. *JCO Precis Oncol*, *6*(6), e2100267. https://doi.org/10.1200/PO.21.00267

Garribba, L., De Feudis, G., Martis, V., Galli, M., Dumont, M., Eliezer, Y., Wardenaar, R., Ippolito, M. R., Iyer, D. R., Tijhuis, A. E., Spierings, D. C. J., Schubert, M., Taglietti, S., Soriani, C., Gemble, S., Basto, R., Rhind, N., Foijer, F., Ben-David, U., . . . Santaguida, S. (2023). Short-term molecular consequences of chromosome mis-segregation for genome stability. *Nature communications*, *14*(1), 1353-1353. https://doi.org/10.1038/s41467-023-37095-7

Geng, H., & Hsieh, P. (2013). Molecular Mechanisms and Functions of DNA Mismatch Repair. *DNA Alterations in Lynch Syndrome: Advances in molecular diagnosis and genetic counselling*, 25-45.

Geurts, B., Zeverijn, L. J., Battaglia, T. W., van de Haar, J., van Berge Henegouwen, J. M., Hoes, L. R., van der Wijngaart, H., Roepman, P., de Leng, W. W. J., Jansen, A. M. L., van der Noort, V., Chalabi, M., Devriese, L. A., Van Herpen, C. M. L., Gelderblom, H., Verheul, H. M. W., & Voest, E. E. (2023). Efficacy and predictors of response of nivolumab in treatment-refractory MSI solid tumors: Results of a tumor-agnostic DRUP cohort. *Journal of clinical oncology*, *41*(16_suppl), 2590-2590. https://doi.org/10.1200/JCO.2023.41.16_suppl.2590

Giuliano, A. E., Connolly, J. L., Edge, S. B., Mittendorf, E. A., Rugo, H. S., Solin, L. J., Weaver, D. L., Winchester, D. J., & Hortobagyi, G. N. (2017). Breast Cancer—Major changes in the American Joint Committee on Cancer eighth edition cancer staging manual. *CA: A Cancer Journal for Clinicians*, *67*(4), 290-303. https://doi.org/10.3322/caac.21393

Gomez, L. C., Sottile, M. L., Guerrero-Gimenez, M. E., Zoppino, F. C. M., Redondo, A. L., Gago, F. E., Orozco, J. I., Tello, O. M., Roque, M., Nadin, S. B., Marzese, D. M., & Vargas-Roig, L. M. (2018). TP73 DNA methylation and upregulation of DeltaNp73 are associated with an adverse prognosis in breast cancer. *J Clin Pathol*, *71*(1), 52-58. https://doi.org/10.1136/jclinpath-2017-204499

Gong, J. G., Costanzo, A., Yang, H. Q., Melino, G., Kaelin, W. G., Jr., Levrero, M., & Wang, J. Y. (1999). The tyrosine kinase c-Abl regulates p73 in apoptotic response to cisplatin-induced DNA damage. *Nature*, *399*(6738), 806-809. https://doi.org/10.1038/21690

Green, A. R., Soria, D., Stephen, J., Powe, D. G., Nolan, C. C., Kunkler, I., Thomas, J., Kerr, G. R., Jack, W., Cameron, D., Piper, T., Ball, G. R., Garibaldi, J. M., Rakha, E. A., Bartlett, J. M., & Ellis, I. O. (2016). Nottingham Prognostic Index Plus: Validation of a clinical decision making tool in breast cancer in an independent series. *The Journal of Pathology: Clinical Research*, *2*(1), 32-40. https://doi.org/10.1002/cjp2.32

Guo, P., Ma, N., Shan, J., Chen, T., Zhang, Y., Zhou, S., & Ma, W. (2019). Exogenous damage causes cell DNA damage through mediated reactive oxygen levels. E3S Web of Conferences,

Gutierrez, R., & O'Connor, T. R. (2021). DNA direct reversal repair and alkylating agent drug resistance. *Cancer Drug Resist*, *4*(2), 414-423. https://doi.org/10.20517/cdr.2020.113

Gutierrez, R., Thompson, Y., & O'Connor, T. R. (2018). DNA direct repair pathways in cancer. *AIMS Medical Science*, *5*(3), 284-302.

Hadi, K., Gundem, G., Levine, M. F., Deshpande, A., Patel, M., Skzrypczak, S., Assaad, M. A., Mosquera, J. M., Elemento, O., & Kung, A. L. (2023). A whole genome sequencing classifier of homologous recombination deficiency. *Cancer Research*, *83*(7_Supplement), 2149-2149.

Hagiwara, K., Harimoto, N., Yokobori, T., Muranushi, R., Hoshino, K., Gantumur, D., Yamanaka, T., Ishii, N., Tsukagoshi, M., & Igarashi, T. (2020). High co-expression of large tenascin C splice variants in stromal tissue and annexin A2 in cancer cell membranes is associated with poor prognosis in pancreatic cancer. *Annals of Surgical Oncology*, *27*, 924-930.

Hahn, W. C., & Weinberg, R. A. (2015). *1 - Cancer: A Genetic Disorder* (Fourth Edition ed.). Elsevier Inc. https://doi.org/10.1016/B978-1-4557-4066-6.00001-9

Hakem, R. (2008). DNA-damage repair; the good, the bad, and the ugly. In *EMBO J* (Vol. 27, pp. 589-605). https://doi.org/10.1038/emboj.2008.15

Hammarlund, J. A., Li, S. Y., Wu, G., Lian, J. W., Howell, S. J., Clarke, R., Adamson, A., Goncalves, C. F., Hogenesch, J. B., Meng, Q. J., & Anafi, R. C. (2023). Subtype-specific circadian clock dysregulation modulates breast cancer biology, invasiveness, and prognosis. *bioRxiv*. https://doi.org/10.1101/2023.05.17.540386

Hanafy, A. K., Morani, A. C., Jensen, C. T., Kamat, A., Eifel, P. J., & Bhosale, P. R. (2023). Ovarian Cancer. *Oncologic Imaging : a Multidisciplinary Approach*, 452-475. https://doi.org/info:doi/10.1016/B978-0-323-69538-1.00027-6

Hanahan, D. (2022). Hallmarks of Cancer: New Dimensions. *Science-Business eXchange*, *12*(1), 31-46. https://doi.org/10.1158/2159-8290.CD-21-1059

Hanahan, D., & Weinberg, R. A. (2000). The Hallmarks of Cancer. In (Vol. 100, pp. 57-70).

Hanahan, D., & Weinberg, R. A. (2011). Hallmarks of cancer: the next generation. *Cell*, *144*(5), 646-674. https://doi.org/10.1016/j.cell.2011.02.013

Haradhvala, N. J., Polak, P., Stojanov, P., Covington, K. R., Shinbrot, E., Hess, J. M., Rheinbay, E., Kim, J., Maruvka, Y. E., Braunstein, L. Z., Kamburov, A., Hanawalt, P. C., Wheeler, D. A., Koren, A., Lawrence, M. S., & Getz, G. (2016). Mutational Strand Asymmetries in Cancer Genomes Reveal Mechanisms of DNA Damage and Repair. *Cell*, *164*(3), 538-549. https://doi.org/10.1016/j.cell.2015.12.050

Hashimoto, S., Anai, H., & Hanada, K. (2016). Mechanisms of interstrand DNA crosslink repair and human disorders. *Genes and Environment*, *38*(1). https://doi.org/10.1186/s41021-016-0037-9

Hashmi, A. A., Bukhari, U., Najam, J., Dowlah, T., Ali, A. H., Diwan, M. A., Anjali, F., Sham, S., Zia, S., & Irfan, M. (2023). Luminal B, Human Epidermal Growth Factor Receptor 2 (HER2/neu), and Triple-Negative Breast Cancers Associated With a Better Chemotherapy Response Than Luminal A Breast Cancers in Postneoadjuvant Settings. *Cureus*, *15*(6).

Head, P. E., Kapoor-Vazirani, P., Nagaraju, G. P., Zhang, H., Rath, S. K., Luong, N. C., Haji-Seyed-Javadi, R., Sesay, F., Wang, S.-Y., & Duong, D. M. (2023). DNA-PK is activated by SIRT2 deacetylation to promote DNA double-strand break repair by non-homologous end joining. *Nucleic acids research*, *51*(15), 7972-7987.

Helbling-Leclerc, A., Garcin, C., & Rosselli, F. (2021). Beyond DNA repair and chromosome instability-Fanconi anaemia as a cellular senescence-associated syndrome. *Cell Death Differ*, *28*(4), 1159-1173. https://doi.org/10.1038/s41418-021-00764-5

Henninger, E. E., & Pursell, Z. F. (2014). DNA polymerase epsilon and its roles in genome stability. *IUBMB Life*, *66*(5), 339-351. https://doi.org/10.1002/iub.1276

Hiatt, R. A., Engmann, N. J., Balke, K., & Rehkopf, D. H. (2020). A Complex Systems Model of Breast Cancer Etiology: The Paradigm II Conceptual Model. *Cancer Epidemiology, Biomarkers & Prevention*, *29*(9), 1720-1730. https://doi.org/10.1158/1055-9965.epi-20-0016

Hoang, L. N., McConechy, M. K., Köbel, M., Anglesio, M., Senz, J., Maassen, M., Kommoss, S., Meng, B., Postovit, L., Kelemen, L. E., Staebler, A., Brucker, S., Krämer, B., McAlpine, J. N., Gilks, C. B., Huntsman, D. G., & Lee, C.-H. (2015). Polymerase Epsilon Exonuclease Domain Mutations in Ovarian Endometrioid Carcinoma. *International journal of gynecological cancer*, *25*(7), 1187-1193. https://doi.org/10.1097/IGC.0000000000000492

Hoeijmakers, J. H. (2007). Genome maintenance mechanisms are critical for preventing cancer as well as other aging-associated diseases. *Mech Ageing Dev*, *128*(7-8), 460-462. https://doi.org/10.1016/j.mad.2007.05.002

Hossain, K. R., Escobar Bermeo, J. D., Warton, K., & Valenzuela, S. M. (2022). New Approaches and Biomarker Candidates for the Early Detection of Ovarian Cancer. *Front Bioeng Biotechnol*, *10*, 819183. https://doi.org/10.3389/fbioe.2022.819183

Hu, H., Cai, W., Wu, D., Hu, W., Dong Wang, L., Mao, J., Zheng, S., & Ge, W. (2021). Ultra-mutated colorectal cancer patients with POLE driver mutations exhibit distinct clinical patterns. *Cancer Med*, *10*(1), 135-142. https://doi.org/10.1002/cam4.3579

Huang, A., Garraway, L. A., Ashworth, A., & Weber, B. (2020). Synthetic lethality as an engine for cancer drug target discovery [ReviewPaper]. *Nat Rev Drug Discov*, *19*(1), 23-38. https://doi.org/10.1038/s41573-019-0046-z

Huang, R., & Zhou, P. K. (2021). DNA damage repair: historical perspectives, mechanistic pathways and clinical translation for targeted cancer therapy. *Signal Transduct Target Ther*, *6*(1), 254. https://doi.org/10.1038/s41392-021-00648-7

Hussain, T., Lee, J., Abba, M. C., Chen, J., & Aldaz, C. M. (2018). Delineating WWOX Protein Interactome by Tandem Affinity Purification-Mass Spectrometry: Identification of Top Interactors and Key Metabolic Pathways Involved. *Front Oncol*, *8*, 591. https://doi.org/10.3389/fonc.2018.00591

Ichimiya, S., Nakagawara, A., Sakuma, Y., Kimura, S., Ikeda, T., Satoh, M., Takahashi, N., Sato, N., & Mori, M. (2000). p73: Structure and function. *Pathology international*, *50*(8), 589-593. https://doi.org/10.1046/j.1440-1827.2000.01090.x

Inoue, K., & Fry, E. A. (2014). Alterations of p63 and p73 in human cancers. *Subcell Biochem*, *85*, 17-40. https://doi.org/10.1007/978-94-017-9211-0_2

Irwin, M. S., & Miller, F. D. (2004). p73: regulator in cancer and neural development. *Cell Death Differ*, *11 Suppl 1*(1), S17-22. https://doi.org/10.1038/sj.cdd.4401452

James, C. R., Quinn, J. E., Mullan, P. B., Johnston, P. G., & Harkin, D. P. (2007). BRCA1, a potential predictive biomarker in the treatment of breast cancer. *Oncologist*, *12*(2), 142-150. https://doi.org/10.1634/theoncologist.12-2-142

Jancalek, R. (2014). The role of the TP73 gene and its transcripts in neuro-oncology. *Br J Neurosurg*, *28*(5), 598-605. https://doi.org/10.3109/02688697.2014.908162

Jiang, M., Jia, K., Wang, L., Li, W., Chen, B., Liu, Y., Wang, H., Zhao, S., He, Y., & Zhou, C. (2020). Alterations of DNA damage repair in cancer: from mechanisms to applications. *Annals of Translational Medicine*, *8*(24), 1685-1685. https://doi.org/10.21037/atm-20-2920

Jilderda, L. J., Zhou, L., & Foijer, F. (2021). Understanding how genetic mutations collaborate with genomic instability in cancer. *Cells (Basel, Switzerland)*, *10*(2), 1-16. https://doi.org/10.3390/cells10020342

Joaquin, A., & Fernandez-Capetillo, O. (2012). Signalling DNA Damage. In *Protein Phosphorylation in Human Health*. InTech. https://doi.org/10.5772/50863

Johanns, T. M., Miller, C. A., Dorward, I. G., Tsien, C., Chang, E., Perry, A., Uppaluri, R., Ferguson, C., Schmidt, R. E., Dahiya, S., Ansstas, G., Mardis, E. R., & Dunn, G. P. (2016). Immunogenomics of Hypermutated Glioblastoma: A Patient with Germline POLE Deficiency Treated with Checkpoint Blockade Immunotherapy. *Science-Business eXchange*, *6*(11), 1230-1236. https://doi.org/10.1158/2159-8290.CD-16-0575

Jost, C. A., Marin, M. C., & Jr, W. G. K. (1997). p73 is a human p53-related protein that can induce apoptosis. *Nature*, *389*(6647), 191-194. https://doi.org/10.1038/38298

Joyce, C., Rayi, A., & Kasi, A. (2024). Tumor-Suppressor Genes. In *StatPearls*. StatPearls Publishing Copyright © 2024, StatPearls Publishing LLC.

Kaelin, W. G., Jr. (2005). The concept of synthetic lethality in the context of anticancer therapy. *Nat Rev Cancer*, *5*(9), 689-698. https://doi.org/10.1038/nrc1691

Kang, S. Y., Kim, D. G., Ahn, S., Ha, S. Y., Jang, K.-T., & Kim, K.-M. (2022). Comparative analysis of microsatellite instability by next-generation sequencing, MSI PCR and MMR immunohistochemistry in 1942 solid cancers. *Pathology, research and practice*, *233*, 153874-153874. https://doi.org/10.1016/j.prp.2022.153874

Karst, A. M., & Drapkin, R. (2010). Ovarian cancer pathogenesis: a model in evolution [Review Article]. *J Oncol*, *2010*, 932371. https://doi.org/10.1155/2010/932371

Kavun, A., Veselovsky, E., Lebedeva, A., Belova, E., Kuznetsova, O., Yakushina, V., Grigoreva, T., Mileyko, V., Fedyanin, M., & Ivanov, M. (2023). Microsatellite Instability: A Review of Molecular Epidemiology and Implications for Immune Checkpoint Inhibitor Therapy. *Cancers*, *15*(8), 2288. https://doi.org/10.3390/cancers15082288

Khan, F. A., & Ali, S. O. (2017). Physiological Roles of DNA Double-Strand Breaks. *J Nucleic Acids*, *2017*, 6439169. https://doi.org/10.1155/2017/6439169

Kim, K. B. (2023). Phase II study of niraparib in patients with advanced melanoma with genetic homologous recombination (HR) mutation/alteration. In: American Society of Clinical Oncology.

Klapacz, J., Pottenger, L. H., Engelward, B. P., Heinen, C. D., Johnson, G. E., Clewell, R. A., Carmichael, P. L., Adeleye, Y., & Andersen, M. E. (2016). Contributions of DNA repair and damage response pathways to the non-linear genotoxic responses of alkylating agents. *Mutat Res Rev Mutat Res*, *767*, 77-91. https://doi.org/10.1016/j.mrrev.2015.11.001

Kong, X., Yan, W., Sun, W., Zhang, Y., Yang, H. J., Chen, M., Chen, H., de Vere White, R. W., Zhang, J., & Chen, X. (2023). Isoform-specific disruption of the TP73 gene reveals a critical role for TAp73γ in tumorigenesis via leptin. *eLife*, *12*. https://doi.org/10.7554/eLife.82115

Konstantinopoulos, P. A., Ceccaldi, R., Shapiro, G. I., & D'Andrea, A. D. (2015). Homologous Recombination Deficiency: Exploiting the Fundamental Vulnerability of Ovarian Cancer. *Science-Business eXchange*, *5*(11), 1137-1154. https://doi.org/10.1158/2159-8290.CD-15-0714

Kopacz-Bednarska, A., & Król, T. (2022). Cisplatin—Properties and clinical application. *Oncology in Clinical Practice*, *18*(3), 166-176.

Kossai, M., Leary, A., Scoazec, J. Y., & Genestie, C. (2018). Ovarian Cancer: A Heterogeneous Disease. *Pathobiology*, *85*(1-2), 41-49. https://doi.org/10.1159/000479006

Krasikova, Y., Rechkunova, N., & Lavrik, O. (2021). Nucleotide Excision Repair: From Molecular Defects to Neurological Abnormalities. *Int J Mol Sci*, *22*(12), 6220. https://doi.org/10.3390/ijms22126220

Kroeger, P. T., Jr., & Drapkin, R. (2017). Pathogenesis and heterogeneity of ovarian cancer. *Curr Opin Obstet Gynecol*, *29*(1), 26-34. https://doi.org/10.1097/GCO.0000000000000340

Kunkel, T. A., & Erie, D. A. (2005). DNA mismatch repair. *Annu Rev Biochem*, *74*, 681-710. https://doi.org/10.1146/annurev.biochem.74.082803.133243

Lagios, M. D. (2020). Duct carcinoma in situ: A personal perspective. *Breast J*, *26*(6), 1132-1137. https://doi.org/10.1111/tbj.13860

Lakhani, S. R., Van De Vijver, M. J., Jacquemier, J., Anderson, T. J., Osin, P. P., McGuffog, L., & Easton, D. F. (2002). The pathology of familial breast cancer: predictive value of immunohistochemical markers estrogen receptor, progesterone receptor, HER-2, and p53 in patients with mutations in BRCA1 and BRCA2. *J Clin Oncol*, *20*(9), 2310-2318. https://doi.org/10.1200/JCO.2002.09.023

Lamghari, Y., Lu, H., & Bentourkia, M. h. (2023). DNA damage by radiation as a function of electron energy and interaction at the atomic level with Monte Carlo simulation. *Zeitschrift für medizinische Physik*, *33*(4), 489-498. https://doi.org/10.1016/j.zemedi.2022.07.003

Lau, T. Y., & Poon, R. Y. C. (2023). Whole-Genome Duplication and Genome Instability in Cancer Cells: Double the Trouble. *International journal of molecular sciences*, *24*(4), 3733. https://doi.org/10.3390/ijms24043733

Laubach, K. N., Yan, W., Kong, X., Sun, W., Chen, M., Zhang, J., & Chen, X. (2022). p73alpha1, a p73 C-terminal isoform, regulates tumor suppression and the inflammatory response via Notch1. *Proc Natl Acad Sci U S A*, *119*(22), e2123202119. https://doi.org/10.1073/pnas.2123202119

Le, D. T., Durham, J. N., Smith, K. N., Wang, H., Bartlett, B. R., Aulakh, L. K., Lu, S., Kemberling, H., Wilt, C., Luber, B. S., Wong, F., Azad, N. S., Rucki, A. A., Laheru, D., Donehower, R., Zaheer, A., Fisher, G. A., Crocenzi, T. S., Lee, J. J., . . . Diaz, L. A., Jr. (2017). Mismatch repair deficiency predicts response of solid tumors to PD-1 blockade. *Science*, *357*(6349), 409-413. https://doi.org/10.1126/science.aan6733

Lebeau, A. (2021). Updated WHO classification of tumors of the breast. *Der Pathologe*, 1-5.

León-Castillo, A., Britton, H., McConechy, M. K., McAlpine, J. N., Nout, R., Kommoss, S., Brucker, S. Y., Carlson, J. W., Epstein, E., Rau, T. T., Bosse, T., Church, D. N., & Gilks, C. B. (2020). Interpretation of somatic POLE mutations in endometrial carcinoma. In *J Pathol* (Vol. 250, pp. 323-335). https://doi.org/10.1002/path.5372

Leon, A. C. S., & Richardson, A. E. (2021). Systemic Therapy for the Treatment of Breast Cancer. In *Breast Cancer and Gynecologic Cancer Rehabilitation* (pp. 81-87). Elsevier.

Leong, C.-O., Vidnovic, N., DeYoung, M. P., Sgroi, D., & Ellisen, L. W. (2007). The p63/p73 network mediates chemosensitivity to cisplatin in a biologically defined subset of primary breast cancers. *The Journal of clinical investigation*, *117*(5), 1370-1380. https://doi.org/10.1172/JCI30866

Leong, C. O., Vidnovic, N., DeYoung, M. P., Sgroi, D., & Ellisen, L. W. (2007). The p63/p73 network mediates chemosensitivity to cisplatin in a biologically defined subset of primary breast cancers. *J Clin Invest*, *117*(5), 1370-1380. https://doi.org/10.1172/JCI30866

Levine, D. A., Mike 1, C. G. A. R. N. G. s. c. B. I. G. G. G. S. B. C. K. L. E. S. A. S. C. L., Heather, W. U. i. S. L. K. C. D. D. F. R. F. L. K.-V. J. M. M. D. O. L. M. S., California, U. o. S., 22 Laird Peter W. 22 Shen Hui 22, J. H. B. S. B. B. M. S. L. P. H. T. J. T. J. V. D. B. D. J. W. D. J., & 23, I. f. S. B. R. S. M. S. I. (2013). Integrated genomic characterization of endometrial carcinoma. *Nature*, *497*(7447), 67-73.

Lewis, T., & Dimri, M. (2023). Biochemistry, DNA Repair [Text]. https://doi.org/https://www.ncbi.nlm.nih.gov/books/NBK560563/

Li, F., Du, Z., Huang, X., Dong, C., & Ren, J. (2021). Analyses of p73 Protein Oligomerization and p73-MDM2 Interaction in Single Living Cells Using In Situ Single Molecule Spectroscopy. *Anal Chem*, *93*(2), 886-894. https://doi.org/10.1021/acs.analchem.0c03521

Li, K., Luo, H., Huang, L., Luo, H., & Zhu, X. (2020). Microsatellite instability: a review of what the oncologist should know [ReviewPaper]. *Cancer Cell Int*, *20*(1), 16. https://doi.org/10.1186/s12935-019-1091-8

Li, Y., & Prives, C. (2007). Are interactions with p63 and p73 involved in mutant p53 gain of oncogenic function? [ReviewPaper]. *Oncogene*, *26*(15), 2220-2225. https://doi.org/10.1038/sj.onc.1210311

Lindsey-Boltz, L. A., Yang, Y., Kose, C., Deger, N., Eynullazada, K., Kawara, H., & Sancar, A. (2023). Nucleotide excision repair in Human cell lines lacking both XPC and CSB proteins. *Nucleic acids research*, gkad334.

Lisio, M. A., Fu, L., Goyeneche, A., Gao, Z. H., & Telleria, C. (2019). High-Grade Serous Ovarian Cancer: Basic Sciences, Clinical and Therapeutic Standpoints [Review]. *Int J Mol Sci*, *20*(4), 952. https://doi.org/10.3390/ijms20040952

Liu, Y., Hu, P., Xu, L., Zhang, X., Li, Z., Li, Y., & Qiu, H. (2023). Current Progress on Predictive Biomarkers for Response to Immune Checkpoint Inhibitors in Gastric Cancer: How to Maximize the Immunotherapeutic Benefit? *Cancers*, *15*(8), 2273. https://doi.org/10.3390/cancers15082273

Logotheti, S., Richter, C., Murr, N., Spitschak, A., Marquardt, S., & Putzer, B. M. (2021). Mechanisms of Functional Pleiotropy of p73 in Cancer and Beyond. *Front Cell Dev Biol*, *9*, 737735. https://doi.org/10.3389/fcell.2021.737735

Logotheti, S., Richter, C., Murr, N., Spitschak, A., Marquardt, S., & Pützer, B. M. (2021). Mechanisms of functional pleiotropy of p73 in cancer and beyond. *Frontiers in Cell and Developmental Biology*, *9*, 737735.

Lord, C. J., & Ashworth, A. (2017). PARP inhibitors: Synthetic lethality in the clinic. *Science*, *355*(6330), 1152-1158. https://doi.org/10.1126/science.aam7344

Lord, C. J., Tutt, A. N., & Ashworth, A. (2015). Synthetic lethality and cancer therapy: lessons learned from the development of PARP inhibitors. *Annu Rev Med*, *66*(1), 455-470. https://doi.org/10.1146/annurev-med-050913-022545

Luo, S., Su, T., Zhou, X., Hu, W.-X., & Hu, J. (2022). Chromosome 1 instability in multiple myeloma: Aberrant gene expression, pathogenesis, and potential therapeutic target. *The FASEB Journal*, *36*(6), e22341. https://doi.org/https://doi.org/10.1096/fj.202200354

Ma, X., Dong, L., Liu, X., Ou, K., & Yang, L. (2022). POLE/POLD1 mutation and tumor immunotherapy. *J Exp Clin Cancer Res*, *41*(1), 216. https://doi.org/10.1186/s13046-022-02422-1

Ma, X. J., Salunga, R., Tuggle, J. T., Gaudet, J., Enright, E., McQuary, P., Payette, T., Pistone, M., Stecker, K., Zhang, B. M., Zhou, Y. X., Varnholt, H., Smith, B., Gadd, M., Chatfield, E., Kessler, J., Baer, T. M., Erlander, M. G., & Sgroi, D. C. (2003). Gene expression profiles of human breast cancer progression. *Proc Natl Acad Sci U S A*, *100*(10), 5974-5979. https://doi.org/10.1073/pnas.0931261100

Maas, A.-M., Bretz, A. C., Mack, E., & Stiewe, T. (2013). Targeting p73 in cancer. *Cancer letters*, *332*(2), 229-236. https://doi.org/10.1016/j.canlet.2011.07.030

Madhusudan, S., & Wilson, D. M. (2013). *DNA repair and cancer : from bench to clinic / editors Srinivasan Madhusudan, David M. Wilson III*. Boca Raton, Fla. ; London : CRC Press.

Makki, J. (2015). Diversity of Breast Carcinoma: Histological Subtypes and Clinical Relevance. In *Clin Med Insights Pathol* (Vol. 8, pp. 23-31). https://doi.org/10.4137/CPath.S31563

Malhotra, G. K., Zhao, X., Band, H., & Band, V. (2010). Histological, molecular and functional subtypes of breast cancers. In *Cancer Biol Ther* (Vol. 10, pp. 955-960). https://doi.org/10.4161/cbt.10.10.13879

Mangogna, A., Munari, G., Pepe, F., Maffii, E., Giampaolino, P., Ricci, G., Fassan, M., Malapelle, U., & Biffi, S. (2023). Homologous Recombination Deficiency in Ovarian Cancer: from the Biological Rationale to Current Diagnostic Approaches. *J Pers Med*, *13*(2). https://doi.org/10.3390/jpm13020284

Mannu, G. S., Wang, Z., Broggio, J., Charman, J., Cheung, S., Kearins, O., Dodwell, D., & Darby, S. C. (2020). Invasive breast cancer and breast cancer mortality after ductal carcinoma in situ in women attending for breast screening in England, 1988-2014: population based observational cohort study. *BMJ*, *369*, m1570. https://doi.org/10.1136/bmj.m1570

Mardis, E. R. (2019). Neoantigens and genome instability: impact on immunogenomic phenotypes and immunotherapy response. *Genome Med*, *11*(1), 71. https://doi.org/10.1186/s13073-019-0684-0

Marinus, M. G. (2012). DNA Mismatch Repair. *EcoSal Plus*, *5*(1), 10.1128/ecosalplus. 1127.1122. 1125. https://doi.org/10.1128/ecosalplus.7.2.5

Marinus, M. G., & Casadesus, J. (2009). Roles of DNA adenine methylation in host-pathogen interactions: mismatch repair, transcriptional regulation, and more. *FEMS Microbiol Rev*, *33*(3), 488-503. https://doi.org/10.1111/j.1574-6976.2008.00159.x

Marnett, L. J., & Plastaras, J. P. (2001). Endogenous DNA damage and mutation. *Trends Genet*, *17*(4), 214-221. https://doi.org/10.1016/s0168-9525(01)02239-9

Matsuda, S., Murakami, M., Ikeda, Y., Nakagawa, Y., Tsuji, A., & Kitagishi, Y. (2020). Role of tumor suppressor molecules in genomic perturbations and damaged DNA repair involved in the pathogenesis of cancer and neurodegeneration (Review). *Biomed Rep*, *13*(3), 10. https://doi.org/10.3892/br.2020.1317

Maxwell, C., & Roskelley, C. (2015). *Genomic Instability and Cancer Metastasis. Mechanisms, Emerging Themes, and Novel Therapeutic Strategies* (Vol. 35).

Maynard, S., Schurman, S. H., Harboe, C., de Souza-Pinto, N. C., & Bohr, V. A. (2009). Base excision repair of oxidative DNA damage and association with cancer and aging. *Carcinogenesis*, *30*(1), 2-10. https://doi.org/10.1093/carcin/bgn250

Medeiros, M. H. (2019). DNA damage by endogenous and exogenous aldehydes. *Journal of the Brazilian Chemical Society*, *30*, 2000-2009.

Mehnert, J. M., Panda, A., Zhong, H., Hirshfield, K., Damare, S., Lane, K., Sokol, L., Stein, M. N., Rodriguez-Rodriquez, L., Kaufman, H. L., Ali, S., Ross, J. S., Pavlick, D. C., Bhanot, G., White, E. P., DiPaola, R. S., Lovell, A., Cheng, J., & Ganesan, S. (2016). Immune activation and response to pembrolizumab in POLE-mutant endometrial cancer. *J Clin Invest*, *126*(6), 2334-2340. https://doi.org/10.1172/JCI84940

Mehrotra, S., & Mittra, I. (2020). Origin of genome instability and determinants of mutational landscape in cancer cells. *Genes*, *11*(9), 1-13. https://doi.org/10.3390/genes11091101

Mei, Y. (2021). Review of the toxicological mechanism of anticancer drug cisplatin. *2350*(1). https://doi.org/10.1063/5.0048435

Melino, G. (2020). Molecular Mechanisms and Function of the p53 Protein Family Member – p73. *Biochemistry (Moscow)*, *85*(10), 1202-1209. https://doi.org/10.1134/S0006297920100089

Messori, L., & Merlino, A. (2016). Cisplatin binding to proteins: A structural perspective. *Coordination Chemistry Reviews*, *315*, 67-89.

Metaxas, G. I., Tsiambas, E., Marinopoulos, S., Adamopoulou, M., Spyropoulou, D., Falidas, E., Davris, D., Manaios, L., Fotiades, P., Mastronikoli, S., Peschos, D., & Dimitrakakis, C. (2023). DNA Mismatch Repair System Imbalances in Breast Adenocarcinoma. *Cancer Diagn Progn*, *3*(2), 169-174. https://doi.org/10.21873/cdp.10197

Mikhova, M., Heyza, J. R., Meek, K., & Schmidt, J. C. (2023). Single-molecule imaging reveals the kinetics of non-homologous end-joining in living cells. *bioRxiv*, 2023.2006. 2022.546088.

Milane, L. S. (2022). The hallmarks of cancer and immunology. *Cancer Immunology and Immunotherapy*, 1-17. https://doi.org/info:doi/10.1016/B978-0-12-823397-9.00001-6

Miller, C. J., & Usdin, K. (2022). Mismatch repair is a double-edged sword in the battle against microsatellite instability. *Expert Reviews in Molecular Medicine*, *24*, e32.

Mir, M. A., & Din, I. M. U. (2023). Molecular Subtypes of Breast Cancer and CDk Dysregulation. In *Therapeutic potential of Cell Cycle Kinases in Breast Cancer* (pp. 133-148). https://doi.org/10.1007/978-981-19-8911-7_6

Mir, M. A., & Qayoom, H. (2023). Introduction to breast cancer. In *Therapeutic potential of Cell Cycle Kinases in Breast Cancer* (pp. 1-22). Springer.

Mishina, Y., Duguid, E. M., & He, C. (2006). Direct reversal of DNA alkylation damage. *Chem Rev*, *106*(2), 215-232. https://doi.org/10.1021/cr0404702

Moll, U. M., & Slade, N. (2004). p63 and p73: roles in development and tumor formation. *Mol Cancer Res*, *2*(7), 371-386.

Momenimovahed, Z., Tiznobaik, A., Taheri, S., & Salehiniya, H. (2019). Ovarian cancer in the world: epidemiology and risk factors. *Int J Womens Health*, *11*, 287-299. https://doi.org/10.2147/IJWH.S197604

Moreno-Villanueva, M. (2016). DNA Damage, DNA Repair, and Micronutrients in Aging. In M. Malavolta & E. Mocchegiani (Eds.), *Molecular Basis of Nutrition and Aging* (pp. 243-249). Academic Press. https://doi.org/10.1016/b978-0-12-801816-3.00018-2

Moschetta, M., George, A., Kaye, S. B., & Banerjee, S. (2016). BRCA somatic mutations and epigenetic BRCA modifications in serous ovarian cancer. *Ann Oncol*, *27*(8), 1449-1455. https://doi.org/10.1093/annonc/mdw142

Mucaki, E. J., & Rogan, P. K. (2019). Expression changes confirm predicted single nucleotide variants affecting mRNA splicing. *bioRxiv*, 549089.

Müller, M., Schilling, T., Sayan, A., Kairat, A., Lorenz, K., Schulze-Bergkamen, H., Oren, M., Koch, A., Tannapfel, A., & Stremmel, W. (2005). TAp73/ΔNp73 influences apoptotic response, chemosensitivity and prognosis in hepatocellular carcinoma. *Cell Death & Differentiation*, *12*(12), 1564-1577.

Mumtaz, S., Ali, S., Mumtaz, S., Pervaiz, A., Tahir, H. M., Farooq, M. A., & Mughal, T. A. (2023). Advanced treatment strategies in breast cancer: A comprehensive mechanistic review. *Sci Prog*, *106*(2), 368504231175331. https://doi.org/10.1177/00368504231175331

Natan, E., & Joerger, A. C. (2012). Structure and kinetic stability of the p63 tetramerization domain. *J Mol Biol*, *415*(3), 503-513. https://doi.org/10.1016/j.jmb.2011.11.007

Nishida, Y., Ishizawa, J., Ruvolo, V., & Andreeff, M. (2018). TP73 Isoforms (TAp73 and ΔNp73) Are Overexpressed in Acute Myeloid Leukemias and Potential Therapeutic Targets to Enhance Anti-Leukemia Activities of Bcl-2 and MDM2 Inhibitors. *Blood*, *132*(Supplement 1), 2629-2629. https://doi.org/10.1182/blood-2018-99-113900

Omran, Z., Dalhat, M. H., Abdullah, O., Kaleem, M., Hosawi, S., Al-Abbasi, F. A., Wu, W., Choudhry, H., & Alhosin, M. (2021). Targeting post-translational modifications of the p73 protein: A promising therapeutic strategy for tumors. *Cancers*, *13*(8), 1916. https://doi.org/10.3390/cancers13081916

Orrantia-Borunda, E., Anchondo-Nuñez, P., Acuña-Aguilar, L. E., Gómez-Valles, F. O., & Ramírez-Valdespino, C. A. (2022). Subtypes of breast cancer. *Breast Cancer [Internet]*.

Orzol, P., Holcakova, J., Nekulova, M., Nenutil, R., Vojtesek, B., & Coates, P. J. (2015). The diverse oncogenic and tumour suppressor roles of p63 and p73 in cancer: a review by cancer site. *Histol Histopathol*, *30*(5), 503-521. https://doi.org/10.14670/HH-30.503

Osterburg, C., & Dotsch, V. (2022). Structural diversity of p63 and p73 isoforms. *Cell Death Differ*, *29*(5), 921-937. https://doi.org/10.1038/s41418-022-00975-4

Oswald, C., & Stiewe, T. (2008). In good times and bad: p73 in cancer. *Cell cycle (Georgetown, Tex.)*, *7*(12), 1726-1731. https://doi.org/10.4161/cc.7.12.6148

Oumarou Hama, H., Aboudharam, G., Barbieri, R., Lepidi, H., & Drancourt, M. (2022). Immunohistochemical diagnosis of human infectious diseases: a review. *Diagn Pathol*, *17*(1), 17. https://doi.org/10.1186/s13000-022-01197-5

Oxford. (2024). *New study assesses long term risk of invasive breast cancer after pre-invasive disease*. @Oxford_NDPH. https://www.ndph.ox.ac.uk/news/new-study-assesses-long-term-risk-of-invasive-breast-cancer-after-pre-invasive-disease

Ozaki, T., & Nakagawara, A. (2005). p73, a sophisticated p53 family member in the cancer world. *Cancer Science*, *96*(11), 729-737. https://doi.org/10.1111/j.1349-7006.2005.00116.x

Parsons, J. L., & Grundy, G. J. (2023). The Base Excision Repair (BER) Pathway. *Encyclopedia of Cell Biology*, 541-551. https://doi.org/info:doi/10.1016/b978-0-12-821618-7.00100-0

Pegington, M., Belcher, J., Barrett, E., Virpal, P., Howell, A., Evans, D., & Harvie, M. (2023). *Weight, weight gain and behavioural risk factors in women attending a breast cancer family history, risk and prevention clinic: an observational study*. https://doi.org/10.21203/rs.3.rs-3027878/v1

Peila, R., Arthur, R., & Rohan, T. E. (2020). Risk factors for ductal carcinoma in situ of the breast in the UK Biobank cohort study. *Cancer Epidemiol*, *64*, 101648. https://doi.org/10.1016/j.canep.2019.101648

Persson, M., Andersson, M. K., Sahlin, P. E., Mitani, Y., Brandwein-Weber, M. S., Frierson, H. F., Jr., Moskaluk, C., Fonseca, I., Ferrarotto, R., Boecker, W., Loening, T., El-Naggar, A. K., & Stenman, G. (2023). Comprehensive molecular characterization of adenoid cystic carcinoma reveals tumor suppressors as novel drivers and prognostic biomarkers. *J Pathol*, *261*(3), 256-268. https://doi.org/10.1002/path.6172

Pikor, L., Thu, K., Vucic, E., & Lam, W. (2013). The detection and implication of genome instability in cancer. *Cancer and metastasis reviews*, *32*(3-4), 341-352. https://doi.org/10.1007/s10555-013-9429-5

Poplawski, T., & Blasiak, J. (2005). [Non-homologous DNA end joining]. *Postepy Biochem*, *51*(3), 328-338. (Naprawa DNA przez niehomologiczne laczenie koncow.)

Pospiech, K., Pluciennik, E., & Bednarek, A. K. (2018). WWOX Tumor Suppressor Gene in Breast Cancer, a Historical Perspective and Future Directions. *Front Oncol*, *8*, 345. https://doi.org/10.3389/fonc.2018.00345

Prashanth, G., Singh, A., Gadewar, M., Lal, B., & Raj, P. (2022). Cisplatin and Nano-particle Formulations of Cisplatin for Cancer Therapy: A Review. *Journal of Pharmaceutical Research International*, 34-49.

Pryor, J. M., Conlin, M. P., Carvajal-Garcia, J., Luedeman, M. E., Luthman, A. J., Small, G. W., & Ramsden, D. A. (2018). Ribonucleotide incorporation enables repair of chromosome breaks by nonhomologous end joining. *Science*, *361*(6407), 1126-1129. https://doi.org/10.1126/science.aat2477

Pulliam, N., Fang, F., Ozes, A. R., Tang, J., Adewuyi, A., Keer, H., Lyons, J., Baylin, S. B., Matei, D., Nakshatri, H., Rassool, F. V., Miller, K. D., & Nephew, K. P. (2018). An Effective Epigenetic-PARP Inhibitor Combination Therapy for Breast and Ovarian Cancers Independent of BRCA Mutations. *Clin Cancer Res*, *24*(13), 3163-3175. https://doi.org/10.1158/1078-0432.CCR-18-0204

Qiagen. (2023). RT2 Profiler PCR Arrays.

Rai, S., Chaitra, D., Pai, D. N., & Honnalli, N. M. (2022). Breast Cancer-An Overview of the Disease. *Current Innovations in Medicine and Medical Science Vol. 8*, 118-128.

Rakha, E., Toss, M., & Quinn, C. (2022). Specific cell differentiation in breast cancer: a basis for histological classification. *J Clin Pathol*, *75*(2), 76-84. https://doi.org/10.1136/jclinpath-2021-207487

Rakha, E. A., Tse, G. M., & Quinn, C. M. (2023). An update on the pathological classification of breast cancer. *Histopathology*, *82*(1), 5-16.

Ray, U., & Raghavan, S. C. (2022). Nonhomologous DNA End Joining in Mammalian Cells. In *Encyclopedia of Cell Biology: Volume 1-6, Second Edition* (Vol. 1, pp. 552-566). Elsevier.

Rayner, E., van Gool, I. C., Palles, C., Kearsey, S. E., Bosse, T., Tomlinson, I., & Church, D. N. (2016). A panoply of errors: polymerase proofreading domain mutations in cancer. *Nature reviews. Cancer*, *16*(2), 71-81. https://doi.org/10.1038/nrc.2015.12

Reardon, J. T., & Sancar, A. (2005). Nucleotide Excision Repair. *Progress in nucleic acid research and molecular biology.*, *79*, 183-235. https://doi.org/info:doi/10.1016/S0079-6603(04)79004-2

Reid, B. M., Permuth, J. B., & Sellers, T. A. (2017). Epidemiology of ovarian cancer: a review. *Cancer Biol Med*, *14*(1), 9-32. https://doi.org/10.20892/j.issn.2095-3941.2016.0084

Research, C. (2024). Ductal carcinoma in situ (DCIS).

Rodríguez, N., Peláez, A., Barderas, R., & Domínguez, G. (2018). Clinical implications of the deregulated TP73 isoforms expression in cancer. *Clinical & translational oncology*, *20*(7), 827-836. https://doi.org/10.1007/s12094-017-1802-3

Rozenberg, J. M., Zvereva, S., Dalina, A., Blatov, I., Zubarev, I., Luppov, D., Bessmertnyi, A., Romanishin, A., Alsoulaiman, L., Kumeiko, V., Kagansky, A., Melino, G., & Barlev, N. A. (2021). Dual Role of p73 in Cancer Microenvironment and DNA Damage Response. *Cells*, *10*(12), 3516. https://doi.org/10.3390/cells10123516

Rufini, A., Agostini, M., Grespi, F., Tomasini, R., Sayan, B. S., Niklison-Chirou, M. V., Conforti, F., Velletri, T., Mastino, A., Mak, T. W., Melino, G., & Knight, R. A. (2011). p73 in Cancer. *Genes Cancer*, *2*(4), 491-502. https://doi.org/10.1177/1947601911408890

Sanchez-Prieto, M., Sanchez-Borrego, R., Lubian-Lopez, D. M., & Perez-Lopez, F. R. (2022). Etiopathogenesis of ovarian cancer. An inflamm-aging entity? *Gynecol Oncol Rep*, *42*, 101018. https://doi.org/10.1016/j.gore.2022.101018

Savinova, A. R., & Gataullin, I. G. (2022). Early diagnostics and screening for ovarian cancer. *Kazan medical journal*, *103*(3), 476-483.

Schuh, A., Dreau, H., Knight, S. J. L., Ridout, K., Mizani, T., Vavoulis, D., Colling, R., Antoniou, P., Kvikstad, E. M., Pentony, M. M., Hamblin, A., Protheroe, A., Parton, M., Shah, K. A., Orosz, Z., Athanasou, N., Hassan, B., Flanagan, A. M., Ahmed, A., . . . Taylor, J. C. (2018). Clinically actionable mutation profiles in patients with cancer identified by whole-genome sequencing. *Cold Spring Harb Mol Case Stud*, *4*(2), a002279. https://doi.org/10.1101/mcs.a002279

Schwartz, D. I., Lindor, N. M., Walsh-Vockley, C., Roche, P. C., Mai, M., Smith, D. I., Liu, W., & Couch, F. J. (1999). p73 mutations are not detected in sporadic and hereditary breast cancer. *Breast Cancer Res Treat*, *58*(1), 25-29. https://doi.org/10.1023/a:1006237031070

Scully, R., Panday, A., Elango, R., & Willis, N. A. (2019). DNA double-strand break repair-pathway choice in somatic mammalian cells. *Nat Rev Mol Cell Biol*, *20*(11), 698-714. https://doi.org/10.1038/s41580-019-0152-0

Selvaraj, C. (2023). Therapeutic targets in cancer treatment: Cell cycle proteins. *Advances in Protein Chemistry and Structural Biology*, *135*, 313-342. https://doi.org/10.1016/bs.apcsb.2023.02.003

Senga, S. S., & Grose, R. P. (2021). Hallmarks of cancer—the new testament. *Open biology*, *11*(1), 200358-200358. https://doi.org/10.1098/rsob.200358

Shaaban, A. M., Hilton, B., Clements, K., Provenzano, E., Cheung, S., Wallis, M. G., Sawyer, E., Thomas, J. S., Hanby, A. M., Pinder, S. E., Thompson, A. M., & Sloane Project Steering, C. (2021). Pathological features of 11,337 patients with primary ductal carcinoma in situ (DCIS) and subsequent events: results from the UK Sloane Project. *Br J Cancer*, *124*(5), 1009-1017. https://doi.org/10.1038/s41416-020-01152-5

Sharma, A., Gupta, P., & Prabhakar, P. K. (2019). Endogenous Repair System of Oxidative Damage of DNA. *Current chemical biology*, *13*(2), 110-119. https://doi.org/10.2174/2212796813666190221152908

Sharma, A., Singh, K., & Almasan, A. (2012). Histone H2AX Phosphorylation: A Marker for DNA Damage. *DNA Repair Protocols*, *920*, 613-626. https://doi.org/10.1007/978-1-61779-998-3_40

Smith, C., & Kitzman, J. O. (2023). Benchmarking splice variant prediction algorithms using massively parallel splicing assays. *Genome Biology*, *24*(1), 294.

Steffens Reinhardt, L., Groen, K., Xavier, A., & Avery-Kiejda, K. A. (2023). p53 Dysregulation in Breast Cancer: Insights on Mutations in the TP53 Network and p53 Isoform Expression. *Int J Mol Sci*, *24*(12), 10078. https://doi.org/10.3390/ijms241210078

Stiewe, T., & Pützer, B. M. (2002). Role of p73 in malignancy: tumor suppressor or oncogene? *Cell Death & Differentiation*, *9*(3), 237-245. https://doi.org/10.1038/sj.cdd.4400995

Stindt, M. H., Muller, P. A. J., Ludwig, R. L., Kehrloesser, S., Dötsch, V., & Vousden, K. H. (2015). Functional interplay between MDM2, p63/p73 and mutant p53. *Oncogene*, *34*(33), 4300-4310. https://doi.org/10.1038/onc.2014.359

Stojic, L., Mojas, N., Cejka, P., Di Pietro, M., Ferrari, S., Marra, G., & Jiricny, J. (2004). Mismatch repair-dependent G2 checkpoint induced by low doses of SN1 type methylating agents requires the ATR kinase. *Genes Dev*, *18*(11), 1331-1344. https://doi.org/10.1101/gad.294404

Strauss, J. D., & Pursell, Z. F. (2023). Replication DNA polymerases, genome instability and cancer therapies. *NAR cancer*, *5*(3), zcad033-zcad033. https://doi.org/10.1093/narcan/zcad033

Su, Y. H., Su, H. W., Liu, C. K., Lu, C. H., & Hsu, S. T. (2023). Early-Stage, BRCA-Associated Ovarian Cancer Detected by Papanicolaou Smear: A Case Report. *Cureus*, *15*(6), e40481. https://doi.org/10.7759/cureus.40481

Surdutovich, E., & Solov'yov, A. V. (2012). Double strand breaks in DNA resulting from double ionization events. *The European Physical Journal D*, *66*, 1-5.

Suzuki, R., Orsini, N., Saji, S., Key, T. J., & Wolk, A. (2009). Body weight and incidence of breast cancer defined by estrogen and progesterone receptor status--a meta-analysis. *Int J Cancer*, *124*(3), 698-712. https://doi.org/10.1002/ijc.23943

Tábuas-Pereira, M., Santana, I., Almeida, M. R., Duraes, J., Lima, M., Duro, D., Kun-Rodrigues, C., Bras, J., & Guerreiro, R. (2022). Rare variants in TP73 in a frontotemporal dementia cohort link this gene with primary progressive aphasia phenotypes. *European journal of neurology*, *29*(5), 1524-1528.

Takedachi, A., Matsuishi, E., Mizusaki, S., Nagasawa, T., Fujikane, R., Hidaka, M., Iwai, S., & Kuraoka, I. (2022). Novel plasmids for the fluorescence-based evaluation of DNA mismatch repair in human cells. *Mutat Res*, *824*, 111779. https://doi.org/10.1016/j.mrfmmm.2022.111779

Tan, T., Sammons, S., Fink, J., Ong, W., Jaradi, B., Waring, P., Chan, Y., Lee, X., Lim, B., & Brady, J. (2023). 4MO Homologous recombination (HR) status of platinum-responsive advanced triple-negative breast cancers (aTNBC) treated with olaparib as maintenance therapy. *ESMO Open*, *8*(1).

Taverna Porro, M. L., & Greenberg, M. M. (2015). Double-strand breaks from a radical commonly produced by DNA-damaging agents. *Chem Res Toxicol*, *28*(4), 810-816. https://doi.org/10.1021/acs.chemrestox.5b00032

Taverniti, V., Krynska, H., Venuti, A., Straub, M.-L., Sirand, C., Lohmann, E., Romero-Medina, M. C., Moro, S., Robitaille, A., & Negroni, L. (2023). The E2F4/p130 Repressor Complex Cooperates with Oncogenic? Np73a To Inhibit Gene Expression in Human Papillomavirus 38 E6/E7-Transformed Keratinocytes and in Cancer Cells. *MSPHERE*.

Tchounwou, P. B., Dasari, S., Noubissi, F. K., Ray, P., & Kumar, S. (2021). Advances in Our Understanding of the Molecular Mechanisms of Action of Cisplatin in Cancer Therapy. *J Exp Pharmacol*, *13*, 303-328. https://doi.org/10.2147/JEP.S267383

Technology, C. S. (2020). *Overview of Immunohistochemistry (IHC) | Cell Signaling Technology*. https://www.cellsignal.co.uk/contents/resources-protocols/immunohistochemistry-(ihc)/overview-of-ihc

Telli, M. L., Timms, K. M., Reid, J., Hennessy, B., Mills, G. B., Jensen, K. C., Szallasi, Z., Barry, W. T., Winer, E. P., Tung, N. M., Isakoff, S. J., Ryan, P. D., Greene-Colozzi, A., Gutin, A., Sangale, Z., Iliev, D., Neff, C., Abkevich, V., Jones, J. T., . . . Richardson, A. L. (2016). Homologous Recombination Deficiency (HRD) Score Predicts Response to Platinum-Containing Neoadjuvant Chemotherapy in Patients with Triple-Negative Breast Cancer. *Clin Cancer Res*, *22*(15), 3764-3773. https://doi.org/10.1158/1078-0432.CCR-15-2477

Temko, D., Van Gool, I. C., Rayner, E., Glaire, M., Makino, S., Brown, M., Chegwidden, L., Palles, C., Depreeuw, J., Beggs, A., Stathopoulou, C., Mason, J., Baker, A. M., Williams, M., Cerundolo, V., Rei, M., Taylor, J. C., Schuh, A., Ahmed, A., . . . Tomlinson, I. (2018). Somatic POLE exonuclease domain mutations are early events in sporadic endometrial and colorectal carcinogenesis, determining driver mutational landscape, clonal neoantigen burden and immune response. *The Journal of pathology*, *245*(3), 283-296. https://doi.org/10.1002/path.5081

Thakur, A., Nigri, J., Lac, S., Leca, J., Bressy, C., Berthezene, P., Bartholin, L., Chan, P., Calvo, E., & Iovanna, J. (2016). TAp73 loss favors Smad-independent TGF-β signaling that drives EMT in pancreatic ductal adenocarcinoma. *Cell Death & Differentiation*, *23*(8), 1358-1370.

Tian, R., Wang, Y., Dong, W., Zheng, X., & Cui, M. (2022). Research progress in the pathogenesis of breast cancer mediated by breast and intestinal flora. *MEDS Clinical Medicine*, *3*(7), 27-32.

Timbres, J., Kohut, K., Caneppele, M., Troy, M., Schmidt, M. K., Roylance, R., & Sawyer, E. (2023). DCIS and LCIS: Are the Risk Factors for Developing In Situ Breast Cancer Different? *Cancers (Basel)*, *15*(17). https://doi.org/10.3390/cancers15174397

Tlsty, T. D., Briot, A., Gualberto, A., Hall, I., Hess, S., Hixon, M., Kuppuswamy, D., Romanov, S., Sage, M., & White, A. (1995). Genomic instability and cancer. *Mutat Res*, *337*(1), 1-7. https://doi.org/10.1016/0921-8777(95)00016-d

Tomlinson-Hansen, S., Khan, M., & Cassaro, S. (2023). *Breast Ductal Carcinoma in Situ*. StatPearls Publishing, Treasure Island (FL).

Trayes, K. P., & Cokenakes, S. E. H. (2021). Breast Cancer Treatment. *Am Fam Physician*, *104*(2), 171-178.

Tubbs, A., & Nussenzweig, A. (2017). Endogenous DNA Damage as a Source of Genomic Instability in Cancer. *Cell*, *168*(4), 644-656. https://doi.org/10.1016/j.cell.2017.01.002

Ursu, R., Truica, R. A., Cojocaru, A., Prepelita, D., Pop, L., Radoi, V., Bacalbasa, N., & Balescu, I. (2022). Genetic factors involved in ovarian cancer. *Romanian medical JouRnal*, *69*(3).

van Gent, D. C., Hoeijmakers, J. H., & Kanaar, R. (2001). Chromosomal stability and the DNA double-stranded break connection. *Nat Rev Genet*, *2*(3), 196-206. https://doi.org/10.1038/35056049

Velmurugu, Y., & Velmurugu, Y. (2017). DNA Mismatch Repair. *Dynamics and Mechanism of DNA-Bending Proteins in Binding Site Recognition*, 159-180.

Vermes, I., Haanen, C., Steffens-Nakken, H., & Reutellingsperger, C. (1995). A novel assay for apoptosis Flow cytometric detection of phosphatidylserine expression on early apoptotic cells using fluorescein labelled Annexin V. *Journal of immunological methods*, *184*(1), 39-51. https://doi.org/10.1016/0022-1759(95)00072-I

Veschetti, L., Treccani, M., De Tomi, E., & Malerba, G. (2023). Genomic Instability Evolutionary Footprints on Human Health: Driving Forces or Side Effects? *International journal of molecular sciences*, *24*(14), 11437. https://doi.org/10.3390/ijms241411437

Vikhreva, P., Melino, G., & Amelio, I. (2018). p73 Alternative Splicing: Exploring a Biological Role for the C-Terminal Isoforms. *Journal of molecular biology*, *430*(13), 1829-1838. https://doi.org/10.1016/j.jmb.2018.04.034

Wang, W.-J., Ho, P.-C., Nagarajan, G., Chen, Y.-A., Kuo, H.-L., Subhan, D., Su, W.-P., Chang, J.-Y., Lu, C.-Y., & Chang, K. T. (2019). WWOX possesses N-terminal cell surface-exposed epitopes WWOX7-21 and WWOX7-11 for signaling cancer growth suppression and prevention in vivo. *Cancers*, *11*(11), 1818.

Wang, Y., Liu, M., Liu, X., & Guo, X. (2023). LINC00963-FOSB-mediated transcription activation of UBE3C enhances radioresistance of breast cancer cells by inducing ubiquitination-dependent protein degradation of TP73. *Journal of translational medicine*, *21*(1), 321-321. https://doi.org/10.1186/s12967-023-04153-z

Welcsh, P. L., & King, M. C. (2001). BRCA1 and BRCA2 and the genetics of breast and ovarian cancer. *Hum Mol Genet*, *10*(7), 705-713. https://doi.org/10.1093/hmg/10.7.705

Wen, J., Wang, Y., Yuan, M., Huang, Z., Zou, Q., Pu, Y., Zhao, B., & Cai, Z. (2021). Role of mismatch repair in aging. *Int J Biol Sci*, *17*(14), 3923-3935. https://doi.org/10.7150/ijbs.64953

Werner, H., & LeRoith, D. (2022). Hallmarks of cancer: The insulin-like growth factors perspective. *Front Oncol*, *12*, 1055589. https://doi.org/10.3389/fonc.2022.1055589

Wilkinson, L., & Gathani, T. (2022). Understanding breast cancer as a global health concern. *British journal of radiology*, *95*(1130), 20211033-20211033. https://doi.org/10.1259/BJR.20211033

Williams, L. N., Herr, A. J., & Preston, B. D. (2013). Emergence of DNA polymerase ε antimutators that escape error-induced extinction in yeast. *Genetics*, *193*(3), 751-770.

Wilson III, D. M. (2007). Processing of nonconventional DNA strand break ends. *Environmental and Molecular Mutagenesis*, *48*(9), 772-782.

Winzer, K.-J., Buchholz, A., Schumacher, M., & Sauerbrei, W. (2016). Improving the prognostic ability through better use of standard clinical data-the Nottingham Prognostic Index as an example. *PLoS One*, *11*(3), e0149977.

Xing, X., Jin, N., & Wang, J. (2022). Polymerase Epsilon-Associated Ultramutagenesis in Cancer. *Cancers*, *14*(6), 1467. https://doi.org/10.3390/cancers14061467

Yemelyanova, A., Vang, R., Kshirsagar, M., Lu, D., Marks, M. A., Shih Ie, M., & Kurman, R. J. (2011). Immunohistochemical staining patterns of p53 can serve as a surrogate marker for TP53 mutations in ovarian carcinoma: an immunohistochemical and nucleotide sequencing analysis. *Mod Pathol*, *24*(9), 1248-1253. https://doi.org/10.1038/modpathol.2011.85

Yi, C., & He, C. (2013). DNA repair by reversal of DNA damage. *Cold Spring Harb Perspect Biol*, *5*(1), a012575. https://doi.org/10.1101/cshperspect.a012575

Yin, L., Duan, J. J., Bian, X. W., & Yu, S. C. (2020). Triple-negative breast cancer molecular subtyping and treatment progress. *Breast Cancer Res*, *22*(1), 61. https://doi.org/10.1186/s13058-020-01296-5

Yoon, J. Y., Roth, J. J., Rushton, C. A., Morrissette, J. J. D., Nathanson, K. L., Cohen, R. B., & Rosenbaum, J. N. (2023). Homologous recombination pathway gene variants identified by tumor-only sequencing assays in lung carcinoma patients. *Transl Lung Cancer Res*, *12*(6), 1236-1244. https://doi.org/10.21037/tlcr-22-749

Yoshida, K., & Miki, Y. (2004). Role of BRCA1 and BRCA2 as regulators of DNA repair, transcription, and cell cycle in response to DNA damage. *Cancer Sci*, *95*(11), 866-871. https://doi.org/10.1111/j.1349-7006.2004.tb02195.x

Yousefzadeh, M. (2022). ENDOGENOUS DNA DAMAGE AS A DRIVER OF AGING AND TISSUE DYSFUNCTION. *Innovation in Aging*, *6*(Suppl 1), 196.

Yu, C. X. (2023). Radiotherapy of early-stage breast cancer. *Precision Radiation Oncology*, *7*(1), 67-79.

Zardavas, D., Irrthum, A., Swanton, C., & Piccart, M. (2015). Clinical management of breast cancer heterogeneity. *Nat Rev Clin Oncol*, *12*(7), 381-394. https://doi.org/10.1038/nrclinonc.2015.73

Zawacka-Pankau, J., Kostecka, A., Sznarkowska, A., Hedström, E., & Kawiak, A. (2010). p73 tumor suppressor protein: A close relative of p53 not only in structure but also in anti-cancer approach? *Cell cycle (Georgetown, Tex.)*, *9*(4), 720-728. https://doi.org/10.4161/cc.9.4.10668

Zhang, X., & Kschischo, M. (2022). Distinct and Common Features of Numerical and Structural Chromosomal Instability across Different Cancer Types. *Cancers (Basel)*, *14*(6). https://doi.org/10.3390/cancers14061424

Zhao, B., Rothenberg, E., Ramsden, D. A., & Lieber, M. R. (2020). The molecular basis and disease relevance of non-homologous DNA end joining. *Nat Rev Mol Cell Biol*, *21*(12), 765-781. https://doi.org/10.1038/s41580-020-00297-8

Zhao, Y., Wang, W., Pan, W., Yu, Y., Huang, W., Gao, J., Zhang, Y., & Zhang, S. (2021). WWOX promotes apoptosis and inhibits autophagy in paclitaxel-treated ovarian carcinoma cells. *Mol Med Rep*, *23*(2), 1-1. https://doi.org/10.3892/mmr.2020.11754

Zheng, J., Zeng, B., Huang, B., Wu, M., Xiao, L., & Li, J. (2024). A nomogram with Nottingham prognostic index for predicting locoregional recurrence in breast cancer patients. *Frontiers in oncology*, *14*.

Zheng, R., Jia, Z., Li, J., Huang, S., Mu, P., Zhang, F., Wang, C., & Yuan, C. (2011). Fast repair of DNA radicals in the earliest stage of carcinogenesis suppresses hallmarks of cancer. *RSC Advances*, *1*(9), 1610-1619. https://doi.org/10.1039/c1ra00523e

Zheng, S., Cao, Y., Randall, J., Yu, H., & Thomas, T. O. (2023). Integrating POLE/POLD1 mutated for immunotherapy treatment planning of advanced stage non-small cell lung cancer. *Thorac Cancer*, *14*(23), 2269-2274. https://doi.org/10.1111/1759-7714.15012

Zheng, Z., Li, M., Zhang, Q., Luo, N., Qi, Y., Sun, T., & Qi, C. (2023). Homologous recombination-related (HRR) gene mutations in patients with glioma and their relevance to genomic characteristics, tumor mutation burden (TMB), and prognosis. In: American Society of Clinical Oncology.